THE UNIVERSITY
of EDINBURGH

THE UNIVERSITY
of EDINBURGH

Host Defence Peptides in Pregnancy; Influences on the Microbiome and Preterm Labour

Tina Louise Baker

Thesis Submitted to the University of Edinburgh for the Degree of Doctor of Philosophy

September 2016

THE UNIVERSITY
of EDINBURGH

Abstract

Although inflammation is a crucial mechanism in response to injury and pathogen clearance, inappropriate or excessive induction of the inflammatory response in pregnancy can cause initiation of the labour cascade and subsequent preterm delivery.

Host Defence Peptides (HDPs) have important anti-microbial properties but are also implicated as multifunctional modulators of immunity and infection. They are predominantly secreted by mucosal epithelial cells and released by leukocytes. The specific HDPs that are the focus of this thesis are Human beta-defensin 3 (hBD3) and Human Cathelicidin (hCAP-18/LL-37). The immunomodulatory effect of HDPs in reproductive tissues in response to infection/inflammation has not been well studied.

In a pregnant state, the hypothesis of this thesis is that HDPs have a dual role in preventing ascending infection, but also preventing an exacerbated inflammatory response that can cause preterm birth by initiation of the labour cascade. To explore this I determine whether bacterial stimuli can regulate HDPs expression in pregnancy tissues. I also explore what interactions HDPs have on the production/induction of important cytokines that are vital to the inflammatory response. With the aid of HDP knockout mice, the role of these peptides in infection/inflammation and continuation of pregnancy is investigated in a mouse-model of induced preterm-labour. To understand how ascending infection might be controlled by HDPs in pregnancy, I explore how HDPs regulate commensal and pathogenic bacteria. This is achieved by interrogating the maternal microbiome at mucosal sites in HDP knockout animals, utilising the bacterial 16S rRNA gene and next generation sequencing.

Results

Placental explants respond to Lipopolysaccharide (LPS) challenge by increasing production of pro-inflammatory cytokines. LL-37 but not hBD3 peptide was able to modulate this inflammation by inhibiting the release of these pro-inflammatory cytokines.

To establish whether HDPs are critical in the continuation of pregnancy I use a LPS induced mouse–model of preterm labour in animals lacking the genes for the HDPs, *Defb14* (*Defb14-/-*), or *Camp* (*Camp-/-*). Intrauterine injection of LPS induced preterm labour in wildtype mice. However, the *Defb14-/-* and *Camp-/-* mice do not have an increased rate of preterm labour. Key inflammatory mediators are increased in response to LPS-induced PTL. *Camp-/-* animals have a similar inflammatory response to wildtype mice when given LPS during pregnancy.

To understand how ascending infection might be controlled by HDPs, I interrogated the maternal microbiome at mucosal sites in HDP knockout animals, utilising the bacterial 16S rRNA gene. I established a workflow for 16S rRNA gene sequencing on next-generation sequencing platforms and a bioinformatic pipeline for data analysis. Using this approach I was able to show the mucosal microbiome of *Camp-/-* animals were significantly different to that of wildtype controls, showing increased diversity in the microbes present.

In murine pregnancy, there were very little global cumulative or progressive shifts in bacteria, with the exception of *Candidatus arthromitus*, which significantly increases with gestation compared to non-pregnancy

This thesis has demonstrated that Host Defence Peptides are expressed in pregnancy tissues and have anti-inflammatory properties in response to bacterial stimuli. It is not clear whether the HDPs, hBD3 and LL-37 are fundamental to the immune defence in pregnancy by preventing excessive inflammation, Although, I have shown LL-37 may have a role in modulation of the maternal microbiota.

Lay summary

Preterm birth occurs in 8% -12% of all pregnancies and is the main cause of death in newborn infants. We still cannot predict which women will have a preterm birth, although infection and inflammation in the area around the baby increases the risk.

There is increasing evidence suggesting that the lining of the female reproductive tract is more than just a physical barrier protecting from invading pathogens. The epithelial cells lining this area secrete proteins that kill invading pathogens and regulate the traffic and activity of incoming immune cells to the area.

The aim of this thesis is to understand how a group of these proteins called, Host Defence Peptides (HDPs), which are present in the reproductive tract, regulate both the 'good' and pathogenic bacteria. This thesis also investigates what role these proteins have on inflammation in response to any invading bacteria. This is of importance in pregnancy as inappropriate or excessive induction of inflammation can cause initiation of the labour cascade leading to preterm delivery.

A better understanding of these defence mechanisms within the female reproductive tract will enlighten strategies to prevent and reduce adverse outcomes in pregnancy.

Declaration

The studies undertaken in this thesis are the unaided work of the author, except where due acknowledgment is made by reference. No part of this thesis has previously been, or is currently being submitted in candidature for another degree.

Chapter 2 - I acknowledge the assistance of Ana Calarrao; Research Assistant, University of Edinburgh, who collected primary tissues from women undergoing elective caesarean section.

Chapter 7 – I acknowledge the assistance of Adrian Thomson; Edinburgh Preclinical Imaging; University of Edinburgh, who assisted in the ultrasound *in-vivo* experiments.

Chapter 5 & 7 – I acknowledge the assistance of Lisa Young and Dr Heather MacPherson who gave me assistance in collecting tissue from *in-vivo* experiments.

Tina Baker

September 2016

Acknowledgments

I would first like to thank my supervisors; Professor Julia Dorin, Dr Donald Davidson and Dr Sarah Stock, for their guidance and support throughout my PhD.

My sincere thanks go to members of the Dorin lab; Dr Fiona Semple, Dr Heather MacPherson, and Dr Sheila Webb for supporting me when times were tough. The last 4 years would most definitely not have been as fun without their friendship.

I would like to thank members of the Tommy's Research team, especially, Ana Calarrao, Dr Sarah Rinaldi, and Dr Lorraine Frew for guidance on experiments.

Finally, I would like to thank my friends and family, for their constant support and encouragement.

Abbreviations

16S rRNA	16S ribosomal RNA
AMP	Antimicrobial peptide
ANOVA	Analysis of variance
AP-1	Activator protein 1
BMDM	Bone-marrow-derived macrophage
BR	Broad range
BV	Bacterial vaginosis
CAL	Calibrator
CCL	Chemokine (C-C) motif ligand
CCR	Chemokine (C-C) receptor
cDNA	Complementary DNA
cffDNA	Cell free fetal DNA
CNV	Copy number variation
COX	Cyclo-oxygenase
CRH	Corticotrophin releasing hormone
CST	Community state types
Ct	Cycle threshold
CXCL	Chemokine (C-X-C) motif ligand
dNTP	Deoxyribonucleotide triphosphate
dsRNA	Double-stranded RNA
DSS	Dextran sulfate sodium
EGFR	Epidermal growth factor receptor
ELISA	Enzyme linked immunosorbent assay
ER	Estrogen receptor
ERK	Extracellular signal-regulated kinases
FISH	Fluorescent in situ hybridization
FRP2	Formyl peptide receptor 2
FRT	Female reproductive tract
GAPHD	Glyceraldehyde-3-phosphate dehydrogenase
GAS	group-A Streptococcus
GBS	group-B-Streptococcus
G-CSF	granulocyte colony-stimulating factor
GR	Glucocorticoid receptor
GWAS	Genome-wide association study
hBD	Human beta defensin
HCL	Hydrochloric acid
HDP	Host defence peptide
hGC	human chorionic gonadotropin
HIV	Human immunodeficiency virus
HNP	Human neutrophil peptides
HPLC	High performance liquid chromatography
HRP	Horseradish peroxidase
HS	High sensitivity
HTS	High throughput sequencing

HUVEC	Human umbilical vein endothelial cells
IL	Interleukin
IL-1Ra	Interleukin-1 receptor antagonist
IRAK	Interleukin-1 receptor associated kinase
IRF	Interferon regulatory factor
JNK	c-Jun N-terminal kinase
LBP	LPS binding protein
LDH	Lactate dehydrogenase
LEfSe	Linear discriminant analysis with effect size
LPS	Lipopolysaccharide
LTA	Lipoteichoic acid
MAPK	Mitogen-activated protein kinase
MDA5	Melanoma differentiation-associated protein 5
MIC	Minimum inhibitory concentrations
MMP	Matrix metalloproteinase
MRSA	Methicillin-resistant Staphylococcus aureus
MyD88	Myeloid differentiation primary response gene 88
NETs	Neutrophil extracellular traps
NF-κB	Nuclear factor kappa B
NK-T	Natural killer T
NO	Nitric oxide
NOD	Nucleotide-binding oligomerization domain-like receptors
NS	No significance
NTC	No template control
NTxC	No treatment control
OTR	Oxytocin receptor
OTU	Operational taxonomic units
PAMP	Pathogen associated molecular patterns
PBS	Phosphate buffered saline
PCOA	Principle co-ordinate analysis
pDCs	Plasmacytoid dendritic cells
PG	Prostaglandin
PGM	Personal genome machine
PMSG	Pregnant mare's serum gonadotropin
polyI:C	Polyinosinic:polycytidylic acid
PPROM	Preterm premature rupture of membranes
PR	Progesterone receptor
PTL	Preterm labour
QIIME	Quantitative insights in to microbial ecology
RA	Rheumatoid arthritis
RANTES	Regulated on activation, normal T cell expressed and secreted
RDP	Ribosomal database project
RNA	Ribonucleic acid
ROS	Reactive oxygen species
RT	Reverse transcriptase
RT-qPCR	Quantitative real time polymerase chain reaction
SCFA	Short chain fatty acids

SEM	Standard error of the mean
SFB	Segmented filamentous bacteria
SLE	Systemic lupus erythematosus
SNP	Single nucleotide polymorphism
SP-A	Surfactant Protein-A
SPF	Specific pathogen free
STAT	Signal transducer and activator of transcription
STI	Sexually transmitted infections
TBE	Tris/Borate/EDTA
TLR	Toll like receptor
TMB	3,3'5,5' Tetramethylbenzidine
TNF	Tumour necrosis factor
TRAF	TNF receptor associated factor
TRIF	TIR domain containing adapter inducing interferon beta
UPGMA	Unweighted pair group method with arithmetic means algorithm
UPL	Universal probe library
USS	Ultrasound sonography
UTR	Untranslated region
VDRE	Vitamin D response element
VRE	Vancomycin-resistant Enterococci

Contents

List of Figures

Chapter 1 Literature Review

Chapter 2 General Materials and Methods

Chapter 3 Host Defence Peptides

Chapter 4 Microbiome - 16S rRNA Gene Sequencing

Chapter 5 Modulation of the Microbiome

Chapter 6 Murine Vaginal Microbiome

Chapter 7 Role of Host Defence Peptides in an Infection/ Inflammation Induced Mouse Model of Preterm Labour

List of Tables

Chapter 1 Literature Review

Chapter 2 General Materials and Methods

Chapter 3 Host Defence Peptides

Chapter 4 Microbiome - 16S rRNA Gene Sequencing

Chapter 5 Modulation of the Microbiome

Chapter 6 Vagina Microbiome

Chapter 7 Role of Host Defence Peptides in an Infection/ Inflammation Induced Mouse Model of Preterm Labour

Chapter 1

Literature Review

Chapter 1 Literature Review

1.1 Labour and Preterm Labour

1.1.1 Preterm Labour

The World Health Organisation estimates that 1 in 10 babies are born preterm (<37 weeks gestation) which is a global annual incidence of 15 million (World Health, 2013). Neonatal preterm labour is the main cause of morbidity and mortality in newborn infants, resulting in a multitude of developmental, neurological and cognitive problems (Galinsky et al., 2013). In addition to the huge burden on quality of life, these long-term associated problems increase the need for medical care and allied services.

In many developed countries antenatal care has greatly increased the survival of extremely premature babies; however, the proportion of babies which survive with major health complications has not changed (Martin et al., 2010). Research into preterm labour has vastly increased in the last decade but this has not translated into a reduction in the incidence of preterm labour and improved neonatal outcomes.

There are several low level risk factors for having a preterm labour; a prior history of a preterm labour, multiple pregnancy, maternal stress, excessive physical work, smoking, excessive alcohol consumption and infection. Gestational diabetes is also associated with a 4-fold increase in the rate of Preterm Labour (Norman et al., 2009b). In addition, pre-existing diabetes is the highest risk factor of any maternal conditions associated with having a premature delivery.

Nearly 40% of preterm deliveries are associated with intrauterine infection (Romero et al., 2006) (Figure 1.2). There are conflicting reports whether antibiotic intervention is beneficial in preventing preterm labour associated with intrauterine infection (Lamont, 2015, King and Flenady, 2002). A review of meta-analysis studies highlighted that the beneficial effects of antibiotics may have been masked by some negative studies which were methodologically flawed (Lamont, 2015). There is however, increasing support that certain prophylactic antibiotics given very early in

pregnancy to those women who have a clinical diagnosis of vaginal bacteria dysbiosis (Bacterial Vaginosis), has benefit (Thinkhamrop et al., 2015).

There is therefore a great need to understand the pathophysiology of infection/inflammation in the context of preterm labour concerning both host-genetic and environmental risk factors. It is of importance to understand how the inflammatory process leads to preterm labour with the end goal of delaying or preventing this process in women.

1.1.2 Term and Preterm Labour Common Components

Preterm and term labour share common terminal pathways characterised by anatomical, biochemical, and endocrine events (Snegovskikh et al., 2006) (Figure 1.1). Labour is a clinical diagnosis characterised by regular painful uterine contraction, progressive cervical effacement and dilatation. The uterine components of this shared pathway include 1) increases in uterine contractility, 2) cervical effacement and dilatation 3) decidual activation. In preterm labour the events are similar, although the stimuli that initiate and contribute to labour may differ. Clinical manifestations in preterm labour include; preterm premature rupture of the membranes (PPROM), preterm uterine contractions and cervical insufficiency. Understanding the upstream molecular mechanisms involved in the onset of labour at term is therefore important when looking at this labour cascade in preterm labour.

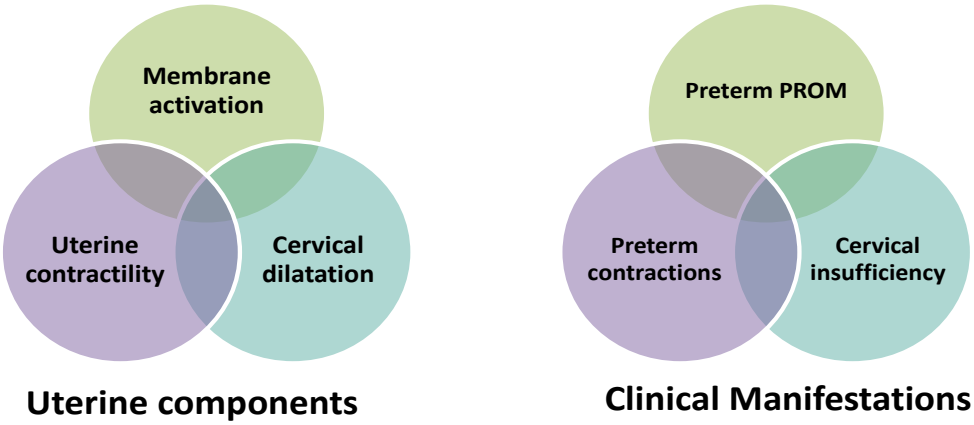

Figure 1.1 Common Components of Term and Preterm Labour
Schematic showing the overlapping factors of parturition at term and in preterm labour. Multiple factors are involved that lead to the clinical diagnosis of labour. (PROM; Preterm Rupture of Membranes)

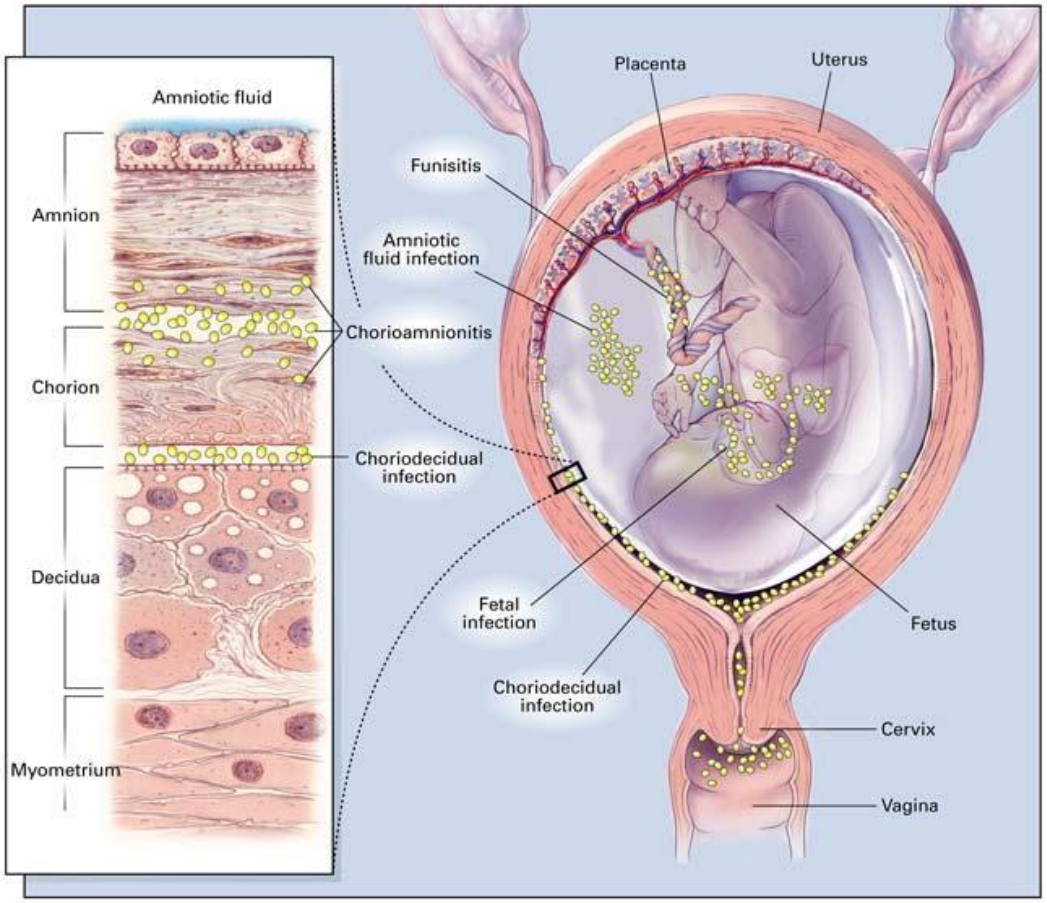

Figure 1.2 Schematic of Types of Infection/Inflammation in Human Pregnancy

The types of inflammation and infection seen at the fetal-maternal interface. Bacterial infections within the uterine compartment can occur between fetal and maternal tissue (choriodecidual infection), within and between the two fetal membranes (chorioamnionitis), within the placenta, in the amniotic cavity or within the umbilical vessels (vasculitis) and cord substance (funisitis). Chorioamnionitis, choriodecidua infection, and amniotic fluid infections are more prevalent in association with ascending infectious agents through the cervix. Source: Goldenberg et al., (2000).

1.1.3 Labour as an Inflammatory Event

Labour is now generally accepted to be an inflammatory event where the emphasis from an anti-inflammatory pregnancy state shifts pro-inflammatory preceding labour (Youssef et al., 2009). At term, an infiltration of neutrophils and macrophages into the cervix and maternal fetal membrane is observed (Osman et al., 2003, Gomez-Lopez et al., 2010), in addition to increases in circulating leukocytes (Yuan et al., 2009). Selective immune cell recruitment from the circulating blood involves the production of chemotactic signals.

NF-κB, a transcription factor family, is increased in the myometrium, the smooth muscle tissue of the womb, and amnion in term labour (Pieber et al., 2001, Lappas and Rice, 2009, Vora et al., 2010). This transcription factor has binding sites in key pro-labour genes controlling their activity (Lindström and Bennett, 2005).

Increase in transcription factor NF-κB, and also AP-1 and STAT (Stein et al., 1993) result in the production of cytokines including IL-6, TNF, IL-1α, IL-1β, and IL-8 within the fetal membranes and uterine lining (Elliott et al., 2001, Lappas et al., 2003). The relative contribution of these inflammatory transcription factors has been shown to be spatial, regardless, alone their activity results in a similar myometrial contractile pathways highlighting redundancy (Migale et al., 2016, MacIntyre et al., 2014). These cytokines can stimulate prostaglandin production that in turn initiate mobilisation of neutrophils (Lockwood et al., 2006, Arcuri et al., 2009). These neutrophils infiltrate the tissue causing the production and release of metalloproteases (MMPs). Prostaglandins directly stimulate myometrial contractions in addition to indirect stimulation by the up-regulation of the oxytocin receptor (COX-2) (Liggins, 1989, Crankshaw and Dyal, 1994). COX-2 is an inducible labour associated gene, which is expressed at term labour in the human myometrium, while release of MMPs can aid tissue remodelling in the cervix and fetal membrane (Heng et al., 2012).

1.1.3.1 Inflammatory Mediators

Microarray studies have highlighted labour is associated with a core inflammatory response when comparing cervical, myometrial and fetal membrane tissue of women before and after the onset of labour (Sharp et al., 2016, Bollapragada et al., 2009, Nhan-Chang et al., 2010). Collectively these studies highlight that the genes up-regulated during term labour are involved in inflammatory response, inflammatory pathway signalling, cytokine-cytokine receptor interaction and extracellular matrix–receptor interactions. Cytokines are cell-signalling molecules and were shown to be the most up-regulated genes in normal term labour (Bollapragada et al., 2009).

1.1.3.2 NF-κB

NF-κB is a transcription factor family that has classic association to infection/ inflammation and is involved in innate and adaptive immune responses. NF-κB is normally inactive in the cytoplasm, but in response to stimuli, such as LPS and pro-inflammatory cytokines, its associated inhibitors, IκB proteins, are phosphorylated and proteolytically degraded. This degradation releases NF-κB dimer that can translocate to the nucleus (Ghosh and Baltimore, 1990, Hayden and Ghosh, 2004). Within the nucleus, NF-κB binds to genes with receptive NF-κB biding sites where it regulates the transcription of the associated genes.

Many key pro-labour genes are regulated by the NF-κB transcription activity (Figure 1.3). Some studies have shown NF-κB to be increased in the amnion, decidua and fetal membrane in normal term labour (Lappas and Rice, 2009, Vora et al., 2010). Although, in the absence of infection, its increased activity has not been conclusively established as other studies failed to confirm its action in fetal membrane tissue from labouring women (Yan et al., 2002). Mouse models of preterm labour have provided evidence for a key involvement for NF-κB in the process of labour. Condon et al., (2004) showed that mice receiving NF-κB locally had delayed onset of preterm labour compared to control injection.

Blocking the activity of NF-κB *in-vitro* can inhibit the expression of IL-8, TNF and IL-6 in amnion, cervical epithelial and chorion-decidual cells (Elliott et al., 2001,

Lappas et al., 2003). It has also been shown to inhibit COX-2 expression and production of prostaglandins in fetal membrane tissues and the release of MMPs (Lindström and Bennett, 2005).

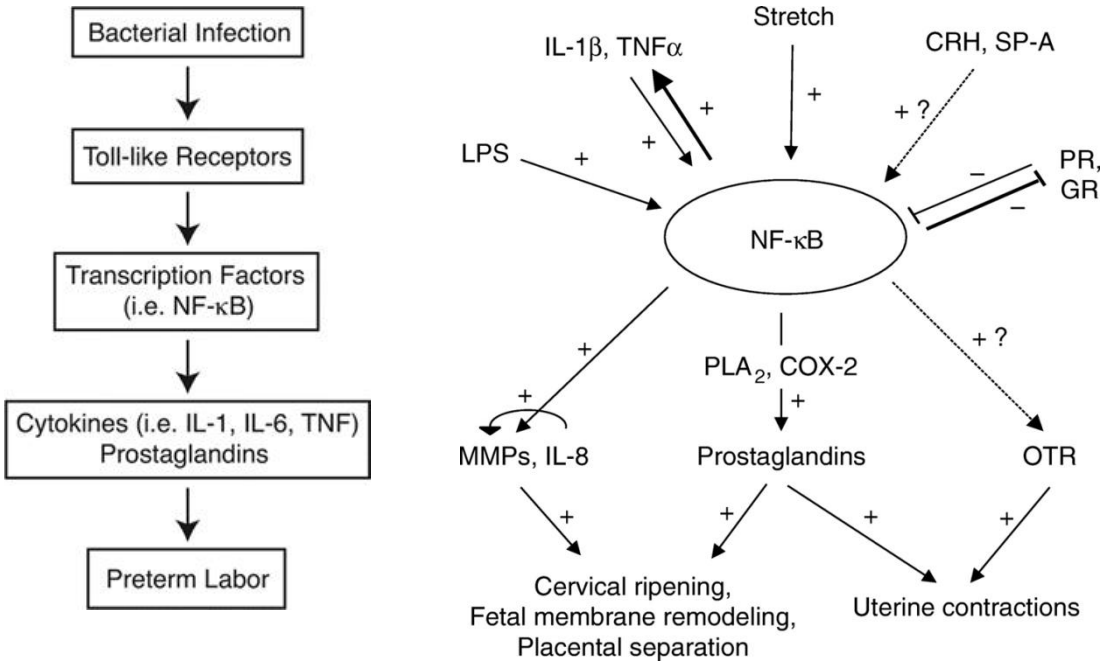

Figure 1.3 Schematic of Core Labour-associated Pathways
Lipopolysaccharide (LPS); Corticotrophin Releasing Hormone (CRH); Surfactant Protein-A (SP-A,); Progesterone Receptor (PR); Glucocorticoid Receptor (GR); Phospholipase A2 (PLA2); Oxytocin Receptor (OTR). Source: Lindström and Bennett (2005)

1.1.3.3 Immune Cells

Neutrophils are a mature type of white blood cell that have vital role in protecting against diseases and infections. They can participate via direct actions such as; phagocytosis, degranulation and generation of neutrophil extracellular traps (NETs). Neutrophils also work by producing cytokines that can recruit and activate further immune cells to the area of infection/inflammation.

Labouring-women at term and preterm have higher total numbers of circulating neutrophils compared to before the initiation of labour. Circulating neutrophils in

labouring women are also more primed than non-labouring neutrophils; they show increased migration potential and have a higher production of reactive oxygen species (Yuan et al., 2009).

The observation of leukocyte influx into reproductive and pregnancy tissues during labour has been widely reported (Osman et al., 2003, Gomez-Lopez et al., 2010). It has also been widely observed in combination with an increase in the neutrophil chemokine IL-8 (CXCL8) mRNA gene transcript. Neutrophils in pregnancy tissues release pro-inflammatory cytokines and MMPs, which degrade the extracellular matrix of the fetal membranes and contribute to the labour cascade. However, it remains to be established whether these leukocytes are a causative factor for the initiation of labour, or predominantly involved in the subsequent tissue remodelling following labour.

In animal studies, term-labour and preterm labour induced by inflammation, results in an influx of neutrophils into the decidua and myometrium (Shynlova et al., 2013a, Shynlova et al., 2013b, Rinaldi et al., 2014). This was not seen when preterm labour was induced by blocking the hormone progesterone with mifepristone (Shynlova et al., 2013a), suggesting a role for decidual neutrophils in labour. Similarly in humans, the number of neutrophils in the decidua of women with infection-associated preterm labour is greater than preterm/term labour not associated with infection (Hamilton et al., 2012). Despite these findings, Rinaldi et al., (2014) showed that neutrophil influx to the decidua is not necessary for initiation of preterm labour in an animal model of PTL. The authors demonstrated that depleting neutrophils did however reduce the amount of IL-1β produced in response to LPS.

Most macrophages are monocyte derived from the blood; however, tissues also have their own type of tissue resident macrophages that are not always derived from the bone marrow. Resident macrophages are mostly involved in homeostasis; patrolling the microenvironment for damage signals from cell death and cells undergoing phagocytosis.

Macrophages have dual functions in the response to inflammation. Macrophages are involved in the pro-inflammatory process of sending signals to recruit more immune

cells, but are also involved in resolution of inflammation and regulating the levels of tissue repair to avoid tissue damage. In response to infection and other intrinsic cell damage signals, they can phagocytose, releasing IL-1β and TNF as potent pro-inflammatory cytokines. In resolving infection, macrophages can produce anti-inflammatory cytokines including TGF-β and IL-10.

Macrophages are important in secreting cytokines, including IL-1β, IL-6, TNF but also MMPs and nitric oxide (NO). Human and rodent studies have shown that uterine macrophage numbers increase with gestation and there is an associated increase in NO production (Tan et al., 2014), although there are conflicting reports of their role in parturition. Some studies in rodents (Shynlova et al., 2013a, Buhimschi et al., 1996, Mackler et al., 1999) have suggested that uterine macrophages are depleted directly prior to the initiation of labour, which is in keeping with the report that NO prevents uterine contractions *in-vitro* (Yallampalli et al., 1993).

Various studies have shown macrophage numbers in the cervix increase during parturition. Elegant studies looking at macrophage surface markers have shown that cervix macrophages are more favoured towards MMP activation and cell matrix remodelling, and less favoured for adhesion and migration. This suggests a key role in functions associated with ripening and dilation of the cervix, which is in keeping with an animal study that showed depleting macrophages prevented cervical remodelling (Gonzalez et al., 2011b). Depleting macrophages also protects mice from LPS-induced PTL suggesting macrophages also have a key role in parturition (Gonzalez et al., 2011b).

Although neutrophils and macrophages are the main infiltrating immune cells, pregnancy tissues also have other resident and patrolling immune cells, including granulocyte-derived mast cells, antigen-presenting dendritic cells and NK-T cells, which are suggested to have a role in mediation of parturition. Adaptive immune cells, such as T cells, B cells and regulatory T cells (T regs), are also resident in pregnancy tissues and participate mostly in fetal-maternal tolerance during pregnancy (reviewed in Gomez-Lopez et al., (2014).

1.1.3.4 Toll Like Receptors

Many cells have pattern recognition receptors (PAMPs) at the cell surface, including the transmembrane TLR proteins. Cells also have multiple intracellular receptors such as NOD domains, which recognise bacterial and extracellular stimuli.

There are 11 transmembrane Toll like receptors described in humans and mice collectively (TLR-1-11) (Akira and Takeda, 2004). These include TLR-4, where the main ligand is LPS, and TLR-3, which detects dsRNA. TLR-2 is involved in the detection of many Gram-positive bacteria products such as lipoteichoic acids (LTA). TLR-9 is essential in the recognition of CpG motifs, which are abundant in many bacteria. TLR-3 and TLR-7-9 are intercellular receptors, while TLR-1, TLR-2, TLR-4-6 and TLR-11 are located at the cell surface.

TLR signalling is mediated by two main pathways; the Myeloid Differentiation Primary Response 88 (MyD88) dependent, and MyD88 independent (Figure 1.4). The MyD88 dependent pathway is common to all the TLRs except TLR-3, whereas the MyD88 independent pathway is distinctive to signalling by TLR-3 and TLR-4(Takeda and Akira, 2001). TLR-4 has a unique property where it can use both MyD88 dependent and independent pathways. TLR-4 co-adaptor molecules include; LPS-binding protein (LBP), cluster of differentiation 14 (CD14) and MD-2 also known as Lymphocyte antigen 96.

Ligand binding in the MyD88 dependent pathway recruits the adapter proteins, IL-1 receptor associated kinases (IRAKs), which when activated interacts with the intracellular signalling molecule TNF Receptor Associated Factor 6 (TRAF6). This activates complexes that signal MAP kinase pathways, JNK, and the NF-κB pathway. The MyD88 independent pathway is mediated by the adaptor protein, TIR-domain-containing adapter-inducing interferon-β (TRIF), which triggers TRAF6, in-turn signalling the NF-κB pathway. TRAF6 also induces an interferon response by increasing the interferon transcription factor, IRF3.

Transcripts for TLR1-10 have been found expressed in multiple tissues of the female reproductive tract and also in pregnancy tissues such as the placenta and fetal

membranes (reviewed in Nasu and Narahara (2010). TLR-2 and TLR-4 are stated to be increased in the myometrium, cervix and fetal membrane of labouring women at term (Kim et al., 2004, Bollapragada et al., 2009, Youssef et al., 2009). Interestingly TLR-2 and TLR-4 are also increased in women with signs of infection (Kim et al., 2004). Spontaneous preterm labour is associated with an increased expression of *TLR4* on maternal human blood monocytes (Pawelczyk et al., 2010).

There is also some evidence that low expression of TLR-4 may be protective against preterm labour (Hirsch et al., 2006). TLR-4, has been shown to mediate inflammation-induced preterm labour in animal models (Elovitz et al., 2003). Elovitz et al., (2003) showed C3H/HeJ, TLR-4 mutant, mice had reduced levels of LPS-induced preterm labour compared to the CD1 strain. In this study, TLR-4 did not reduce the rate of fetal demise, whereby those animals that had no preterm labour still displayed high rates of LPS-induced fetal death.

Interestingly, genetic variation in TLR-4 and TLR-9 have been associated with incidences of dysbiosis in the vaginal microbiota, suggesting host-immune genotype is important in maintaining bacteria homeostasis (Royse et al., 2012, Macones et al., 2004).

Pioli et al., (2004) show TLRs have spatial expression patterns in the female reproductive tract. Hirata et al. (2007) went on to show the expression of many of these TLRs alters during the menstrual cycle (Hirata et al., 2007). TLR-1-9 are also in the female reproductive tract of mice, where they similarly show temporal and spatial expression patterns throughout estrus in the vagina and uterus (Soboll et al., 2006, Hickey et al., 2013).

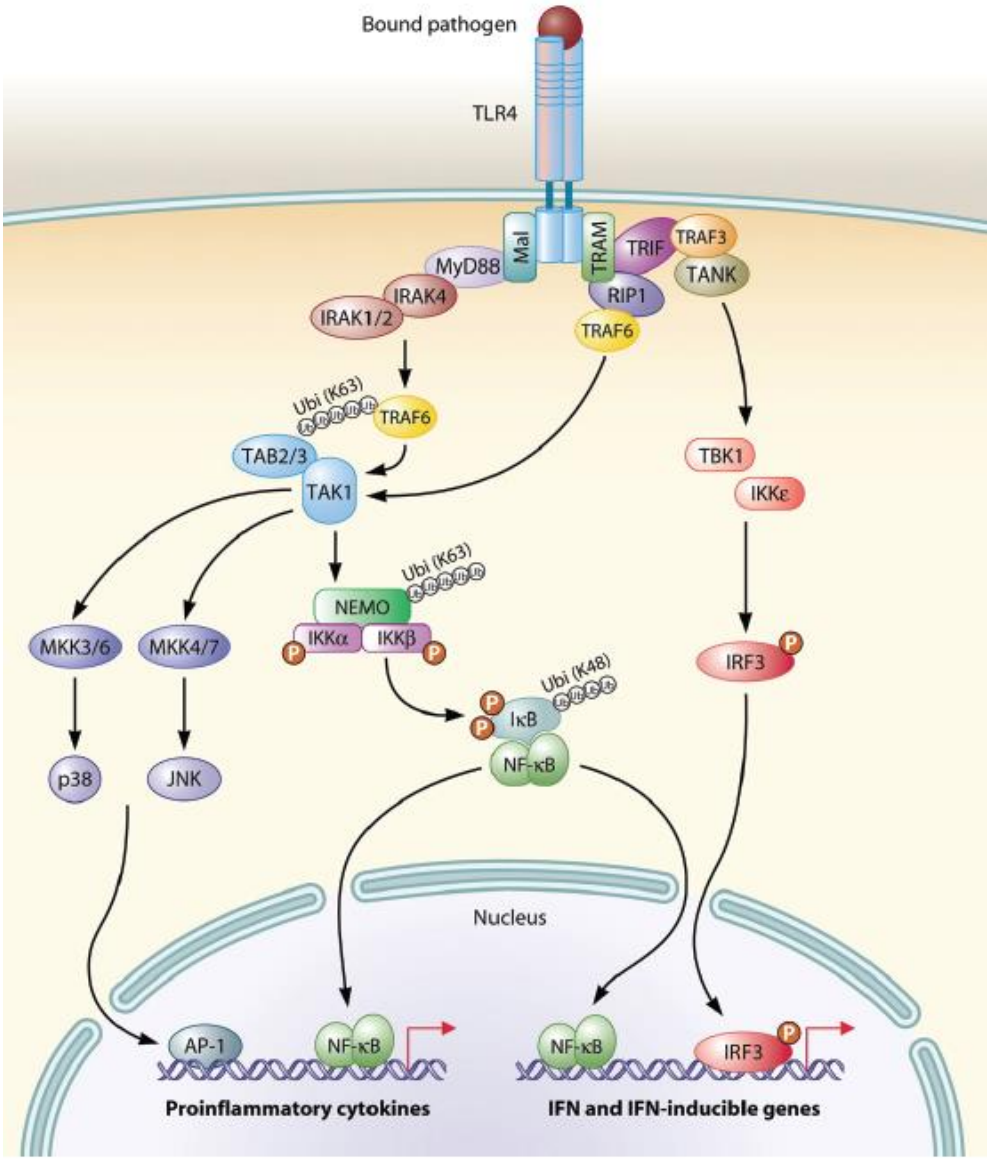

Figure 1.4 Schematic of the TLR-4 Signalling Pathway
TLR-4 singling through both the MyD88 (MyD88 dependent) and TRIF pathways (MyD88 independent). Source: Mogensen (2009)

1.1.4 Onset of Labour at Term

Humans first maintain pregnancy by the production of progesterone in the corpus lutum; this is then superseded by placental progesterone production. In humans labour is not associated with a systemic withdrawal of progesterone (Elovitz and Mrinalini, 2004). However, emerging evidence suggests there may be local functional progesterone withdrawal prior to the onset of labour (Pieber et al., 2001, Mesiano et al., 2002).

In contrast in mice, placental progesterone is not thought to supersede that of the corpus lutum and so removal of the ovaries during pregnancy induces labour (Condon et al., 2004). The onset of labour in mice has been proposed to involve Surfactant Protein A (SP-A) which is released from the pup lung. SP-A causes mobilisation of macrophages from the amniotic fluid into the maternal tissues of the uterus, this process activates pro-inflammatory cytokines such as IL-1β that in turn stimulates NF-κB activation (Condon et al., 2004, Mendelson and Condon, 2005). However, the causative factor that initiates the inflammatory cascade in Human term labour still remains unclear.

1.1.5 Infection/Inflammation and Preterm Labour

There are many infectious agents that when contracted by the mother can transfer to fetus and cause inflammation and fetal demise. Infectious agents include; *Toxoplasma gondi* (toxoplasmosis), Cytomegalovirus, Herpes simplex virus, and Lyme disease. However, these infections do not explain the infection/inflammation seen in most preterm births. A local immune response in the decidua and chorion is more commonly associated with preterm labour (Galinsky et al., 2013, Vrachnis et al., 2010). These are frequently caused by ascending opportunistic commensal bacteria from the vagina, through the cervix and into the fetal membrane (Allam et al., 2013, DiGiulio et al., 2010). The upper genital tract is generally considered sterile prior to the onset of labour (Jones et al., 2009) nonetheless nearly 40% of preterm deliveries are associated with intrauterine infection and/or clinical inflammation (Romero et al., 2006). Studies investigating bacterial DNA in placenta

and fetal membranes discovered women who present with preterm labour have a greater diversity of bacteria in these tissues (Prince et al., 2016, Aagaard et al., 2014). It is therefore important to investigate the role of local infection when considering premature labour.

1.1.6 Mechanisms for Inflammation/Infection

NF-κB can also be activated by pro-inflammatory cytokines in response to pathogens such as endotoxins from bacterial cell walls.

The surface of many immune cells including leukocytes, dendritic cells, epithelial cells and trophoblasts, have pattern recognition receptors (e.g. TLRs) which when stimulated by bacterial endotoxin or pro-inflammatory cytokines release transcription factors including NF-κB, STAT, and AP-1. This in turn results in the production of cytokines and chemokines, such as IL-6, TNF, IL-1β, and IL-8, within the uterine lining and the fetal membranes (Figure 1.3).

The involvement of cytokines/chemokines in maternal and fetal inflammation has been well investigated in humans. Experimentally, animal models have been used which allow for collection of gestational tissues at various time-points during pregnancy.

Systemic LPS treatment in pregnant mice induces maternal inflammation and preterm labour that is associated with rises in amniotic fluid cytokines (IL-1 and IL-6) and maternal serum cytokines (IL-1, TNF, and IL-6) (Baumann et al., 1993, Fidel et al., 1994).

A similar cytokine response was seen in a localised fetal inflammatory model, where heat-killed *E.coli* was injected into ligated uterine horns (Hirsch et al., 2006). These cytokines can stimulate the production of prostaglandins, which initiate mobilisation of neutrophils. These neutrophils infiltrate tissue causing the production and release of metalloproteases (MMPs) and induction of COX-2. COX-2 is expressed at term labour in the human myometrium and also animal cervical fibroblasts (Sato et al., 2001), there is also some evidence that low expression may be protective against

preterm labour (Hirsch et al., 2006). As discussed previously, TLR-4 has been shown to mediate inflammation-induced preterm labour in animal models (Elovitz et al., 2003).

Prostaglandins produced in the amnion can stimulate uterine contractions when in proximity to the uterine lining (Cheung et al., 1992). This activity is supressed during pregnancy by the release of prostaglandin dehydrogenase in chronic tissue which acts as a buffer for its activity (Cheung et al., 1992). In the context of an amniotic infection, activity of prostaglandin dehydrogenase is reduced, which allows the prostaglandins to reach the myometrium which in-turn can lead to premature contractile activity (Van Meir et al., 1996). Infection can also increase MMPs, which can weaken the chorion amniotic membrane causing it to prematurely rupture (Catalano et al., 2010). Increased concentrations of iNO and prostaglandins in amniotic fluid are also associated with intrauterine infection and continue to propagate the labour cascade (Bethea et al., 1998).

LPS and exposure to some bacteria can cause hypoxia-inducing oxidative stress and apoptosis in the placenta and fetal membranes (Garnier et al., 2008). Increases in cell turn-over and apoptosis at the fetal-maternal interface could result in increased apoptotic bodies and cell-free fetal DNA (cffDNA) from the placenta entering the maternal circulation (Bischoff et al., 2005). High levels of cffDNA, which is hypomethylated and a TLR-9 agonist, have previously been associated with preterm labour, preterm rupture of the membrane and preeclampsia (Farina et al., 2005, Jakobsen et al., 2012, Lim et al., 2013).

1.1.7 Therapeutics for Preterm Labour

Research into preterm labour has vastly increased in the last decade but this has not translated into a reduction in the incidence of preterm labour. There are few treatment options for preventing a preterm birth to improve neonatal outcomes.

A cervical cerclage is a suture inserted close to the cervix during pregnancy. It is used in women with short cervical length with the aim of preventing early opening of

the cervix. Kindinger et al., (2016) demonstrated that the type of material used for the suture can affect the vaginal microbiome and inflammatory cytokine profile.

Drugs can be used in an attempt to supress the myometrial contractions in women who are high risk of preterm labour. The main mechanisms for these tocolytic drugs are to reduce the supply and transfer of intracellular calcium in the myometrium, which is a key component in processes for myometrial contractions. Inhibitors for the oxytocin receptor COX-2 are also used as tocolytic treatment; as COX-2 is the rate-determining step for Prostaglandin synthesis and Prostaglandins directly stimulate myometrial contractions.

Progesterone also acts on suppressing the availability and transport of intracellular calcium ions and Prostaglandin synthesis in myometrial tissue. There have been multiple randomised control-studies which show a reduction in PTL with weekly injections of 17α-hydroxy progesterone caproate (Meis et al., (2003) reviewed in Norwitz and Caughey (2011)). This protective effect was also shown in a study which applied progesterone daily to the vagina (da Fonseca (2003) reviewed in Norwitz and Caughey (2011)). Progesterone was not shown to be effective for women presenting with PROM (Briery et al., 2011) or multiple pregnancies (Rouse et al., (2007), Durnwald et al., (2010), Norman et al., (2009a) reviewed in Norwitz and Caughey (2011)). Reviews have suggested that progesterone can also improve neonate morbidity and mortality. Although recent published results from the OPTIMUM randomised placebo-controlled trial, looking at progesterone as a prophylaxis, showed no harm or benefit from vaginal progesterone on neonatal outcome at 2 years of age, moreover no benefit to preterm labour (Norman et al., 2016).

There are conflicting reports whether antibiotic intervention is beneficial in preventing preterm labour associated with intrauterine infection (Lamont, 2015, King and Flenady, 2002). There is however, increasing support that certain prophylactic antibiotics given very early in pregnancy to those women who have a clinical diagnosis of vaginal bacteria dysbiosis has benefit (Thinkhamrop et al., 2015).

Novel drug development and clinical trials, especially in pregnancy is very restricted, so looking towards currently available drugs already used for other conditions may prove a quicker mode for translational medicine. An encouraging human study looking into administration of chloroquine chemoprophylaxis, a known TLR-9 inhibitor and antimalarial agent, in pregnant mothers in West Africa reported lower rates of preterm labour in those who had a 'complete' course of chloroquine (Sirima et al., 2003).

Taken together, the development of preventative therapies for preterm labour requires a mechanistic understanding of how key modifiers of the inflammatory processes respond to bacterial infection during pregnancy.

1.2 Host Defence Peptides

Antimicrobial peptides provide the first line of defence against infectious pathogens in multicellular organisms. Peptides with antimicrobial functions have also been defined in archaea, fungi, plants and bacteria. Over 1,972 animal host defence peptides are currently described and they are evolutionarily conserved (Wang et al., 2016). Structurally, antimicrobial peptide families are very diverse, but they are categorised by their sequence composition and protein confirmation.

The most studied cationic antimicrobial peptides in humans are the Defensins and Cathelicidin. Due to the discovery that these antimicrobial peptides have an array of additional immunomodulatory properties (Figure 1.5), they are commonly adopting the broader name of Host Defence Peptides (HDPs).

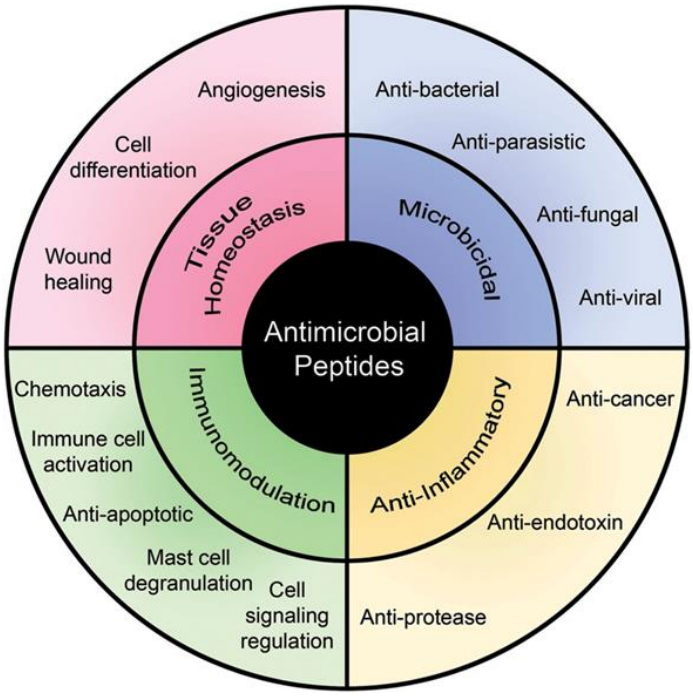

Figure 1.5 Overview of HDPs Modes of Action
HDPs have potent microbicidal activity against a broad spectrum of bacteria, fungi, and viral organisms; acting directly on the invading pathogens (blue). They can supress the inflammatory process by binding and blocking receptors but also directly binding to bacterial pathogens (yellow). They also influence immune response by attracting inflammatory cells, inducing an inflammatory state, modulating apoptotic cell death and cell degranulation (green). HDPs can play a role in tissue homeostasis; including the induction of angiogenesis (pink). Source: Yarbrough et al., (2015)

1.2.1 Defensins

1.2.1.1 Defensins

Human defensins are small cationic peptides, predominantly released by epithelial cells at mucosal surfaces where their main role is in host innate immunity. In addition to acting directly on invading pathogens, they also influence immune response by attracting inflammatory cells and inducing an inflammatory state. There is also evidence to suggest that certain defensins can function to modulate apoptotic cell death (Yamaguchi et al., 2007) and some have immunosuppressive activity (Shi et al., 2007, Semple et al., 2010)

Defensins are divided into three categories; alpha-defensins, beta-defensins, and theta-defensins. Alpha and theta defensins arose from ancestral beta-defensin genes. In other species such as snakes, beta-defensin derivatives have become specialised as toxins (crotamines). Almost all defensins contain a canonical six-cysteine motif and have a beta-sheet structure. They are distinguishable by their; genomic organisation, the spacing of these cysteines, and their disulphide bond interactions. *In-silico* analysis has predicted 28 defensin like sequences at 5 loci in the human genome based on the six- cysteine motif (Schutte et al., 2002).

Alpha-defensins and beta-defensins are found in most vertebrate species. Leukocytes and Paneth cells (specialised cells in the small intestine), are the main source of alpha-defensins. Beta-defensins are expressed in a variety of tissues and cell types, including epithelial cells, macrophages and dendritic cells.

In humans and many higher mammals, beta-defensin sequences have been found to cluster together on chromosome arrangements. In humans, 10 beta-defensins are clustered on an 8MB region of chromosome 8p23.1. Seven of the genes in this region (*DEFB103 – DEFB108* and *DEFB4*) are arranged in a copy number variable (CNV) cluster, which ranges from 2-7 copies. CNV has been shown to some extent to be correlated to protein level and CNV of this loci has been linked to the inflammatory disease psoriasis (Hollox et al., 2008). A few beta-defensins are expressed constitutively, for example Human beta-defensin 1 (hBD1). While other beta-

defensins, such as Human beta-defensin 3 (hBD3) and Human beta-defensin 2 (hBD2), are inducible upon stimulation with bacteria or cell damage signals. Interestingly many beta-defensins are expressed in the male and female reproductive tract. The epididymis expression of beta-defensins is segmental and influences sperm maturation (Zhou et al., 2013).

In mice, the genomic arrangement containing the alpha-defensins is flanked by two beta-defensin regions. Mice have 27 beta-defensins, 26 cryptdin genes (defensin related) and multiple defensin pseudogenes. Mouse defensins are highly repetitive in nature with regard to their chromosomal position; this arrangement supports a positive diversifying-selection model of evolution (Patil et al., 2004, Patil et al., 2005). Unlike humans, mice have no neutrophil alpha defensins but they have multiple cryptdin alpha-defensins in the small intestine.

There are several published beta-defensin mouse knockouts. Two studies suggest that *Defb1* homozygous null mice retain *Haemophilus influenzae* in the lung, and *Staphylococcus* spp. in the bladder longer than wildtype mice. This implicates a role of *Defb1* in respiratory and urinary tract infection, resistance and pathogen clearance (Morrison et al., 2002, Moser et al., 2002). There has been direct evidence linking gut alpha-defensins to the modulation of microbiota in mice. Salzman et al., (2010) demonstrated that Paneth cell alpha-defensins contributed to mucosal host defence and regulate the composition of murine intestinal microbiota.

1.2.1.2 Beta-defensins

In humans, seven of the beta-defensin genes on chromosome 8 are copy number variable and five of these, *DEFB4* (encodes peptide hBD2), *DEFB103* (encodes hBD3), *DEFB106*, *DEFB105* and *DEFB107*, have a mouse orthologue (Table 1.1).

Murine Gene Name	Human Gene Ortholog	Human Protein Ortholog	Common Name
Defb1 (57%)	*DEFB1*	hBD1	Beta-defensin 1
Defb4 (45%)	*DEFB4*	hBD2	Beta-defensin 2
Defb12/ Defb35	*DEFB105*	-	
Defb13	*DEFB107*	-	
Defb14 (69%)	*DEFB103*	hBD3	Beta-defensin 3
Defb15/ Defb34	*DEFB106*	-	
Defa5	*DEFA5*	HD5	Alpha Defensin 5
-	-	HNP 1-3	Human Neutrophil Peptide 1-3

Table 1.1 Mouse and Human Orthologous Defensin Genes
Percentage of sequence identity between human and mouse at the protein level to the mature peptide are shown in parentheses.

Impaired stimulation of hBD2 and hBD3 has been characterised in Crohn's disease (Wehkamp et al., 2003, O'Neil et al., 1999). In addition, genome wide CNV profiling highlighted a predisposition to Crohn's disease with low hBD2 CNV (Fellermann et al., 2006).

Human beta-defensin 1 (hBD1) is not located within the copy number variable region on chromosome 8p23.1, and is ubiquitously expressed in human epithelia cells. Reduction of hBD1's disulphide bonds exposes its powerful antimicrobial activity against *Candida albicans*, (the opportunistic pathogenic fungus), *Bifidobacteria*, and *Lactobacillus* species (commensal Gram-positive bacteria) (Schroeder et al., 2011).

Murine beta-defensins are not copy number variable; however, they are contained within an extended locus of 27 beta-defensins and may demonstrate redundancy. Many human and mouse beta-defensins show epididymis-specific expression patterns. Human beta-defensin 126 (*DEFB126*) is an epididymis-specific secretory protein which has the ability to inhibit LPS-induced inflammation in macrophage cell lines (Liu et al., 2012). This could have a role in the female reproductive tract, where *DEFB126* in semen could suppress inflammatory response in the vaginal epithelium. Other HDPs also display this immunomodulatory activity in macrophage cell lines (discussed below).

A major site of beta-defensin expression is in the male reproductive tract of both humans and mice. Zhou et al., (2013) has shown that homozygous deletion of 9 beta-defensins on mouse chromosome 8 results in infertility in male mice. Infertile mice displayed reduced sperm motility, increased sperm fragility and increased spontaneous acrosome reaction. This is partly due to defects in sperm microtubule formation and consequently results in increased intracellular calcium content.

Many human and mice beta-defensins have chemotactic properties. hBD1, hBD2 and hBD3 are able to induce chemotaxis through CCR6 (Hoover et al., 2002, Oppenheim and Yang, 2005). Similarly, the mouse *Defb4* and *Defb14* genes, orthologues of genes encoding hBD2 and hBD3 respectively, also have chemotactic activity for CCR6-expressing cells (Rohrl et al., 2008, Rohrl et al., 2010).

1.2.1.3 Human beta-defensin-3 (hBD3)

DEFB103 gene, which encodes hBD3, has two exons; the first exon contains sequence for the 5'UTR and pre-protein, while the second exon contains the sequence for the mature protein. The six-cysteine motif spacing, which forms the di-sulphide bonds in hBD3, is different from the other defensins, namely hBD2 and hBD1. However, the general shape of these defensins is similar despite lack of identity between family members (Bauer et al., 2001). hBD3 is the most cationic and when folded has the ability to form symmetrical amphipathic dimers (Dhople et al., 2006); this is thought to be responsible for its salt in-sensitivity compared to other HDPs.

1.2.1.3.1 Expression and Regulation

hBD3 is found highly expressed in psoriatic skin (Harder et al., 2001) (where it was first isolated) but also in cells of the oral cavity, endometrium, placenta, and immune cells. A broad range of bacteria (Gram-positive and Gram-negative) in addition to pro-inflammatory cytokines such as IL-1β, TNF-α and INF-γ are able to induce/increase the expression of hBD3.

hBD3 in human keratinocytes is increased by bacterial challenge via stimulation of the epidermal growth factor receptor (EGRF). In gingival fibroblasts, hBD3 expression increases in response to infection with C*andida albicans* (Gursoy and Kononen, 2012). Oral squamous cells (Shuyi et al., 2011), gingival epithelial cells and dendritic cells (Yin et al., 2010) all show a marked increase in hBD3 in response to LPS treatment *in-vitro*.

In women, hBD3 and other defensins are known to show temporal expression patterns in the reproductive tract during the menstrual cycle; where higher levels of hBD3 are seen in the early and late secretory phase (King et al., 2003b, Das et al., 2007).

DEFB103 at the transcript level is inhibited by corticosteroids (Duits et al., 2001); these corticosteroids can also inhibit pro-inflammatory cytokines and cell surface markers (Barnes, 2006). The activity of hBD3 can be impaired through the direct inhibition and degradation of the protein. Saliva and serum can inhibit the microbicidal activity of hBD3 to Gram-positive and Gram-negative bacteria (Maisetta et al., 2005). hBD3 was also found to have reduced killing activity to Gram-positive bacteria in low pH environments (Abou Alaiwa et al., 2014). Cysteine proteases and streptococcal inhibitor complement produced by group-A Streptococcus (GAS) can also directly degrade hBD3 peptide (Cogen et al., 2010).

1.2.1.3.2 Antimicrobial and Immunomodulatory Properties

hBD3 is known for its potent antimicrobial activity against a broad spectrum of bacteria, fungi, and viral organisms. hBD3 can act on many Gram-negative and Gram-positive bacterial species including methicillin-resistant *Staphylococcus aureus* (MRSA) and vancomycin-resistant *Enterococci* (VRE) (Harder et al., 2001). The exact mechanisms of how hBD3 kills bacteria are not fully understood, but are thought to involve ionic interactions with the bacterial cell surface, blockage of bacterial biosynthetic pathways, and bacteria cell wall lipid interaction (Sahl et al., 2005). *Staphylococcus aureus* when treated with non-folded hBD3 shows rapid perforation in the exterior cell wall (Midorikawa et al., 2003). Folded proteins of

hBD3 also show a similar activity suggesting disulphide structure is not essential for the antibacterial mode of action (Harder et al., 2001).

hBD3 can supress biofilm production in single organisms of *Pseudomonas aeruginosa* and *Staphylococcus aureus,* but also biofilms of multiple-species (Zhu et al., 2013, Lee et al., 2013). Studies have shown that hBD3 not only represses the initiation and maturation of biofilms, but also represses those already established (Zhu et al., 2013).

hBD3 and *DEFB14* have potent anti-inflammatory effects on human and mouse primary monocyte derived macrophages. This action effectively inhibits the LPS-activated TLR4-induced TNF and IL-6 response, through both the MyD88 and TRIF pathways. This effect has been shown both *in-vitro* and *in-vivo* (Semple et al., 2010, Semple et al., 2011). hBD3 can act in synergy with other HDPs. For example, LL-37 and hBD3 have a combined effect reducing the LPS-induced secretion of cytokines in gingival cells (Bedran et al., 2014).

Semple et al., (2015) showed that hBD3 exacerbates the production of INF-β in response to polyI:C, a viral mimic and TLR-3 agonist, in both human and mouse primary macrophages. Conversely, the authors showed reduction of CXCL10 in response to this TLR-3 agonist in the presence of hBD3. This effect was also seen *in-vivo* where co-treatment of mice with hBD3 peptide and polyI:C enhanced the increase in INF-β, compared to polyI:C treatment alone. Using macrophages from knockout mice, Semple et al., (2015) went on to show that hBD3 suppressive effects were mediated by TICAM1 (TRIF in mouse), while the exacerbating effects were mediated by MDA5 (IFIH1 in mouse).

In addition, hBD3 can bind to CpG and self-DNA to form net complexes; these complexes are up-taken by pDCs and induce an INF-α response, acting as a TLR-9 agonist (Tewary et al., 2013). Such complexes are increased in patients with autoimmune disease (Gilliet and Lande, 2008).

1.2.1.4 Murine Orthologue of hBD3; Mouse *Defb14*

Mouse beta-defensin 14 (*Defb14*) has the highest sequence identity to hBD3 protein; sharing 69% sequence identity at the protein level. Multiple studies have confirmed similar activity of the human and mouse peptide suggesting they are functional orthologues (Rohrl et al., 2008, Semple et al., 2010).

Like hBD3, DEFB14 exhibits broad-spectrum antimicrobial activity. *Defb14* responds to INF-γ and TGF-α treatment in keratinocytes (Hinrichsen et al., 2008), which were also identified as stimuli of hBD3 in human keratinocytes (Harder et al., 2004). hBD3 and *DEFB14* have the same potent anti-inflammatory effects on human and mouse primary monocytes (Semple et al., 2010, Semple et al., 2011). Moreover, hBD3 and *Defb14* also have similar expression profiles in the female and male reproductive tract (King et al., 2003b, Hickey et al., 2013, Zhou et al., 2013, Garcia-Lopez et al., 2010)

1.2.2 Cathelicidin

1.2.2.1 Cathelicidin

Cathelicidins are cationic antimicrobial peptides, found mostly in neutrophils, keratinocytes and epithelial cells, which have a vital role in protecting against diseases and infections.

Multiple cathelicidins have been identified in mammals such as sheep, goat and pigs. However, rodents and humans have only one gene for cathelicidin. The gene encoding the sole human cathelicidin, *CAMP* is located on chromosome 3p21.3 and is comprised of 4 exons. The N-terminal and the coding regions of the first three exons, which include the cathelin and signal domain, are highly conserved. Exon 4 codes the antimicrobial peptide domain. The 16kDa preprotein, hCAP18, does not exhibit antimicrobial activity and can either be immediately cleaved, or stored as a proprotein in granules without the signal domain. Extracellular proteolytic cleavage of the C-terminal of hCAP18 by proteinases 3, or kallikrein generates the active LL-37 peptide (Sorensen et al., 2001, Yamasaki et al., 2006, Garcia-lopez et al., 2010).

The LL-37 peptide has cationic and amphipathic properties forming an alpha- helical structure.

Alternative microbicidal active forms of LL-37 have been reported in select environments (Sorensen et al., 2001, Sorensen et al., 2003, Murakami et al., 2004). These alternative fragments can be formed either by the additional degradation of LL-37 by host/bacterial proteases, or by alternative cleavage of the pro-protein. hCAP18 in seminal fluid can be processed by gastricsin derived from the prostatic gland to form an antimicrobial peptide of 38 amino acids (Sorensen et al., 2003). This peptide, ALL-38, has the same antimicrobial properties as LL-37 (Sorensen et al., 2003). Gastricsin cleavage only occurs at low pH, akin to what is seen in the vagina suggesting a mechanistic involvement preventing infection following sexual intercourse. LL-37 is found to have reduced killing activity to Gram-positive bacteria in low pH environments (Abou Alaiwa et al., 2014). Serine proteases in sweat can also degrade LL-37 into reduced fragments; KR-20, RK-31, and KS-30 (Murakami et al., 2004).

1.2.2.2 Expression and Regulation

CAMP gene expression is found at varying levels in many cell types; hCAP18/LL-37 is also present in many bodily fluids such as breast milk, sweat, saliva and vaginal secretions (reviewed in Durr et al., (2006)). *CAMP* is commonly upregulated in many immune and epithelial cells when challenged in infectious disease. Leukocytes and epithelial cells can rapidly release hCAP18/LL-37 molecules extracellularly following uncontrolled cell death, infection and degranulation (reviewed in Durr et al., (2006)). TLR activation and various cytokines can also directly upregulate *CAMP* gene expression (Mookherjee et al., 2006).

Upstream of the *CAMP* gene is a SINE repeat, which contains the putative Vitamin D response element (VDRE). This is the primary element that is bound by Vitamin D receptor (VDR) and responsible for the Vitamin D induced expression of *CAMP* in many cell and tissue types. This element is not highly conserved, and is absent in all other higher vertebrates including mouse.

Bacteria produce short chain fatty acids such as butyrate from fermentation of dietary fibres in the colon. SCFAs such as butyrate can also regulate the expression of *CAMP* gene (Kida et al., 2006). In the gut, SCFA's are mostly anti-inflammatory involved in promoting gut barrier function and homeostasis. SCFA's demonstrate anti-inflammatory function by inhibiting NF-Kb signally by the suppression of pro-inflammatory cytokines (Zeuthen et al., 2008, Segain et al., 2000). In contrast, SCFA's in the vagina show more of a pro-inflammatory response in those women with bacterial vaginosis (Mirmonsef et al., 2012, Aldunate et al., 2015). The difference in SCFA immune response could be inherent properties of the cell type, pH, and TLR ligand combination in the different environments (Mirmonsef et al., 2012).

Immune-Mediated Inflammatory Diseases

Chronic inflammatory disease has associations with dysregulation of the careful cytokine/chemokine homeostatic balance. Several HDP, including LL-37 are elevated in systemic lupus erythematosus (SLE) (Kreuter et al., 2011), and rheumatoid arthritis (RA) (Paulsen et al., 2002).

Some conditions are associated with a downregulation of hCAP18/LL-37. Morbus Kostmann is a condition where patients display reduced neutrophil counts and no LL-37 in granulocytes, these patients also commonly display severe periodontal disease (Putsep et al., 2002). Without treatment Morbus Kostmann patients die from bacterial infection in infancy. Patients treated with recombinant granulocyte colony-stimulating factor (G-CSF), retain reduced neutrophil defensins and absolute deficiency in LL-37. Crohn's, atopic dermatitis and chronic ulcers are all reported to be associated with a decrease in *CAMP* gene expression or hCAP18/LL-37 levels (Schauber et al., 2006, Sun et al., 2016, Reinholz et al., 2012).

Mice null for *Camp*, the murine orthologue of LL-37/hCAP18, have many inducible phenotypes; showing increased vulnerability to bacterial infections of the gastrointestinal tract (Chromek et al., 2012), urinary tract (Chromek et al., 2006), skin (Nizet et al., 2001), lung (Kovach et al., 2012), and eye (Huang et al., 2007).

The mechanisms for the anti-inflammatory and immunomodulatory activities of human and mouse cathelicidin are very complex. Involving such processes as, intracellular uptake, endocytic mobilisation and receptor interaction (reviewed in Choi et al., (2012). These mechanisms result in signalling pathways being altered and activation of various transcription factors.

Receptors

The most classic LL-37 receptor is formyl peptide receptor 2 (FRP2), but there are also others such as CXR2, EGFR, and P2X7 (De et al., 2000). Major downstream pathways of these receptors involve activation of protein kinases, the release of intracellular calcium, and NF-kB activation. Activation of these receptors and signalling pathways cause cell proliferation, mobilisation and cytokine release. These processes are important for the immunomodulatory activity of LL-37 in chemotaxis, angiogenesis and tissue repair (Carretero et al., 2008, Koczulla et al., 2003). The ability for LL-37 to cross the cell membrane where it can bind proteins, such as GAPDH intracellularly has also been shown to be an important factor in LL-37's immunomodulatory activity (Mookherjee et al., 2009). It has been shown that cells such as vaginal epithelial and placenta cells express the classic LL-37 receptor FRP2 (Dong and Yin, 2014, Frew, 2013), but it is unclear if this is the main receptor for the immunomodulatory properties of LL-37 in these cells (Frew, 2013).

1.2.2.3 Antimicrobial Properties

LL-37 like hBD3, is known for its broad-spectrum antimicrobial activity; acting on many Gram-positive, Gram-negative bacteria, viruses, and also on the yeast *Candida albicans* (reviewed in Vandamme et al., (2012)). LL-37 preferentially binds to bacteria where its antibacterial action involves disrupting cell membrane integrity using a toroidal pore carpet like mechanism (Oren et al., 1999, Henzler Wildman et al., 2003, Lee et al., 2011). This process involves LL-37 binding parallel to the membrane, where oligomers and monomers cause membrane strain and subsequent translocation into the periplasm. This process of LL-37 molecules translocating into the periplasm opens pores and causes leakage (Oren et al., 1999). Antifungal properties of LL-37 are based on interaction with fungal cell wall and membrane

ROS production (Rapala-Kozik et al., 2015). Antiviral properties of LL-37 have been shown by its ability to directly interact with the viral envelope (Currie et al., 2016). In addition, this peptide has shown strong inhibitory effects on the HIV-1 reverse transcriptase where it can inhibit HIV-1 replication in PBMCs and T-cells (Bergman et al., 2007).

Like hBD3, LL-37 has been reported to have anti-biofilm activity at sub-minimum inhibitory concentrations (MIC) of a number of organisms, namely, *Staphylococcus epidermidis* (Hell et al., 2010) *Staphylococcus aureus* (Mishra et al., 2016, Dean et al., 2011), *Pseudomonas aeruginosa* (Overhage et al., 2008) and *Escherichia coli* isolates (Kai-Larsen et al., 2010). This feature is not unique to all cathelicidins where the mouse peptide, CAMP, did not show anti-biofilm activity on *Pseudomonas aeruginosa* (Overhage et al., 2008). In addition to its activity against pre-establish biofilms, LL-37 peptide can also inhibit biofilm formation of *Staphylococcus aureus* (MRSA) (Dean et al., 2011). In animal *in-vivo* infection-models, LL-37 peptide prevents *Escherichia coli* and *Candida albicans* from adhering to the urinary tract cell wall, stopping subsequent biofilm formation (Chromek et al., 2006, Tsai et al., 2011).

1.2.2.4 Modulation of Inflammation/Infection

Chemotactic Properties

LL-37 can act as a direct chemoattractant for cell types including; neutrophils, iDCs, eosinophils, T lymphocytes and monocytes (Tjabringa et al., 2006, Soehnlein et al., 2008, Chertov et al., 1997, Wang et al., 1996). Tjabringa et al., (2006) showed that eosinophils and neutrophils are directly mobilised by LL-37 using a calcium chamber assay. Soehnlein et al., (2008) went on to show a direct LL-37-induced mobilisation of inflammatory-monocytes.

At and around the site of infection, low/modest physiological concentrations of LL-37 induces the secretion of chemokines such as IL-8. This process also indirectly recruits additional innate immune cells to the area. LL-37 induces secretion of these cytokines in innate immune cells such as macrophages, but also in epithelial cells

and fibroblasts (Bowdish et al., 2004, Montreekachon et al., 2011). IL-8 is a chemokine, which promotes the attraction of neutrophils, and along with LL-37 works to respond to the infection. After treatment with LL-37, primary monocytes can produce CCL20, CCL4, and CXCL1 *in-vitro* (Niyonsaba et al., 2010, Vandamme et al., 2012). LL-37 on macrophages can also up-regulate the expression of receptors including the IL-8 receptor, IL-8RB, and CCR2 (Scott et al., 2002). Human umbilical vein endothelial cells (HUVEC) and RAW cells also release CCL2 after LL-37 treatment, (Vandamme et al., 2012).

Chemokine/Cytokines	Alternative name	Receptor
CXCL8	IL-8	CXCR1,CXCR2
CCL2	MCP-1	CCR2
CXCL10	IP-10	CXCR3
CCL5	RANTES	CCR1, CCR3, CCR5
CXCL1	GROα	CXCR2
CCL4	MIP-1β	CCR5

Table 1.2 Chemokine/Cytokines and Receptor Nomenclature

Immune-cell Modulation

In addition to attracting immune cells to combat infection, LL-37 is capable of modulating their action once recruited to the site. In mast cells, LL-37 peptide causes increases of IL-4, IL-2, and IL-6, and also causes cell degranulation that results in histamine being released (Niyonsaba et al., 2001). This activity in mast cells has also been shown for hBD2 peptide (Niyonsaba et al., 2001, Niyonsaba et al., 2002). Histamine works as a 'alarmin' causing blood vessels to dilate; increasing capillary permeability, thus allowing more white blood cells to reach the site of infection/inflammation.

LL-37 can promote sensing of CpG motifs through TLR-9 from bacterial DNA in plasmacytoid dendritic cells (pDCs) and human B lymphocytes (Hurtado and Peh, 2010). This sensing is highly dependent on the structure and methylation status of the

CpG motifs. ODNs, which have a natural phosphodiester backbone (akin to human genomic DNA), can also elicit a similar response when un-methylated.

LL-37 increases the life span of neutrophils at the site of infection; suppressing neutrophil apoptosis via FPR2 and P2X7 receptor (Nagaoka et al., 2006). The effect of LL-37 on apoptosis in other cells shows an alternate effect, depending on the dose of peptide used. High concentrations of the peptide in lung epithelial cells promote apoptosis (Barlow et al., 2006), whereas suppression of apoptosis has been observed in primary human keratinocytes and HaCaT cells (immortalised human keratinocytes) (Chamorro et al., 2009).

Neutrophil extracellular traps (NETs) are shown to contain LL-37 (Ciornei et al., 2005) which is able to induce their formation and stabilisation (Neumann et al., 2014). Interestingly the bacterial killing properties of LL-37 when bound to NET DNA are diminished, suggesting it might be having an alternate role here.

LL-37 DNA Aggregates

LL-37 can bind to extracellular self-DNA fragments forming aggregates, which are taken up by pDCs. These aggregated particles enter pDCs through lipid-raft-mediated endocytosis and are retained in early endocytic compartments, which in-turn triggers a robust TLR-9 mediated interferon response (Gilliet and Lande, 2008). Gilliet and Lande, (2008) have subsequently shown hBD3 has the same properties to form DNA complexes. One study proposed that such activation of pDCs is central to the pathogenesis of SLE (Lande et al., 2011).

TLR Pathway Suppression

Apart from indirectly recruiting immune cells and directly inducing cytokines, LL-37 has other modulatory roles sensing signals from cell damage and pathogen associated molecular patterns (PAMPs). LL-37 like hBD3, in the presence of exogenous inflammatory stimuli has the ability to target inflammatory pathways such as NF-κB signalling by TLRs, supressing certain pro-inflammatory responses. LL-37 has a high affinity to LPS and is able to neutralise its inflammatory effects (Mookherjee et

al., 2006). RAW cells treated with LPS, a TLR4 agonist, release less TNF and NO when treated with LL-37, hence supressing inflammation (Scott et al., 2002).

Extracellular LL-37, and the mouse orthologue CAMP, can form complexes with LPS by directly binding to it; these complexes prevent LPS interaction with TLR-4 signalling molecules (Scott et al., 2000, Scott et al., 2011). The formation of these complexes is due to the physicochemical properties of LL-37/CAMP, such as its charge, helicity, amphipathicity and hydrophobicity. It has also been suggested that LL-37 can exhibit anti-endotoxic effects by binding the CD14 receptor directly, or by dissociating LPS oligomers; both mechanisms prevent binding to the LPS binding receptors (LBP) (Suzuki et al., 2011).

1.2.2.5 Wound Healing and Tissue Remodelling

As previously mentioned LL-37 can activate the FPR2 and P2X7 receptors on epithelial cells and fibroblasts. It is proposed that this results in a similar proliferative effect as EGFR activation. In endothelial cell lines, it has also been suggested that LL-37 acts on the FPR2 receptor to induce angiogenesis (Salvado et al., 2013). One study showed electroporation of a LL-37 plasmid in an ischemic hind limb model upregulated antigenic chemokines, and also reduced muscular atrophy (Steinstraesser et al., 2014).

1.2.3 HDPs and the Female Reproductive Tract

Cells in the female reproductive tract are a major source of multiple microbicides. Reproductive tract epithelial cells, cervical glands, and neutrophils generate a wide-range of HDPs that target viruses, bacteria and fungi, both directly and indirectly (Figure 1.6).

LL-37 is found at high levels in fetal skin, amniotic fluid, vaginal fluid and the vernix caseosa (reviewed in Yarbrough et al., (2015)). Steady state defensin expression is cell specific and compartmentalised in the female reproductive tract in

pregnant and non-pregnant women. hBD1-4 and human alpha defensin 5 (HD5) have all been reported to be expressed with distinctive temporal profiles in the endometrial epithelium, vagina and cervix (King et al., 2003a, Fleming et al., 2003, Quayle et al., 1998). The kinetics of this differential expression most likely reflects the differing immunological requirements along the length of the female reproductive tract.

In women, HDPs are known to show temporal expression patterns during the menstrual cycle (King et al., 2003b). The mechanism of menses shares many characteristics of acute inflammatory processes, involving localised increase in pro-inflammatory cytokines, prostaglandins, and leukocyte migration. In women, hBD3 is higher in the early and late secretory phase of the menstrual cycle (Fleming et al., 2003). Hickey et al., (2013) found that in non-pregnant mice *Defb14* also had specific estrus cycle mRNA expression profiles in the vagina and uterus. Like hBD3, LL-37 is not uniformly expressed throughout the cycle. Mice null for *Camp*, the murine orthologue of LL-37/hCAP18 have increased susceptibility to bacterial urinary tract infections (Chromek et al., 2006). *Defb1* homozygous knockout mice also have increased susceptibility to urinary tract infections whereby they were shown to retain *Staphylococcus* spp. in the bladder longer than wildtype mice (Morrison et al., 2002).

Like LL-37, multiple alternative fragments of hBD1 with varying amino-acid termini have been found in the human reproductive and urogenital system (Valore et al., 1998, Zucht et al., 1998, Valore et al., 2002). These alternative forms have been isolated in vaginal lavage fluids and urine, where they appear to have different levels of antibacterial activity under specific conditions (Zucht et al., 1998).

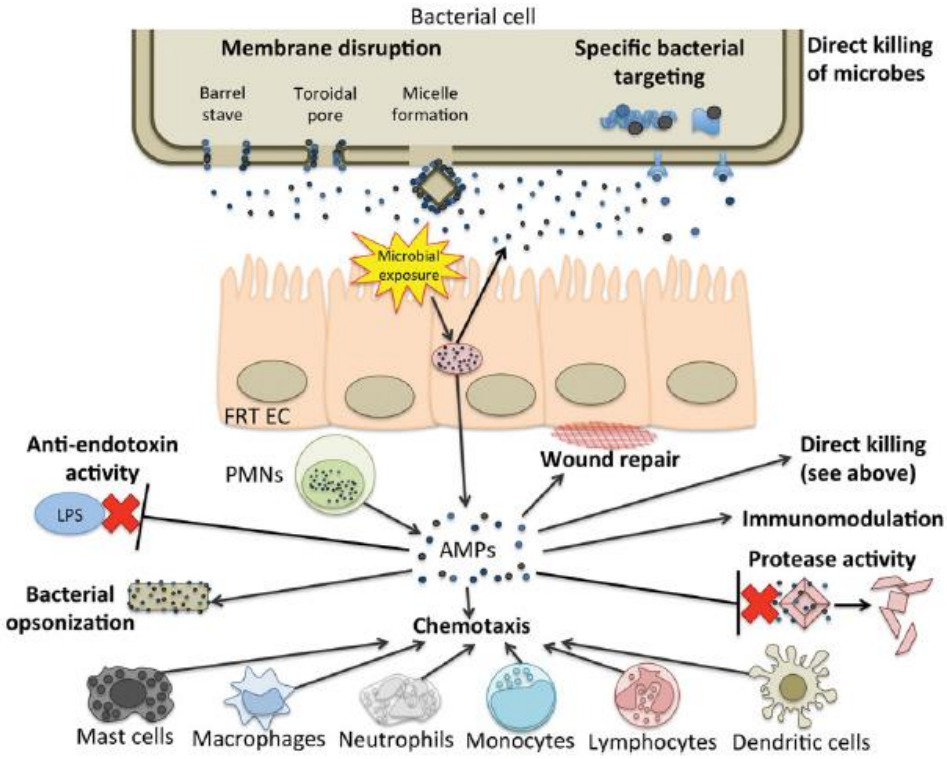

Figure 1.6 Mechanisms for HDPs in Epithelial Cells of the Female Reproductive Tract

Mechanisms for HDPs in female reproductive tract epithelial cells (FRT EC). HDP have potent microbicidal activity against a broad spectrum of bacteria, they can supress the inflammatory process by binding and blocking receptors but also directly binding to bacterial pathogens. They also influence immune response by attracting inflammatory cells, inducing an inflammatory state, modulating apoptotic cell death and cell degranulation. HDPs play a role in tissue homeostasis; including the induction of angiogenesis. Source: Yarbrough et al., (2015)

1.2.4 HDPs and Preterm Labour

The development of preventative therapies for preterm labour requires a mechanistic understanding of how the pro-inflammatory profile is induced. HDPs have been shown to have multiple roles in this pro-inflammatory process.

Researchers have found that an immune genotype variation in human *DEFB1* may contribute clinically to women who deliver preterm (James et al., 2013). This retrospective genotyping study highlighted rs1799946, a SNP in *DEFB1*, to be associated with a doubled risk of preterm delivery and four-fold increase in the risk of extreme preterm delivery (<28 weeks) (James et al., 2013). A second SNP, rs1047031, was found to be protective. However, a larger GWAS study, which included a different SNP in the *DEFB1* gene, failed to highlight an association of this locus to preterm labour (Uzun et al., 2013).

Women with elevated concentrations of cervicovaginal HNPs at 24-29 weeks of gestation have a greater risk of delivering preterm (before 32 weeks) (Balu et al., 2003). Further work on human extra-placental membrane in *ex-vivo* cultures has shown increased hBD2 in the amnion when the choriodecidua were exposed to group B streptococcus (GBS) (Boldenow et al., 2013).

An *in-vitro* study on human gingival fibroblasts found that hBD3 is pro-inflammatory and increases both COX-2 expression and prostaglandin E2 (PGE_2). COX-2 is an inducible labour associated gene, which is expressed at term labour in the human myometrium and also in rabbit cervical fibroblasts (Sato et al., 2001). The importance of this effect in cervical and myometrial stromal fibroblasts in mouse and human has yet to be determined.

As previously discussed, the active form of Vitamin D is a potent inducer of *CAMP*/LL-37. LL-37 is upregulated by Vitamin D in placental explants and primary human trophoblasts in a dose-dependent manner (Liu et al., 2009). This response is similar to that observed in primary cultures of human macrophages (Martineau et al., 2007). hBD2 but not hBD3 also shows a similar Vitamin D response in keratinocytes (Wang et al., 2010).

1.3 Mouse Models of Preterm Labour

Nearly 40% of preterm deliveries are associated with intrauterine infection (Romero et al., 2006). Mouse preterm labour models have focused on stimulation with agents to create an infection and/or inflammatory state; such as heat-killed *E.coli*, heat killed bacteria, LPS, group B streptococci (GBS), Lipoteichoic acids (LTA), TNF and IL-1β (Elovitz et al., 2003). Stimulation of the TLR4 pathways with LPS has been the central method of invoking preterm labour in animal models (Table 1.3). Live and heat-killed bacteria have also been used for preterm-labour models, however the reproducibility has been reported to be low (Reznikov et al., 1999). In humans, amniotic fluid cultures from most preterm births are negative for bacteria (Romero et al., 2007), although amniotic inflammatory cytokines and LPS binding proteins have been shown to be increased (Gardella et al., 2001). This lack of bacterial detection could be due to the limitations of the culture-dependent detection method. There is however, evidence to support signal transduction to the amnion when the choriodecidua is stimulated with bacteria (Boldenow et al., 2013), this could account for the increase in inflammatory response in the amnion without direct bacterial invasion.

The mode of agent administration has a large impact on the immune response mounted against the endogenous stimulating agent in animal models; intravaginal (i.vag), intraperitoneal (i.p) intracervical (i.c) intrauterine (i.u) have all been used as routes of administration.

The i.p model of preterm labour most likely mimics that associated with sepsis and severe bacteraemia (Elovitz et al., 2003). As most women with preterm labour do not present with elevated white blood cells or symptoms of illness, a localised model of inflammation at the maternal-fetal interface would likely recapitulate what is seen in women. In addition, systemic models of induced preterm-birth in mice are highly variable, with high incidence of maternal morbidity (Aisemberg et al., 2013).

A more recent model for preterm labour involves intrauterine (i.u) administration of an agent; this involves performing a mini-laparotomy in the late stage of pregnancy

to expose the gestational uterine horn and inject between two fetal sacs. Administering LPS using this method is reported to induce high preterm labour rates while maintaining low maternal mortality. However, the biological relevance of delivering a bolus of purified LPS into the uterus in the hope of mimicking human ascending bacterial infection could be questioned.

There has been one study that used medical endoscope to navigate through the murine cervix to administer infectious agents (Reznikov et al., 1999), however, due to the dense mucus plug and small opening, results were highly variable and others have failed to replicate this method.

Reznikov et al., (1999) developed a mouse model of infection/inflammation-induced preterm labour by injecting *E.coli* intracervical (i.c) in pregnant mice. In this model, the expression of fetal and/or maternal cytokines was demonstrated to up-regulate a number of uterine factors such as prostaglandin hormones, prostaglandin receptors and matrix metalloproteinases, which leads to premature initiation of parturition.

There has been some work on an intravaginal (i.vag) model of preterm labour, where the agent is applied distal to the cervix and causes preterm labour by transcending the cervix and/or through signal transduction (Gonzalez et al., 2011b, Gonzalez et al., 2011a). The mucus plug during pregnancy is very dense and the quantity of agent breeching this barrier is likely to be small, therefore higher loads of agent are needed.

There is variability across animal studies which use LPS as the inflammatory agent, this could be due to several compounding factors, such as serotype of the LPS used (Migale et al., 2015). The gestational age at which LPS is administered to induce preterm labour is also a factor in animal models as early administration can lead to resorption (Aisemberg et al., 2013).

Reference	Route	Conc.	Mouse Strain	n =	Gestation	PTB	Time-points/ Comments
Reznikov et al., (1999)	Intracervical	5mg/kg LPS	CD1, HS, C57BL, IL-1β-/-(C57BL)	100% n=56 total	14/15	48hrs	Controls taken 24hr after administration
Reznikov et al., (1999)	Intracervical	*E.coli* 10^4	CD1, HS, C57BL, IL-1β-/-(C57BL)	60-75% n=34 total	14/15	48 hrs	Controls taken 24hr after administration
Burd et al., (2011)	Intrauterine	250µg/mouse LPS	CD1	N/A	18.5	6 hrs	Culled after 6 hrs
Gonzalez et al., (2011b)	Intravaginal	250µg/mouse LPS	C57BL6	94.7%	15	36 hrs	
Salminen et al., (2008)	Intraperitoneal	25µg/mouse	C57BL6 FVB	58% -38%	16/17	17 hrs	Less than 20µg/mouse no PTL
Sykes et al., (2013)	Intrauterine	20µg/mouse	CD1	100%	16	7.7hrs	No pup survival >10µg
Sykes et al., (2013)	Intrauterine	2.5µg/mouse	CD1	100%	16	48 hrs	
Wakabayashi et al., (2013)	Intraperitoneal	100µg/kg	C3H/HeN		15.5	72 hrs	
Rinaldi et al., (2015)	Intrauterine USS guided	20µg/mouse	C57BL6	6/7	17	36 hrs	No pup survival 6/7

Table 1.3 Animal Models used to Study Infection/Inflammation-induced Preterm Labour
Summary of literature using *in-vivo* models of TLR-4 stimulation to induce preterm labour

1.4 Microbiome

Researchers have often quoted that the numbers of microbial cells in the human body easily out-number the human cells 10:1. New data suggested this was a vast overestimate and the number of human and bacterial cells in an average adult male is actually about equal 1:1 (Sender and Milo, 2016). Nonetheless, bacterial cells offer a plethora of microbial genes, providing important metabolic functions that have specific selections based on co-adaptions.

The term ‘Microbiome’ refers to the full composition of genetic material of all the microorganisms in a community. This includes the widely reported prokaryotic entities but also eukaryotic, archaea and viral organisms, more frequently being referred to as the ‘virome’. This thesis interrogates the prokaryotic organisms of the microbiome using the general term bacteria.

Bacteria are an essential part of human health; they break down un-digestible food fibres, and also provide a source of Vitamin K and Biotin. Many selections in the bacterial gene complement can be induced by alterations in the host-environment, such as antibiotic exposure (Langdon et al., 2016), dietary changes (Aron-Wisnewsky and Clement, 2016) and hormone regulation (Sudo, 2014). Selective metabolic functions also occur in other animal species. Rodents lacking exposure to microorganisms (germ free) display severely stunted growth, reduced cardiac output, reduced cell proliferation and other pathologies (Schwarzer et al., 2016, Blanton et al., 2016).

The majority of the time the relationship between host and bacteria is synergistic, existing in perfect homeostasis. However, disruptions or aberrations in this relationship can sometimes cause pathologies and disease. Pathogenic microorganisms are not the only causes of disease; disruption in commensal bacteria that are typically held in check by the microbial network and host immune defence factors can also be causative.

Recent studies have provided evidence that some inflammatory diseases can be caused or associated with community disturbance, often referred to as dysbiosis (Srinivasan and Fredricks, 2008, Carding et al., 2015).

The ‘hygiene hypothesis’ suggests that, reducing the diversity of pathogens humans are exposed to in early childhood leads to defects in the establishment of normal immune tolerance (Strachan, 1989). This causes an increase in susceptibility to allergic diseases such as asthma and hay fever (Strachan, 1989), but also autoimmune and chronic inflammatory diseases such as type 1 diabetes and multiple sclerosis (Bach, 2002).

Historically much of our understanding of the human microbiome had come from culture-based approaches, but as many human-associated bacteria are not easily cultivable, culture-independent approaches such 16S rRNA gene sequencing are becoming ever important. The bacterial 16S Ribosomal RNA gene is approximately 1500bp and consists of nine hyper-variable regions (V1-V9), that when sequenced can be used to identify bacteria taxonomy to the species or genus level. The Human Microbiome Project is an initiative which, using high throughput technologies, aims to characterise the microbiome across body sites associated with both health and disease (Peterson et al., 2009).

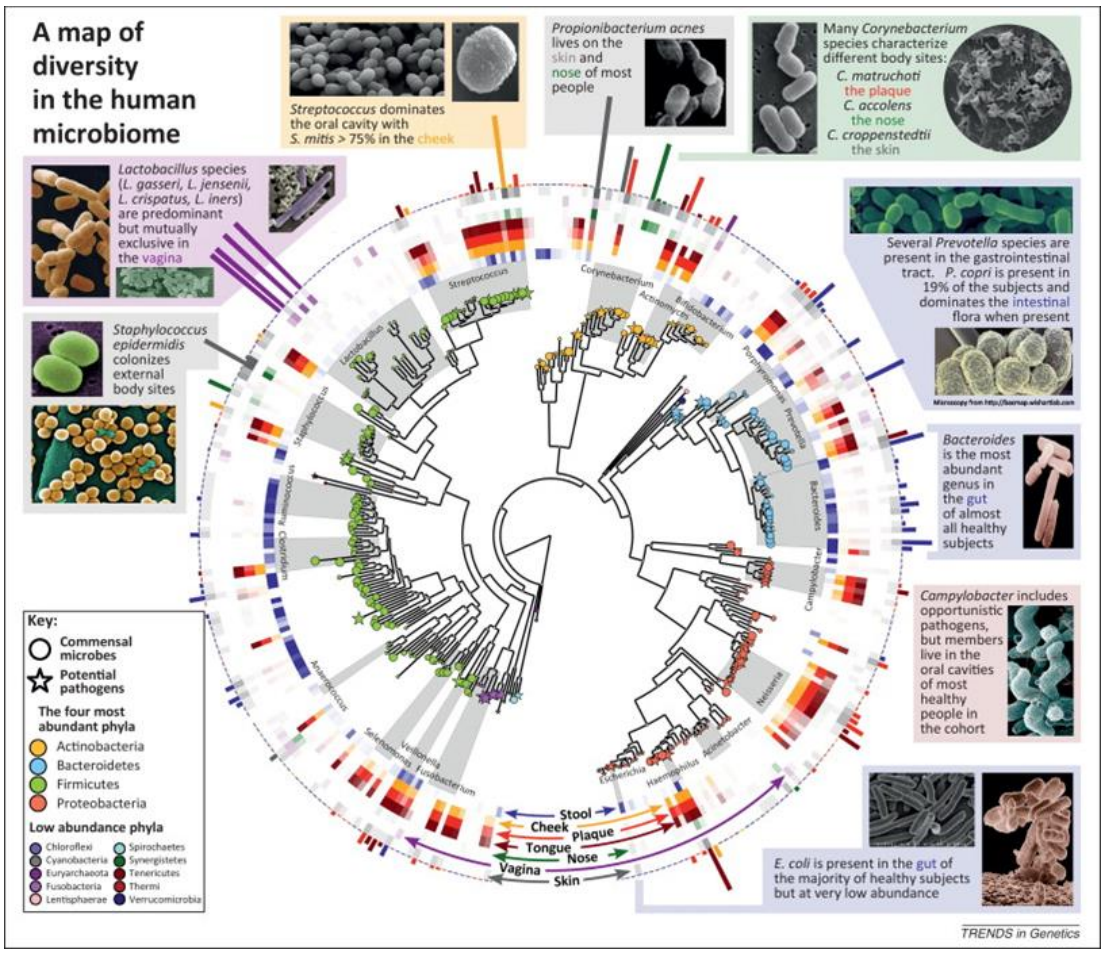

Figure 1.7 Human Microbiome Diversity
Phylogenetic tree of the common human phyla found at various body sites. The coloured rings are coded by body site and the height of the bars are proportional to the relative abundance at each site. Source: Morgan et al., (2013)

Both culture-independent and dependent approaches have widely established that humans are dominated by just 4 main phyla (*Bacteroidetes*, *Firmicutes*, *Actinobacteria* and *Proteobacteria*), which show site-specific distributions (Dethlefsen et al., 2007) (Figure 1.8). The highest bacterial load in humans and animals is in the colon, whereas the bacterial load in the vagina is much lower. The relative abundance at the phylum level within body sites tends to be consistent between individuals. For instance, multiple large studies show the healthy human

colon is dominated by *Bacteroidetes* and *Firmicutes* (Dethlefsen et al., 2007, Lay et al., 2005, Eckburg et al., 2005). The composition in the vagina at the phylum level shows a little more variation, most women are dominated by just *Firmicutes* in the vagina, but some women have a dominance of *Actinobacteria* phyla (Dethlefsen et al., 2007).

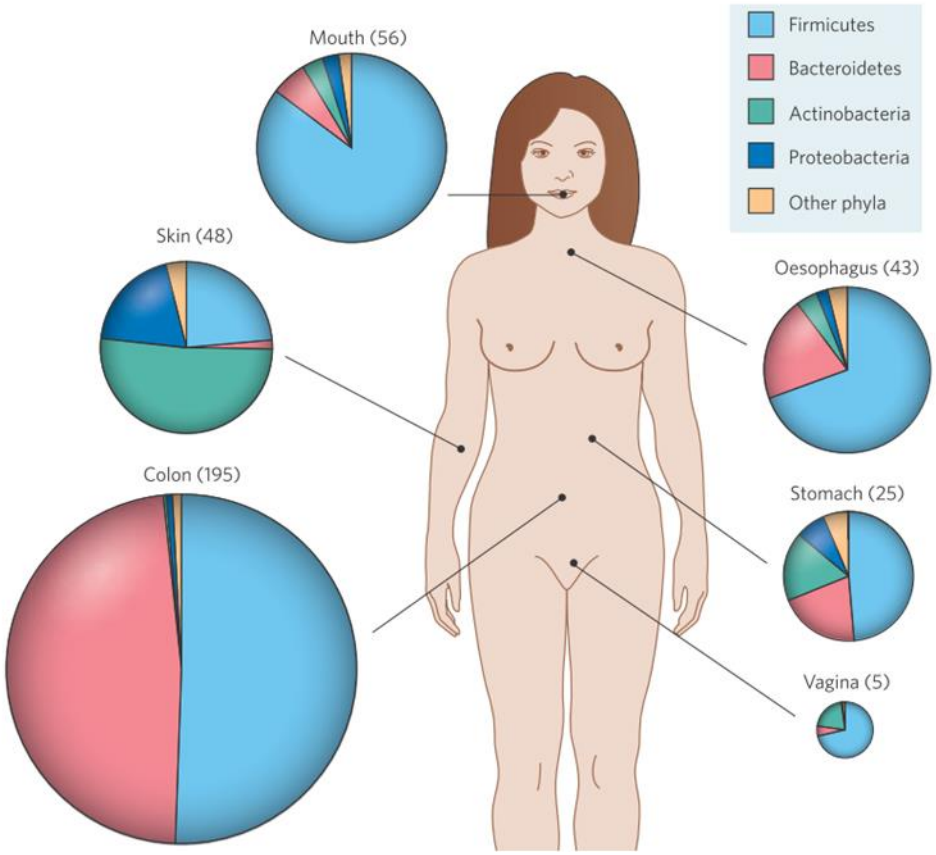

Figure 1.8 The Human Microbiome; Site Specific Distribution of Phyla
Coloured proportions represent the percentage of each 4 main phyla found in different body-sites as determined by 16S rRNA gene sequencing (n=11 women). The area of the pie chart somewhat represents the bacterial load, the number in parentheses shows the mean number of phylotypes (approximated species level taxa). Source: Dethlefsen et al., (2007)

1.4.1 The Vaginal Microbiome

1.4.1.1 Vaginal Microbiome Development

The mode of delivery (caesarean or vaginal) has impact on the baby's whole-body biota, including the gastrointestinal tract, skin and first colonisation of the baby's reproductive tract (Dominguez-Bello et al., 2010).

Through childhood, the vaginal microbiota is sparsely populated with a variety of anaerobic bacteria, with few or no *Lactobacilli* spp. (Hammerschlag et al., 1978, Hill et al., 1995). In adolescence estrogen levels rise and *Lactobacilli* spp. become more prevalent while anaerobic populations begin to diminish (Thoma et al., 2011, Alvarez-Olmos et al., 2004). At reproductive age, estrogen cycling stimulates the thickening of the vaginal epithelium and in turn glycogen production, which is when *Lactobacilli* spp. become most abundant. *Lactobacilli* spp. help to maintain low pH by metabolising glycogen to produce lactic acid (Linhares et al., 2011). There is evidence that amylase is a key component in this process by breaking down glycogen into smaller components for *Lactobacillus* spp to metabolise (Spear et al., 2014). At menopause estrogen levels decline, the vaginal epithelium thins, *Lactobacilli* spp. diminish and anaerobes become more prevalent again (Muhleisen and Herbst-Kralovetz, 2016). This is akin to the adolescent microbial profile suggesting a strong hormonal factor in driving microbial composition.

1.4.1.2 Vaginal Microbiome Stability

Most of our understanding of the vaginal microbiome has come from reproductive age women; fewer studies have been done on the stability of the vaginal microbiome in childhood or post-menopause.

In a large study Ravel et al., (2011) recruited 396 healthy women across 4 ethnic groups, and sequenced their vaginal bacteria to assign taxonomic species. Bacterial profiling in these 396 women confirmed variability of bacterial at the phyla level between individuals. However, hierarchal clustering at the species level showed the bacteria complement could be classified into so-called community state types (CST),

of which there are 5. These community state types are defined by the dominance or absence of certain *Lactobacillus* spp. (Table 1.4). Ravel et al., (2011) concluded at 95% confidence that women in North America will fit into one of these community state types. Nonetheless, it still remains that one in every 20 women will not have a bacteria profile which fits into one of these 5 groups.

Community State Type Group	Dominant Bacteria/ Defining Feature
Group I	*Lactobacillus crispartus*
Group II	*Lactobacillus gasseri*
Group III	*Lactobacillus iners*
Group IV	Little/no *Lactobacillus* spp., *Atopobium, Prevotella, Sneathia, Gardnerella*
Group V	*Lactobacillus jenseni*

Table 1.4 Human Vaginal Community State Types (CST)
Vaginal community state type group of reproductive age women. Summary as described by Ravel et al., (2011)

CST IV, which is a group defined as having very little *Lactobacillus* spp., is interesting concerning vaginal homeostasis. Women with CST IV have a high Nugent score (Gram stain scoring system from vaginal swabs) because of the lack of *Lactobacilli* spp., however they are reported healthy and have not presented with symptomatic Bacterial Vaginosis (BV), which is dysbiosis of the vaginal microbiota. This is interesting as it highlights that the metabolic functions of bacteria in the vagina are most likely conserved. *Lactobacillus* spp. are not the only bacteria to produce lactic acid; *Streptococcus* spp. and *Megaspherea* spp. are also lactic acid producing bacteria (LAB). Community sate types vary across ethnic groups (Ravel et al., 2011); CST IV has a more frequent occurrence in black and Hispanic populations, which interestingly is also the ethnic group which displays the highest incidences of BV and PTL (Burris et al., 2011, Ness et al., 2003).

Longitudinal sampling (16 weeks) of women's vaginal bacteria show that CST is not a stable trait (Gajer et al., 2012). Women can transition between CST; some shifts are temporal and consistent but others are more permanent. What factors are responsible

for driving these dynamic shifts remains to be determined. It is likely that estrogen, mechanism of menses, host genetics, microbicides and environmental factors all might play a role. Knowledge of CST kinetics is important because each community state type might differ in a risk to invasive diseases. A women's relative risk therefore might be a factor of the duration spent in the more vulnerable community state types or transitioning between them.

1.4.1.3 Vaginal Microbiome Dysbiosis

Bacterial Vaginosis (BV) is a dysbiosis of the normal proportions of commensal microbial species in the vagina, commonly shifting towards a depletion of *Lactobacilli* spp., which are proposed to be the protective species in the healthy vagina. BV affects 30% of women of reproductive age, has a high rate of reoccurrence and is associated with a high risk of secondary infections (Lambert et al., 2013).

Bacterial Vaginosis is a disease associated with increased inflammatory cytokines in cervicovaginal secretions and mucosal epithelial cell damage (reviewed in Kumar et al., (2011)). It has been proposed that this damage to the vaginal epithelial surface may play a role in the increased susceptibility of women with BV to sexually transmitted secondary infections/disease such as *Neisseria gonorrhoeae*, *Chlamydia trachomatis* and HIV (Taha et al., 1998, Wiesenfeld et al., 2003). A recent study suggests that the shedding of epithelial cells seen in patients with BV may be caused by a single organism, *Gardnerella vaginalis* (Gilbert et al., 2013).

Genetic variation in immune-regulatory genes such as TLR-4, TLR-9, IL-8, IL-6 and TNF are associated with incidences of BV, suggesting host-immune genotype is important in the disease (Royse et al., 2012, Macones et al., 2004).

The standard treatment for BV in the UK is a course of oral/intravaginal antibiotics, commonly metronidazole or in some cases clindamycin. As most women following this treatment course will clinically present with recurrent BV, metronidazole is partly ineffective as a treatment (Menard, 2011).

1.4.2 Vaginal Microbiome in Pregnancy

Using bacterial 16S rRNA gene sequencing Aagaard et al., (2012) compared the vaginal microbiome of pregnant women to those women not pregnant. Aagaard et al., (2012) showed that the pregnant bacterial complement is different, being less diverse to those women not pregnant. Romero et al., (2014) sampled women through pregnancy and classified their community state types as described by Ravel et al., (2011). The authors found the vaginal community of pregnant women differed to that of non-pregnant women; having a higher abundance of *Lactobacillus vaginalis*, *Lactobacillus gasseri*, *Lactobacillus crispatus*, and *Lactobacillus jensenii*. CSTs in pregnant women were also more stable than non-pregnant women; showing less CST shifts, which rarely included CST IV (group with little *Lactobacillus* spp.).

MacIntyre et al., (2015) included vaginal samples taken after delivery and showed the postpartum community has a rapid decrease in *Lactobacillus* spp. The authors displayed *Prevotella* and *Anaerococcus* spp. were increased in replacement of the diminished *Lactobacilli* in a high proportion of postpartum women. It was proposed the quick drop in estrogen levels postpartum is causing this alteration in community structure.

1.4.2.1 Bacterial Vaginosis in Pregnancy

Although not generally a reportable disease, the occurrence of BV in pregnancy has been estimated to be around 50% (Nelson and Macones, 2002). There have been many studies that link dysbiosis of the vaginal microbiota, clinical BV and preterm labour (Gravett et al., 1986, Svare et al., 2006). BV identified before 20 weeks gestation has been indicated in preterm delivery and chorioamnionitis (Svare et al., 2006). There is increasing support that certain prophylactic antibiotics given very early in pregnancy to those women who have a clinical diagnosis of BV has benefit (Thinkhamrop et al., 2015).

Bacterial vaginosis is associated with lower vaginal concentrations of hBD3, but not hBD2 or HNP-3, in pregnant women (Balu et al., 2003, Mitchell et al., 2013). Interestingly, maternal Vitamin D deficiency is associated with BV in the first

trimester of pregnancy, and Vitamin D can induce hCAP18/LL-37 and hBD2 gene expression in multiple cells (Wang et al., 2004b).

1.4.2.2 Vaginal Microbiome and Preterm Labour

Many bacterial species have been isolated from the amniotic fluid, placenta and chorion/amnion from pregnancies that have delivered preterm. The most common species observed are commensal bacteria from the lower genital tract and bacteria associated with bacterial vaginosis. Other bacteria such as those associated with STI's and the gingival cavity have also been isolated from amniotic samples (Han et al., 2004, Mitchell et al., 2013).

Hyman et al., (2014) studied the vaginal microbial diversity of women at high and low risk of preterm labour. The authors concluded that there were differences in the overall diversity between the two risk groups; showing a correlation between high alpha diversity and preterm labour (Hyman et al., 2014). As previously mentioned the type of material used in a cervical cerclage can have an impact on the vaginal microbiome (Kindinger et al., 2016). Using braided sutures over monofilament sutures increases the risk of women developing vaginal dysbiosis, inflammation, and preterm labour (Kindinger et al., 2016). Taken together, this supports the hypothesis that infection-induced preterm labour is associated with vaginal disruption of commensal bacteria as well as invading pathogens.

1.4.3 Modulation of Vaginal Microbiome

Vaginal *Lactobacilli* dominance in reproductive age women could be a protective mechanism to reduce pathogenies in the newborn infant. A baby's first whole-body microbiome is highly correlated with the organisms exposed to at the peri-partum period. Those babies born by caesarean-section have microbiota resembling the mothers' skin, whereas those born by natural delivery have microbiotas resembling the mother's vagina. Multiple studies suggest that caesarean-section babies have a higher incidence of allergic disease such as asthma, where the incidence was 20%

higher in caesarean section children (Sevelsted et al., 2016, Sevelsted et al., 2015). Caesarean section babies also pick-up more MRSA infections following birth than vaginally delivered babies (CDC, 2006).

If the types of microbes in the mother's vagina are pathogenic at the time of delivery, these can also be passed on to baby. *Lactobacillus* dominance during pregnancy could therefore have selective protective effects. Indeed as previously mentioned, Romero et al., (2014) had shown that Community state type IV (group defined by little/no *Lactobacillus* spp.) transition and occurrence was rarely seen in pregnant women.

Probiotics have been considered as a therapy to colonise the vagina, by preventative prophylaxis or to treat dysbiosis/pathogenic infection. Probiotics have the ability to, selectively displace pathogenic organisms, provide metabolic compounds of different kinetics, and directly compete with the resident bacteria. *In-vitro* studies have shown that *Lactobacillus* spp. can disrupt biofilms of common BV associated bacteria and inhibit the growth of urogenital pathogens including yeast. Clinical studies have taken *Lactobacillus* spp. probiotics into women as a therapy for BV (Bradshaw and Brotman, 2015). The most promising *Lactobacillus* spp. in these studies is *Lactobacillus rhamnosus* GR-1, and *Lactobacillus reuteri* RC-14 (Martinez et al., 2009). Studies have shown that orally administered *Lactobacillus rhamnosus* GR-1, and *Lactobacillus reuteri* RC-14 can be recovered from the vagina (Reid and Burton, 2002), highlighting possible fecal-vaginal transfer of microorganisms. Combinations of these bacteria are currently sold as oral live-cultures to promote urogenital microbial health.

1.4.4 Murine Vaginal Microbiome

Animals offer researchers a vital tool by providing a model to test out host-microbiome interactions under controlled environmental conditions. They also allow for infectious models that help understand pathogenicity. Mice are used in many

reproductive tract disease investigations, such as humanised mice as a model to study vaginal transmission of HIV (Deruaz and Luster, 2013).

There has been very little work done on the commensal bacteria of the mouse reproductive tract, presumably due to its extremely low bacterial load and dependency on microbial burden in each animal facility.

Previous bacterial species identified to reside in the murine reproductive tract has been through culture-dependent techniques (Noguchi et al., 2003). More work has focused on colonisation and clearance of exogenous bacteria both in a probiotic approach and in infectious models (Reid and Burton, 2002, Meysick and Garber, 1992).

There is very little known about the species level richness of bacteria that colonise the murine vaginal mucosa. Publications that use techniques such as qPCR and culture-dependent methods have shown that in contrast to humans, only a small percentage of female mice harbour *Lactobacillus* species at the vaginal mucosa (Noguchi et al., 2003, McGrory and Garber, 1992). Such culture-dependent studies listed *Streptococci*, gram-negative rods, *Bacteroidaceae* and *Staphylococci* as found in the non-pregnant vagina, however, these observations were not consistent and were highly variable (Noguchi et al., 2003).

MacManes (2011) conducted a study looking at two different strains of wild mice, one known to be promiscuous and the other monogamous. By using 16S rRNA gene cloning and sanger sequencing MacManes (2011) showed that there was a greater degree of diversity in the vaginal bacteria of the promiscuous strain of mice.

After review of the literature, only one study attempts to categorise the vaginal microbiome of lab animals using high throughput16S rRNA gene sequencing (Barfod et al., 2013). Barfod et al., (2013) study highlighted that the vaginal community of BALB/c mice is highly variable. Although the authors only had n=8 samples they showed the vaginal community had two sub-clusters. One sub-cluster appeared to be closely related to the lung microbiota, whereas the other sub-cluster did not show similarity to either of the other two sample sites the authors

investigated (lung and cecum). *Streptococcus* (Gram-positive) was attributed to the separation of the two clusters; the authors also listed *Acinetobacter, Sphinogmonas, Enterococcus* and *Polaromonas* as genera from the vaginal mucosa.

1.4.5 The Gut Microbiome

Microbes in the gut are essential for the break down of complex carbohydrates where they can manipulate host metabolism by altering nutrient availability. The presence and abundance of each bacterial group is fundamental since different species differentially metabolise these nutrients.

The stomach has the lowest bacterial loads of the gastrointestinal tract, where stomach acids maintain low bacteria numbers, the load then increases further from the stomach as pH levels become less acidic and more favourable for anaerobic growth. The mammalian gastrointestinal tract is dominated by two main phyla, *Firmicutes* and *Bacteroidetes.* Shifts in the ratio of these two phyla have been observed in many conditions such as obesity (Ley et al., 2006, Ley et al., 2005). Diet, age, host genetics, and local immune defence also influence on the community composition of these phyla (Mariat et al., 2009, Ussar et al., 2015, Salzman et al., 2007). The Human Microbiome Project is an initiative which, using high throughput technologies, aims to characterise the microbiome across body sites associated with both health and disease (Peterson et al., 2009).

The gut epithelium, as the outermost single cell layer of the gut, secretes many antimicrobial peptides including LL-37, defensins, but also S100 proteins, and C-type leptins. Speciality cells such as Paneth cells also selectively secrete HDPs such as the human alpha defensin 5 (HD5) and human alpha defensin 6 (HD6). Interestingly HD6 has the ability to polymerize forming nanonets that are believed to prevent bacteria translocating across the gut wall (Chu et al., 2012). These Paneth cell defensins have also been shown to have anti-viral properties (Wang et al., 2013, Hazrati et al., 2006).

Gut epithelia cells have multiple pattern recognition receptors, including the transmembrane TLRs, and also intracellular NOD receptors (Lavelle et al., 2010). These pattern recognition receptors are not uniformly expressed along the gastrointestinal tract. This is most probably a co-adaption strategy, to allow host tolerances of commensal and mutualistic species. For example in the gut, in a steady state, the numbers of TLR-4 and TLR-2 molecules are reduced, whereas TLR-3 (viral ligand) and TLR-5 (flagellin ligand) are more abundant. Another co-adaption strategy to allow tolerances of commensals is the mucus barrier; this layer reduces the ability of the effector molecules to sense bacteria. The colonic mucus barrier has two constantly renewing layers; the innermost is predominantly kept sterile.

Germ-free mice have shown that bacteria are essential for the development of normal gut epithelium. The major adaptor molecule MyD88 is essential for signalling via TLRs. The gut epithelia of MyD88 knockout mice show abnormal development (Frantz et al., 2012) and mice are consequently more susceptible to DSS colitis (Araki et al., 2005). This was supported in a conditional MyD88 knockout which displayed down regulation of mucus genes, antimicrobial peptides, and had compromised antibacterial immunity (Frantz et al., 2012).

In the absence of infection and inflammation beta-defensins in humans and mice are not prominently expressed in the small intestine, although in the colon beta-defensins have been shown to be important (Meyer-Hoffert et al., 2008).

Crohn's and IBD are linked to key deficiencies in HD5 and HD6 Paneth cell function (Wehkamp and Stange, 2010). Impaired induction of hBD2 and hBD3 have also been characterised in Crohn's disease (Wehkamp et al., 2003, O'Neil et al., 1999). Genomic variation in several defensin genes have been linked to the disease. Genome wide CNV profiling highlighted that low hBD2 copy number predisposes to Crohn’s disease (Fellermann et al., 2006), while a SNP in the *DEFB1* gene (encodes hBD1) was associated with an increased risk (Kocsis et al., 2008).

LL-37/*Camp* is upregulated during ileitis/colitis dependent on the level of inflammation (Schauber et al., 2006), and mice null for *Camp* have more severe phenotype in a DSS induced colitis model (Koon et al., 2011, Tai et al., 2013).

Addition of exogenous *CAMP* could reverse some of the phenotypic severity of DSS treatment in *Camp-/-* animals, such as cytokine production, apoptosis and mucus production (Tai et al., 2013). Intracolonic CAMP peptide treatment in mice pre-infected with *Clostridium difficile* also show large improvements in phenotypic consequences of the pathogen (Hing et al., 2013). Mice showed better colonic histology score, reduced apoptosis and supressed induction of myeloperoxidase (MPO) and TNF-α. Although, endogenous cathelicidin was not shown to have protective benefits in a similar model which delivered *Clostridium difficile* toxin A, to *Camp-/-* and wildtype mice (Hing et al., 2013), suggesting LL-37 has more effect on live bacteria in this model.

Graft versus host disease, a possible deadly side effect of bone marrow and stem cell transplants, targets Paneth cells and causes subsequent impairment of defensin secretion in mice; including *Defa1*, *Defa4*, and *Defa5* (Eriguchi et al., 2012). Interestingly, giving *Blautia* spp. to mice could protect them from graft versus host disease (Jenq et al., 2015).

There has been direct evidence linking gut alpha-defensins to the modulation of microbiota in mice. Salzman et al., (2010) demonstrated that Paneth cell alpha-defensins contributed to mucosal host defence and regulate the composition of murine intestinal microbiota. Mice deficient in defensins displayed increased *Firmicutes* and decreased *Bacteriodes* in the gut. Whereas mice expressing the human defensin (HD5) have *Firmicutes* decreased and increased *Bacteriodes* when compared to wildtype littermates.

1.4.6 Gut Microbiome in Pregnancy

There are vast metabolic changes that occur during pregnancy, especially in late gestation, which could affect microbial communities. Different points in gestation have different biochemical and physiological changes that could also have temporal and dynamic impact on the microbiome. Indeed, alterations in the maternal gastrointestinal microbiome have been implicated in metabolic adaptations to pregnancy (Koren et al., 2012, Collado et al., 2008). Body weight is an obvious contributing factor; pre-pregnancy weight has been linked to microbial change, where obese mothers display higher bacterial diversity (Collado et al., 2008). Koren et al., (2012) demonstrated that the gut microbiome of pregnant women changed dramatically between the first and the third trimester, showing an increase in inter-individual diversity. The authors also showed that the bacterial load of the gut changed with gestation; increasing from the first to the third-trimester. Conflicting reports whether pregnancy is truly connected with substantial shifts in gut bacteria, has come from a larger longitudinal study that failed to show significant remodelling of the gut microbiota in pregnant women (DiGiulio et al., 2015).

Aims and Hypothesis

The work in this thesis is based on the hypothesis that Host Defence Peptides play a fundamental role in mucosal immune defence. In a pregnant state, the hypothesis is that HDPs have a dual role in preventing ascending infection, but also preventing an exacerbated inflammatory response that can cause preterm birth by initiation of the labour cascade.

To explore this I determine whether bacterial stimuli can regulate HDPs expression in pregnancy tissues. I also explore what interactions HDPs have on the production/induction of important cytokines, which are vital to the inflammatory response.

As hBD3 and LL-37 suppress the inflammatory response of cells to LPS through TLR-4, the hypothesis is that *in-vivo* they might offer protection from preterm birth caused by inflammation. With the aid of HDP knockout mice, the role of these peptides in infection/inflammation and continuation of pregnancy is investigated in a mouse-model of induced preterm-labour.

Infection-induced preterm labour in women is associated with vaginal disruption of commensal bacteria as well as invading pathogens. To understand how ascending infection might be controlled by HDPs in pregnancy, I explore how HDPs regulate commensal bacteria. This is achieved by interrogating the maternal microbiome at mucosal sites in HDP knockout mice, utilising the bacterial 16S rRNA gene and next generation sequencing.

Chapter 2

General Materials and Methods

Chapter 2 General Materials and Methods

2.1 Animal Experiments

All mice were sourced ‘in-house’ and kept under specific pathogen free (SPF) conditions at the University of Edinburgh. Mice were permitted food and water *ad libitum* and maintained in 12-hour cycle of light and dark. Animal experiments were conducted under a UK Home Office licence in line with the Animals Scientific Procedure Act (1986). For full details of reagents and supplies, see Appendix on page 314.

2.1.1 Fertility Experiments

Virgin female mice were set-up in mating pairs within genotype with a stud male. During timed male exposure (96 hours), females were checked for the occurrence of a vaginal plug each morning. Once a vaginal plug was found the female was removed and monitored for subsequent confirmation of pregnancy. On day 17 of gestation females were culled and the number of viable fetus *in-utero* counted. The fertility of *Camp-/-* and *Defb14-/-* mice was determined by looking at several pregnancy indices; plug rate, pregnancy rate and first litter size. The plug rate was determined as the fraction of female mice where a copulatory plug was found, compared to the total number set-up. Subsequent pregnancy rate is the fraction of the plugged females who continued pregnancy to gestational day 17, compared to the total number plugged. First litter sizes are described here as the number of viable fetus found *in-utero* in pregnant dams on day 17 of gestation.

2.1.2 Preterm Birth Model; Laparotomy Method

Virgin female mice were set-up in mating pairs with a Stud male of the same genotype and checked for a copulatory plug each morning. The day the copulatory plug was found is determined to be Day 0. On day 17 of murine gestation, pregnant dams were anaesthetised for surgery using Isoflurane with oxygen as standard (Isoflurane flow rate 5% for initial anaesthetisation, thereafter by 2.5% for maintenance). Vetergesic analgesic [0.05mg/kg] and intra-operative fluid support [25mls/kg] of sterile physiological saline [Sodium Chloride 0.9%] were both given subcutaneously. A laparotomy was then performed which involves making a small incision into the abdomen, where the uterine horns can be externalised from the abdominal cavity (Figure 2.1). Treatment of either 25µl sterile physiological saline [Sodium Chloride 0.9%] or 25µl of Ultrapure LPS (*E.coli* O111:B4) [0.8µg/µl] were injected between the first and second fetal sac using a Hamilton 33-gauge needle. The uterine horn selected for injection was the side with the greater number of fetuses. Uterine horns were then returned to the cavity; the abdominal wall was closed with rolling sutures and the skin closed with interrupted sutures. Dams initially recovered in post-surgery heated chambers and then transferred to cages with video recording equipment for observation. Labour was defined as the time when a single pup was delivered or found in the lower vagina, either by video or by observations.

Non-surgery and non-aesthetic control animals were also set-up in cages in parallel on Day 17 (NTxC).

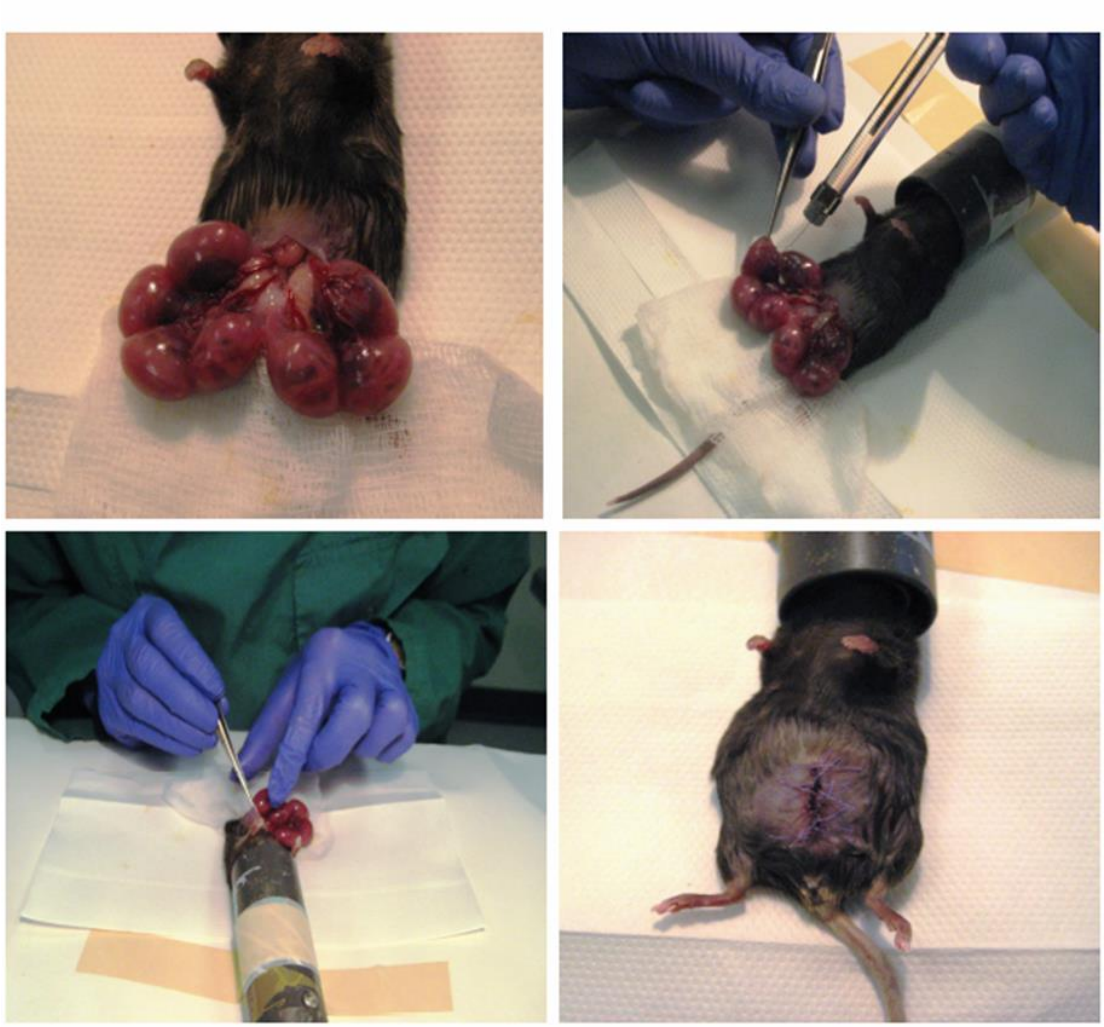

Figure 2.1 Mouse Model of Preterm Labour; Laparotomy Method
(a) Exposed uterine horns, (b) Intra-uterine injection of agent, (c) Uterine horns returned to abdominal cavity, (d) abdominal wall sutured closed. Source: Frew (2013).

2.1.3 Preterm Birth Model; Ultrasound Method

On day 17 of murine gestation, pregnant dams were anaesthetised using Isoflurane with oxygen as standard (Isoflurane flow rate 5% for initial anaesthetisation thereafter by 2.5% for maintenance). Treatment of either 25µl sterile physiological saline [Sodium Chloride 0.9%] or 25µl of LPS Ultrapure [0.8µg/µl] / [0.04µg/µl] were injected between two fetal sacs guided by ultrasound sonography (Figure 2.2). Dams were allowed to initially recover in post-procedure heated chambers and then transferred to cages with video recording equipment for observation. Labour was defined as the time when a single pup was delivered or found in the lower vagina, either by video or by observations.

Non-surgery and non-aesthetic control animals were also set-up in cages in parallel on Day 17 (NTxC).

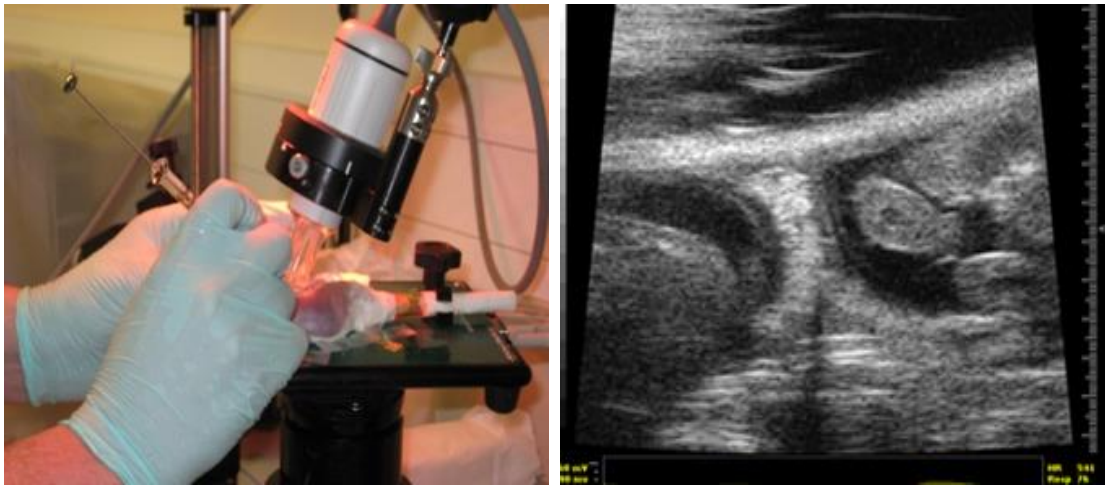

Figure 2.2 Mouse Model of Preterm Labour; Ultrasound guided Injection Method
(a) Intra-uterine injection of agent, (b) sonogram showing two fetal sacks and site of intra-uterine injection. Source: Adrian Thomson; Edinburgh Preclinical Imaging; University of Edinburgh.

2.1.4 Interval to Delivery and Number of Live-Born Pups

Labour was defined as the time when a single pup was delivered or found in the lower vagina, either by video or by observation. Interval to delivery was recorded for each animal as the number of hours between injection and labour. Preterm labour is defined as an interval of <36 hours. The number of live-born pups was determined at the first observation following labour; any pups found live *in-utero* were not counted as 'live-born'. The proportion of live-born pups was the number of viable fetus counted at the time of injection divided by the number of live-born.

2.1.5 Timed Collection

Preterm labour model was conducted as detailed in section 2.1.3, but animals were culled 6-hours post treatment by lethal CO_2 exposure, where tissue (placenta, fetal membrane, uterus, vagina, and cervix) and blood serum were collected for molecular analysis. In parallel non-anaesthetic non-treatment day 17 pregnant females (NTxC) were also culled for control tissue and blood serum for comparison.

Immediately after CO_2 lethal exposure blood was collected by cardiac puncture using a 21-gauge needle into BD Microcontainers®. Blood was allowed to sit for 20 minutes and then centrifuged at 8000 rpm for 5 minutes. The serum was then collected and centrifuged at 14000 rpm for 10 minutes at 4°C to pellet any remaining blood cells, supernatant was then stored at -80°C.

All tissue collections and dissections were conducted on large sterile petri-dishes kept on ice. Where possible tissues were divided into 3 portions; 1) For RNA extraction; collected in RNA*later*®, kept at 4°C and extracted within 48 hours. 2) For protein extraction; snap frozen on dry ice and stored at -80°C. 3) For histology; collected into 4% solution of paraformaldehyde, fixed overnight and then transferred to 70% ethanol.

The uterus was carefully dissected to release all fetal sacs. Uterine tissues were collected from both uterine horns (right and left), mid-way from the cervix. Fetal membranes were dissected from the placenta and pooled where possible, according to which uterine horn the fetal sac was obtained. One placenta from the left and right horn was dissected into two parts for RNA and Protein, a separate placenta from each horn was selected for histology. Vagina and cervix were excised internally, releasing any connecting tissues. Cross-sections of the cervix and vagina were taken for histology; remaining vagina and cervix tissue was collected for RNA extraction.

2.1.6 Microbiome Sample Collection

Sampling and methods for microbiome analysis are described in Chapter 4. For full details of reagents and supplies, see Appendix on page 314.

2.1.7 HDP Expression in the Murine Reproductive Tract Experiments

2.1.7.1 Estrus Cycling and Staging

Eight week old C57BL/6N mice were super-ovulated with pregnant mare's serum gonadotropin (PMSG) and human chorionic gonadotropin (hCG) combination. Specifically, mice were given intraperitoneal administration of 5 IU of PMSG, 48 hours later mice received intraperitoneal administration of 5 IU hCG. Animals were culled 18 hours after hCG injection by lethal CO_2 exposure, where tissue (placenta, fetal membrane, ovary, uterus, vagina, and cervix) were collected for molecular analysis. Prior to tissue collection, vaginal cell cytology was also conducted to confirm all mice were in estrus stage at the time of collection (see below).

2.1.7.2 Vaginal Cell Cytology

Estrus cycling in mice is continuous but there are discrete phases; diestrus, proestrus, estrus and metestrus. Mouse estrus cycling is accompanied with vaginal manifestations in vaginal morphology and cell cytology. Cytological estrus staging requires the collection and staining of vaginal cells to characterise the proportions of; leukocytes, cornified squamous epithelial cells, and nucleated epithelial cells. Crystal violet was used for vaginal cell cytology in this study as described by McLean et al., (2012) (Figure 2.3). In brief, 200µl of sterile H_2O is lavaged in the mouse vagina, smeared onto a glass slide and then air dried. Once dry, crystal violet solution 0.1% (w/v) is applied for 1 minute then the slide is washed in sterile water for a further 1 minute. Slides are mounted in glycerol and imaged immediately. The number of cornified squamous epithelial cells, leukocytes, and nucleated epithelial cells are counted and the relative ratio of these cell types is used to determine estrus stage according to the tool published by Byers et al., (2012).

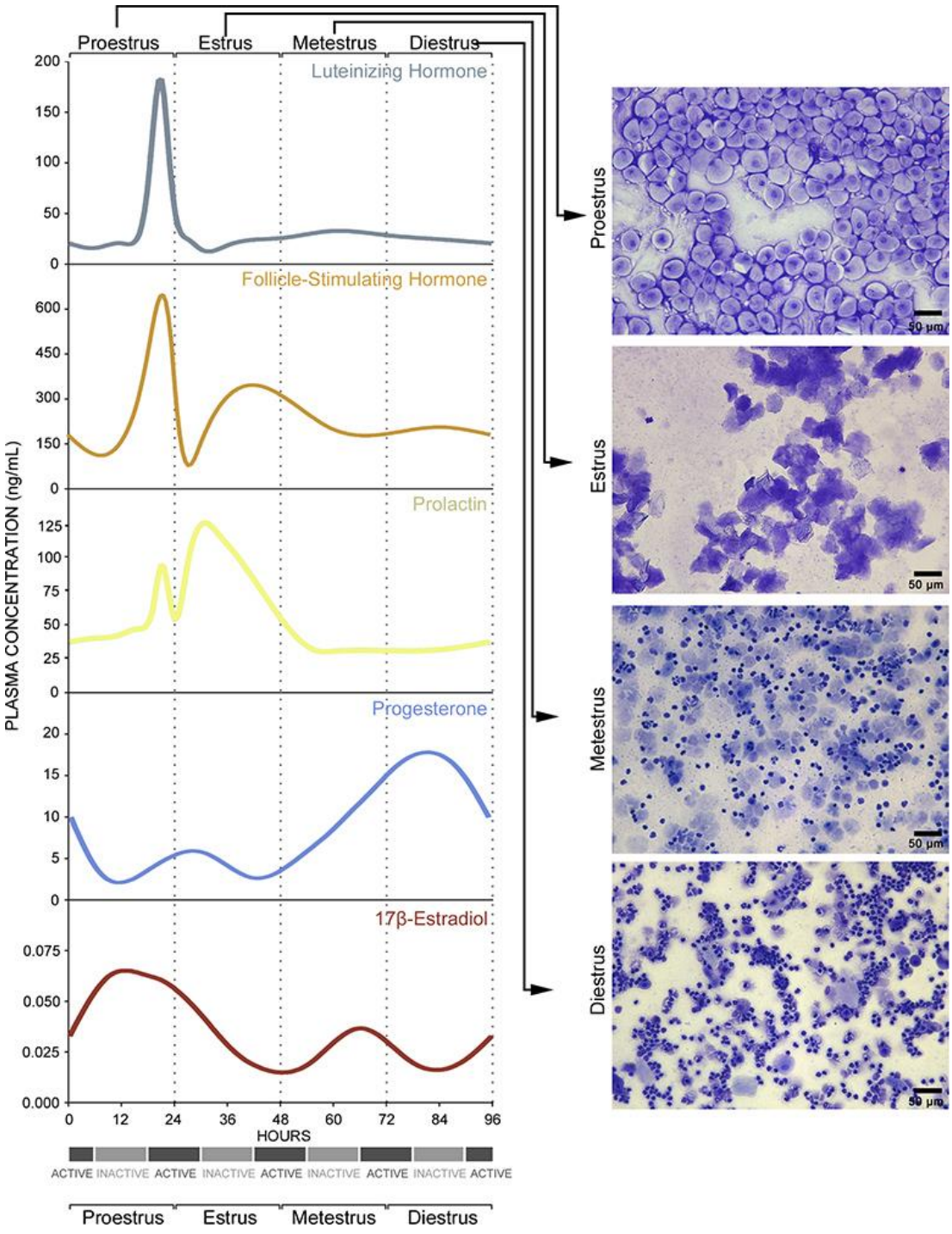

Figure 2.3 Mouse Vaginal Cytology for Estrus Staging
Diestrus stage is mostly dominated by leukocytes, proestrus is mostly dominated by nucleated epithelial cells and estrus is mostly dominated by cornified epithelial cells. Metestrus has both nucleated epithelial cells and leukocytes. Source: McLean et al., (2012)

2.2 Molecular

2.2.1 RNA Extraction and Reverse Transcription

Two methods of RNA extraction were used in this study. All human tissues were extracted using the TRI reagent method; while all murine tissues were extracted using the RNA Bee method. The TRI Reagent method is the protocol of choice for the Edinburgh Reproductive Biobank and was implemented for uniformity across study-sets. For full details of reagents and supplies, see Appendix on page 314.

2.2.1.1 TRI Reagent Method

Tissue was transferred to 2ml tubes containing 1ml of TRI reagent® with sterile stainless steel bead. Homogenisation was supported using TissueLyser I for 2 x 3 minutes at 25HZ. Samples were left to incubate for 15 minutes at room temperature then centrifuged at 14,000 rpm for 15 minutes maintained at 4°C. The supernatant was then transferred to phase-lock tubes and 200µl of bromochloropropane added, samples were then left to participate at room temperature for 15 minutes. Samples were centrifuged at 14,000 rpm for 15 minutes maintained at 4°C; the aqueous phase was then collected into equal volume of ice cold 70% ethanol. To isolate the RNA the RNeasy kit was used following the manufactures protocol. Isolated RNA was quantified on the Nanodrop ND-1000 at 260nm and 280nm as standard; all RNA is stored at -80°C.

2.2.1.2 RNA Bee Method

Tissue was transferred to 2 ml Lysing Matrix D tubes, containing 1ml of RNA Bee, then homogenised for 30 seconds at 5000 rpm on the Precellys®24 lyser. 100µl of chloroform was added and samples were left to incubate on ice for 5 minutes. Samples were then centrifuged at 10000 rpm for 15 minutes maintained at 4°C. The subsequent upper aqueous phase was transferred to a new tube containing equal parts of ice-cold isopropanol. Samples were then incubated at -20°C for 20 minutes and centrifuged at 10000 rpm for 20 minutes maintained at 4°C to pellet the RNA. Pellets

were washed twice with 75% ice cold ethanol and RNA was re-suspended in 20-100µl RNase and DNase-free water.

2.2.1.3 Reverse Transcription

High-Capacity cDNA Reverse Transcription Kit was used to reverse transcribe RNA following the manufactures protocol for a 20µl reaction using oligo (dT) primers and 1µg of each RNA sample. Where possible a representative reverse transcription negative (RT-NEG) and template negative (NTC-NEG) were included in each batch. cDNA was stored at -20°C until required.

2.2.2 RT-qPCR

The amount of mRNA transcript was quantified using qPCR, where the cDNA is amplified for specific genes of interest in the presence of fluorescent reporter probes and quenchers. The majority of the gene expression analysis in this study was done using pre-designed Taqman probes, which have been optimised for use on the ABI PRISM® 7000 Sequence Detection System. These probes were sourced from Applied Biosystems and are listed in Table 2.1. Some gene expression analysis was supported on the LightCycler® 480 Real-Time PCR System. For this approach, primers for specific genes of interest were designed to be compatible with the universal hydrolysis probes system (UPL), utilising the Universal ProbeLibrary Assay Design Center (Table 2.2).

Several qPCR negatives (PCR-NTC) and reverse transcription negatives (RT-NEG) and calibrators were run on every plate. The individual calibrators (CAL) are detailed in each chapter.

2.2.2.1 Taqman Assay (ABI PRISM)

A reaction mix containing the ABI Taqman Mastermix (x2), template, reference gene Primer-Probe Assay (x20) or the primer-probe mix for the gene of interest were set up as per manufacturer's instructions. cDNA template was diluted 1:2.5 in molecular grade water prior to reaction. All Taqman PCR primers are intron-spanning and the ABI assay ID numbers are given in Table 2.1. Samples were run in triplicate and PCR cycling and fluorescence detection was supported on the ABI PRISM® 7000 Sequence Detection System. Standard 4 stage PCR cycling method was used; 50°C for 2 minutes, 95°C for 10 minutes, [95°C for 15 seconds, 60°C for 1 minute] repeated for 35 cycles.

Gene	**Human/Mouse**	**ABI Assay ID**
Defb14	Mouse	Mm00806979_m1
Camp	Mouse	Mm00438285_m1
Cxcl1	Mouse	Mm04207460_m1
Cxcl2	Mouse	Mm00436450_m1
Il-1β	Mouse	Mm00434228_m1
Tnf	Mouse	Mm00443258_m1
Ptgs2	Mouse	Mn00478374_m1
Atcb	Mouse	4352341E (cat number)
DEFB103 (hBD3)	Human	Hs00218678_m1
CAMP (LL-37)	Human	Hs00189038_m1
ACTB	Human	4310881E (cat number)
18S	Eukaryotic	4319413E (cat number)

Table 2.1 Taqman Assay Probes

2.2.2.2 Universal ProbeLibrary Assay (Roche LightCycler)

A reaction mix containing the LightCycler Mastermix, template, reference gene primer-probe mix or the primer-probe mix for the gene of interest were set up as per manufacturers instruction. All samples were run in triplicate and PCR cycling and fluorescence detection was supported on the LightCycler® 480 Real-Time PCR System. cDNA template was diluted 1:2.5 in molecular grade water prior to reaction. All PCR primers were synthesised by Sigma and are intron-spanning; the primer sequences and corresponding UPL probe ID numbers are given in Table 2.2. The efficiencies of each primer and probe-set were evaluated using a serial dilution of a calibrator cDNA sample (epididymis cDNA). All efficiencies were within the acceptable range of E= 1.9-2.1. Mouse beta-actin (*Actb*) predesigned primer-probe mix was used as the reference gene control for all samples. For all primer-probe pairs the PCR cycling parameters were; 95°C for 10 minutes, [95°C for 15 seconds, 60°C for 30 seconds, 72°C for 1 second] repeated for 35 cycles.

Gene	**Forward Primer (5'-3')**	**Mouse UPL probe ID #**
Defb1	CCTGGCTGCCACCACTAT	2
Defb4	CAGTCATGAGGATCCATTACCTT	2
Defb6	GCTCTTTGCCTTTATCCTGGT	94
Defa5	CAGGCTGATCCTATCCACAAA	103
Actb	N/A	Pre-designed primer-probe mix

Table 2.2 Primers and Probes Designed in Universal ProbeLibrary Assay Design Center

2.2.2.3 RT-qPCR analysis method

All qPCR in this study were set up in technical triplicates where any intra-sample outliers were removed. Ct value is the cycle at which the fluorescence signal crosses a threshold, where the threshold is an estimate of the first point where samples are in exponential phase above background. Ct values were normalise to the reference gene and then samples compared to calibrator using the formula $2^{-\Delta\Delta CT}$. This gives a fold change in gene expression of the target relative to the calibrator. This method also allows comparison across multiple plates if the same calibrator is used. Where two reference genes were used as the control, their geometric mean was used to normalise the Ct value of the gene of interest.

2.2.3 ELISA

ELISA quantitatively measures the amount of a protein of interest in solution by comparing to a known sample using a serial dilution. Sandwich ELISA involves coating a plate with monoclonal antibody raised against the protein of interest. After the protein of interest is bound to this primary antibody, a secondary antibody that has an epitope for the protein is then bound. These secondary antibodies are coupled to substrates that allow for detection and quantitative measurement.

All ELISA kits in this study were R&D duosets, the detection range for each protein is given in Table 2.3. All ELISA in this study were conducted using the following protocol. Flat-bottom ELISA plates were coated with 50µl of capture antibody, diluted appropriately in PBS, and incubated overnight at room temperature. Plates were then washed 3 times in PBS-Tween (0.05%) to remove unbound antibody and blocked for 2 hours in 0.5% (v/v) Reagent Dilute Concentrate in PBS. After removal of the blocking solution, 50µl of sample was added to the plate in duplicate. In this study all blood serum and cell culture supernatants were diluted 1:5 in Reagent Diluent. Serial dilution of standards were also made in Reagent diluent and added in duplicate in 50µl volumes. Plates were incubated overnight at 4°C and then washed 3 times in PBS-Tween (0.05%). Appropriate biotinylated detection antibody was

applied and incubated overnight at 4°C, thereafter washed 3 times in PBS-Tween (0.05%). Following this, 50µl of HRP-conjugated antibody was applied to each well and incubated at room temperature for 30 minutes. Wells were washed 3 times in PBS-Tween (0.05%), and then 50µl of substrate (TMB solution) was added to each well to detect activity. Reactions were stopped with 25µl of acid solution (1N HCL). The intensity of the colour was measured using spectrophotometry with absorbance at 450nm and corrected for background at 570nnm.

R&D duosets	Detection Range
Human TNF DuoSet ELISA	2000 – 31 pg/ml
Human Il-8 DuoSet ELISA	2000 – 31 pg/ml
Human IL-1β DuoSet ELISA	250 – 4 pg/ml
Human RANTES DuoSet ELISA	2000 – 31 pg/ml
Human IL-6 DuoSet ELISA	1300 – 20 pg/ml
Human IP-10 DuoSet ELISA	1000 – 16 pg/ml
Mouse IL-6 DuoSet ELISA	2000 – 31 pg/ml
Mouse TNF DuoSet ELISA	2000 – 31 pg/ml
Mouse IL-1β DuoSet ELISA	1000 – 16 pg/ml

Table 2.3 R&D duosets ELISA

2.3 HDPs in Placental Explants Experiment

Placenta was obtained from women undergoing elective Caesarean section at 38-39 weeks. All women were healthy, non-smokers with a normal BMI. Women had no indication of infection and all were singleton pregnancies.

Full thickness placental lobule was collected from the central cotyledons region of the placenta and transported directly to the lab in PBS. Placenta tissue was washed 5 times in sterile PBS and the chorionic surface removed. Any visible connective tissue deposits and blood clots were also removed. Villous tissue was obtained from the middle cross-section where 0.05g was placed in each well of a 24-well flat bottom culture dish. Each well contained 1ml of pre-warmed RPMI 1640 media with 10% fetal calf serum (FCS) and penicillin and streptomycin [50ug/ml]. Tissues were left to acclimatise for 1 hour in 5% CO_2 at 37°C before treatments applied. Treatments and concentrations are detailed in section 3.3.2. The scrambled LL-37 peptide sequence is RSLEGTDRFPFVRLKNSRKLEFKDIKGIKREQFVKIL. All treatments were applied in triplicate and cultures incubated in 5% CO_2 at 37°C for 3 hours, unless detailed otherwise. Culture supernatant was collected and centrifuged at 800 rpm for 10 minutes maintained at 4°C to remove debris. To further pellet red blood cells this supernatant was transferred to a new tube and centrifuged at 8000 rpm for 10 minutes maintained at 4°C. Final supernatants were used immediately for LDA assay or stored in aliquots at -80°C. Placenta tissue was blotted dry on sterile paper and collected in RNA*later* for RNA extraction as described in section 2.2.1.1. For full details of reagents and supplies, see Appendix on page 314.

2.3.1 LDH assay

Cytotoxicity of each treatment was measured using Pierce™ LDH Cytotoxicity Assay Kit following the manufactures protocol.

2.4 HDPs in Human Term Labour study

Human myometrium, fetal membrane, and placenta tissue was obtained from the Edinburgh Reproductive Biobank; REC number 13/ES/0126. Informed consent was obtained and approved under South East Scotland Scottish Academic Health Sciences Collaboration (SAHSC) Human Annotated BioResource (HAB). Tissues were collected from healthy singleton pregnancies undergoing elective Caesarean section. All samples were collected into RNA*later* and stored at -80°C until RNA extraction. For full details of reagents and supplies, see Appendix on page 314.

Chapter 3

Host Defence Peptides

Chapter 3 Host Defence Peptides

3.1 Introduction

Nearly 40% of all preterm deliveries are associated with intrauterine infection and/or clinical inflammation (Romero et al., 2006). The female reproductive tract has biochemical and physiological barriers to prevent bacteria ascending from the vagina into the amniotic cavity during pregnancy. These physiological barriers include the cervix and fetal membranes which also produce multiple Host Defence Peptides; key mediators in defence against invading pathogens. HDPs are released by epithelial cells, trophoblastic cells and immune cells where their action can be by disrupting bacteria cell membranes, but also by an array of immunomodulatory processes.

Labour is generally accepted to be an inflammatory event where the emphasis from an anti-inflammatory pregnancy state shifts pro-inflammatory preceding labour (Youssef et al., 2009).

hBD3 and the murine orthologue DEFB14 have potent anti-inflammatory effects shown both *in-vitro* and *in-vivo* (Semple et al., 2010, Semple et al., 2011). Exposure of human and mouse primary monocytes to LPS in the presence of hBD3 effectively inhibited the TLR-4 mediated TNF, IL-6 and type I interferon responses (Semple et al., 2010). This inhibitory response has been shown to be through both the MyD88 and TRIF pathways. Contrastingly, a study has also suggested hBD3 can be pro-inflammatory when mediated by TLR1/2 (Funderburg et al., 2007). Funderburg et al., (2007) displayed that hBD3 increases the production of co-stimulatory molecules on monocytes and dendritic cells enhancing their chemoattractant potential. The chemoattractant property of hBD3 has also been shown in many other cell types, such as T cells, immature dendritic cells and macrophages (Wu et al., 2003, Yang et al., 1999). Other pro-inflammatory properties of hBD3 are displayed in its potential to exacerbate the MDA5 cytoplasmic receptor in response to dsRNA, a viral ligand mimic (Semple et al., 2015).

LL-37 has been shown to have biphasic action, having both pro-inflammatory and anti-inflammatory functions. In human monocytes, exogenous LL-37 can inhibit the release of the pro-inflammatory cytokine TNF in response to LPS. This has also been shown for the mouse peptide CAMP on BMDMs (Pinheiro da Silva et al., 2009). LL-37 can also inhibit the pro-inflammatory response to PAMPS in other myeloid cells (Mookherjee et al., 2006). The anti-endotoxic effects of LL-37 and the mouse orthologue CAMP have been mostly attributed to their ability to directly bind to LPS (Scott et al., 2000, Scott et al., 2011).

With regard to promoting inflammation, exogenous LL-37 *in-vitro* increases the production of cytokines and chemokine such as IL-8 and IL-6 in lung epithelial cells (Tjabringa et al., 2003, Pistolic et al., 2009), skin cells (Niyonsaba et al., 2007), and cervical epithelial cells (Frew et al., 2014). LL-37 also preferentially promotes apoptosis in lung epithelial cells in the presence of an infection (Barlow et al., 2006) and is a potent modifier of dendritic cell differentiation (Davidson et al., 2004).

In a pregnant state the hypothesis of this chapter is that HDPs have a dual role, in preventing ascending infection, and also preventing an exacerbated inflammatory response that can cause preterm birth by initiation of the labour cascade. The immunomodulatory effects of LL-37 and hBD3 in reproductive tissues in response to bacterial stimuli has not been well studied. The spatial function most likely reflects the differing immunological requirements along the length of the female reproductive tract and pregnancy tissues.

This chapter investigates whether the HDPs, hBD3 and LL-37, are affected by the inflammatory cascade of normal term labour. This was done by looking at the mRNA gene expression in the myometrium, amnion/chorion, and placenta of women in either labour at term or not in labour at term. These tissues were chosen for the relative ease of collection.

To test the anti-inflammatory properties of HDPs in pregnancy I investigated the effects of endogenous LL-37 and hBD3 on placental explants in response to bacterial stimuli. This response could have additionally been tested placental cell lines,

however, it is reported that different trophoblast cell lines express differences in cell surface markers when cultured in isolation (Nakada et al., 2011, Grasso et al., 2014).

I also determined the expression of the mouse orthologues of LL-37 and hBD3; *Camp* and *Defb14* respectively, in the mouse female reproductive tract in pregnancy.

3.2 Experimental Details

3.2.1 Patient Characteristics

HDPs in Labour Study

Human myometrium, fetal membrane, and placenta tissue were obtained from the Edinburgh Reproductive Biobank. Tissues were collected from healthy singleton pregnancies from women undergoing caesarean sections. All non-labouring women had no evidence of cervical dilatation. Those women in labour had spontaneous induction of labour but failed to progress and underwent caesarean section. All samples were selected on the criteria that women were non-smokers, had healthy BMI with no signs of an infection including chorioamnionitis

Clinical Details	**Non-Labour (n=7)**	**Labour (n=8)**
Maternal Age (years)	38 ± 1.4	31 ± 2.1
Maternal BMI (kg/m^2)^	27 ± 0.87	23 ± 1.2
Gestation at collection (weeks)	39 ± 0.22	41 ± 0.29
Parity	1.1 ± 0.26	0.38 ± 0.18
Sex of baby (M; F)	2 ; 5	4 ; 4
Dilatation at CS	nil	6 ± 2.5 cm

Table 3.1 Clinical Details of Patients; HDPs in Labour study
Data presented as mean and SEM. ^ at first trimester antenatal visit.

HDPs in Placental Explants Study

Placenta was collected from women undergoing elective caesarean section at 38-39 weeks and immediately processed for *ex-vivo* experiments as detailed in section 2.3. All women were healthy non-smokers with a normal BMI, had no indication of infection, and were all singleton pregnancies.

Clinical Details	**No Labour (n=3)**
Maternal Age (years)	33 ± 2.4
Maternal BMI (kg/m^2)^	28 ± 1.4
Gestation at collection (weeks)	39 ± 0.12
Parity	1.0 ± 0.20
Sex of baby (M; F)	2 ; 1
Dilatation at CS	nil

Table 3.2 Clinical Details of Patients; HDPs in Placental Explants study
Data presented as mean and SEM. ^ at first trimester antenatal visit.

3.2.2 Assays and Statistical Analysis

RT-qPCR; HDPs in Labour Study

The level of *DEFB103*, *CAMP*, and *TNF* gene transcripts in myometrium, placenta and amnion/chorion tissues was measured by RT-qPCR as described in section 2.2.2. As detailed, the Ct values were normalised to the geometric mean of the reference genes, ACTIN and 18S. Values were then compared to a calibrator sample (CAL) which was from myometrial tissue. *CAMP* and *DEFB103* expression data was log transformed prior to analysis. Unpaired t-test was conducted that compared the labouring to non-labouring samples within each tissue type**.**

RT-qPCR; HDPs in Placental Explants Study

The level of *DEFB103*, *CAMP*, and *TNF* gene transcripts in placenta was measured by RT-qPCR as previously described. Samples were normalised to a calibrator (CAL) from a placenta explant tissue that received no treatment.

For *TNF* gene transcript (excluding hBD3 treatment), a two-way ANOVA with Tukey's post-test compared to no-peptide treatments within LPS groups was performed. Significant interactions in LPS treatment were identified with Bonferroni's post-test compared to no-treatment groups. As there was no hBD3 peptide only group, the effect of hBD3 peptide was measured by paired t-test between LPS [100ng/ml] alone and LPS [100ng/ml] + hBD3 [25µg/ml] group.

Significant differences in the level of *DEFB103* and *CAMP* in response to LPS were conducted using a paired t-test comparing no-treatment to LPS alone.

RT-qPCR; HDPs in Murine Reproductive Tract

The mouse beta-defensins; *Defb1*, *Defb4*, *Defb6*, *Defb14*, the alpha defensin, *Defa5*, and the murine cathelicidin, *Camp*, transcripts were measured in ovary, uterus, cervix and vagina by RT-qPCR as described in section 2.2.2. The Ct values were normalised to the reference gene, *Actb*. Where a calibrator was used to normalise values; the calibrator was from epididymis tissue. Data presented as mean fold change and SEM relative to either the calibrator (CAL) or mean expression in the ovary.

ELISA; HDPs in Placental Explants Study

To detect the amount of secreted protein in culture supernatants from human placenta explants post-treatment, ELISA's were conducted as described in section 2.2.3. The proteins of interest were TNF, IL-8, IL-6, IL-1β, IP-10, and RANTES.

All ELISA data is presented as the mean concentration ± SEM. Two-way ANOVA was used to highlight the effect of the presence of LPS and LL-37 compared to control peptide. Significant interactions in peptide treatment were identified with

Tukey's post-test. A two-way ANOVA with Dunnett's post-test for matched samples was conducted on the data looking at LPS effect over time. One-way ANOVA with Dunnett's post-test was conducted when comparing dose of LL-37 with LPS treatment.

As there was no hBD3 peptide only group, the effect of hBD3 peptide was measured by paired t-test between LPS [100ng/ml] alone and LPS [100ng/ml] + hBD3 [25µg/ml] groups for each secreted cytokine.

3.3 Results

3.3.1 HDPs in Human Term Labour

The level of *DEFB103* (Figure 3.1) and *CAMP* (Figure 3.2) gene transcripts was measured by RT-qPCR in myometrium, placenta and amnion/chorion tissues collected from term pregnancies of women not in labour (n=7) and in labour (n=8).

3.3.1.1 Human beta-defensin 3 in Term-Labour

There was a small but significant increase in *DEFB103* levels in myometrium from women in labour compared to myometrium from women not in labour (unpaired t-test; P <0.05) (Figure 3.1). Compared to non-labouring samples, labour increased the average *DEFB103* expression in the myometrium 18.7 ± 13.4 fold. Labour, however, did not affect the mRNA expression level of *DEFB103* in the placenta or amnion/chorion in this study.

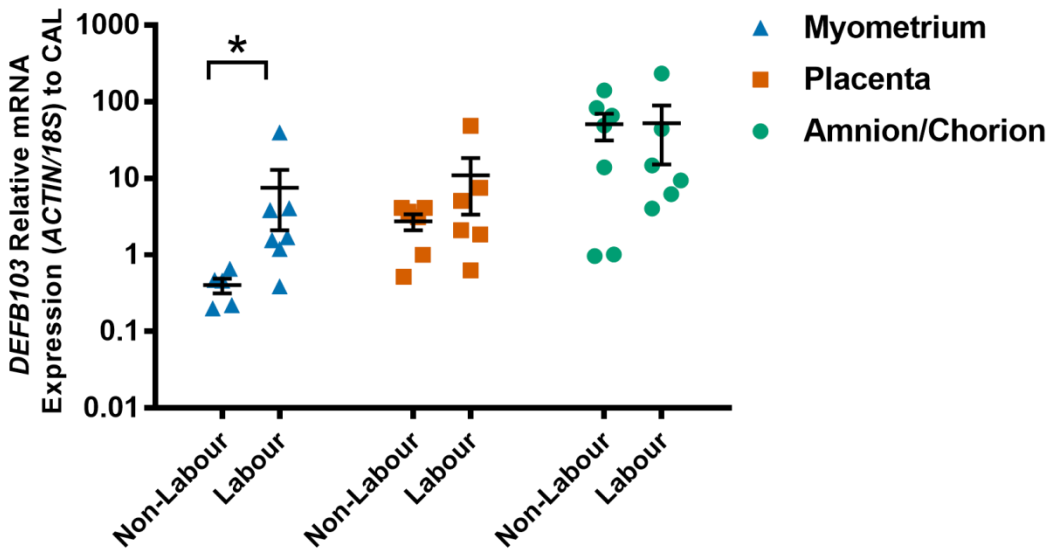

Figure 3.1 Expression of *DEFB103* (hBD3) during Term Labour
Relative *DEFB103* mRNA gene expression in myometrium, placenta and amnion/chorion tissues collected from non-labouring women (n=≥5) and women in labour (n=≥5). Normalised to β-*ACTIN* and *18S*, relative to calibrator (CAL). (Unpaired t-test; *, P <0.05)

3.3.1.2 Human Cathelicidin in Term-Labour

There was a small but significant increase in *CAMP* mRNA gene expression in placenta tissue from women in labour compared to placenta from women not in labour (unpaired t-test; P <0.05) (Figure 3.2). Placental tissue from women in labour displayed a 6.8 ± 3.1 mean fold increase compared to tissue from women not in labour. Labour did not affect the mRNA expression level of *CAMP* in the myometrium or amnion/chorion.

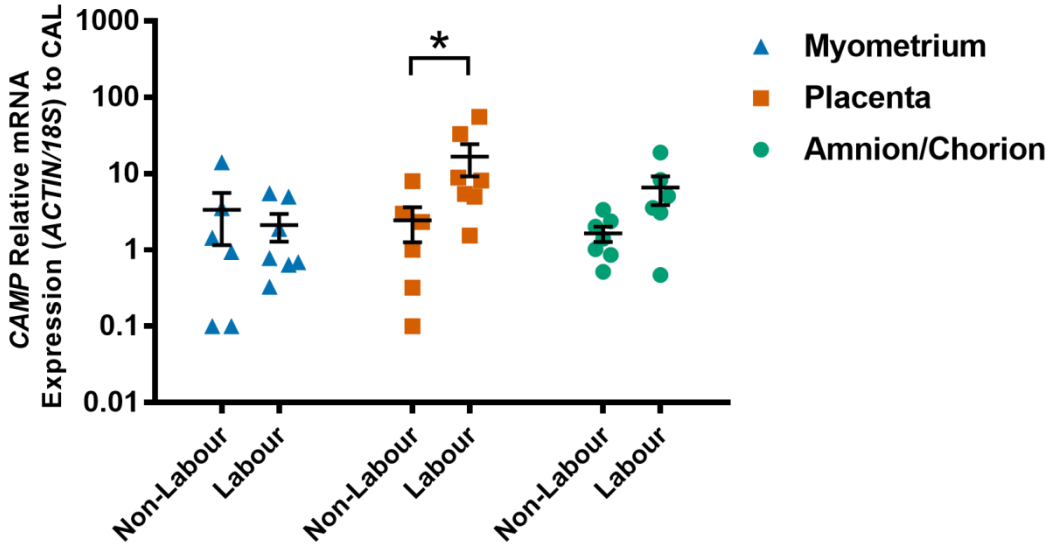

Figure 3.2 Expression of *CAMP* (LL-37) during Term Labour
Relative *CAMP* gene expression in myometrium, placenta and amnion/chorion tissues collected from non-labouring women (n=≥6) and women in labour (n=≥6). Data presented as mean and SEM, normalised to *β-ACTIN* and *18S*, relative to calibrator (CAL). (Unpaired t-test; *, P <0.05)

3.3.2 HDP Anti-inflammatory effect on Placental Explants

To investigate the effects of HDPs on the inflammation caused by infection, placenta tissue explants were cultured with LPS in combination with exogenous peptides of hBD3, LL-37 and scrambled LL-37 control. Placenta was collected from women undergoing caesarean section at term (n=3), but prior to the initiation of labour. The main read-out of inflammation was the secreted pro-inflammatory cytokine TNF, which was assessed by ELISA in culture supernatants as described in section 2.2.3. Other secreted cytokine levels were also determined; IL-8, IL-6, IL-1β, IP-10 (CXCL10), and RANTES (Regulated on Activation, Normal T Cell Expressed and Secreted) as measured by ELISA. *TNF* mRNA gene expression levels were assessed by RT-qPCR as described in section 2.2.2.

Cytotoxicity assay showed that LPS and exogenous HDP treatments did not induce any significant cell death in the doses and time-points investigated here compared to background (section 2.3.1; data not shown).

3.3.2.1 LPS Dose and Time Response in Placental Explants

The time and dose-responsive effects of LPS on placental explants was determined by culturing at two LPS doses, 1µg/ml or 100ng/ml for 24 hours. Culture supernatants were taken at 1, 3, 6 and 24 hours post treatment, and the amount of the pro-inflammatory cytokine TNF was measured by ELISA (Figure 3.3).

1µg/ml and 100ng/ml of LPS both increased TNF secretion significantly compared to non-LPS treated samples at all time-points considered (two-way ANOVA with Dunnett's post-test; $P < 0.0001$). 100ng of LPS appeared to produce less secreted TNF compared to 1µg at all time-points, but this was not significant in this small sample size with repeated measures. Nonetheless, as the lower dose of 100ng LPS could elicit a robust TNF response, this dose was chosen for subsequent experiments to be closer to physiological/clinical levels of LPS (Guo et al., 2013). As TNF protein levels in this system peak at 6-hours; culture supernatants in subsequent experiments were collected at 3-hours post treatment to capture initial TNF response before saturation.

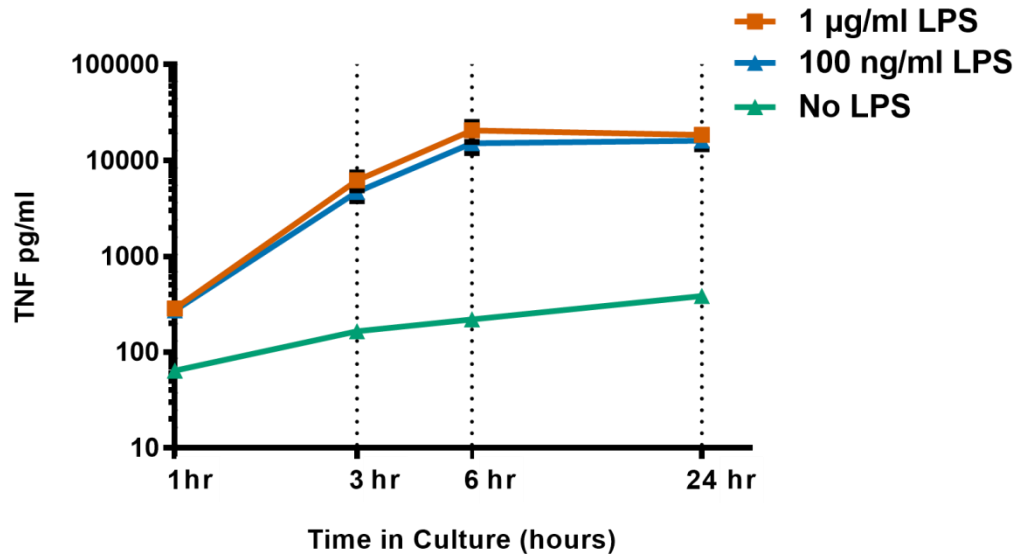

Figure 3.3 Placental Explants; TNF levels in LPS dose and Time Response

TNF protein levels from cultures supernatants as measured by ELISA. Presented as mean and SD of technical replicates, n=3 per group. All treated samples are from one patient. (Two-way ANOVA with Dunnett's post-test; P <0.0001 for LPS effect at all time-points, no significant difference in 1µg compared to 100ng LPS dose at any time-point; Bonferroni's post-test)

3.3.2.2 LL-37 Dose Response in Placental Explants

The effect of LL-37 on LPS-induced inflammation in the placenta was determined by culturing explants with increasing doses of exogenous LL-37 peptide in the presence of 100ng/ml of LPS. Culture supernatants were taken at 3-hours post treatment and the amount of the secreted pro-inflammatory cytokine TNF was measured by ELISA (Figure 3.4).

In placental explants from all 3 patients; increasing the dose of LL-37 peptide reduced the levels of secreted TNF in response to 100ng/ml of LPS. This reached statistical significance at 25µg/ml of LL-37 (one-way ANOVA with Dunnett's post-test; **, P <0.01 compared to LPS alone).

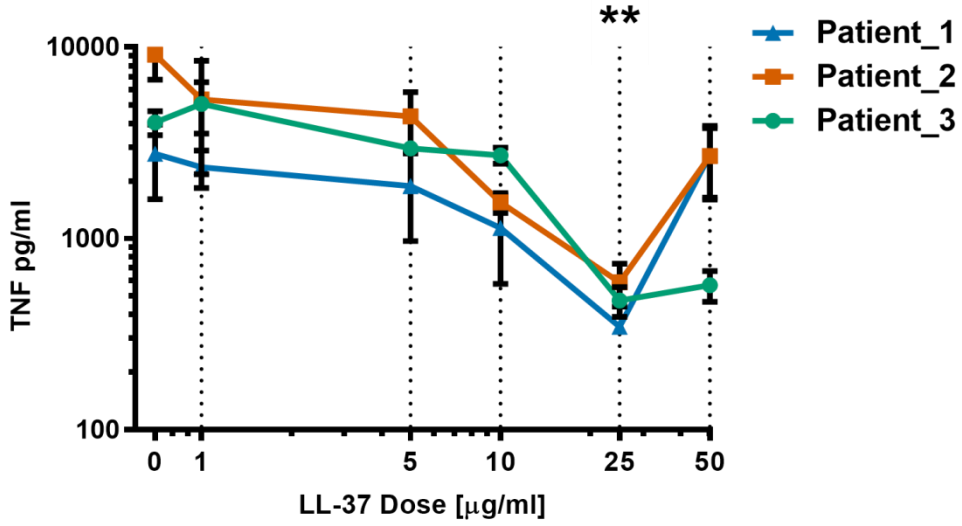

Figure 3.4 Placental Explants; TNF levels in LL-37 Dose Response
TNF protein levels from cultures supernatants with 100ng/ml of LPS and increasing doses of LL-37. All data presented as mean and SD of technical replicates, n=3 per group. (one-way ANOVA with Dunnett's post-test; **, P <0.01 compared to LPS alone)

3.3.2.3 HDPs in Placental Explants

To confirm that the anti-inflammatory effects of LL-37 were specific to the addition of the peptide, scrambled peptide control (Control) was also used as a treatment at the optimal dose seen for LL-37, [25µg/ml]. In addition, placental explants were also treated with hBD3 peptide at 5µg/ml; a dose previously shown to have anti-inflammatory functions in human and mouse macrophages (Semple et al., 2010). The secreted cytokines; TNF, IL-8, IL-6, IL-1β, IP-10, and RANTES were measured by ELISA (Figure 3.5). *TNF* (Figure 3.6), *CAMP* and *DEFB103* (Figure 3.7) mRNA gene expression levels were also assessed in these treated placenta tissues by RT-qPCR.

Exogenous scrambled control peptide or LL-37 alone, had no effect on the secretion of IL-1β, IL-8 or IL-6 (two-way ANOVA's with Tukey's post-test) (Figure 3.5). LL-37 treatment alone however, did show a small but significant decrease in TNF protein level in culture supernatants (Figure 3.5.c) (two-way ANOVA with Tukey's post-test; $P < 0.05$ compared to no treatment).

Addition of 100ng/ml of LPS to placental explants robustly and significantly increased the levels of; IL-8 ($P < 0.01$), IL-6 ($P < 0.05$), TNF ($P < 0.0001$), and IL-1β ($P < 0.0001$) in culture supernatants collected 3-hours post treatment (two-way ANOVA; Bonferroni's post-test; no treatment compared to LPS only). LPS treatment alone did not increase the levels of IP-10 or RANTES (Figure 3.5.e, Figure 3.5.f).

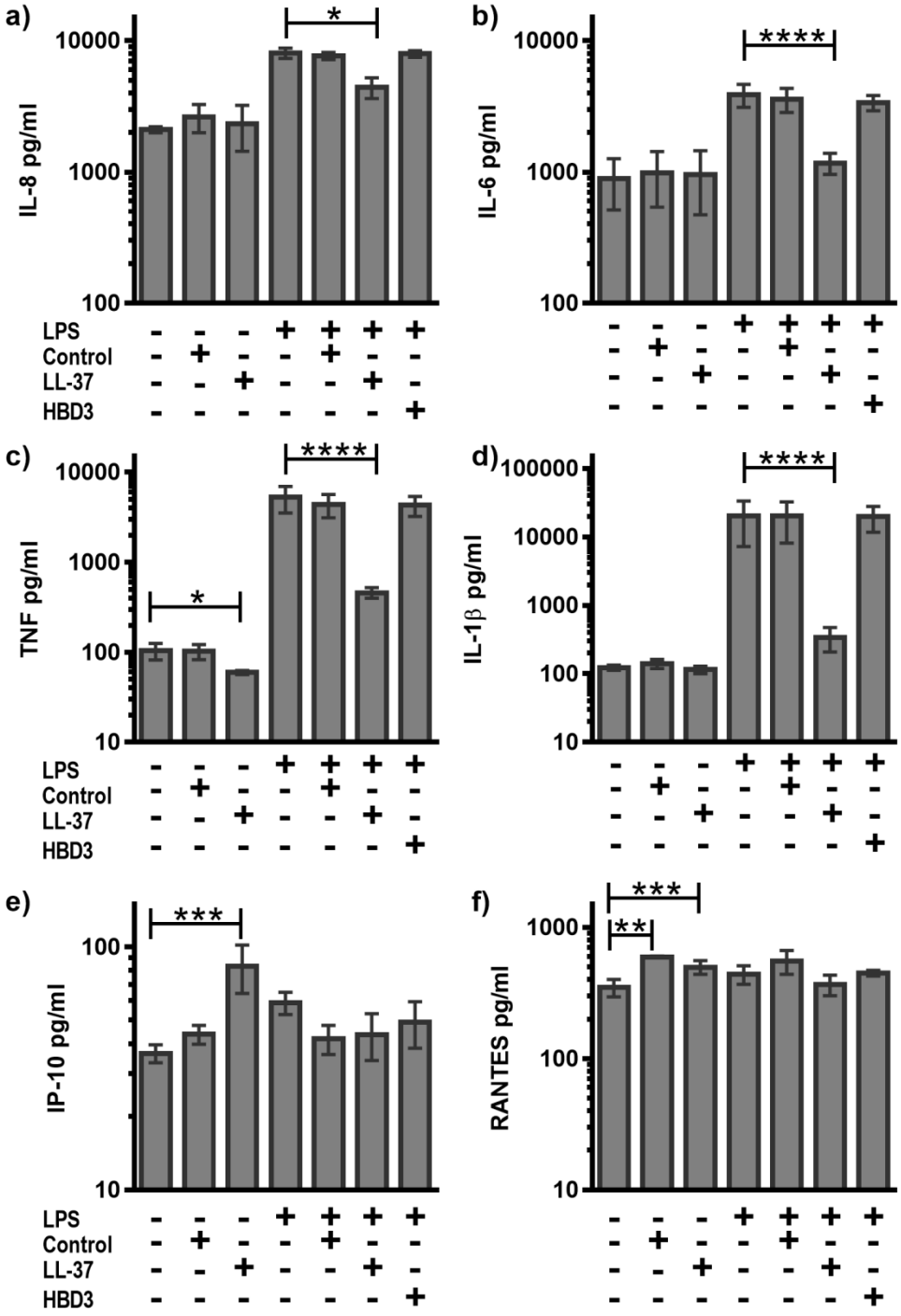

Figure 3.5 Effects of HDPs on Cytokine Secretion in Placenta Explants
Placenta explant cultures (n=3 patients) cytokine secretion after treatment; LPS [100ng/ml], control scrambled peptide [25µg/ml], LL-37 [25µg/ml] and hBD3 [5µg/ml]. (a) IL-8 (b) IL-6 (c) TNF (d) IL-1β (e) IP-10 and (f) RANTES protein measured by ELISA in culture supernatants 3 hours post-treatment. All data presented as mean concentration and SEM. (Two-way ANOVA (excluding hBD3 treatment), with Tukey's post-test; *, P <0.05, **, P <0.01, ***, P<0.001 compared to no-peptide treatments within LPS groups. Paired t-test comparing hDB3+LPS with LPS alone; NS difference)

LL-37 was able to significantly reduce the LPS induced increase in IL-8 ($P < 0.05$), IL-6 ($P < 0.0001$), TNF ($P < 0.0001$), and IL-1β ($P < 0.0001$). The addition of scrambled control peptide did not result in any significant change in levels of any cytokine compared to LPS treatment alone (two-way ANOVA with Tukey's post-test; compared to LPS alone).

hBD3 treatment did not have an effect on the levels of any of the cytokines measured in an environment of 100ng/ml of LPS (paired t-test, hBD3+LPS compared to LPS alone).

Although IP-10 and RANTES did not respond to LPS treatment, LL-37 peptide treatment alone did result in increased IP-10 ($P < 0.001$) and RANTES ($P < 0.001$) compared to no-treatment. As scrambled control peptide was also able to induce a significant RANTES response this effect does not look peptide specific. In addition IP-10 levels were at the lower limits of detection in this system and more likely subject to error.

To investigate whether the levels of TNF were also affected at the mRNA level, *TNF* gene expression was measured in the placental explants in response to LPS and HDPs by RT-qPCR (Figure 3.6). Exogenous scrambled control peptide or LL-37 alone had no effect on *TNF* gene expression (two-way ANOVA with Tukey's post-test). Addition of 100ng/ml LPS to placental explants significantly increased *TNF* ($P < 0.01$) in tissue collected 3-hours post treatment (two-way ANOVA; Bonferroni's post-test; no treatment compared to LPS only). Exogenous LL-37 ($P < 0.05$) but not scrambled control peptide was able to significantly reduce the LPS-induced rise in *TNF* mRNA expression.

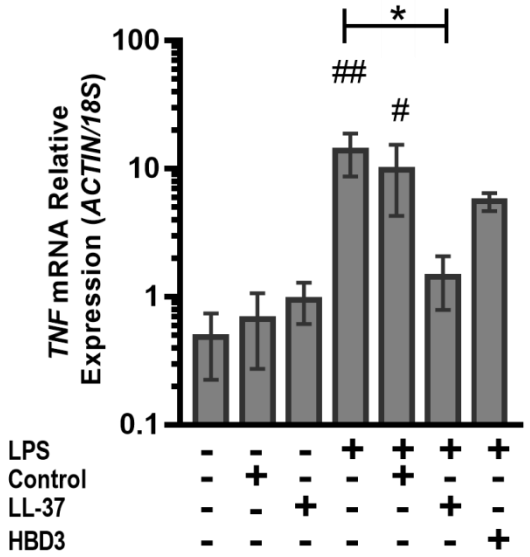

Figure 3.6 Effects of HDPs on *TNF* Gene Expression in Placenta Explants

Relative *TNF* gene expression levels in placenta explant cultures (n=3 patients) after treatment with; LPS [100ng/ml], control scrambled peptide [25µg/ml], LL-37 [25µg/ml] and hBD3 [5µg/ml]. Data presented is mean fold-increase and SEM, normalised to *β-ACTIN* and *18S*, relative to CAL (Two-way ANOVA (excluding hBD3 treatment) with Tukey's post-test; *, $P < 0.05$ compared to no-peptide treatments within LPS groups. Two-way ANOVA (excluding hBD3 treatment) with Bonferroni's post-test; ##, $P < 0.01$ no-treatment compared to LPS only. Paired t-test between LPS alone and LPS + hBD3; NS difference)

Levels of endogenous *DEFB103* (hBD3) and *CAMP* (LL-37) were measured by RT-qPCR in placental explants from no treatment compared to LPS [100ng/ml]. There was a trend for both of the HDPs to be increased following LPS treatment but neither reached significance in the sample size of 3 (paired t-test)

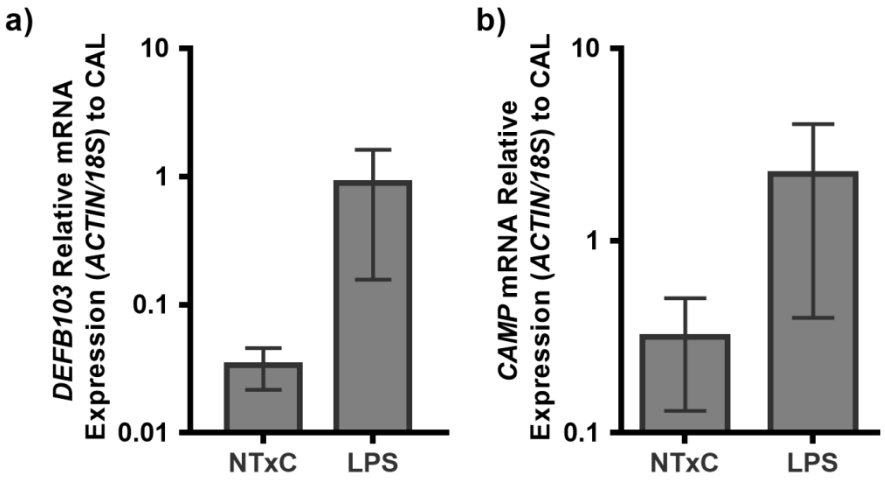

Figure 3.7 Endogenous *DEFB103* and *CAMP* mRNA in Placental Explants

Relative (a) *DEFB103* and (b) *CAMP* gene expression levels in placenta explant cultures (n=3 patients) with no-treatment (NTxC) or LPS [100ng/ml]. Data presented is mean and SEM, normalised to *β-ACTIN* and *18S* relative to calibrator (CAL). (Paired t-test: NS difference)

3.3.3 HDPs in the Murine Reproductive Tract

The relative expression of multiple defensin genes and cathelicidin were determined by RT-qPCR in non-pregnant C57BL/6N mice (n=6) (Figure 3.8). To account for variation in HDP gene expression during estrus cycling; mice were super-ovulated with PMSG/hCG combination prior to tissue collection as detailed in section 2.1.7.1. Vaginal lavages were also taken and stained with crystal violet to confirm vaginal cell cytology was similar across all mice as described in section 2.1.7.2. The genes considered were the mouse beta-defensins; *Defb1*, *Defb4*, *Defb6*, *Defb14*, the alpha defensin *Defa5*, and the murine cathelicidin *Camp*. Relative gene expression results are displayed compared to samples from the ovary, which was the site of lowest expression of all the defensins but not cathelicidin.

All beta-defensins investigated in this chapter show spatial expression patterns along the female reproductive tract. Beta-defensins were found to be highly expressed in tissues of the lower reproductive tract; the vagina and cervix. Comparatively there was lower expression of beta-defensins in tissues collected from the upper reproductive tract; the uterus and ovary. The mouse cathelicidin, *Camp*, displayed contrasting mRNA gene expression patterns to that of beta-defensins. *Camp* was only expressed at low levels in the vagina and had higher expression in the cervix, uterus and ovary (Figure 3.8.f).

Defb1 was expressed in vaginal tissues 2840 ± 476 fold higher than tissue from the ovary (Figure 3.8.a). Similarly, although high variation in a small sample size, the vaginal expression of *Defb6* and *Defb4* was on average 377 ± 134 and 5416 ±1476-fold higher respectively, compared to the expression in the ovary (Figure 3.8.b, Figure 3.8.d). *Defa5* was expressed in all tissues of the reproductive tract but did not show any spatial expression pattern (Figure 3.8.e).

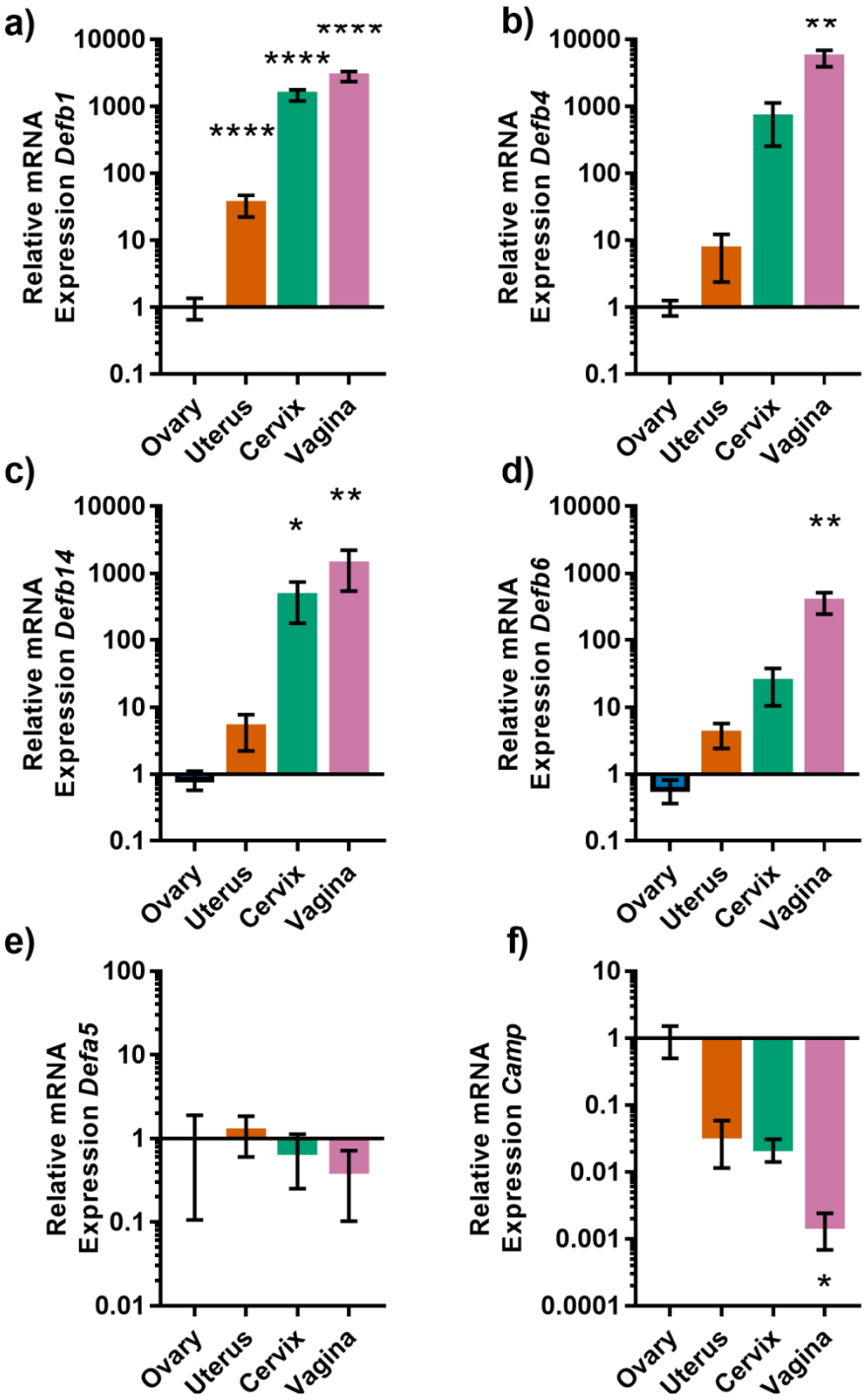

Figure 3.8 HDPs Gene Expression in the Mouse Reproductive Tract
Relative gene expression of (a) *Defb1*, (b) *Defb4*, (c) *Defb14*, (d) *Defb6*, (e) *Defa5*, and (f) *Camp* in non-pregnant mouse (n=6) tissue from ovary, uterus, cervix and vagina. Data presented as mean fold change and SEM, normalised to *β-Actin*, relative to ovary. (one-way ANOVA with Dunnett's post-test compared to ovary; *, P <0.05, **, P <0.01, ***, P<0.001, ****, P<0.0001)

3.3.3.1 Murine *Defb14* (*hBD3* orthologue) in Pregnancy

The mRNA gene expression of *Defb14* was assessed in the uterus, placenta and fetal membrane of C57BL/6N mice on day 17 of gestation (Figure 3.9). The uterus and placenta were positive for low levels of *Defb14* mRNA transcript but this was not reliably detected in fetal membrane tissues from the same animals in a steady-state.

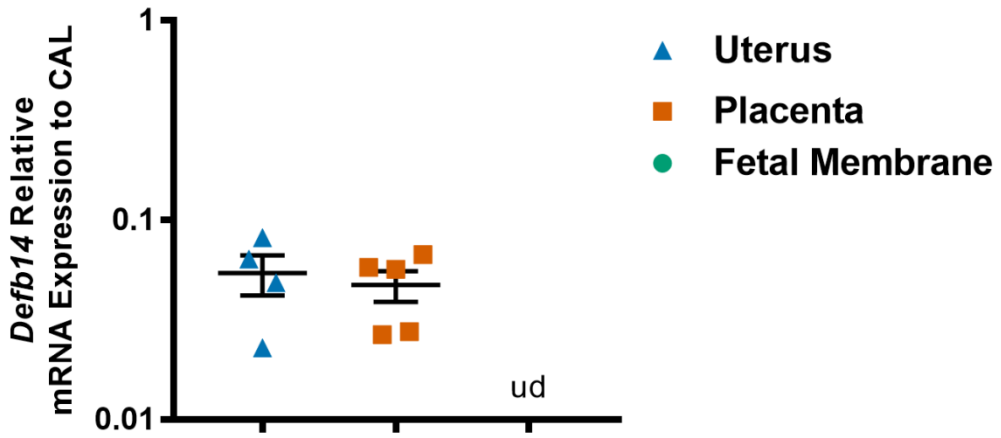

Figure 3.9 *Defb14* Gene Expression in Mouse Pregnancy Tissues
Relative *Defb14* gene expression in uterus (n=4), placenta (n=5) and fetal membrane tissues (n=5) in C57BL/6N mice. Data presented as mean and SEM, normalised to *β-Actin*, relative to calibrator (CAL). ud = undetected.

3.3.3.2 Murine *Camp* (LL-37 orthologue) in Pregnancy

The mRNA gene expression of *Camp* was also assessed in the uterus, placenta and fetal membrane of C57BL/6N mice on day 17 of gestation (Figure 3.10). All tissues were positive for low levels of *Camp* gene by RT-qPCR. In a steady-state, the expression of *Camp* in the placenta and fetal membrane is higher than in the uterus.

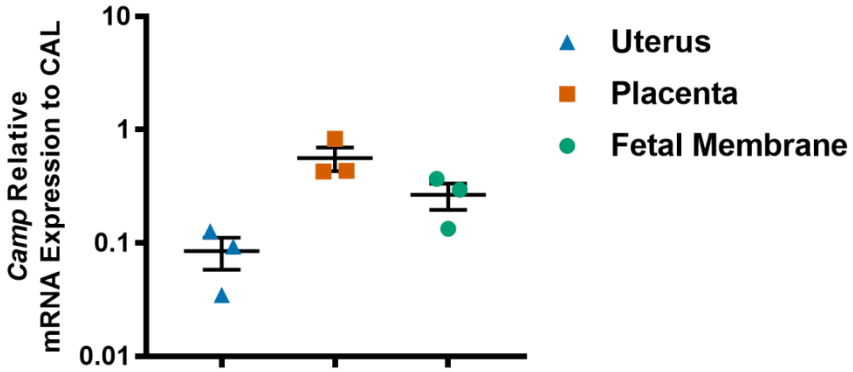

Figure 3.10 *Camp* Gene Expression in Mouse Pregnancy Tissues
Relative *Camp* gene expression in uterus (n=3), placenta (n=3) and fetal membrane tissues (n=3) in C57BL/6N mice. Data presented as mean and SEM, normalised to *β-Actin*, relative to calibrator (CAL).

3.4 Discussion

HDPs in Labour

In tissues and cells not of the reproductive tract, HDPs have been shown to modulate inflammation. Infection and inflammation are frequently associated with preterm labour in women. Preterm and term labour share a common terminal pathway characterised by anatomical, biochemical, and endocrine events (Snegovskikh et al., 2006). One aim of this chapter was to determine the effect of human term labour on the expression of HDPs in the fetal membranes, myometrium and placenta of women.

There was a small but significant increase in *DEFB103* levels in labouring tissue of the myometrium compared to non-labouring tissue. In humans, six of the beta-defensin genes on chromosome 8 are copy number variable, this includes *DEFB103*. Copy number has been shown to correlate with the protein expression and peptide level (Hollox et al., 2008, Jansen et al., 2009, Fellermann et al., 2006). The beta-defensin copy number of the women in this chapter was not determined, and could account for some inter- patient variation in gene transcript levels.

In the placenta there was a slight increase in *CAMP* gene expression in labour compared to non-labouring women. No difference in *CAMP* gene level was seen in the myometrium or amnion/chorion. This leads to the conclusion that resident epithelial cells of the myometrium and fetal membrane are not upregulating *CAMP* during labour.

LL-37 is a chemoattractant for the stimulation and mobilisation of neutrophils and eosinophils (Tjabringa et al., 2003). As leukocytes infiltrate uterine tissues around the time of labour (Osman et al., 2003), it was estimated that the myometrial samples in this chapter might have shown an increase in *CAMP* in labouring women. Although there may be leukocytes infiltrating to the myometrium in labouring samples; this is not contributing to mRNA gene transcript in this chapter. LL-37 peptide is stored pre-processed in neutrophils so it may have activity in labour at the protein level. Investigation of protein expression levels of LL-37 and co-localisation

with leukocyte markers would provide evidence for these cells supplying additional stores of LL-37 during labour. Indeed this is what Lim et al., (2015) had shown in the fetal membrane and myometrium. Lim et al., (2015) displayed that in labouring women, immunostaining for hCAP18/LL-37 co-localised with infiltrating leukocytes but also increased in resident amnion epithelium, chorionic trophoblasts and decidua, which is not what I found in this chapter at the mRNA gene transcript level.

HDPs in Placenta Explant Cultures

In this chapter, I have shown that LL-37 was able to significantly reduce the LPS induced increase in IL-8, IL-6, TNF, and IL-1β in placenta explant cultures. This anti-inflammatory effect of LL-37 *ex-vivo* is likely due to LL-37 directly binding to LPS. LL-37 can downregulate signalling through TLR-4 when coadministered with LPS by preventing the interaction with LPB, essential for TLR-4 activation. Not all of LL-37 anti-inflammatory properties are due to direct binding to LPS; pre-treatment with LL-37 prior to LPS can also suppress TNF protein production (Mookherjee et al., 2006). LL-37 can also act through disruption of TLR-4 receptor complex function when LPS is already bound to macrophage receptors (Rosenfeld et al., 2006). All actions can result in lower levels of pro-inflammatory cytokine production. It would be interesting to further investigate the mechanism of LL-37's anti-inflammatory action in placental explants. This could be achieved using inhibitors of known LL-37 receptors to elude what proportion of the effect might be due to actions other than LL-37 and LPS binding.

It would be interesting to investigate whether the mouse peptide, *CAMP* is also anti-inflammatory on murine placental tissues. This can be achieved by primary culture of mouse placental tissue with exogenous *CAMP* and LPS. *Camp-/-* mice also provide an additional control to that of human experiments where the endogenous *CAMP* contributing to the LPS response can be accounted for. The *in-vivo* equivalent to this has already somewhat been done in Chapter 7 of this thesis, where LPS was given intrauterine during pregnancy in wildtype and Cathelicidin knockout animals. In placental tissue, with a low dose of intrauterine LPS (1µg), there was a small but significant reduction in the chemokine *Cxcl1* and *Ptgs2* (Figure 7.13). The number of

animals in this treatment group was small and this difference was not seen when a higher dose of 20µg LPS was used.

It was surprising that RANTES was not increased in response to LPS in the placenta explant cultures in this chapter. Higher expression of RANTES (CCL5) and IL-8 (CXCL8) has been shown in trophoblast cell lines (Swan-71) after stimulation with LPS (Grasso et al., 2014). Interestingly, after interacting with maternal monocytes, these trophoblast cells did not modulate the expression of RANTES and IL-8 by LPS stimulation (Grasso et al., 2014). In this chapter, the placental explant cultures have high levels of blood, where maternal monocytes could modulate the expression of these cytokines. Moreover, there are conflicting reports as to whether placenta tissues express RANTES. Villous trophoblast only express very small amounts of RANTES (Nakada et al., 2011) whereas trophoblast cell lines (Swan-71, SVneo) express high amounts of RANTES which is increased in response to LPS and TNF (Grasso et al., 2014). This might be the reason for the difference in levels of RANTES in placenta explant cultures seen in this chapter compared to that reported in cell lines.

hBD3 has been shown to have potent anti-inflammatory effects on human and mouse primary monocytes in response to LPS (Semple et al., 2010, Semple et al., 2011). However, in this chapter, hBD3 treatment did not have an effect on the levels of any of the cytokines measured in an environment of 100ng/ml of LPS on placental explants. Only a single dose of hBD3 peptide [5µg/ml] was used in this chapter as this has previously been shown to have anti-inflammatory effects *in-vitro*. It would be ideal to conduct a dose response for hBD3 to further test any anti-inflammatory effects in the placenta.

Other defensins are present in the female reproductive tract, including Human beta-defensin 126 (*DEFB126*), an epididymis-specific secretory protein, which has the ability to inhibit LPS-induced inflammation in macrophage cell lines (Liu et al., 2012).

HDPs in Mouse Pregnancy

There are only a few studies that investigate defensins and cathelicidins in the mouse female reproductive tract (Hickey et al., 2013, Soboll et al., 2006). Hickey et al., (2013) measured the expression of several defensin genes in the murine vagina and uterus at different stages of estrus. In line with what this paper reported, in this chapter I have shown that many defensins are expressed at specific spatial patterns along the reproductive tract. Estrus cycling in mice is continuous but there are discrete phases; diestrus, proestrus, estrus and metestrus. In this chapter I used hormones to induced estrus in mice, which coincides with ovulatory follicle growth and vaginal neutrophil accumulation. I found beta-defensins including *Defb14* and *Defb4* were highly expressed in the lower reproductive tract during this phase which has continuous exposure to bacteria. Most defensins displayed reduced expression the further up the reproductive tract, which is presumably a sterile environment. Mice in the estradiol-dominant phase have peak defensin expression and it has been shown that treating mice directly with estradiol can protect against pathogens (Kaushic et al., 2003, Kaushic et al., 2000). The load of commensal bacteria in the vagina is also elevated in estrus compared to other stages (Noguchi et al., 2003). Estradiol treatment *in-vitro* has also been shown to enhance the production of HDPs, namely beta-defensin 2 (human orthologue of *Defb4)* in uterine epithelial cells. However, in humans the phase of the menstrual cycle dominated by progesterone has been shown to display more resistance to infection with various pathogens (reviewed in Wira et al., (2010). Another reason for lower defensin expression in the uterus could be to support implantation of the fetus that is immunologically different to the host.

Defb1 homozygous knockout mice have increased susceptibility to urinary tract infections whereby they were shown to retain *Staphylococcus* spp. in the bladder longer than wildtype mice (Morrison et al., 2002). *Defb6* has been shown to have tissue-specific expression in skeletal muscle along with esophagus, tongue, and trachea (Yamaguchi et al., 2001). *Defa5* has been found in epithelial cells of the vagina and is highly expressed in Paneth cells, the secretory granules of the small intestine.

In this study *Camp* mRNA was expressed highly in the ovary during estrus, the reasons for this are not clear but as *Camp* and LL-37 have been shown to be involve in tissue repair it could be playing a role in proliferation of the ovarian surface.

Pattern recognition receptors are not uniformly expressed along the reproductive tract and also show temporal expression patterns that coincide with estrus cycling in mice. The numbers of TLR-2 and TLR-5 molecules are higher in the vagina than uterus, whereas in general, TLR-4 is higher in the uterus than in the vagina (Hickey et al., 2013). This is most probably a co-adaption strategy, to allow host tolerances of commensal and mutualistic species while still being effective to detect invading pathogens. This has also been shown in humans where TLR-4 and the NOD-2 receptor are found at higher levels in the upper reproductive tract and reduces the further down the reproductive tract (Pioli et al., 2004, Hart et al., 2009). Other TLRs are more uniformly expressed along the reproductive tract, namely TLR-9, TLR-8 and TLR-7 (Hart et al., 2009), these TLRs in mice also displayed more consistent expression in the vagina and uterus regardless of the stage of estrus (Hickey et al., 2013, Soboll et al., 2006).

Whether changes in HDP levels alter the vaginal microbiome directly has not been established, but changes in levels are accompanied by alterations of commensal and pathogenic bacteria in humans and in mice (Mitchell et al., 2013, Fan et al., 2008, Soboll et al., 2006, Frew et al., 2014).

3.5 Summary

In summary, in this chapter I have shown:

- *DEFB103* and *CAMP* are expressed in myometrium, placenta and amnion/chorion tissues in term pregnancy.
- *DEFB103* expression was upregulated in the myometrium during normal labour, whereas *CAMP* expression was upregulated in the placenta.
- Placental explants respond to LPS challenge by increasing production of pro-inflammatory cytokines.
- LL-37 but not hBD3 peptide was able to modulate LPS induced inflammatory response by inhibiting the release of pro-inflammatory cytokines in the placenta.
- Beta-defensins; *Defb1*, *Defb4*, *Defb6, Defb14*, and the cathelicidin *Camp* show spatial expression patterns along the female reproductive tract in mice.

Chapter 4

Microbiome - 16S rRNA Gene Sequencing

Chapter 4 Microbiome - 16S rRNA Gene Sequencing

4.1 Introduction

Several methods for bacterial species identification and quantification are available to researchers; these methods classify bacteria to varying taxonomic levels and all have their associated advantages and disadvantages. Culture based studies can cause misrepresentation of some species due to selection in culture conditions. There are various indirect molecular based methods for measuring cell viability, such as membrane staining, membrane potential, flow cytometry and reporter gene analysis. Fluorescent in situ hybridization (FISH) is a commonly used technique for localisation and quantification of bacterial species. FISH probes, usually for the taxa specific expanse of the 16S rRNA gene, can be used on tissues sections of interest for localising bacterial taxa. FISH probes are advancing the specificity of genus-specific identification, however, the throughput and multiplexing capability is still limited compared to broad range techniques such as 16S rRNA gene sequencing. Whole-genome shotgun metagenomic sequencing can also be undertaken for microbiome analysis, where the entire genomic content in a sample is sequenced. This is becoming an ever more popular method for public health surveillance in analysis of outbreaks, but also in the study of antimicrobial resistance mechanisms and pathogenicity. While full genome sequencing generally can offer researchers the ability to classify bacteria to a greater taxonomic level, there is often a compromise with regards to sequencing depth. A metagenomic approach sequences the entire genomic content of a sample, which depending on how and where the sample is collected from can contain high levels of host DNA. This is not ideal when trying to keep the per sample cost low, as greater depth is needed to obtain microbial sequences. Target gene approaches such as 16S rRNA gene sequencing can offer increased read depth, which puts this approach in a better position to highlight low-abundant taxa that may be overlooked in shotgun sequencing.

The objectives of this chapter were to establish a next generation sequencing workflow for microbial species identification in murine vaginal and fecal samples. This microbiome analysis utilises the 16S rRNA gene as a target for phylogenetic

reconstruction and species identification. The microbiome field has yet to establish a gold standard for looking at microbial communities; workflows need to be tailored and validated for specific sites of interest. Multiple considerations are needed at almost every point of the workflow. In relation to sample processing, consideration is needed in; sampling method, sample storage duration, sample storage temperature and method of DNA extraction. Multiple considerations are also required when selecting a 16S rRNA gene interrogation method with regards to the amplicon primers, amplicon length, and sequencing platform limitations. Having sufficient read quality, read depth and choosing an appropriate method for OTU picking are also important factors in microbial species identification. Chimeric reads produced by PCR artifacts can lead to the false discovery of unique organisms and effect community inference. In this regard optimisation is needed to keep PCR cycles to the minimum needed for amplification, in addition to the stringent downstream bioinformatic filtering of proposed chimeric reads. Employing a paired end sequencing approach has the added benefit of sequence overlap, which helps to reduce sequencing artefact contribution to community inference. There are many bioinformatic tools available to researchers interrogating the 16S rRNA gene. Quantitative Insights in to Microbial Ecology (QIIME) (Caporaso et al., 2010b) and Mothur (Schloss et al., 2009) are among the most highly used. As 16S rRNA gene sequencing is becoming an ever popular choice from microbial species analysis there is an increasing amount of rRNA sequence data accessible in open databases such as SILVA (Quast et al., 2013), Ribosomal Database Project (RDP) (Cole et al., 2009), and Greengenes (DeSantis et al., 2006b).

4.2 Targeted 16S rRNA Gene Amplification

The bacterial 16S Ribosomal RNA gene is approximately 1500bp and consists of nine hyper-variable regions (V1-V9), that when sequenced can be used to identify bacteria taxonomy to the species or genus level (Figure 4.1). The microbial field has mixed opinion as to which hypervariable region provides the highest number of operational taxonomic units (OTUs) when using next generation sequencing

platforms. It is becoming increasingly clear this is dependent on the diversity of bacteria in the community sampled (Chakravorty et al., 2007). Nossa (2010) looked at sequence data from all nine hyper-variable regions and proposed that in human foregut samples the V3 and V4 region is the least effective at class level bacterial identification. However, Whiteley et al., (2012) regarded sequencing the V6 region not acceptable for environmental samples and suggested the V3-V4 region provides a more representative result. Recent *in-silico* work on human fecal samples demonstrated that the V3-V4 and V4-V5 regions would most likely give more OTUs than the other variable regions (Claesson et al., 2010). However, this predicted advantage was not seen in actual sequencing analysis (Claesson et al., 2010), most likely due to accumulation bias from the primers and the extraction method employed.

Comparable to other mucosal body sites, such as the gastrointestinal tract, the human vagina has considerably less bacterial species in terms of both diversity and bacterial load (Cho and Blaser, 2012, Ravel et al., 2011). At the current level of sequencing, the human vaginal microbiome is establishing around 200 bacterial assigned OTUs across study sets (Ravel et al., 2011, Drell et al., 2013, Martin et al., 2013). A large study on the human vaginal microbiome suggested that the V1-V2 region has greater variability than the V3 region for species identification of *Lactobacillus* and *Prevotella,* giving potential higher OTU counts (Ravel et al., 2012). In addition the V1-V3 region has been reported to have a higher degree of accuracy in classifying species (Kim et al., 2011), and also less species specific bias (Vilo and Dong, 2012).

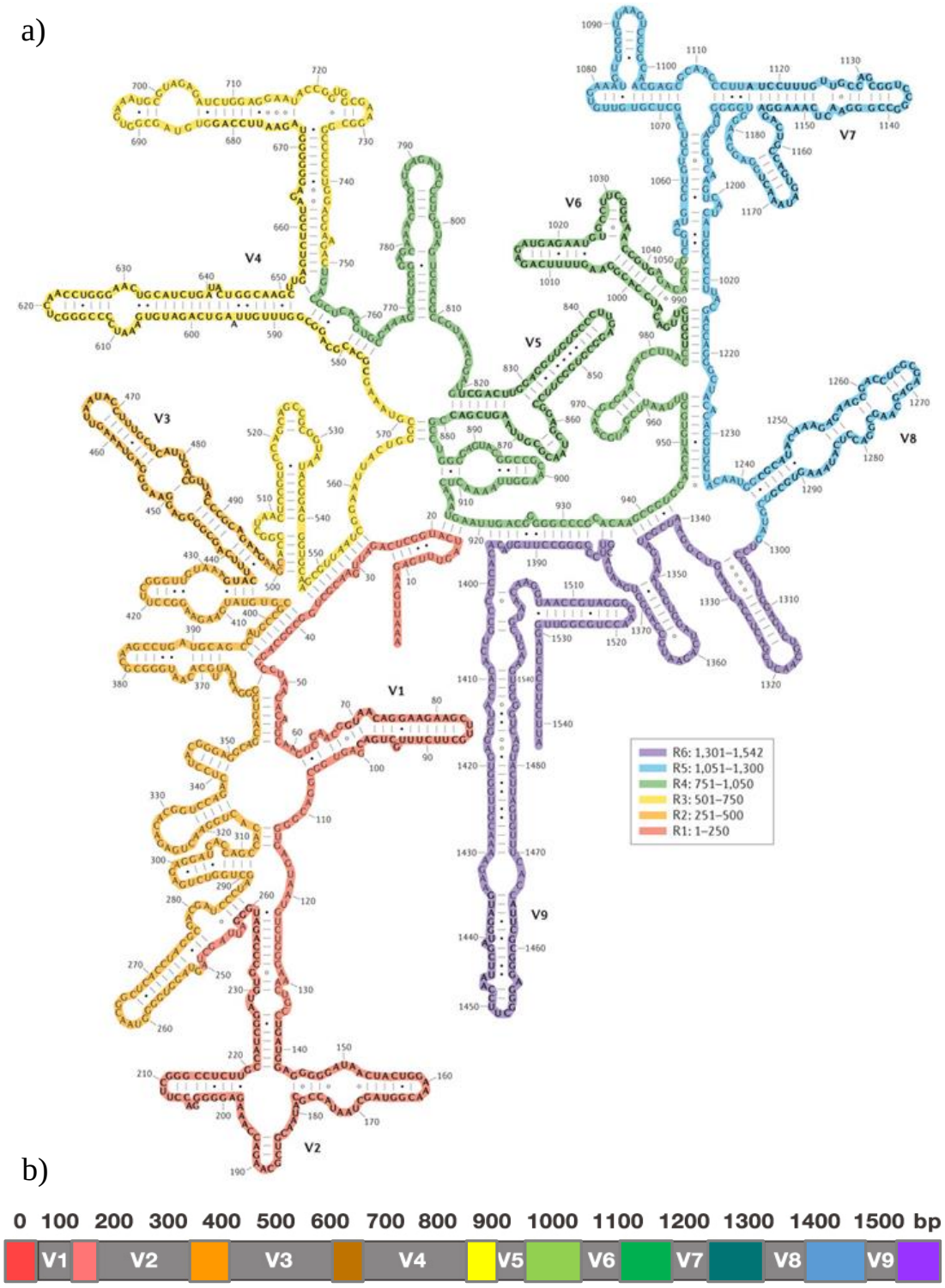

Figure 4.1 Schematic of the 16S rRNA Gene Variable Regions
(a) The predicted secondary structure of the 16S Ribosomal RNA gene (*E.coli*). Source: Yarza et al., (2014). (b) Schematic of the 16S Ribosomal RNA gene that is 1500bp and consists of nine hyper-variable regions (V1-V9). Variable regions are in grey, the colour regions represent conserved interspaced expanses. (Adapted from http://www.alimetrics.net/)

4.3 16S rRNA Copy Number qPCR

For quantification of 16S rRNA copy number, I optimised a qPCR assay using universal reference primers for the 16S rRNA gene and comparing to a sample of known copy number (gift from Nita Salzman).

The generation of the qPCR amplicon was detected using SYBR Green as the intercalating dsDNA dye. The unbound SYBR Green dye exhibits minimal fluorescence, upon binding to DNA the fluorescence is increased 100-fold. Therefore during qPCR, the increase in SYBR Green fluorescence is directly proportional to the quantity of dsDNA produced.

The universal primer sequences for 16S rRNA copy number assay were; UniF340 (5'- ACTCCTACGGGAGGCAGCAGT-3') and UniR514 (5'- ATTACCGCGGCTGCTGGC-3') which amplify a 179bp product spanning the V3 region of the 16S rRNA gene.

A 20µl reaction mix containing the qPCR reaction mastermix, reference gene primers and template were made as detailed in Table 4.1. For fecal samples the optimised template input was 1µl of a 1:100 dilution of extraction product in sterile molecular grade water. For the vaginal samples, which have a lower bacterial load, 1µl of extraction product, was used as the template. DNA extraction methods are detailed in section 4.7. All samples were run in triplicate and PCR cycling and fluorescence detection was supported on the LightCycler® 480 Real-Time PCR System using the parameters detailed in Table 4.2.

For absolute quantification, a 5-serial dilution of the sample of known copy number was used to create a standard curve. Ct value is the cycle at which the fluorescence signal crosses a threshold, where the threshold is an estimate of the first point where samples are in exponential phase above background. The Ct values of the standards are then used to determine the concentration of target DNA. Several qPCR negatives (PCR-NTC) and extraction negatives (EXT-NEG) and calibrators (*E.coli* DNA) were run on every qPCR plate. The efficiencies of the primers were evaluated using the

serial dilution of the sample of known copy number; this was determined to be within the acceptable range of E= 1.9-2.1.

Component	Final Concentration / Reaction	20µl Reaction
LightCycler490 SYBR	x1	10
Primer F [20µM]	0.4 µM	0.2
Primer R [20µM]	0.4 µM	0.2
Template	Variable	1.0
H_20	/	8.6

Table 4.1 qPCR Reaction Mix for 16S rRNA Copy Number Assay

Temperature	Time	Number of Cycles
50°C	2 minutes	x 1
95°C	10 minutes	x 1
95°C	30 seconds	x 45
63°C	30 seconds	

Table 4.2 qPCR Cycle Parameters for 16S rRNA Copy Number Assay

4.4 16S rRNA Gene Sequencing Primer Design

4.4.1 *In-silico* Variable Region Evaluation

The variable region chosen to sequence for bacterial identification in this study is the V1-V2 region of the 16S rRNA gene. This region was highlighted as a good candidate; firstly as literature suggested it has an advantage for discrimination of *Lactobacillus* spp. (Ravel et al., 2012), secondly this region displayed higher discrimination potential in a test-dataset, 'TEST-SET', I created *in-silico* (detailed below).

The 'TEST-SET' was comprised of 949 full length 16S rRNA sequences from species likely to be encountered in the; murine female reproductive tract (highlighted in culture studies), murine gastrointestinal tract (highlighted in 16S rRNA studies)

and sequences of species known to colonise the human vagina (highlighted in 16S rRNA studies). The two regions highlighted as potential candidates were the, V1-V2 region and the V4-V5, as amplicon products from both regions would be less than 500bp, which was a criterion for selection. Three pairwise percent identity matrixes were calculated in Clustal2.1 (Larkin et al., 2007) for; the full length 16S rRNA, the V1-V2 and the V4-V5 regions. Pairwise identity above 97% would suggest sequences are indistinguishable when clustering OTUs for microbial identification. The identity matrix for the full length 16S rRNA region calculated that 0.003% of the pairs had sequence similarity above 97%. The V1-V2 region matrix revealed only 0.0009% of the sequence pairs had higher than 97% similarity, whereas for the V4 - V5 matrix this was 0.01%. Therefore in this test data-set sequencing the V1-V2 region will identify more OTUs than if the V4-V5 region were sequenced. As the 'TEST-SET' contains the species which are likely to be encountered in this study the V1-V2 region was chosen as the desired amplicon region of the 16S rRNA gene.

The 16S rRNA V1-V2 hypervariable region is flanked by more conserved regions common to all bacteria, this allows for universal primer hybridisation and amplification. Even in the denoted 'conserved' regions no primer sites are totally conserved; where one primer pair will not amplify 100% of bacteria species even with miss-matches allowed. Deciding which one/ones to use depends on the complement of bacteria in the sample and each pair could slightly bias towards a certain type of bacteria (Milani et al., 2013). In the literature, there are over 30 forward and reverse primers that have been used as universal probes for the V1-V2 region (Klindworth et al., 2013). Klindworth et al., (2013) provides a great review of common universal 16S rRNA gene primers and conducted *in-silico* evaluation on coverage against the SILVA database.

4.4.2 *In-silico* Variable Region Primer Evaluation

An optimized primer set comprising of 27f-YM (universal forward 5'-AGAGTTTGATYMTGGCTCAG-3') and 338r (universal reverse 5'-TGCTGCCTYCCGTAGGAGT-3') were chosen to amplify the V1-V2 region based on the following criteria; the size of product did not exceed 500bp, annealing

temperatures were within 5°C, universal coverage of > 90% 16S rRNA sequences in SILVA database (v119), and universal coverage of > 90% 16S rRNA sequences in the 'TEST-SET'. The forward primer 27f-YM has 92.2% coverage (one mismatch) and the reverse primer 338r has 95.2% coverage of bacterial sequences in the SILVA database (one mismatch). The forward primer is commonly referred to as 27f-YM as it ends at *E.coli* position 27 of the 16S rRNA gene and has the degenerate bases YM. The forward 27f-YM represents four discrete primer sequences. The reverse primer sequence 338r, which ends at *E.coli* position 388, also has a degenerate base that represents two discrete primer sequences.

Sequencing in this study was done on two platforms; the Ion Torrent PGM (life technologies) and the Illumina MiSeq. Each platform has associated platform specific primer sequences that are incorporated into the fusion primers, detailed in section 4.8.2 and 4.8.1 respectively. On both platforms 27f-YM (universal forward) and 338r (universal reverse) were used as the complementary sequence for 16S rRNA gene amplification.

For the MiSeq primers only, mixtures of four forward 27f primers were used to maximise discovery of all bacterial species. This mixture has been shown to eliminate PCR bias and maintain the best ratio of *Lactobacillus* spp. to *Gardnerella* spp. as determined by qPCR (Frank et al., 2008, Romero et al., 2014). The forward primer mix consisted of 4 parts 27f-YM (the universal forward), and one part of each 27f-Bif, 27f-Bor and 27f-Chl, these primers are specific for the amplification of *Bifidobacteriaceae*, *Borrelia* and *Chlamydiales* respectively (Table 4.7). The universal primer 27f-YM alone would not amplify these species in stringent conditions. The degenerate bases within the forward primer mix provide seven discrete primer sequences.

For reference, the universal forward primer (27f-YM) best matches 'S-D-Bact-0008-b-S-20', and the universal reverse primer (338r) best matches 'S-D-Bact-0338-a-A-19' in Klindworth et al., (2013) nomenclature.

4.5 Contamination Considerations

An important consideration for microbial sequencing is contamination from laboratory equipment, molecular grade water, PCR reagents and extraction kits. Many of the extraction kits used for microbiome analysis are known to have low level contaminants (Salter et al., 2014). This is of particular importance with low biomass samples such as from the murine vagina in this study. It is often not possible to exclude these contaminates without additional sequencing of various negative controls from each kit batch.

In this study extraction kits were ordered in bulk from the same manufacture lot number to reduce and account for any lot specific contamination. For quality control, extraction negatives were included in every batch of extractions. To reduce potential contamination, equipment was cleaned with 70% alcohol, UV treated where suitable, and then cleaned with RNAzap. Extractions and subsequent PCRs were carried out in a designated PCR clean-room.

4.6 Sampling method

Fecal Sampling

Clean autoclaved cages were used as collection containers for fecal sampling of each mouse. One fecal pellet per mouse was immediately collected using disposable sterile forceps into sterile 2ml tubes and kept at 4°C within 20 minutes and -80°C within 2 hours. As the bacterial load in murine fecal samples is very high there was little optimisation needed with regards to sampling approach and yield.

Vaginal Sampling

As the murine vagina has low biomass, different sampling methods were compared to evaluate bacterial load recovery. One sampling method was a vaginal lavage, where 200µl of sterile physiological saline [Sodium Chloride 0.9%] is washed in the vagina 5 times and then extracted as detailed in section 4.7 using the PowerSoil®

DNA Isolation Kit. In the second method, whole vaginal tissue were internally excised, cut longitudinally and then extracted. To determine whether there are higher bacteria yield from vaginal lavages as compared to whole vaginal tissue extractions, the 16S rRNA gene copy number was determined as previously described. Although there was no significant difference in the mean bacteria yield between methods (P; 0.1791), there was a trend for whole tissue extraction to be more consistent and the coefficient of variation was smaller (Figure 4.2). For this reason this study adopted post-mortem sampling of whole vaginal tissue for bacterial extraction.

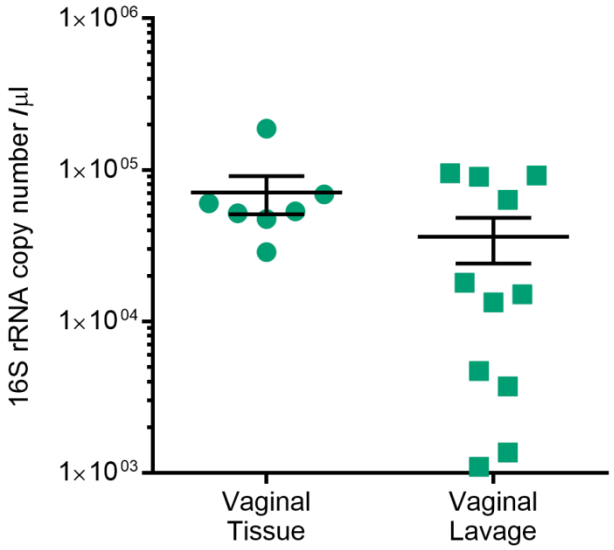

Figure 4.2 16S rRNA Copy Number; Murine Vaginal Sampling Optimisation
Copy number of 16S rRNA gene per µl as determined by qPCR for whole vaginal tissue (n=7) and vaginal lavage (n=11) extracted using the PowerSoil® DNA Isolation Kit. (NS difference; Mann–Whitney U test)

4.7 Bacterial DNA Extraction

The method of bacterial DNA extraction has a profound impact in community structure as different methods can have bias in the lysis of certain bacterial cell walls (Milani et al., 2013, Wesolowska-Andersen et al., 2014). Two different extraction kits were used in this study for microbial DNA isolation, the PowerSoil® Isolation Kit and the FastDNA® SPIN Kit. DNA extractions using either kit were carried out according to the manufacturer's instructions. The PowerSoil® DNA Isolation Kit is the method of choice for the Human Microbiome Project (Human Microbiome, 2010) and was initially used in this study for samples sequenced on the Ion Torrent platform. However, recent publication suggested that for low biomass samples, the FastDNA® SPIN Kit with bead-beating may yield better results and less bias towards *Bacteroidetes* phylum than the PowerSoil® DNA Isolation Kit (Milani et al., 2013, Wesolowska-Andersen et al., 2014). FastDNA® SPIN Kit for DNA extraction gave more consistent bacterial yields from vaginal tissue than the PowerSoil® DNA Kit (Figure 4.3). This method was adopted for all samples both fecal and vaginal run on the MiSeq platform.

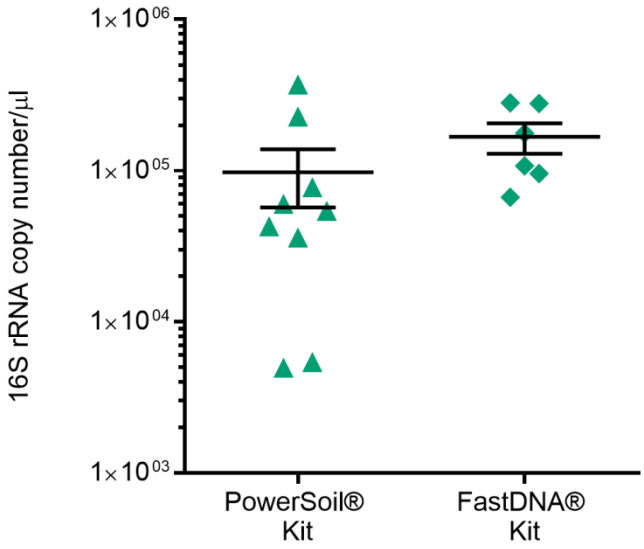

Figure 4.3 16S rRNA Copy Number; Extraction Kit Optimisation
Copy number of 16S rRNA gene per µl as determined by qPCR for whole vaginal tissue using the PowerSoil® DNA Isolation Kit (n=9) or the FastDNA® SPIN Kit (n=6) (NS difference; Mann–Whitney U test)

4.8 Library Preparation

4.8.1 Illumina MiSeq Primer Design and PCR Optimisation

The number of sequence reads generated on an Illumina MiSeq lane vastly exceeds the number of reads needed per sample for species identification. For this reason and to reduce per-sample sequencing costs, amplicon libraries were pooled in a 64-plex.

The complementary forward and reverse primer regions have been designed to be as universal as possible for bacterial species likely to be encountered in biological specimens from the vagina, but also murine gastrointestinal sites. Specific consideration has been given to accurately represent bacterial species common to the vagina by mixing 4 different forward primers in specific proportions (see section 4.4.2).

For multiplexing capability, the forward and reverse primers are indexed with TruSeq index sequences. Primers have been designed such that they contain the correctly orientated standard MiSeq sequencing and indexing primer sites that are compatible with MiSeq HP10, HP11 and HP12. These Illumina sequencing and indexing primers are contained within the reagent cartridge as standard. To account for possible low complexity in the library pool, heterogeneity spacers were incorporated into the designed fusion primers. To reduce oligo crosstalk, oligonucleotides with TruGrade™ processing were synthesised from IDT (Integrated DNA Technologies). Full MiSeq primer sequences are given in Table 4.7 and Table 4.8. Primers were checked for possibility of secondary structure formation and primer dimers.

Optimisation is required to get strong amplification results using fusion primers. To optimise PCR conditions for MiSeq library preparation several PCR parameters were compared, namely; template volume, template 16S rRNA copy number, cycle number, annealing temperature, polymerase, and use of reducing agents.

Component	Final Concentration / Reaction	50µl Reaction
Q5® Reaction Buffer 5x	x1	10
dNTPs [10mM]	0.1mM	1
Primer F [10µM]	0.1µM	0.5
Primer R [10µM]	0.1µM	0.5
Q5 *Taq*	0.01U/µl	0.2
Q5® High GC Enhancer 5x	x1	10
Template	Variable *	Variable
H20	/	# to 50µl vol

Table 4.3 PCR Reaction Mix; MiSeq 16S rRNA Amplicon Library
* 2ng for fecal samples/ 20,000 copies of 16S rRNA for vaginal samples/ 5µl PCR nested PCR product

For fecal samples, the optimised template input was 2ng of extracted DNA as quantified by Qubit™ 2 Fluorometer using Qubit dsDNA BS Assay Kit following the manufacture's protocol. For the vaginal samples, which have higher host DNA contribution to total DNA, the copy number of 16S rRNA gene was determined by qPCR as previously described. Template volumes equal to 20,000 copies or 12µl (max volume) were added to each PCR reaction.

All amplifications were performed in a 50µl total reaction mixture volume according to Table 4.4. Q5® High-Fidelity DNA Polymerase reaction Buffer contains 2mM Mg^{2+}.

Temperature	Time	Number of Cycles
98°C	30 seconds	x 1
98°C	10 seconds	x20 Fecal Samples + Nested x30 Vaginal Samples
50°C	30 seconds	
72°C	30 seconds	

Table 4.4 PCR Cycle Parameters; MiSeq 16S rRNA Amplicon Library

A large proportion of samples from the murine vagina did not show specific bands at x20 and x30 PCR cycles using the conditions described in Table 4.4 and Table 4.5. Various additional attempts were made to optimise the conditions for these low biomass samples; including changing the PCR annealing temperature, reducing agent and PCR approach. A nested PCR protocol was adopted which involves two rounds of PCR. The first round of PCR used the universal primer sequences 8f (5'-AGAGTTTGATYMTGGCTCAG-3') and 805r (5'-GACTACCAGGGTATCTAAT-3') to amplify an extended region of the 16S rRNA gene spanning V1 to V4. Unincorporated primers and dNTPs were enzymatically digested using ExoSAP-IT® according to the manufacturer's instructions. 5µl of the cleaned PCR product is then used as the template for the second round of PCR, which uses the MiSeq fusion primers and PCR conditions previously detailed in Table 4.4. The PCR cycle conditions and reaction mix used in both steps were the same, only the primers were changed. This type of nested PCR approach is known to have effect downstream on community inference and structure (Yu et al., 2015). Therefore for consistency and validity a nested PCR approach was adopted for all vaginal samples sequenced on the MiSeq platform, including those samples that had a specific band at x20 cycles in the one-step method.

PCR product size and purity of the amplified library were checked by performing gel electrophoresis as described in section 4.8.3. A single specific band is seen in all products of a size around 500bp (Figure 4.4); extraction and PCR negative show no specific band.

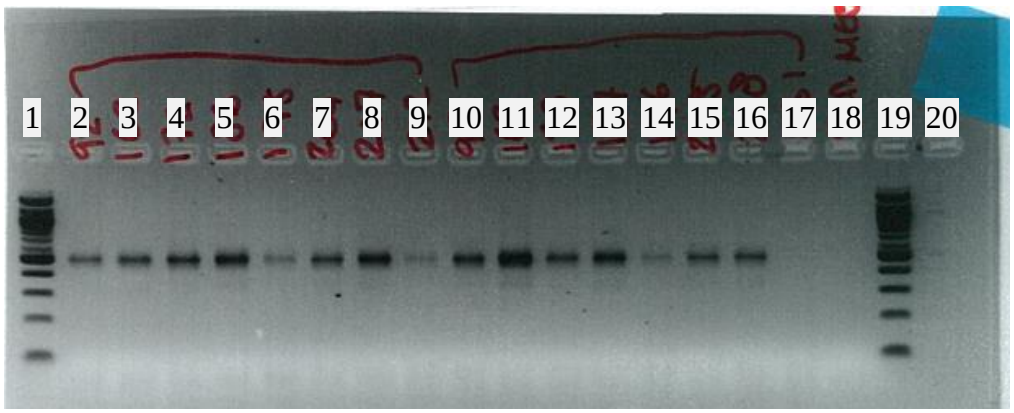

Figure 4.4 Gel Photo; MiSeq 16S rRNA Amplicon Library
Representative gel electrophoresis showing a single specific band in all products of a size around 500bp on a 2% agarose gel, with 100bp ladder (Lane 1 and 19). Lane 17 is extraction negative (EXT-NEG), lane 18 is the non-template control PCR negative (PCR-NTC). Lanes 2 – 16 are from fecal extractions using x20 PCR cycles. Lane 20 is blank.

4.8.2 Ion Torrent PGM Primer Design and PCR Optimisation

Microbial sequencing on the Ion Torrent PGM platform using the 400bp Sequencing Chemistry Kit and PGM 314 chip took advantage of dual-indexed fusion-primers to reduce per sample cost. Forward and reverse fusion primers were designed to include the sequences 27f and 338r respectively (as described in section 4.4.2) to amplify the V1-V2 variable region of the 16S rRNA gene. I designed these primers to include, at the 5' end, one of two adaptor sequences (adaptor trP1 or adaptor A) linking to a unique barcode tag (IonXpressBarcode). Short linkers 'Key' and 'Barcode-Adapter' sequences were also included. All primers were HPLC synthesised by Sigma® Life Science; the complete list of Ion Torrent fusion-primers used in this study are shown in Table 4.9. Primers were checked for possibility of secondary structure formation and primer dimers.

To optimise PCR conditions for Ion Torrent PGM library preparation, several PCR parameters were compared as before, namely; template volume, template 16S rRNA copy number, cycle number, annealing temperature, polymerase, and use of reducing agents.

For fecal samples the optimised template input was 1.5ng of extracted DNA, as determined by Qubit™ 2 Fluorometer using Qubit dsDNA BR Assay Kit. For the vaginal samples, which have higher host DNA contribution to total DNA, the copy number of 16S rRNA gene was determined by qPCR. Template volumes equal to 20,000 copies or 12µl (max volume) were added to PCR reaction.

All amplifications were performed in a 50µl total reaction mixture volume according to Table 4.5. Q5® High-Fidelity DNA Polymerase reaction Buffer contains 2mM Mg^{2+}.

Component	Final Concentration / Reaction	50µl Reaction
Q5® Reaction Buffer 5x	x1	10
dNTPs [10mM]	0.2mM	1
Primer F [10µM]	0.2µM	1
Primer R [10µM]	0.2µM	1
Q5 *Taq*	0.01U/µl	0.2
Q5® High GC Enhancer 5x	x1	10
Template	1.5ng / 20,000 copies	Variable
H20		* to 50µl vol

Table 4.5 PCR Reaction Mix; Ion Torrent 16S rRNA Amplicon Library

The optimised PCR thermocycler conditions for amplification are given in Table 4.6. For vaginal samples the number of cycles was increased to 30. PCR product size and purity were checked by performing gel electrophoresis as described in section 4.8.3. A single specific band is seen in all products of a size around 420bp and extraction (EXT-NEG) and PCR negatives (PCR-NTC) show no specific band (Figure 4.5).

Temperature	Time	Number of Cycles
98°C	2 minutes	x 1
98°C	30 seconds	x20 Fecal Samples + Nested x30 Vaginal Samples
60°C	30 seconds	
72°C	40 seconds	

Table 4.6 PCR Cycle Parameters; Ion Torrent 16S rRNA Amplicon Library

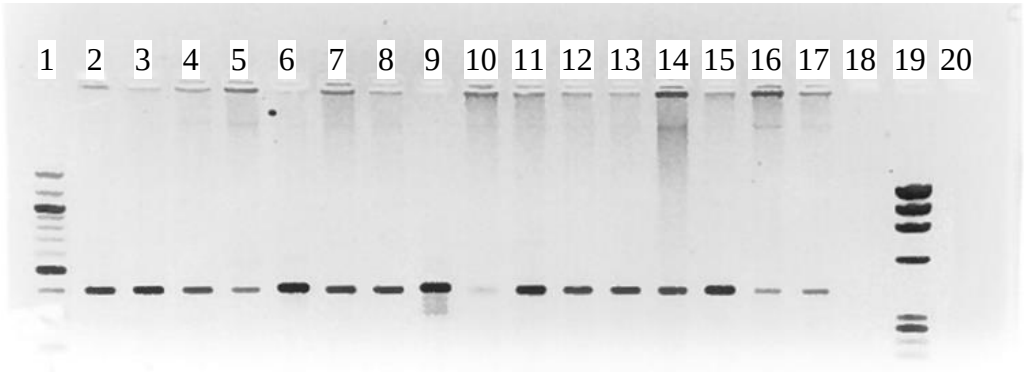

Figure 4.5 Gel Photo; 16S rRNA Amplicon Library
Representative gel electrophoresis showing a single specific band in most products of a size around 420bp on a 2% agarose gel, with 100bp ladder (Lane 1) and PhiX ladder (Lane 19). Lane 18 is extraction negative (EXT-NEG), Lane 20 is non-template control PCR negative (PCR-NTC). Lanes 2-17 are from vaginal extractions using x30 PCR cycles.

Forward Primer Name	P7 Grafting Sequence:	Index (i7):	P7 Sequencing Primer:	Heterogeneity Spacer:	16S rRNA Complementary Region (V1)
27F_YM_MISEQ_D701	CAAGCAGAAGACGGCATACGAGAT	CGAGTAAT	GTGACTGGAGTTCAGACGTGTGCTCTTCCGATCT		AGAGTTTGATYMTGGCTCAG
27F_YM_MISEQ_D702	CAAGCAGAAGACGGCATACGAGAT	TCTCCGGA	GTGACTGGAGTTCAGACGTGTGCTCTTCCGATCT		AGAGTTTGATYMTGGCTCAG
27F_YM_MISEQ_D703	CAAGCAGAAGACGGCATACGAGAT	AATGAGCG	GTGACTGGAGTTCAGACGTGTGCTCTTCCGATCT	T	AGAGTTTGATYMTGGCTCAG
27F_YM_MISEQ_D704	CAAGCAGAAGACGGCATACGAGAT	GGAATCTC	GTGACTGGAGTTCAGACGTGTGCTCTTCCGATCT	T	AGAGTTTGATYMTGGCTCAG
27F_YM_MISEQ_D705	CAAGCAGAAGACGGCATACGAGAT	TTCTGAAT	GTGACTGGAGTTCAGACGTGTGCTCTTCCGATCT	GT	AGAGTTTGATYMTGGCTCAG
27F_YM_MISEQ_D706	CAAGCAGAAGACGGCATACGAGAT	ACGAATTC	GTGACTGGAGTTCAGACGTGTGCTCTTCCGATCT	GT	AGAGTTTGATYMTGGCTCAG
27F_YM_MISEQ_D707	CAAGCAGAAGACGGCATACGAGAT	AGCTTCAG	GTGACTGGAGTTCAGACGTGTGCTCTTCCGATCT	CGA	AGAGTTTGATYMTGGCTCAG
27F_YM_MISEQ_D708	CAAGCAGAAGACGGCATACGAGAT	GCGCATTA	GTGACTGGAGTTCAGACGTGTGCTCTTCCGATCT	CGA	AGAGTTTGATYMTGGCTCAG
27F_Bif_MISEQ_D701	CAAGCAGAAGACGGCATACGAGAT	CGAGTAAT	GTGACTGGAGTTCAGACGTGTGCTCTTCCGATCT		AGGGTTCGATTCTGGCTCAG
27F_Bif_MISEQ_D702	CAAGCAGAAGACGGCATACGAGAT	TCTCCGGA	GTGACTGGAGTTCAGACGTGTGCTCTTCCGATCT		AGGGTTCGATTCTGGCTCAG
27F_Bif_MISEQ_D703	CAAGCAGAAGACGGCATACGAGAT	AATGAGCG	GTGACTGGAGTTCAGACGTGTGCTCTTCCGATCT	T	AGGGTTCGATTCTGGCTCAG
27F_Bif_MISEQ_D704	CAAGCAGAAGACGGCATACGAGAT	GGAATCTC	GTGACTGGAGTTCAGACGTGTGCTCTTCCGATCT	T	AGGGTTCGATTCTGGCTCAG
27F_Bif_MISEQ_D705	CAAGCAGAAGACGGCATACGAGAT	TTCTGAAT	GTGACTGGAGTTCAGACGTGTGCTCTTCCGATCT	GT	AGGGTTCGATTCTGGCTCAG
27F_Bif_MISEQ_D706	CAAGCAGAAGACGGCATACGAGAT	ACGAATTC	GTGACTGGAGTTCAGACGTGTGCTCTTCCGATCT	GT	AGGGTTCGATTCTGGCTCAG
27F_Bif_MISEQ_D707	CAAGCAGAAGACGGCATACGAGAT	AGCTTCAG	GTGACTGGAGTTCAGACGTGTGCTCTTCCGATCT	CGA	AGGGTTCGATTCTGGCTCAG
27F_Bif_MISEQ_D708	CAAGCAGAAGACGGCATACGAGAT	GCGCATTA	GTGACTGGAGTTCAGACGTGTGCTCTTCCGATCT	CGA	AGGGTTCGATTCTGGCTCAG
27F_Bor_MISEQ_D701	CAAGCAGAAGACGGCATACGAGAT	CGAGTAAT	GTGACTGGAGTTCAGACGTGTGCTCTTCCGATCT		AGAGTTTGATCCTGGCTTAG
27F_Bor_MISEQ_D702	CAAGCAGAAGACGGCATACGAGAT	TCTCCGGA	GTGACTGGAGTTCAGACGTGTGCTCTTCCGATCT		AGAGTTTGATCCTGGCTTAG
27F_Bor_MISEQ_D703	CAAGCAGAAGACGGCATACGAGAT	AATGAGCG	GTGACTGGAGTTCAGACGTGTGCTCTTCCGATCT	T	AGAGTTTGATCCTGGCTTAG
27F_Bor_MISEQ_D704	CAAGCAGAAGACGGCATACGAGAT	GGAATCTC	GTGACTGGAGTTCAGACGTGTGCTCTTCCGATCT	T	AGAGTTTGATCCTGGCTTAG
27F_Bor_MISEQ_D705	CAAGCAGAAGACGGCATACGAGAT	TTCTGAAT	GTGACTGGAGTTCAGACGTGTGCTCTTCCGATCT	GT	AGAGTTTGATCCTGGCTTAG
27F_Bor_MISEQ_D706	CAAGCAGAAGACGGCATACGAGAT	ACGAATTC	GTGACTGGAGTTCAGACGTGTGCTCTTCCGATCT	GT	AGAGTTTGATCCTGGCTTAG
27F_Bor_MISEQ_D707	CAAGCAGAAGACGGCATACGAGAT	AGCTTCAG	GTGACTGGAGTTCAGACGTGTGCTCTTCCGATCT	CGA	AGAGTTTGATCCTGGCTTAG
27F_Bor_MISEQ_D708	CAAGCAGAAGACGGCATACGAGAT	GCGCATTA	GTGACTGGAGTTCAGACGTGTGCTCTTCCGATCT	CGA	AGAGTTTGATCCTGGCTTAG
27F_Chl_MISEQ_D701	CAAGCAGAAGACGGCATACGAGAT	CGAGTAAT	GTGACTGGAGTTCAGACGTGTGCTCTTCCGATCT		AGAATTTGATCTTGGTTCAG
27F_Chl_MISEQ_D702	CAAGCAGAAGACGGCATACGAGAT	TCTCCGGA	GTGACTGGAGTTCAGACGTGTGCTCTTCCGATCT		AGAATTTGATCTTGGTTCAG
27F_Chl_MISEQ_D703	CAAGCAGAAGACGGCATACGAGAT	AATGAGCG	GTGACTGGAGTTCAGACGTGTGCTCTTCCGATCT	T	AGAATTTGATCTTGGTTCAG
27F_Chl_MISEQ_D704	CAAGCAGAAGACGGCATACGAGAT	GGAATCTC	GTGACTGGAGTTCAGACGTGTGCTCTTCCGATCT	T	AGAATTTGATCTTGGTTCAG
27F_Chl_MISEQ_D705	CAAGCAGAAGACGGCATACGAGAT	TTCTGAAT	GTGACTGGAGTTCAGACGTGTGCTCTTCCGATCT	GT	AGAATTTGATCTTGGTTCAG
27F_Chl_MISEQ_D706	CAAGCAGAAGACGGCATACGAGAT	ACGAATTC	GTGACTGGAGTTCAGACGTGTGCTCTTCCGATCT	GT	AGAATTTGATCTTGGTTCAG
27F_Chl_MISEQ_D707	CAAGCAGAAGACGGCATACGAGAT	AGCTTCAG	GTGACTGGAGTTCAGACGTGTGCTCTTCCGATCT	CGA	AGAATTTGATCTTGGTTCAG
27F_Chl_MISEQ_D708	CAAGCAGAAGACGGCATACGAGAT	GCGCATTA	GTGACTGGAGTTCAGACGTGTGCTCTTCCGATCT	CGA	AGAATTTGATCTTGGTTCAG

Table 4.7 MiSeq Forward Primer Sequences

Primers are split into components for ease of visualisation. All Primers shown 5'-3' across the row left to right.

Reverse Primer Name	P5 Grafting Sequence:	Index (i5):	P5 Sequencing primer:	Heterogeneity Spacer:	16S rRNA Complementary Region (V2):
338R_MISEQ_D501	AATGATACGGCGACCACCGAGATCTACAC	TATAGCCT	ACACTCTTTCCCTACACGACGCTCTTCCGATCT		TGCTGCCTYCCGTAGGAGT
338R_MISEQ_D502	AATGATACGGCGACCACCGAGATCTACAC	ATAGAGGC	ACACTCTTTCCCTACACGACGCTCTTCCGATCT		TGCTGCCTYCCGTAGGAGT
338R_MISEQ_D503	AATGATACGGCGACCACCGAGATCTACAC	CCTATCCT	ACACTCTTTCCCTACACGACGCTCTTCCGATCT	A	TGCTGCCTYCCGTAGGAGT
338R_MISEQ_D504	AATGATACGGCGACCACCGAGATCTACAC	GGCTCTGA	ACACTCTTTCCCTACACGACGCTCTTCCGATCT	A	TGCTGCCTYCCGTAGGAGT
338R_MISEQ_D505	AATGATACGGCGACCACCGAGATCTACAC	AGGCGAAG	ACACTCTTTCCCTACACGACGCTCTTCCGATCT	TC	TGCTGCCTYCCGTAGGAGT
338R_MISEQ_D506	AATGATACGGCGACCACCGAGATCTACAC	TAATCTTA	ACACTCTTTCCCTACACGACGCTCTTCCGATCT	TC	TGCTGCCTYCCGTAGGAGT
338R_MISEQ_D507	AATGATACGGCGACCACCGAGATCTACAC	CAGGACGT	ACACTCTTTCCCTACACGACGCTCTTCCGATCT	CTA	TGCTGCCTYCCGTAGGAGT
338R_MISEQ_D508	AATGATACGGCGACCACCGAGATCTACAC	GTACTGAC	ACACTCTTTCCCTACACGACGCTCTTCCGATCT	CTA	TGCTGCCTYCCGTAGGAGT

Table 4.8 MiSeq Reverse Primer Sequences

Primers are split into components for ease of visualisation. All Primers shown 5'-3' across the row left to right.

Forward Primer Name	Ion Torrent Adapter: A/trP1	KEY	IonXpressBarcode	Barcode Adapter	16S rRNA Complementary Region (V1/V2)
IT_27F_YM_Index_1	CCATCTCATCCCTGCGTGTCTCCGAC	TCAG	CTAAGGTAAC	GAT	AGTTTGATYMTGGCTCAG
IT_27F_YM_Index_2	CCATCTCATCCCTGCGTGTCTCCGAC	TCAG	TAAGGAGAAC	GAT	AGTTTGATYMTGGCTCAG
IT_27F_YM_Index_3	CCATCTCATCCCTGCGTGTCTCCGAC	TCAG	AAGAGGATTC	GAT	AGTTTGATYMTGGCTCAG
IT_27F_YM_Index_4	CCATCTCATCCCTGCGTGTCTCCGAC	TCAG	TACCAAGATC	GAT	AGTTTGATYMTGGCTCAG
IT_27F_YM_Index_5	CCATCTCATCCCTGCGTGTCTCCGAC	TCAG	CAGAAGGAAC	GAT	AGTTTGATYMTGGCTCAG
IT_27F_YM_Index_6	CCATCTCATCCCTGCGTGTCTCCGAC	TCAG	CTGCAAGTTC	GAT	AGTTTGATYMTGGCTCAG
IT_27F_YM_Index_7	CCATCTCATCCCTGCGTGTCTCCGAC	TCAG	TTCGTGATTC	GAT	AGTTTGATYMTGGCTCAG
IT_27F_YM_Index_8	CCATCTCATCCCTGCGTGTCTCCGAC	TCAG	TTCCGATAAC	GAT	AGTTTGATYMTGGCTCAG
IT_27F_YM_Index_9	CCATCTCATCCCTGCGTGTCTCCGAC	TCAG	TGAGCGGAAC	GAT	AGTTTGATYMTGGCTCAG
IT_27F_YM_Index_10	CCATCTCATCCCTGCGTGTCTCCGAC	TCAG	CTGACCGAAC	GAT	AGTTTGATYMTGGCTCAG
IT_27F_YM_Index_11	CCATCTCATCCCTGCGTGTCTCCGAC	TCAG	TCCTCGAATC	GAT	AGTTTGATYMTGGCTCAG
IT_27F_YM_Index_12	CCATCTCATCCCTGCGTGTCTCCGAC	TCAG	TAGGTGGTTC	GAT	AGTTTGATYMTGGCTCAG
IT_27F_YM_Index_13	CCATCTCATCCCTGCGTGTCTCCGAC	TCAG	TCTAACGGAC	GAT	AGTTTGATYMTGGCTCAG
IT_27F_YM_Index_14	CCATCTCATCCCTGCGTGTCTCCGAC	TCAG	TTGGAGTGTC	GAT	AGTTTGATYMTGGCTCAG
IT_27F_YM_Index_15	CCATCTCATCCCTGCGTGTCTCCGAC	TCAG	TCTAGAGGTC	GAT	AGTTTGATYMTGGCTCAG
IT_27F_YM_Index_16	CCATCTCATCCCTGCGTGTCTCCGAC	TCAG	TCTGGATGAC	GAT	AGTTTGATYMTGGCTCAG
IT_338R	CCTCTCTATGGGCAGTCGGTGAT				TGCTGCCTYCCGTAGGAGT

Table 4.9 Ion Torrent Forward and Reverse Primer Sequences

Primers are split into components for ease of visualisation. All Primers shown 5'-3' across the row left to right.

4.8.3 Gel Electrophoresis

To qualitatively confirm products were of a desired size, PCR products were loaded on an agarose gel (2%; w/v) containing ethidium bromide and exposed to electrophoresis at 110 V for 1 hour in TBE buffer. Gels were visualised under UV light to determine the presence and size of PCR amplicons. For all samples, a 12µl volume was loaded into each well; 5µl of PCR product mixed with 5µl of sterile water and 2µl of loading dye. For size comparison PCR products were compared against 100bp ladder and/or PhiX.

4.8.4 Sample clean-up

Post-PCR samples were purified by one round of Agencourt AMPure XP (Beckman Coulter) DNA purification beads to remove primer dimers and short fragments. Manufacturer's instructions were followed apart from the ratio of DNA to beads. A ratio of 1: 0.8 DNA to beads was used for better size selection of larger fragments.

4.8.5 DNA Quantification, Quality Control, and Equimolar Pool

The integrity of the clean-up PCR-product was subsequently analysed on the 2100 Bioanalyzer Instrument using an Agilent DNA 1000 Chip Kit for size determination. Total dsDNA was measured on the Qubit™ 2 Fluorometer using Qubit dsDNA HS Assay Kit following the manufacturer's instructions. For Illumina MiSeq samples only, an additional qPCR using KAPA Library Quantification Kit was performed following the manufacturer's instructions. This qPCR is specific to the Illumina sequence primers and gives an accurate measure of copies of DNA amplicons with Illumina adapters. KAPA qPCR was conducted with three technical replicates at two dilutions per library; 1:1000 and 1:10000 as suggested by the manufacturer's protocol.

The concentration (determined by Qubit and/or KAPA qPCR) and average size (determined by Bioanalyzer) of each sample was used to make an equimolar amplicon library pool which was diluted appropriately prior to sequencing. The

concentration and average size of each sample was also used to highlight samples below threshold that were subsequently dropped from processing. Purity of the equimolar pool was determined as before using the KAPA Library Quantification kit and size determined using the Bioanalyzer Instrument.

4.9 Sequencing and Base Calling

For MiSeq libraries, bridge amplification was supported on the MiSeq platform in 2 x 300 Paired End (PE) mode using the 600-cycle MiSeq Reagent v3 kit, at Edinburgh Genomics; University of Edinburgh. After sequencing, the FASTQ reads were filtered by the Illumina software to remove TruSeq indexes and demultiplexed.

For Ion Torrent libraries**,** emulsion PCR was supported on the Ion OneTouchTM 400 Template Kit v2 according to the manufacturer's instructions. Sequencing of the library was carried out on the 314 chip using the Ion Torrent Personal Genomic Machine (PGM) system and using the Ion Sequencing 400 kit at the MRC-Human Genetics Unit, Edinburgh. After sequencing, the FASTQ reads were filtered by the PGM software to remove sub-threshold and polyclonal sequences.

4.10 QIIME and Mothur

Quantitative Insights into Microbial Ecology (QIIME) is a Linux-based open source software package that aids analysis of microbial communities from high throughput sequencing (HTS) technologies (Caporaso et al., 2010b). QIIME packaged utilises many other open source tools including; FastTree 2.1.3 (Price et al., 2010), RDP Classifier (Wang et al., 2007), PyNAST algorithm (Caporaso et al., 2010a) and UCHIME (Edgar et al., 2011). QIIME allows for; demultiplexing, aligning, screening, assigning OTUs, calculating diversity, hypothesis testing, and data visualisation.

Mothur is also an open-source software program for microbial bioinformatics (Schloss et al., 2009). Mothur has all the similar functions to QIIME for data processing with built in function for RDP Classifier (Wang et al., 2007), NAST algorithm (DeSantis et al., 2006a) and UCHIME (Edgar et al., 2011).

4.11 Downstream Quality Filtering and Data Analysis; MiSeq

Parameters for Processed Paired Reads

FASTQ files were received from Edinburgh Genomics (University of Edinburgh) already demultiplexed based on sample specific TrueSeq index sequences that were incorporated into the fusion primers. To search and trim the degenerate 16S rRNA primer sequence and any excess heterogeneity spaces from the 5' end, Cutadapt was used in paired-end mode (Martin, 2011). A maximum of 6% error was allowed in primer sequence and any untrimmed reads were discarded. On average 97% of raw read-pairs passed Cutadapt filtering. FASTQ files were then passed to Trimmomatic (Bolger et al., 2014) to remove read pairs where one or both reads have an average phred33 score of <Q20, and trim sequences that fall below <Q20 in a rolling window of 15nt. Low quality bases below phred33 Q6 were masked with an N, prior to generating contigs, using fastq_masker (FASTX-Toolkit). On average 98% of paired reads passed Trimmomatic filtering. Figure 4.6 shows a representative graphical display of FASTQ summary data from raw reads and processed reads generated from a randomly selected sample. Raw quality of each independent MiSeq lane was variable, however, profiles post processing were consistent with Figure 4.6.

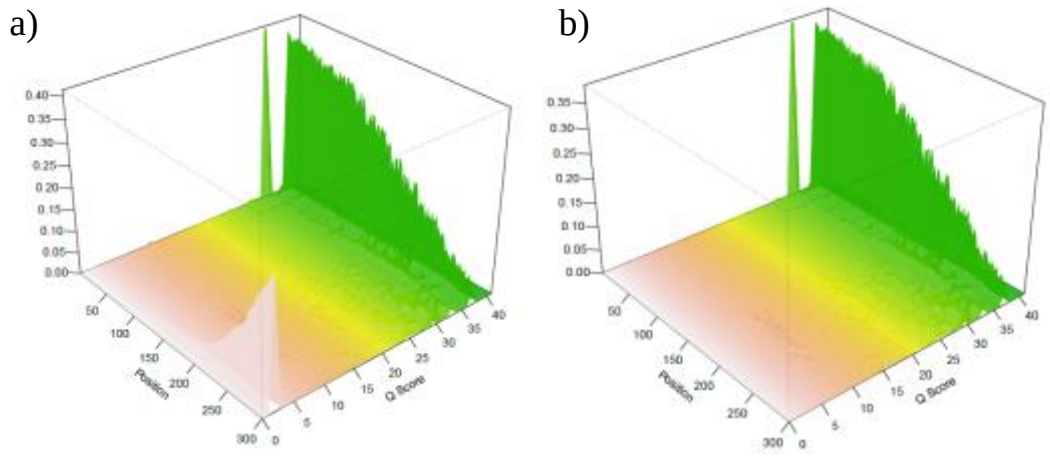

Figure 4.6 Overview of MiSeq Sequencing Quality Output; FASTQ 3D plots
Read Position vs. Quality Score vs. Frequency (x, y, z respectively) (a) Raw paired reads (b) Processed paired reads. Representative data from one randomly selected sample.

Contigs, Chimera filtering, OTU Picking and Tree building

Contigs from paired-end reads were generated in Mothur (Schloss et al., 2009). To ensure sequence reads are a true representation of 16S rRNA gene and not sequencing artifacts; sequences with ambiguous bases, homopolymers of >6, and a contig length above 350bp were removed.

To ensure sequence reads are a true representation of 16S rRNA gene and not PCR artifacts, reads were screened for chimeras using Mothur (Schloss et al., 2011) which is based on UCHIME (Edgar et al., 2011) and USEARCH (Edgar, 2010). The operational taxonomic units (OTUs) were picked *de novo* and clustered at 97% sequence similarity using the Nearest Alignment Space Termination (NAST) algorithm for alignment (DeSantis et al., 2006a). The taxonomy of each OTU was assigned using naive Bayesian classification that is based on the RDP Classifier 8-kmers method (Wang et al., 2007) which is integrated in Mothur (bootstrap threshold 80%) using SILVA (v119) database. FastTree 2.1.3 (Price et al., 2010) intergraded in QIIME (Caporaso et al., 2010b), was used to build approximately-maximum-likelihood phylogenetic trees.

4.12 Downstream Quality Filtering and Data Analysis; Ion Torrent

Parameters for Processed Reads

Ion Torrent raw FASTQ sequencing reads were first quality filtered using tools in Galaxy (web-based platform for biological data) then directed into QIIME (version 1.8.0), for OTU calling, taxonomy identification and diversity measurements. To ensure sequence reads are a true representation of 16S rRNA gene and not sequencing artifacts reads were quality filtered and trimmed. The workflow I designed in Galaxy quality filters and trims the sequence reads based on the following criteria (see appendix for full details).

i) Only reads with perfect match to a barcode sequence are kept; barcode is trimmed

ii) Only reads with a maximum of 2 mismatches in the complementary primer sequence are kept; complementary primer trimmed

iii) Reads are trimmed when the average quality score drops below Phred score 25 in a sliding window of 6bp.

iv) Reads outside the rage of 150–500bp post trimming are discarded.

v) Reads containing homopolymers of more than 8bp are discarded.

Sequences are then binned by sample (demultiplexed) and the remaining high quality FASTQ sequences are sent to QIIME for chimera filtering, OTU picking and tree building.

Chimera filtering, OTU Picking and Tree building

Before OTU picking, reference-based and *de novo* based chimera detection was carried out using USEARCH 6.1 (Edgar, 2010) against the full Greengenes database (13_8 release). OTUs were picked at 97% sequence similarity using an open-reference approach. This approach first clusters the sequences against the Greengenes database using UCLUST (Edgar, 2010), those sequences which do not cluster are then sent for *de novo* OTU picking. Representative FASTA sequences for each OTU were aligned to the Greengenes database (13_8 release) using PyNAST (re-implemented NAST aligner (Caporaso et al., 2010a)). Taxonomy was assigned using the RDP Classifier (Wang et al., 2007) with a bootstrap threshold of 60%. FastTree 2.1.3 (Price et al., 2010) intergraded in QIIME, was used to build approximately-maximum-likelihood phylogenetic trees.

4.13 R Package

The resulting OTU tables were imported into R for filtering and statistical analysis using multiple R packages for data manipulation, such as; Phyloseq, ggplot2, and Hclust. Phyloseq is an R-Package which manipulates the raw OTU data generated elsewhere (such as in QIIME or Mothur), and together with analytical and graphical packages (such as vegan, ape, picante and ggplot2) provides a tool for analysis and visualisation of phylogenetic data. Phyloseq also has functions to rarefy data and calculate diversity, however, for the most part these functions were used in QIIME and phyloseq was primarily used in this study for data manipulation and generating 2D PCoA plots.

4.14 Rarefaction Curves

Sufficient sequencing depth is needed to capture the full representation of bacterial species in a sample. To establish whether the depth of sequencing truly captures the community, a method commonly called rarefaction can be employed. Rarefaction is a technique used in ecology to measure species richness as a function of sampling effort. Rarefaction can be thought of as a method for random resampling, whereby diversity measures are then calculated for each simulated sequencing effort. The rate of increase in diversity measure is an inherent property of the microbial community of that sample, whereby a plateau suggest the majority of the species in the community have been found.

In this study multiple rarefactions are done for each sample, diversity measures calculated and shown graphically on rarefaction curve plots. The diversity measures calculated for rarefaction were; species richness (S_{obs}), Chao1 Estimate (Chao, 1987), Shannon Diversity (Shannon, 1948) and Inverse Simpsons Index (Simpson, 1949); these diversity measures are described in more detail below.

4.15 Alpha Diversity Analysis

Bacterial diversity at the community level is evaluated using two principle measures; alpha and beta diversity. Alpha diversity is a measure of diversity 'within' a sample and can be assessed using various metrics. Most measures take into account both species richness and evenness. Richness refers to how many different species (OTUs) there are present, whereas evenness describes their distribution.

The alpha diversity measures used in this study are; Observed species (S_{obs}), Chao1 Estimate, Shannon Diversity and Inverse Simpsons Index. Observed species is a measure of the unique OTUs in each sample and Chao1 is an estimate of species richness which uses the ratio of singletons to doubletons (Chao, 1987). Low abundant OTUs should therefore not be removed prior to analysis. Simpson's index is a measure of the probability that upon randomly selecting an individual from a community, the individual has already been observed (Simpson, 1949). Shannon Diversity measure is more sensitive to species richness, giving higher weight to low abundant OTUs/species (Shannon, 1948).

4.15.1 Statistical analysis of alpha diversity

Where alpha diversity between two groups were compared (e.g. Fecal vs. Vaginal); a unpaired student t-test was performed. Continuous parametric data between more than two groups was compared using a one way analysis of variance (ANOVA). Longitudinal data within-subject across the 4 time-points was compared using repeated measures ANOVA (RM-ANOVA) and Tukey's post-test. Linear mixed regression was applied to the Alpha Diversity measures across collection time-points. A P value of less than 0.05 was determined to be significant for all measures.

4.16 Beta Diversity Analysis

While Alpha Diversity is descriptive for inferring community structure, it represents only the dispersion pattern of the OTUs. Alpha Diversity will not tell us if the same bacteria are shared between samples. Beta diversity measures are used to describe the similarity or dissimilarity between two different samples. Beta diversity, like alpha diversity is dependent on the depth of sequencing and the metric used. A popular method which uses the phylogenetic tree as the measure for similarity is a technique called UniFrac (Lozupone and Knight, 2005). UniFrac takes into account the shared species between two samples, their abundance and their phylogenetic relationship. It measures pairwise distances and returns a value between 0, where two communities are identical, and 1, where communities are totally unrelated. The higher the beta diversity, the less similar the communities are. Unweighted UniFrac distance is a qualitative description of similarity whereas weighted UniFrac distance takes into account the quantitative occurrence of the OTUs/species. Weighted UniFrac distance therefore attributes more power to highly abundance OTUs/species than unweighted UniFrac measure.

The UniFrac distances from all samples are approximated visually using Principle Co-ordinate Analysis (PCoA). PCoA is a method of dimensionality reduction that aims to recapture whatever patterns are in the data but reduce the number of dimensions using a new co-ordinate system. PCoA is related to the commonly used statistical method principle component analysis (PCA) which is analogous to Euclidian distance and not UniFrac measures. 2D PCoA plots in this thesis were created and visualised using phyloseq; an R package (McMurdie and Holmes, 2013). Ultimately ordination is a visualisation method, but any spatial separation seen in 2D PCoA plots can be tested for statistical significance using hypothesis testing on the raw data (described below).

4.16.1 Statistical analysis of beta diversity

Where beta diversity between two groups was compared, a parametric two sample t-test with Bonferroni correction was performed. This was supported with non-parametric testing using 999 Monte Carlo permutations and Bonferroni-corrected.

Adonis

Adonis is a nonparametric statistical method that first identifies the central points in the data, centroids, and then radially calculates the squared deviations out from these points. This produces an effect size value (r^2) which is the level of variance in the data that can be attributed to the specified category (e.g. genotype or gestation). In addition this method provides a P value from permutations of the raw data (999) using multiple F-tests (sequential sums of squares).

ANOSIM

ANOSIM is a test which determines whether two or more groups of samples (e.g. C57BL/6J vs. *Camp-/-*) are significantly different by relating the distances 'between' the groups, to the distances 'within' the groups, and providing an *r* value. A positive *r* value close to 1.0 signifies that the groups are highly dissimilar. Significance is supported by 999 permutations of the similarity matrix.

4.16.2 Jack-knife and UPGMA bootstrapped trees

A rooted dendrogram (tree) is constructed from the pairwise UniFrac distance matrix using Unweighted Pair Group Method with Arithmetic Means algorithm (UPGMA) to infer structure. Jack-knife replicates are used to estimate uncertainty in distance matrix and involves dropping one/many observations from a sample each time and recalculating the distance. Together with bootstrapped hierarchical clustering, UPGMA provides an estimate to the uncertainty of the points in PCoA plots. Jack-knifing in this study was set at 100 replicates at 45,000 sequences (75% per sample sequences). Those nodes which are consistent across jack-knife replicates are robust for microbial inference. Bootstrap values on the branch indicate how much support is given to that branch on a phylogenetic tree.

4.17 Significant Taxa (LEfSe)

Linear Discriminant Analysis with Effect Size (LEfSe) is an all-against-all multi-class comparison tool used to highlight biological consistency and estimate effect size (Segata et al., 2011). LEfSe was used to detect which taxa were enriched in different genotypes; C57BL/6J vs. *Camp-/-*. LEfSe first applies a nonparametric (Kruskal -Wallis) rank sum test to the OTU data to detect OTUs and classifications with significant differential abundances. Stringent alpha values of 0.01 for Kruskal-Wallis were set in this study. This is then followed by a biological consistency estimate which involves pairwise rank sum tests (Wilcoxon). Linear Discriminant Analysis is then used to estimate an effect size of the differentially abundant taxa; threshold of 3.0 was chosen for a logarithmic LDA score.

4.18 Mock Community

To measure the error rate of MiSeq microbial sequencing in this workflow, a mock community was co-sequenced along with samples detailed in Chapter 5. The mock community HM-278D was sourced from BEI (https://www.beiresources.org/) and contained an even mixture of 20 bacterial species listed in Table 4.10. Reference sequences of the 20 species contained 115 unique 16S RNA operons. These 115 sequences were aligned and trimmed to the V1-V2 region for comparison to the sequenced 'Mock' sample. Using seq.error in Mothur the error rate was determined to be 0.00673%. This is very low and confirms the quality control and pre-processing parameters employed in this workflow are more than adequate for robust microbial species inference.

Bacteria	**Strain**	**NCBI**
Rhodobacter sphaeroides	strain ATH 2.4.1	NC_007493
Acinetobacter baumannii	strain 5377	NC_009085
Actinomyces odontolyticus	strain 1A.21	NZ_AAYI02000000
Bacillus cereus	strain NRS 248	NC_003909
Bacteroides vulgatus	strain ATCC®8482	NC_009614
Clostridium beijerinckii	strain NCIMB 8052	NC_009617
Deinococcus radiodurans	strain R1 (smooth)	NC_001263, NC_001264
Enterococcus faecalis	strain OG1RF	NC_017316
Escherichia coli	strain K12 sub-strain MG1655	NC_000913
Helicobacter pylori	strain 26695	NC_000915
Lactobacillus gasseri	strain 63 AM	NC_008530
Listeria monocytogenes	strain EGDe	NC_003210
Neisseria meningitidis	strain MC58	NC_003112
Propionibacterium acnes	strain KPA171202	NC_006085
Pseudomonas aeruginosa	strain PAO1-LAC	NC_002516
Staphylococcus aureus	strain TCH1516	NC_010079
Staphylococcus epidermidis	FDA strain PCI 1200	NC_004461
Streptococcus agalactiae	strain 2603 V/R	NC_004116
Streptococcus mutans	strain UA159	NC_004350
Streptococcus pneumoniae	strain TIGR4	NC_00302

Table 4.10 Mock Community HM-278D Species List
Genomic DNA from Microbial Mock Community A (Even, Low Concentration), v3.1 (sourced from BEI https://www.beiresources.org/)

Further investigation of the sequenced Mock community showed that there were 81 unique OTUs generated from this sample. This was reduced to 50 OTUs once rarefied to 60,000 sequences (Table 4.11). As there are only 20 species in the mock community the number of OTUs returned in an ideal scenario should be 20. However, there are always some erroneous and chimeric sequences that pass even very stringent quality filtering. The spurious OTUs were found to make only a small contribution to the total number of sequences, whereby most are in fact singletons or doubletons that would be filtered out in subsequent downstream beta-diversity analysis (Table 4.11).

Once taxonomy were assigned for the OTUs from the mock community, it was apparent that *Rhodobacter sphaeroides* had not amplified in either of the Mock samples. Three clusters of *Streptococcus* OTUs were distinguished, but taxonomy assignment did not attribute a genus classification at 97% sequence identity. At 97% sequence similarity, the OTU picking method failed to highlight two OTU clusters for the two *Staphylococcus* spp. in the mock community. After removal of single and double sequences, the only spurious taxonomic classification of bacteria not in the mock community was *Ralstonia* spp.. However, only 15 out of 150,023 total sequences in the mock sample were assigned to this taxonomy.

The mock sample that underwent the nested PCR protocol 'Mock_Nested' has a greater number of OTUs, singlets, and doublets (Table 4.11). This was expected as combined increase of PCR cycle number can amplify chimeric reads. The nested mock community proportions of the 19 taxonomic groups identified are also more varied, which highlights the primer bias in the first round of PCR, especially in favour of *Helicobacter* (Figure 4.7)

	MOCK OTU Count	**MOCK_NESTED OTU Count**
All Reads 150,000	81 (48)	182 (108)
Rarefied to 60,000	50 (26)	104 (60)

Table 4.11 Sequenced Mock Community OTU Counts
Number of single and double sequences given in parenthesis.

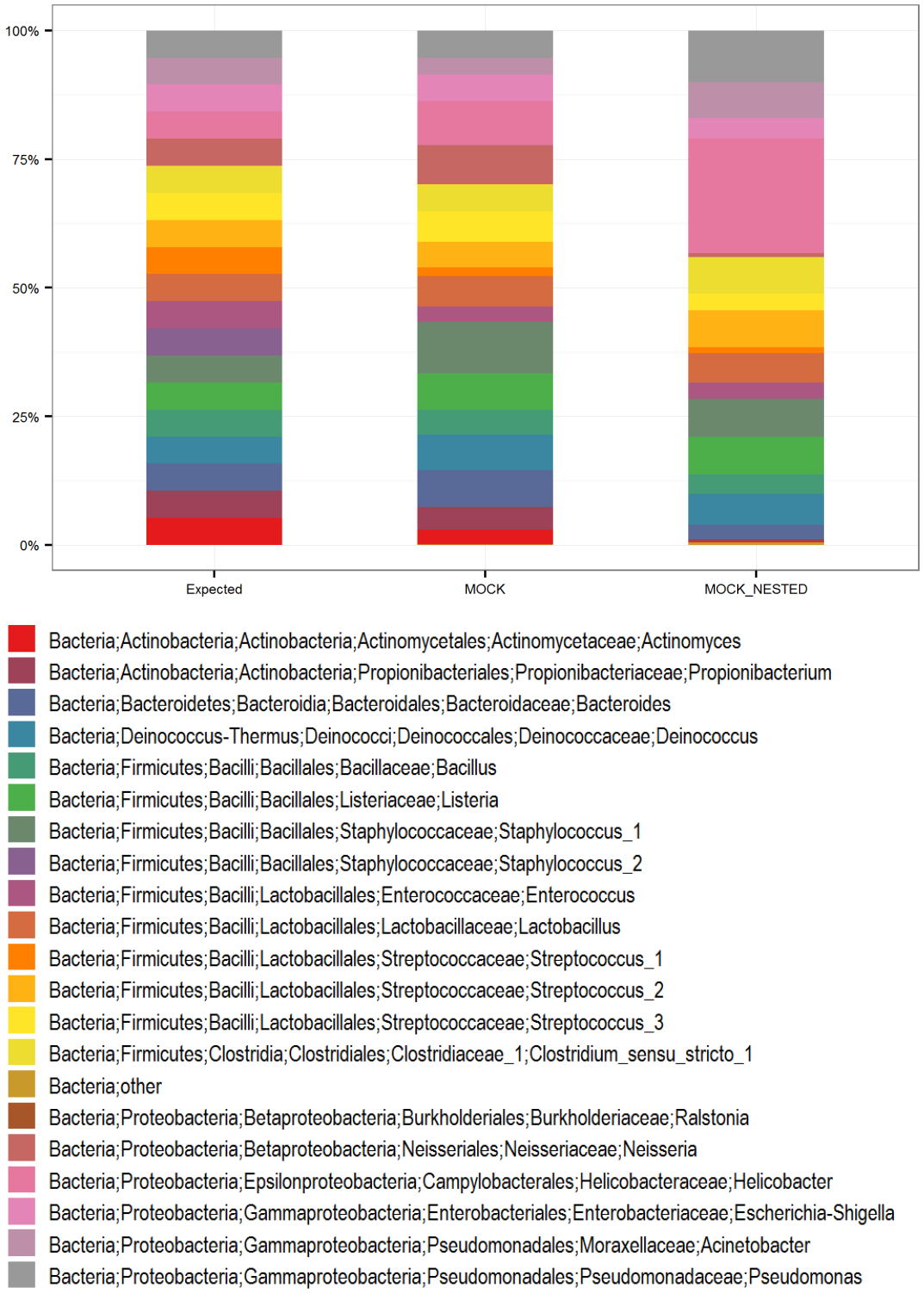

Figure 4.7 Mock Community Relative Abundance

Bar plot of relative bacterial abundance determined by OTUs and grouped at the genus level. The expected proportions of HM-278D are shown in the left bar, the middle bar describes the actual proportions seen in the mock community sample that underwent x20 PCR cycles (method for fecal samples). The right bar shows the actual proportion from the mock community sample which underwent nested PCR protocol (method for vaginal samples).

Further analysis of the mock sample sequenced highlighted which taxa had positive and negative bias for amplification (Figure 4.8). In an ideal scenario each taxa's contribution to the total number of sequence reads would be 5%. *Helicobacter* shows the most positive bias having nearly 8% of the sequence reads attributed to this genus. After *Rhodobacter*, which is not amplified, one of the *Streptococcus* spp. shows the greatest negative bias.

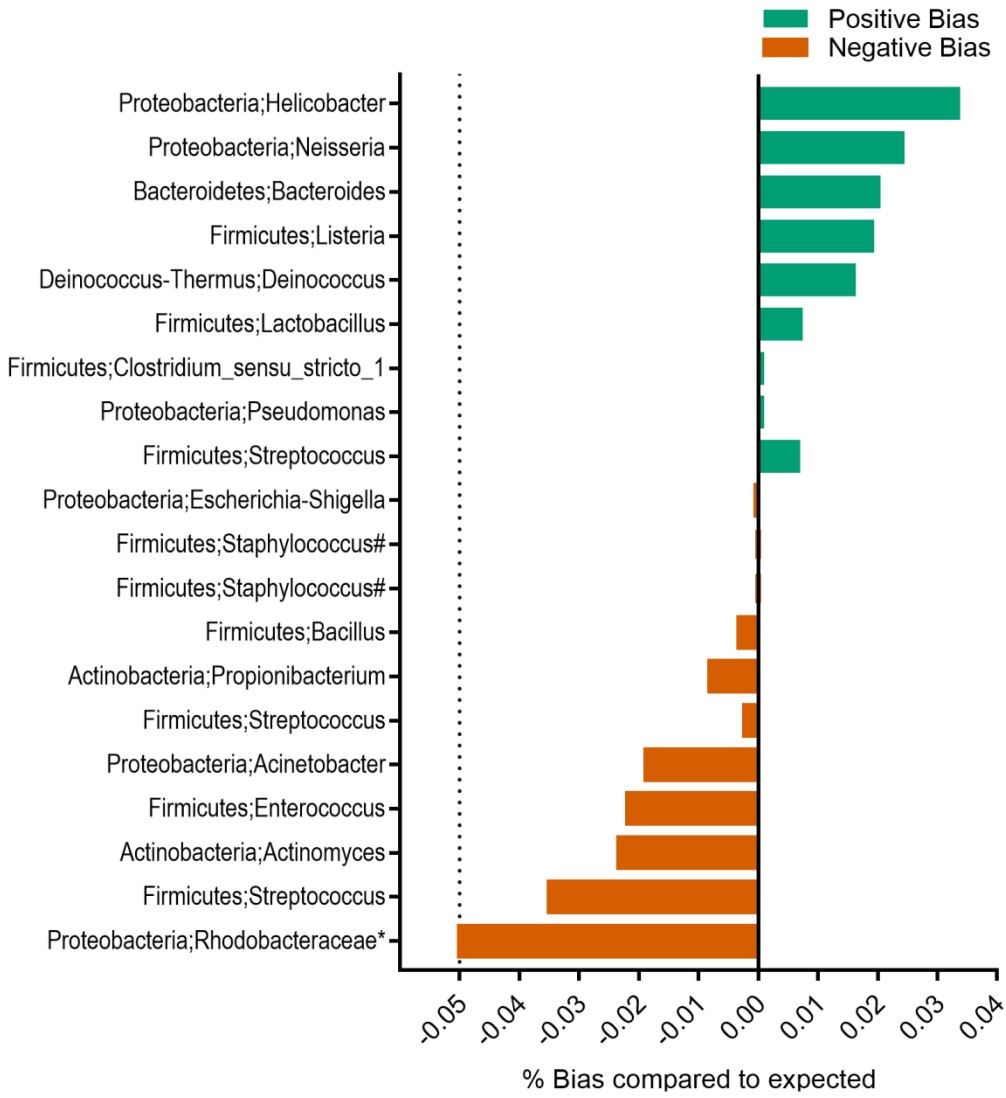

Figure 4.8 Percentage Bias in Sequenced Mock Community
Positive and negative amplification bias of each genus compared to an expected 5% contribution in HM-278D. #Analysis was unable to differentiate OTUs between the two species of *Staphylococcus*. No sequences were assigned to the *Rhodobacter* genus.

4.19 Discussion

This chapter details a method for looking at the microbiome across body sites and has been optimised to consider the murine fecal and vaginal bacterial community. After review of the literature and *in-silico* work I deduced the V1-V2 region would provide the highest discrimination potential for species identification in the murine vagina and gastrointestinal tract. In this chapter I conducted *in-silico* primer evaluation to generate and confirm the suitability of universal sequencing primers to amplify the V1-V2 region of the 16S rRNA gene.

As the murine vagina has a low bacteria burden, different sampling methods were evaluated for 16S rRNA gene recovery, this highlighted that whole vaginal tissue provides the most consistent bacterial yield.

Different extraction methods used to isolate and extract bacterial DNA from ecological samples can give a varied representation of species diversity and abundance (Milani et al., 2013). Milani et al., (2013) found large variations in proportions of the contributing bacteria depending on the extraction method used; mechanical and/or enzymatic. Milani et al., (2013) concluded that *Faecalibacterium* and *Bacteroides* (gut microbial taxa), might be over-represented in human gut metagenomic studies as a result of this bias. Although I did not directly compare the bias in extraction methods in this study, I favoured the FastDNA® SPIN Kit with bead-beating over the PowerSoil® DNA Isolation Kit due to this reported reduction in bias towards *Bacteroidetes* phylum.

Reagent contamination is emerging as a key factor in microbiome studies especially in low-biomass sites. Salter et al., (2014) demonstrated this using low concentrations of *Salmonella* DNA, where low biomass was associated with inflated spurious sequences of various taxonomic assignments. Ultra-pure polymerases and ultra-pure molecular grade water were used in this study with the aim of reducing potential contaminants.

Co-sequencing of a mock community on the MiSeq platform highlighted that the error rate in sequencing microbial communities in this optimised workflow was

extremely low, only 0.00673%. The mock community also highlights *Ralstonia* as a species for possible PCR reagent contamination, although only 15 out of 150,023 total sequences in the mock sample were attributed to this clade. Molecular grade water is a common source of this bacterium (Grahn et al., 2003, Barton et al., 2006, Laurence et al., 2014). The mock community also highlights that the primers in this study are not suitable for picking up bacteria in the *Rhodobacter* genus as no OTUs were assigned to this taxonomy.

Consideration was given in this study to keep the number of PCR cycles to a minimum as to reduce the affliction of PCR artifacts, such as chimeras, inflating OTU clusters (Acinas et al., 2005). A study comparing 15x and 30x PCR cycles showed a 30% inflation of chimeric amplicons with increased cycle number (Ahn et al., 2012).

In this study, for the low biomass vaginal samples, a nested PCR approach was adopted. This approach was a compromise of controlling the number of chimeric reads while allowing for workable concentrations of PCR product to be obtained. Sequencing artifacts are also kept to a minimum by doing paired end sequencing (MiSeq only) and employing stringent downstream chimera checking. Using the most current database for taxonomic assignment is essential but there are still sequences that are poorly annotated.

A limitation in this study was in the optimisation required to get strong amplification results using fusion-primers; which are known to be difficult due to the extended primer length and off target amplification. There are similar low cost methods of multiplexing that allow barcodes and sequencing adaptors to be added without having to incorporate target-specific sequences for each fusion primer. These methods employ a two-step PCR protocol, where shorter ‘tail’ sequences are incorporated in the first universal 16S rRNA amplification. The second PCR is then specific to the tail sequence allowing for barcodes and sequencing adapters to be added at this stage. Any processes involving two PCR steps, as I have shown in this chapter, has the disadvantage of potential inflation of PCR artifacts and amplification

bias. A robust study comparing multiplexing approaches for 16S rRNA sequences has yet to determine the associated bias in the various approaches.

OTUs were clustered using a cut-off of 97% sequence identity to seed in database, which is generally accepted to represent species level. There is however some debate whether this cut-off is too conservative (Mizrahi-Man et al., 2013). Collectively, for the MiSeq data-set, only 0.01630% of the sequences did not align with the V1-V2 region of the 16S rRNA gene, of all those sequences that did align, only 0.09143% were identified as non-bacterial (e.g. chloroplast, mitochondria and Archaea and unknown) with a cut off of 80% to bacteria kingdom. Collectively this means that only 0.5418% of total sequences passing quality filtering were not identifiable as bacterial. This low value is evidence of the specificity of the primers used in this study and appropriate quality filtering.

Low nucleotide diversity in the first few cycles of sequencing on the Illumina platform is known to cause problems with base calling and the cluster identification algorithms, which impacts greatly on sequence quality (Krueger et al., 2011). To bypass/rectify this problem researchers often "spike-in" a PhiX shotgun library to increase diversity and gain better sequence quality. The amount of PhiX spike can range for 10% but some times as high as 50-80% depending on the complexity of targeted library (Mitra et al., 2015). This obviously has enormous impact on the per sample cost, as the majority of sequences are being assigned to PhiX and not the 16S rRNA gene of interest. In this study I attempt to reduce this problem by the incorporation of random nucleotides of varying lengths into the forward and reverse fusion-primers, known as 'heterogeneity' spacers. Cluster density of all MiSeq runs in this study was respectable, and raw sequence quality was above threshold; with >78% raw reads having an average quality of >Q20. This is suggestive that the heterogeneity spacers employed have reduced possible issues with low complexity and improved sequence quality.

Cross-study comparisons with regards to 16S rRNA gene studies should be approached with some caution. Although the discussed factors in 16S rRNA protocols are important to consider, variation attributed to the choice of extraction

method and variable regions were still shown to be less than the variation attributed to differences between individual samples and body sites (Wesolowska-Andersen et al., 2014, Lozupone et al., 2013). There is however still a need for a gold standard library preparation and bioinformatic protocol for looking at microbial communities.

4.20 Summary

In this chapter I have detailed a method for looking at the microbiome across body sites; specifically optimising protocols to consider the murine fecal and vaginal bacterial communities. Co-sequencing of a mock community highlights this workflow is robust for broad taxonomic classification, but is not suitable for picking up bacteria in the *Rhodobacter* genus. The mock community also highlights *Ralstonia* as a species for possible low level PCR reagent contamination.

Chapter 5

Modulation of the Microbiome

Chapter 5 Modulation of the Microbiome

5.1 Introduction

Animals offer researchers a vital tool by providing a model to test out host-microbiome interactions under controlled environmental conditions. They also allow for infectious models that help understand pathogenicity. Gastrointestinal bacteria have an important role in maintaining multiple physiological processes. LL-37/*Camp* is upregulated during ileitis/colitis dependent on the level of inflammation (Schauber et al., 2006), and *Camp* null mice have more severe phenotype in a DSS induced colitis model (Koon et al., 2011). Addition of exogenous *Camp* could reverse some of the phenotypic severity of DSS treatment in *Camp*-/- animals, such as cytokine production, apoptosis and mucus production (Tai et al., 2013). In this chapter I look at the direct consequences of the cathelicidin gene on gut microbial diversity and structure, by interrogating the microbiome of *Camp*-/- animals.

There are vast metabolic changes that occur during pregnancy, especially in late gestation, which could impact on microbial communities. Indeed, alterations in the maternal gastrointestinal bacteria have been implicated in metabolic adaptations to pregnancy (Koren et al., 2012, Collado et al., 2008). However, there are conflicting reports with regards to whether pregnancy causes the modulation of gut bacterial composition, with a large longitudinal study failing to show significant remodelling of the gut microbiota in pregnant women (DiGiulio et al., 2015). This study investigates whether there is remodelling in the diversity and composition of the murine gastrointestinal and vaginal microbiome in pregnancy.

The aims of this study were;

1) To establish whether the microbiome of animals lacking cathelicidin are altered across body sites.

2) To investigate whether there are gestational related changes in the female murine gut microbiome.

3) To establish whether the vaginal microbiome is affected by pregnancy, results and discussion presented in Chapter 6

5.2 Experimental Methods

5.2.1 *Camp-/-* Microbiome and Pregnancy Microbiome Study

Virgin female and male mice of either wildtype C56BL6/J Ola Hsd (n=10♀/10♂) or *Camp-/-* (n=8♀/♂8) genotype (congenic on C57BL/6J Ola Hsd) had fecal samples collected on day 0. Within genotype, these animals were set-up in mating pairs and females were checked for a copulatory plug over 4 consecutive days. On day 4 female animals were removed from the mating and singly housed for the remainder of the experiment. Subsequently, the majority of the female animals became pregnant; with the remainder providing the non-pregnant control group. In parallel, littermate female virgin mice, not exposed to any males, were singly housed on Day 0 providing the non-plug control group. Fecal samples were collected from females on day 4, day 10 and day 17, when animals were culled on day 17 vaginal tissue was also collected. A subset of pregnant wildtype mice continued to term, where fecal and vaginal samples were collected postpartum on day 22.

All fecal and vaginal tissue samples were stored at -20°C within 2 hours of collection and DNA was extracted within 3 weeks. Sample extraction, multiplexing and library preparation was conducted as described in Chapter 4 using the MiSeq protocols.

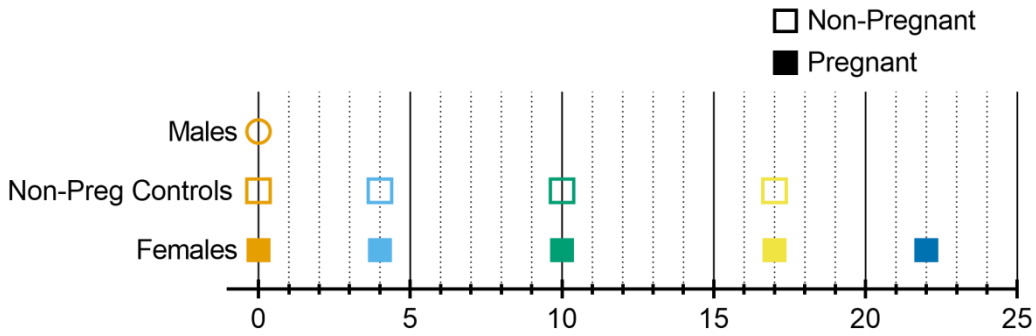

Figure 5.1 Experimental Timeline for *Camp-/-* Microbiome Study
Fecal samples were taken from male and female mice on Day 0 at the start of the experiment. Female animals were longitudinally sampled on Day 4, Day 10, Day 17 and a subset on Day 22. Non-plug female control animals were also longitudinally sampled on Day 4, Day 10, and Day 17. Animals were culled on Day 17 or Day 22 and vaginal tissue was also collected.

	C57BL6/J				*Camp-/-*			
	Pregnant	Non-Pregnant	Non-Plug Controls	Males	Pregnant	Non-Pregnant	Non-Plug Controls	Males
Day 0	8	2	2	10	6	2	2	8
Day 4	8	2	2		6	2	2	
Day 10	8	2	2		6	2	2	
Day 17	8 (5)	2 (2)	2 (2)		6 (6)	2 (2)	2 (2)	
Day 22	3 (3)							

Table 5.1 Experimental Sample Number for *Camp-/-* Microbiome Study
Table displaying the number and genotypes of animals at each collection time-point in this study. Numbers given are for fecal sampling; vagina sample numbers are given in parentheses.

5.3 Results

5.3.1 Data Summary

The full 16S rRNA gene sequencing performed on the Illumina MiSeq platform consisted of 139 samples; two mock communities, 114 murine fecal samples and 22 murine vaginal samples. Amplicon libraries were sequenced on 6 independent MiSeq lanes. Bioinformatic and quality filtering done on the raw data are described in section 4.11, but in brief; runs were demultiplexed and barcodes and indexes removed using Illumina software. Raw sequence read quality filtering and primer trimming was done using Cutadapt and Trimmomatic. The total number of raw reads prior and post data processing is given in Table 5.2. Quality filtering the raw reads reduced the number of paired end reads from 31,640,538 (raw paired reads) to 30,279,366 reads (processed paired reads) (Figure 5.2).

Contigs were made in Mothur and screened as detailed in section 4.11. Chimeras were removed by UCHIME and operational taxonomic units (OTUs) were picked *de novo* and clustered at 97% sequence similarity using the NAST algorithm. The taxonomy was assigned by RDP classifier (Bootstrap threshold 80%) using SILVA (v119) as the reference database. This further quality screening reduced the number of processed paired end reads from 30,279,366 (processed paired reads) to 24,306,711 contig sequences (filtered contigs) (Figure 5.2).

	Raw Paired Reads	Processed Paired Reads	Filtered Contigs
Paired read #:	31,640,538 (100%)	30,279,366 (100%)	24,306,711 (100%)
Number of Q>=20 reads:	31,083,664 (98.24%)	30,279,366 (100%)	NA
Number of Q>=30 reads:	24,869,462 (77.86%)	23,287,860 (76.91%)	N/A
Read Length:	300 ± 0.00	279 ± 1.18	316 (Contig length)
GC Content	55.80% ± 4.64	55.89% ± 4.69	N/A
N base Count	691,892	218,510	0

Table 5.2 MiSeq Sequence Quality Summary
Summary data for raw paired reads, processed paired reads, and filtered contigs for n=139 samples on 6 MiSeq lanes. A Phred +33 quality score of Q20 is predicted 99% accuracy in base calling; Q30 has 99.9% predicted accuracy.

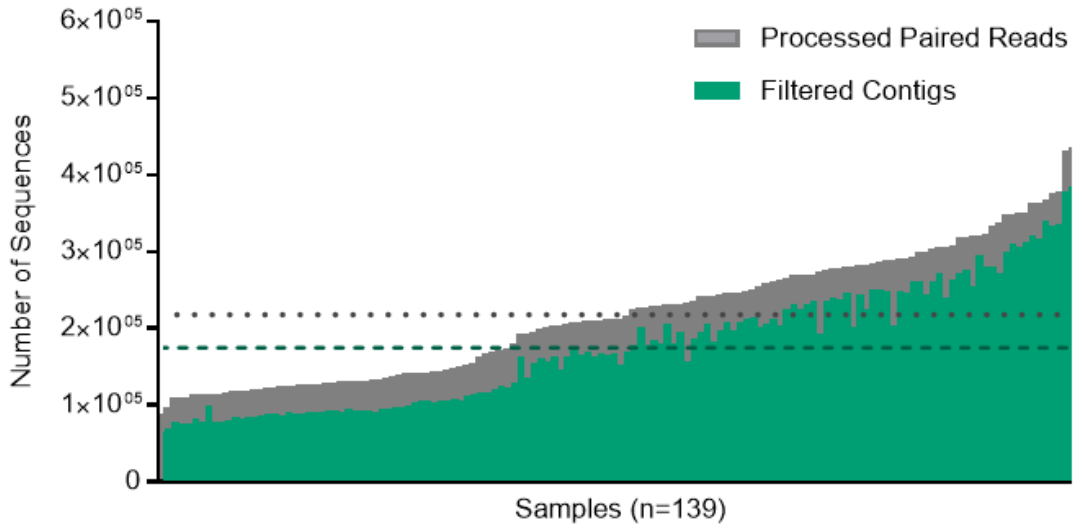

Figure 5.2 MiSeq Processed Paired Reads and Filtered Contigs
Processed paired reads and quality filtered contig counts of all n=139 samples. Grey dotted line represents mean processed paired read count at 217,837 sequences. Green dashed line represents mean filtered contigs count at 174,860 sequences.

5.3.2 Taxa Summary

In this study 2,257 OTUs were identified collectively in the full data-set, many of these were low abundant OTUs. Sub-sampling each sample to 60,000 sequences (discussed in section 5.3.5) reduced the number of OTUs to 915 across the data-set. Removal of singletons and doubletons further pruned the OTU count to 908. These 908 OTUs represent 143 unique genera, 82 unique family level classifications, 50 unique orders, 29 unique classes and 15 different phyla (Figure 5.3).

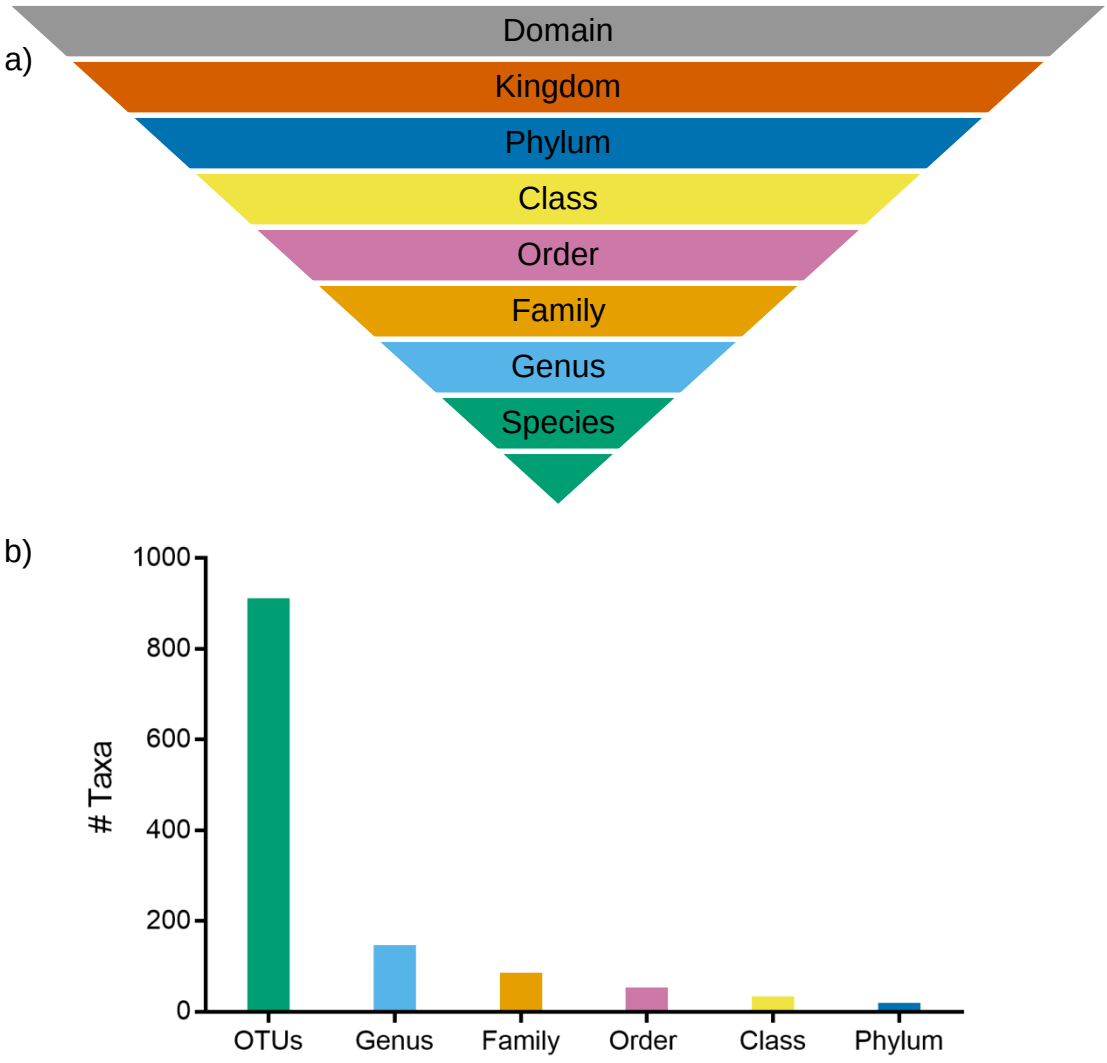

Figure 5.3 Taxonomic Classification Hierarchy
(a) Schematic view of taxonomic classification hierarchy. (b) Distribution of taxonomic classification of the 908 OTUs identified in this study.

5.3.3 Subsets

Subset 1 - Fecal vs. Vaginal

To examine the murine fecal microbiome in relation to vaginal bacterial communities, Subset 1 consisted of the full data-set minus the two mock community samples, which are evaluated in section 4.18. This subset includes the full data of vaginal (n=22) and fecal samples (n=115).

Subset 2 - *Camp-/-* vs. C57BL/6J

To determine whether there is any genotypic difference in the fecal microbiome in *Camp-/-* compared to wildtype C57BL/6J animals, the data was further partitioned to only include fecal samples from the *Camp-/-* pregnancy microbiome study (n=99; 42 *Camp-/-* , 57 C57BL/6J).

Subset 3 - C57BL/6J; Gestational effect

To examine whether the fecal microbiome varied longitudinally both in a non-pregnant and pregnant state, fecal samples were further partitioned to only include the wildtype C57BL/6J animals which were longitudinally sampled at 4 time-points over 17 days (n=44 samples; 16 non-pregnant, 28 pregnant).

Subset 4 - Vaginal Microbiome; *Camp-/-* vs. C57BL/6J, Pregnant vs. Non-pregnant

This subset included only the vaginal samples (n=22), and is detailed and discussed in Chapter 6.

5.3.4 Rarefaction Curves

As deep sequencing was performed in this study, it would be assumed that the depth of sequencing is sufficient for robust conclusions to be made. However, this needs to be empirically established as a true representation is dependent on community complexity. To establish whether the depth of sequencing truly captures the community, a method commonly called rarefaction was employed (discussed in section 4.14).

Multiple rarefactions to a maximum sampling depth of 60,000 sequences were calculated for each sample and species richness (S_{obs}), Chao1 Estimate, Shannon Diversity, and Inverse Simpsons Index, were computed for each simulated sequencing effort (Figure 5.4). Specifically, 10 rarefactions at 10 increasing depths (6,000 integers) were conducted on the data. Maximum rarefaction at 60,000 was chosen as this is the number of sequences from the lowest sample.

Visual assessment of the rarefaction plots reveal that the diversity and complexity of the vaginal community is considerably lower than the fecal samples, as expected, displayed by lower amplitude on the rarefaction curves (Figure 5.4). A common trend was seen in all mean diversity measures in both fecal and vaginal samples, whereby a steep increase up-to 6,000 is observed followed by a plateau to varying degrees (Figure 5.4). The number of observed OTUs (S_{obs}) can sometimes never reach a true plateau, as this is often a factor of sequencing chemistry error and stringency of OTU alignment. Chao1 estimates species richness based on the ratio of singletons to doubletons in the sample and is therefore also a factor of S_{obs}. Chao1 and S_{obs} show a steady increase with sampling effort after 6,000 sequences but this is not adding to the complexity of community structure. This can be seen by the Shannon Diversity and Inverse Simpson Index, which are stable past 6,000 sequences. This suggests that many OTUs are present in low abundance. Overall the curves reach an acceptable plateau somewhere before 6,000, highlighting that sequence depth >6,000 is more than adequate to capture a true representation of the community. Subsequent beta-diversity measures were calculated on a single subsampled population of 60,000 sequences per sample.

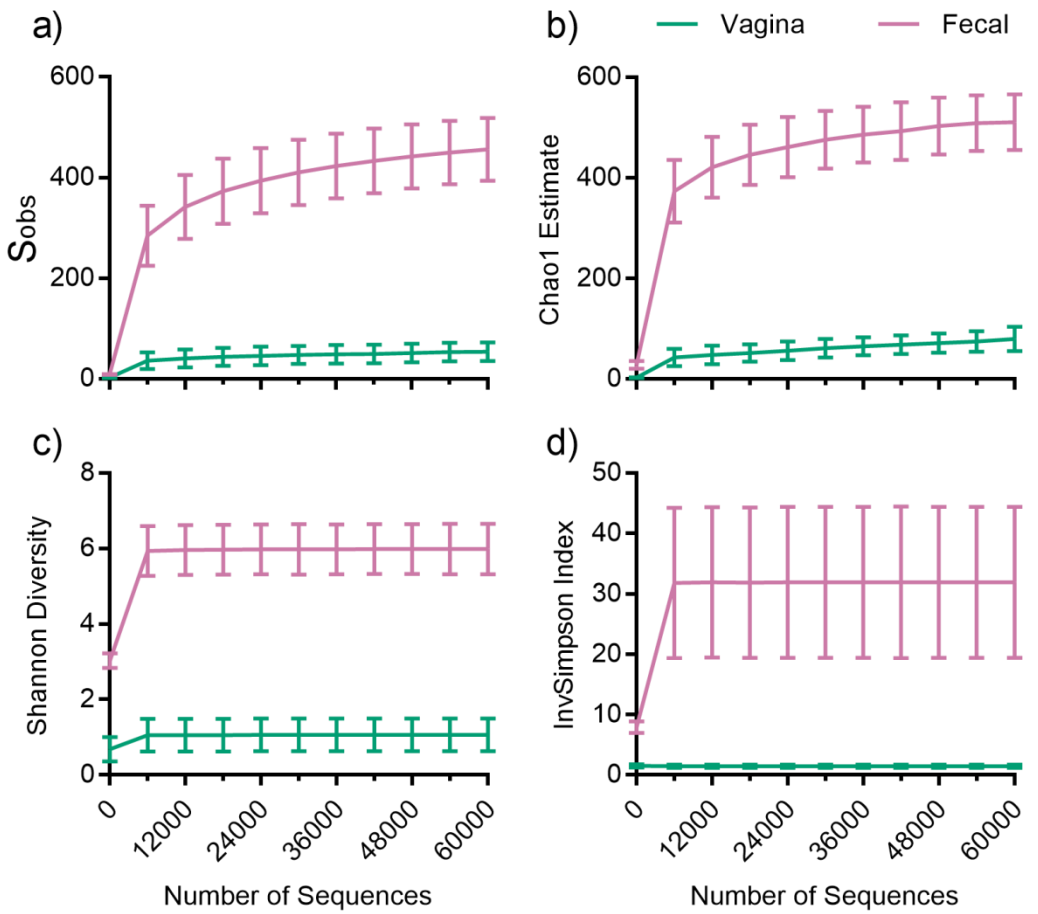

Figure 5.4 Rarefaction Curves - Fecal and Vaginal
Rarefaction curves created for (a) Observed OTUs (S_{obs}) (b) Chao1 Estimate (c) Shannon Diversity (d) Inverse Simpsons Index of fecal (n=122) and vaginal (n=22) samples. Rarefaction plots are displayed as diversity measure versus simulated sequencing effort at 10 iterations per depth, to maximum depth of 60,000 sequences. Error bars display SEM grouped by sample site.

5.3.5 Subsampling; Single Rarefaction

Although library quantification steps, such as KAPA qPCR (detailed in section 4.8.5), were used in this study, there was still a degree of unequal contribution of each library to the sequencing reads (Figure 5.2). In addition, as sequencing in this chapter was conducted over 6 independent MiSeq lanes, there is additional variability in depth due to lane specific characteristics. Although there is some debate about whether subsampling (single rarefaction) to normalise 16S rRNA amplicons is essential (McMurdie and Holmes, 2014); to minimise artificial inflation of diversity from samples with greater coverage I performed subsampling to a depth of 60,000. This was done as the biological questions I will be asking are based on beta-diversity measures, which have sensitivity to sample size. This subsampling depth was chosen as it is the number of sequences of the lowest sample.

5.3.6 The Murine Fecal Microbiome in Relation to Vaginal Bacterial Communities (Subset 1)

5.3.6.1 Alpha Diversity

Alpha diversity is a measure of diversity 'within' a sample and can be assessed using various metrics. Observed species (S_{obs}), Shannon Diversity, and Inverse Simpson Index were calculated for each sample on the rarefied but unfiltered OTU data (Figure 5.5). As expected the vaginal community has a significantly lower number of observed species, lower Shannon Diversity and lower Inverse Simpsons Index than the fecal samples ($P<0.0001$ for all). The mean Shannon Diversity measure for fecal sample is 5.98 ± 0.06, whereas the mean value for vaginal samples is 1.06 ± 0.1. This indicates that the fecal microbiome is significantly more complex than the vaginal community. This is a result of the vaginal microbiome being dominated by just a few high abundant OTUs. The most abundant genera found in the vaginal samples are *Ralstonia, Streptococcus* and *Staphylococcus*.

Figure 5.5 Alpha Diversity Fecal vs. Vaginal
Boxplots representing median, IQR, whisker length represents 1.5x IQR of the (a) Observed species, (b) Shannon Diversity and (c) Inverse Simpson Index measures calculated for all samples and grouped by sample site; vagina (n=22) or fecal (n=115). All measures indicate that the fecal community is statistically more complex than the microbial community of the vagina. (****P;<0.0001, Unpaired t-test).

5.3.6.2 Beta Diversity

While Alpha Diversity is descriptive for inferring community structure, the identity of each species is not considered; therefore it will not tell us if the same bacteria are shared between samples. Beta diversity, specifically weighted and unweighted UniFrac distance, was calculated between the vaginal and fecal samples and visualised using Principle co-ordinate Analysis (PCoA). As expected, these pairwise comparisons show substantial variation in bacteria community membership (unweighted UniFrac) and substantial variation in community structure (weighted UniFrac) between the two body sites (Figure 5.6).

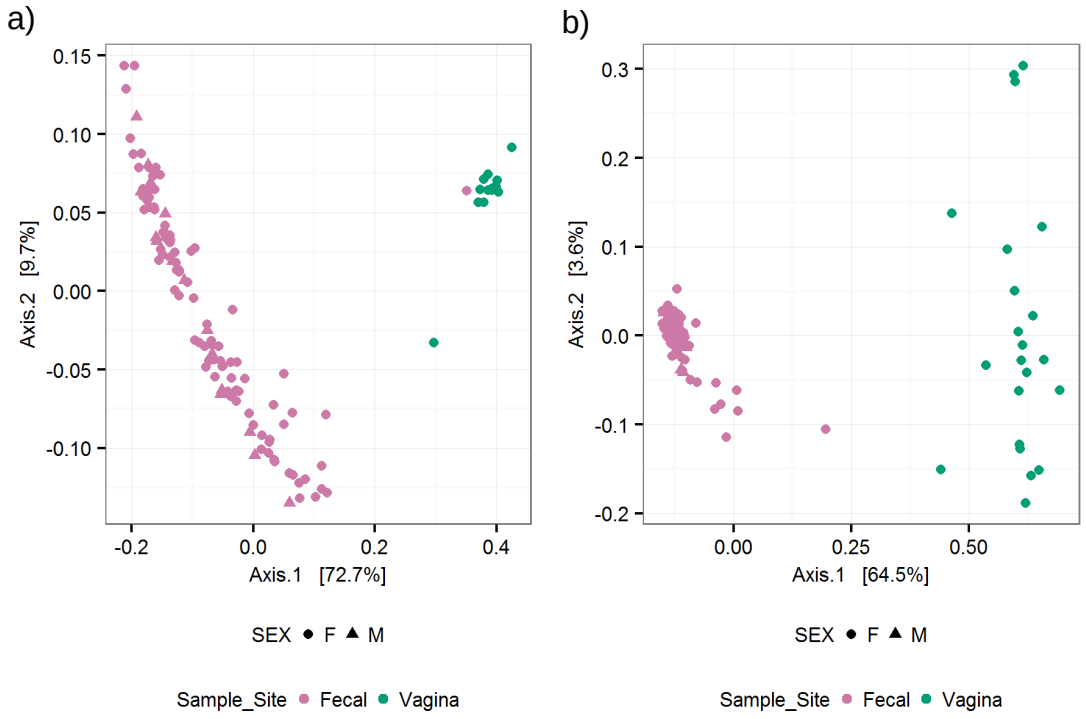

Figure 5.6 UniFrac Distance 2D PCoA plots of Vagina and Fecal Community
(a) Unweighted and (b) weighted UniFrac 2D PCoA plots illustrating the relationship between the bacterial diversity of fecal (n=115) samples compared to vaginal (n=22) samples. Points are coloured by sample group and shape by sample sex. Each point represents an individual sample.

5.3.6.3 Sample Cross Contamination

Due to the close proximity of the murine vagina and anus it is possible that cross-contamination during sampling can occur. To determine whether this is a common occurrence the shared taxa between the two sites were compared. There were 188 overlapping OTUs between the vaginal and fecal samples (Figure 5.7.a). This portion is higher than expected, inferred from what Barfod et al., (2013) had detailed comparing the cecum and vagina. Due to the high depth of sequencing I conducted in this study, many of these shared OTUs are low abundant; less than 100 sequences. If only OTUs with an abundance of >0.1% are considered, the number of shared OTUs is reduced to 50 (data not shown), these shared OTUs represent only 4 different genus level classifications (Figure 5.7.b); *Staphylococcus*, *Lactobacillus*, S24-7-Family, and *Pseudomonas*. This is more in keeping with the proportions of shared taxa detailed in Barfod et al., (2013).

The contribution of *Pseudomonas* to the fecal community is highly skewed by one animal that had predominately *Pseudomonas* sequences. *Pseudomonas* should therefore not be defined as a common fecal bacterium in this study. *Staphylococcus*, *Lactobacillus*, and *Pseudomonas* have previously been reported in the vagina of laboratory and wild mice (MacManes, 2011, Barfod et al., 2013). S24-7 is mostly a mouse gut associated bacteria, sequences from this genus are most likely due to low level contamination from fecal material. The contribution of S24-7 sequences in the vagina is 0.22% compared to fecal sample where 44.6% of sequences are from this clade. To conclude there is very little overlap between fecal and vaginal microbiota, which would be indicative of high levels of cross-contamination during sampling.

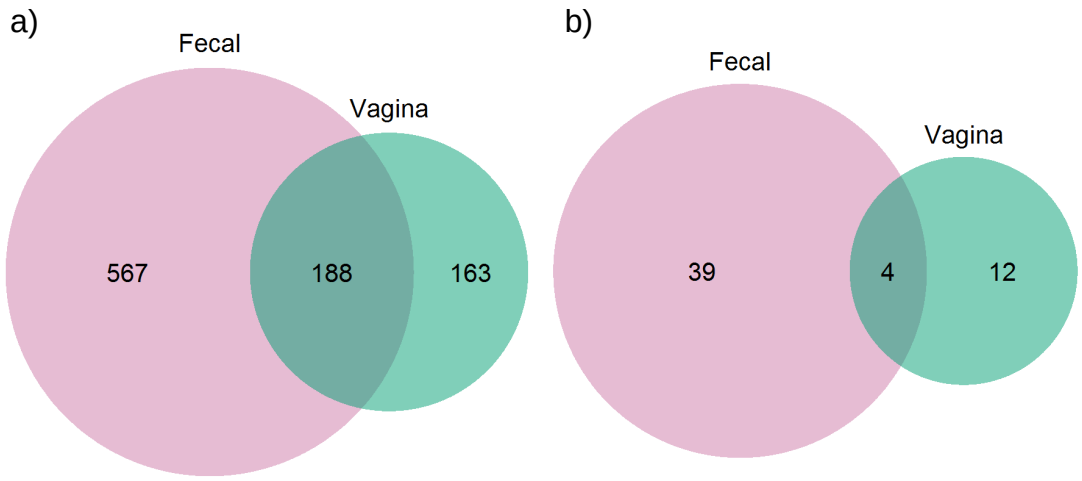

Figure 5.7 Venn diagram of Shared Taxa between Fecal and Vaginal Samples

(a) Displays the number of shared OTUs between fecal and vaginal samples in Subset 1. (b) Shared genus between fecal and vaginal samples from Subset 1 where only OTUs with >0.1% total contribution are considered. Vaginal (n=22) Fecal (n=115).

5.3.7 Fecal Microbiome of *Camp-/-* Animals (Subset 2)

To establish whether *Camp-/-* animals have altered diversity and composition of the fecal microbial community compared to wildtype animals, 16S rRNA sequences from *Camp-/-* samples (n=42) and C57BL/6J samples (n=57) were compared. Alpha diversity measures were compared between these sample populations, in addition, the UniFrac distances were also recomputed on this subset.

5.3.7.1 Phylum Level Classification

The 648 unique OTUs in Subset 2 represented 9 phylum level classifications (Figure 5.8). The murine fecal samples were dominated by two main phyla, *Bacteroidetes* (gram negative) and *Firmicutes* (gram positive), contributing on average 56.78% and 39.57% of the sequences respectively. Seven other phyla were represented but only at very low levels of less than 1%. *Bacteroidetes* and *Firmicutes* collectively made up around 96% of the sequences; this is slightly inflated over other studies that have shown 70–80% contribution of these two phyla (Salzman et al., 2003, Salzman et al., 2007). In this study the relative abundance of *Tenericutes* (0.52% ± 0.02%) and *Deferribacteres* (0.51% ± 0.01%) are lower than seen in other 16S rRNA studies (Turnbaugh et al., 2008, Nagalingam et al., 2011). *Tenericutes* have commonly been shown to contribute around 3-5% of sequences in other 16S rRNA investigations. This clade is highly sensitive to diet, where increases in *Mollicute*, a subclass of *Tenericutes,* have been observed in obese animals (Turnbaugh et al., 2008). In contrast *Mollicute* spp. are decreased in animals as a result of DSS treatment (Nagalingam et al., 2011).

At the phylum level, C57BL/6J and *Camp-/-* samples have a very similar contribution of sequences to the 9 phyla. C57BL/6J have on average 54.63% ± 6.99% sequences classified as *Bacteroidetes,* whereas in the *Camp-/-* samples the average contribution is 58.24% ± 9.48%. For *Firmicutes,* the average contribution in C57BL/6J samples is 41.88% ± 5.36% and 38.01% ± 6.19% in *Camp-/-* samples.

The significance of these differences is estimated using Linear Discriminant Analysis with Effect Size (LEfSe) described later in section 5.3.7.6.

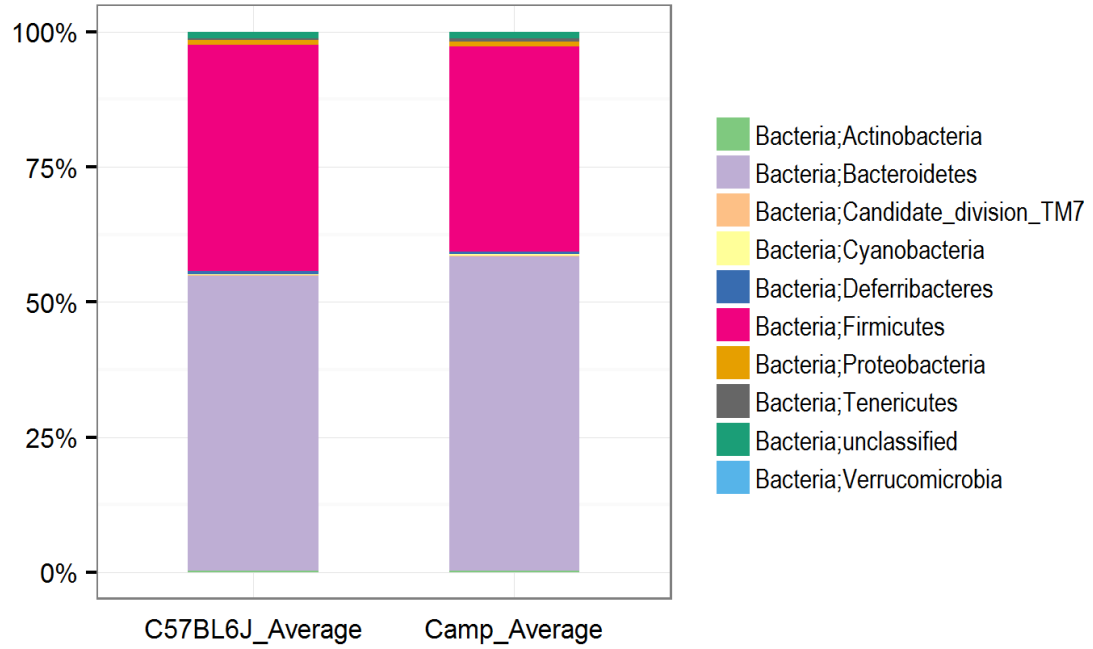

Figure 5.8 Phylum Level Classification in *Camp-/-* vs. C57BL/6J Fecal Samples

Average relative abundance of sequences at the phylum level of C57BL/6J (n=57) and *Camp-/-* (n=42) samples.

Phylum	C57BL/6J	C57BL/6J SD	*Camp-/-*	*Camp-/-* SD
Bacteria;Actinobacteria	0.21%	0.03%	0.26%	0.04%
Bacteria;Bacteroidetes	54.63%	6.99%	58.24%	9.48%
Bacteria;Candidate_division_TM7	0.08%	0.01%	0.08%	0.01%
Bacteria;Cyanobacteria	0.25%	0.03%	0.28%	0.05%
Bacteria;Deferribacteres	0.57%	0.07%	0.47%	0.08%
Bacteria;Firmicutes	41.88%	5.36%	38.01%	6.19%
Bacteria;Proteobacteria	0.85%	0.11%	0.82%	0.13%
Bacteria;Tenericutes	0.35%	0.04%	0.64%	0.10%
Bacteria;Verrucomicrobia	0.00%	0.00%	0.02%	0.00%
Bacteria;unclassified	1.18%	0.15%	1.18%	0.19%

Table 5.3 Phylum Level Classification in *Camp-/-* vs. C57BL/6J Fecal Samples

Average percentage contribution and standard deviation (SD) of sequences to each phylum in C57BL/6J (n=57) and *Camp-/-* (n=42) samples.

5.3.7.2 Genus Level Classification

The 648 unique OTUs in Subset 2 represented 78 genus level classifications. Figure 5.9.a and Table 5.4 show the relative abundance of these genera in each sample (n=99). Genera with a contribution of <0.5% sequences have been grouped and represented as 'low OTUs' for ease of visualisation.

Bacteroidetes

Ten *Bacteroidetes* genera were identified which represent six different families. The most dominant *Bacteroidetes* in the fecal samples were found to be S24-7 family of bacteria, contributing on average 44.98% of the sequences. The next abundant genera of *Bacteroidetes* were, *Alistipes*, *Bacteroides* and *RC9 gut group*, contributing 3.65%, 2.74% and 1.29% average sequences respectively.

S24-7 family, a butyrate-producing bacterium predominantly only seen in rodents, covers the largest component of mouse fecal sequences assigned in the *Bacteroidetes* phylum. *Alistipes* spp. are found in the gastrointestinal tract of both humans and mouse. It has been reported to be the most significantly overrepresented taxa in older mice (Langille et al., 2014), which is consistent to what has been shown in humans, suggesting parallel age related microbial shifts in this taxa (Claesson et al., 2012). Gastrointestinal *Bacteroides* are an abundant and well-studied member of the mammalian commensal microbiota providing many beneficial activities, including the metabolism of complex carbohydrates and glycosylation (Comstock, 2009, Hooper et al., 2001).

Firmicutes

Forty *Firmicutes* genera were identified, representing nineteen different families. The most dominant *Firmicutes* were *Lactobacillus* with 11.23% contribution, followed by *Blautia,* an unclassified *Lachnospiraceae,* and an unclassified *Ruminococcaceae,* with 8.99%, 6.31% and 3.27% average sequence contributions respectively.

Lactobacillus spp. colonise the gut and mucosal sites of most mammals where they can adhere to the non-secreting stomach epithelium, continuously seeding the content of the stomach. Interestingly the absence of *Lactobacillus reuteri* in the gut of mice causes autism-like behaviours, which can be reversed by probiotic inoculation of this bacterium (Buffington et al., 2016). The mechanisms of this are still unclear but *Lactobacillus reuteri* has been shown to increase the levels of the oxytocin hormone (Buffington et al., 2016). Other *Lactobacillus* species have also been found to have cognitive effects in mice (Bravo et al., 2011).

Blautia is a genera often associated with the production of beneficial Short-chain fatty acids (SCFAs), which are also thought to work in helping suppress inflammation. Interestingly giving *Blautia* spp. to mice could protect them from graft versus host disease (Jenq et al., 2015).

Lachnospiraceae family is abundant in the digestive tracts of many mammals but is rarely found at other sites, it is also a group often associated with the production of SCFAs. Members of this family in humans have been linked to obesity and colon cancer, mainly due to the association with the production of Butyric acid. Although this property is not conserved as not all species of *Lachnospiraceae* have genes related to Butyric acid production (Meehan and Beiko, 2014).

Ruminococcaceae is a family normally found just in the ruminant gut, although species within this family have also been seen in human gastrointestinal samples (Wang et al., 2004a).

Shared Taxa

77 of the 78 genera were common to C57BL/6J and *Camp-/-* samples. The only genera not shared were the low abundant *Akkermansia*. C57BL/6J samples collectively had no sequences from this clade; *Camp-/-* animals had 0.02% average *Akkermansia* contribution. Although, this clade was not consistently seen in all *Camp-/-* animals; only 11/42 had *Akkermansia* sequences. The most abundant genera, S24-7 family, are higher in the *Camp-/-* samples; 47.32% compared to C57BL/6J samples which have on average 43.25%. *Lactobacillus* was higher in the

wildtypes displaying 11.82% compared to *Camp-/-* samples which had 10.43% average contribution. Lower abundant genera also show differences such as *Allobaculum*, which is 2.02% in C57BL/6J and 0.95% in *Camp-/-*mice. The significance of these differences, and all other OTUs, is estimated using Linear Discriminant Analysis with Effect Size (LEfSe) as described later in section 5.3.7.6.

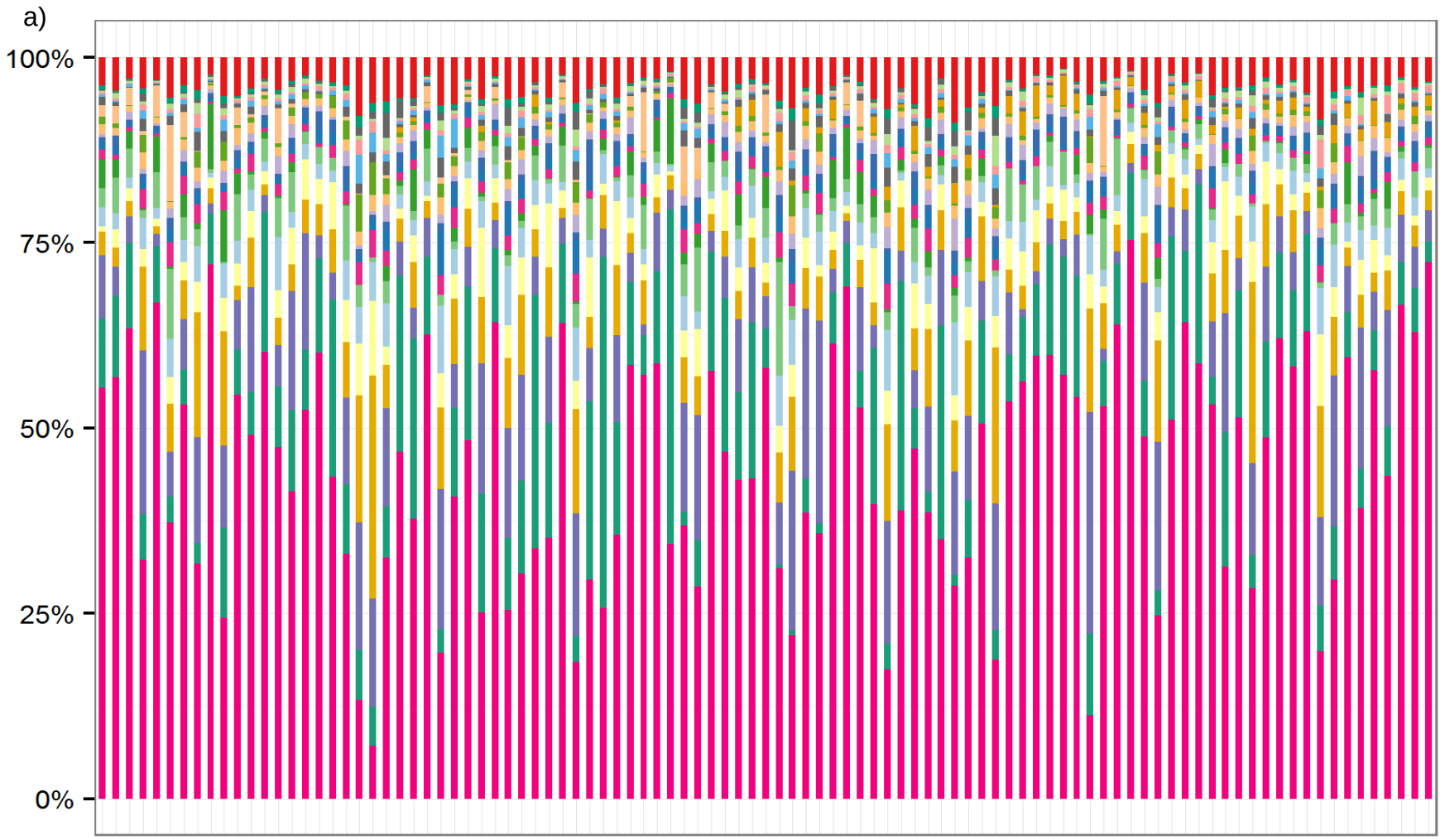
a)
100%
75%
50%
25%
0%

b)

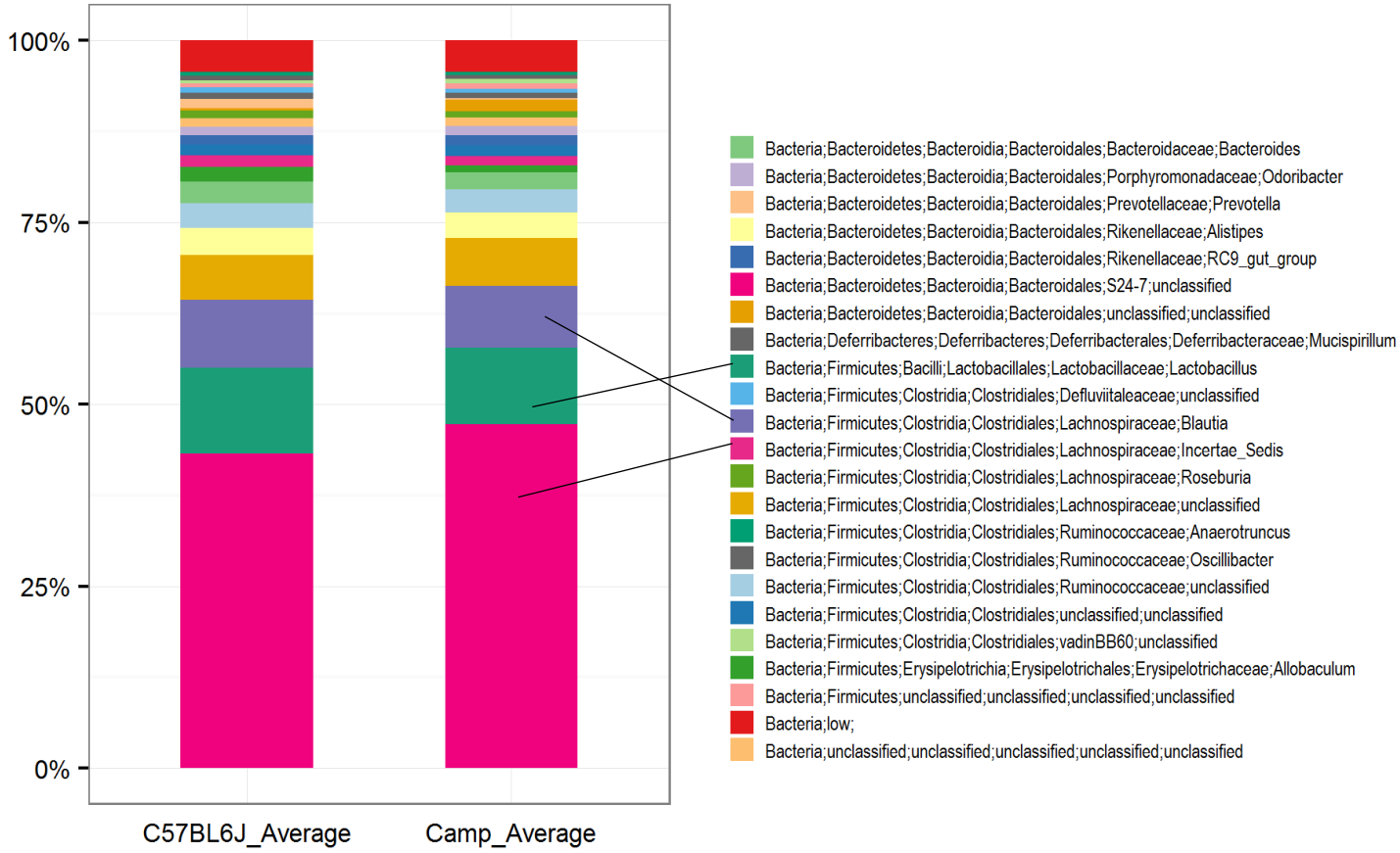

Figure 5.9 Genus Level Classification in *Camp-/-* vs. C57BL/6J Fecal Samples

(a) Relative abundance of each genus level sequence contribution in n=99 fecal samples. (b) Average relative abundance of C57BL/6J (n=57), *Camp-/-* (n=42) fecal samples. For visual clarity, only the 23 most abundant genera are displayed. Those genera with an abundance <0.5% have been combined and displayed as 'Low' (red).

Taxon	C57BL/6J	*Camp-/-*
Bacteria;Bacteroidetes;Bacteroidia;Bacteroidales;S24-7;unclassified	43.25%	47.32%
Bacteria;Firmicutes;Bacilli;Lactobacillales;Lactobacillaceae;Lactobacillus	11.82%	10.43%
Bacteria;Firmicutes;Clostridia;Clostridiales;Lachnospiraceae;Blautia	9.34%	8.52%
Bacteria;Firmicutes;Clostridia;Clostridiales;Lachnospiraceae;unclassified	6.10%	6.58%
Bacteria;Bacteroidetes;Bacteroidia;Bacteroidales;Rikenellaceae;Alistipes	3.70%	3.57%
Bacteria;Firmicutes;Clostridia;Clostridiales;Ruminococcaceae;unclassified	3.38%	3.12%
Bacteria;Bacteroidetes;Bacteroidia;Bacteroidales;Bacteroidaceae;Bacteroides	3.05%	2.33%
Bacteria;Firmicutes;Erysipelotrichia;Erysipelotrichales;Erysipelotrichaceae;Allobaculum	2.02%	0.95%
Bacteria;Firmicutes;Clostridia;Clostridiales;Lachnospiraceae;Incertae_Sedis	1.60%	1.32%
Bacteria;Firmicutes;Clostridia;Clostridiales;unclassified;unclassified	1.49%	1.45%
Bacteria;Bacteroidetes;Bacteroidia;Bacteroidales;Rikenellaceae;RC9_gut_group	1.22%	1.37%
Bacteria;Bacteroidetes;Bacteroidia;Bacteroidales;Porphyromonadaceae;Odoribacter	1.14%	1.35%
Bacteria;unclassified;unclassified;unclassified;unclassified;unclassified	1.18%	1.18%
Bacteria;Firmicutes;Clostridia;Clostridiales;Lachnospiraceae;Roseburia	1.06%	0.76%
Bacteria;Bacteroidetes;Bacteroidia;Bacteroidales;unclassified;unclassified	0.34%	1.64%
Bacteria;Bacteroidetes;Bacteroidia;Bacteroidales;Prevotellaceae;Prevotella	1.32%	0.22%
Bacteria;Firmicutes;Clostridia;Clostridiales;Ruminococcaceae;Oscillibacter	0.85%	0.76%
Bacteria;Firmicutes;Clostridia;Clostridiales;Defluviitaleaceae;unclassified	0.71%	0.54%
Bacteria;Firmicutes;unclassified;unclassified;unclassified;unclassified	0.49%	0.73%
Bacteria;Firmicutes;Clostridia;Clostridiales;vadinBB60;unclassified	0.51%	0.65%
Bacteria;Deferribacteres;Deferribacteres;Deferribacterales;Deferribacteraceae;Mucispirillum	0.57%	0.47%
Bacteria;Firmicutes;Clostridia;Clostridiales;Ruminococcaceae;Anaerotruncus	0.56%	0.47%
Bacteria;low OTUs (<0.5%)	4.29%	4.27%

Table 5.4 Genus Level Classification *Camp-/-* vs. C57BL/6J Fecal Samples

Average percentage contribution of sequences to each genera in C57BL/6J (n=57) and *Camp-/-* (n=42) samples. Those genera with an abundance <0.5% have been combined and displayed as 'Low OTUs'. The significance of any differences including samples of low abundance is evaluated using Linear Discriminant Analysis with Effect Size (LEfSe) as described later in section 5.3.7.6.

5.3.7.3 Alpha Diversity

The alpha diversity measures; S_{obs}, Shannon Diversity and Inverse Simpsons Index were calculated for each sample on the rarefied but unfiltered OTU data (Figure 5.10). There was no significant difference in any alpha diversity metric between the C57BL/6J and the *Camp-/-* samples (two sample t-test). All measures indicate that the fecal communities are equally complex within each genotype.

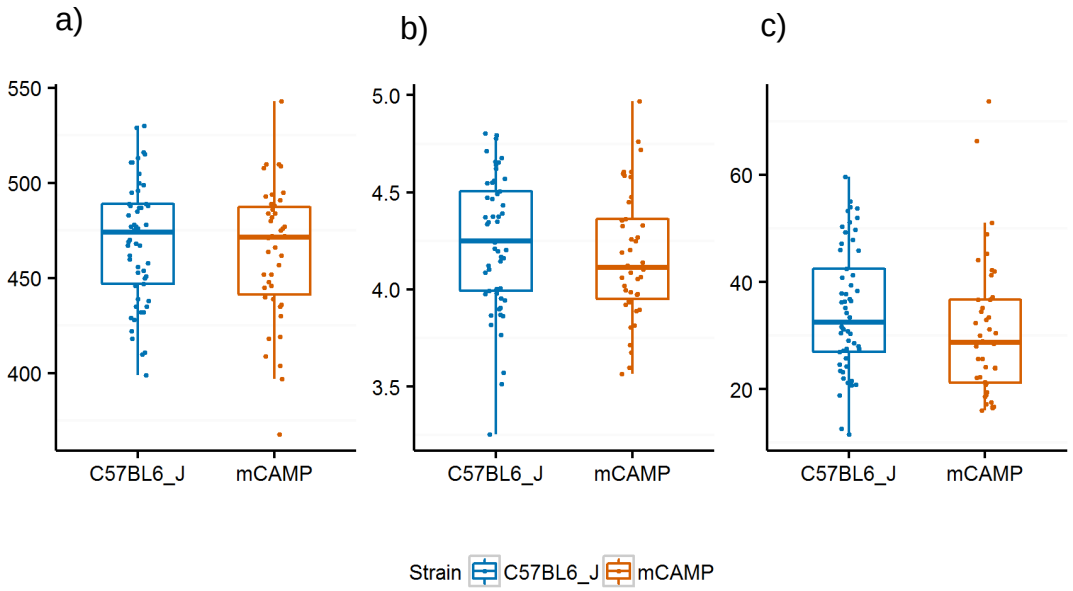

Figure 5.10 Comparison of Alpha diversity for C57BL/6J vs. *Camp-/-*
Boxplots representing median, IQR, whisker length represents 1.5x IQR of the (a) observed species S_{obs} (b) Shannon Diversity (c) and Inverse Simpsons Index calculated for all samples and grouped by genotype; C57BL/6J (n=57) and *Camp-/-* (n=42). All measures indicate that the fecal communities are equally complex (NS: two sample unpaired t-test).

5.3.7.4 Beta Diversity

The pairwise qualitative difference between sample diversities (unweighted UniFrac) distances reveals there is a highly significant difference in the diversity within genotypes compared to between genotypes ($P<0.0001$), whereby *Camp-/-* knockout animals are significantly more diverse than the wildtype controls ($P<0.0001$) (Figure 5.11). The diversity between genotypes is also significantly more than the diversity within each genotype respectively ($P <0.0001$ for both). Nonparametric p-values were also calculated using 999 Monte Carlo permutations and Bonferroni-corrected, all tested pairs give $P <0.01$.

That is to say animals are more similar to other animals of the same genotype than they are to another animal of the opposite genotype. In addition the *Camp-/-* animals have more bacterial diversity than the wildtype animals.

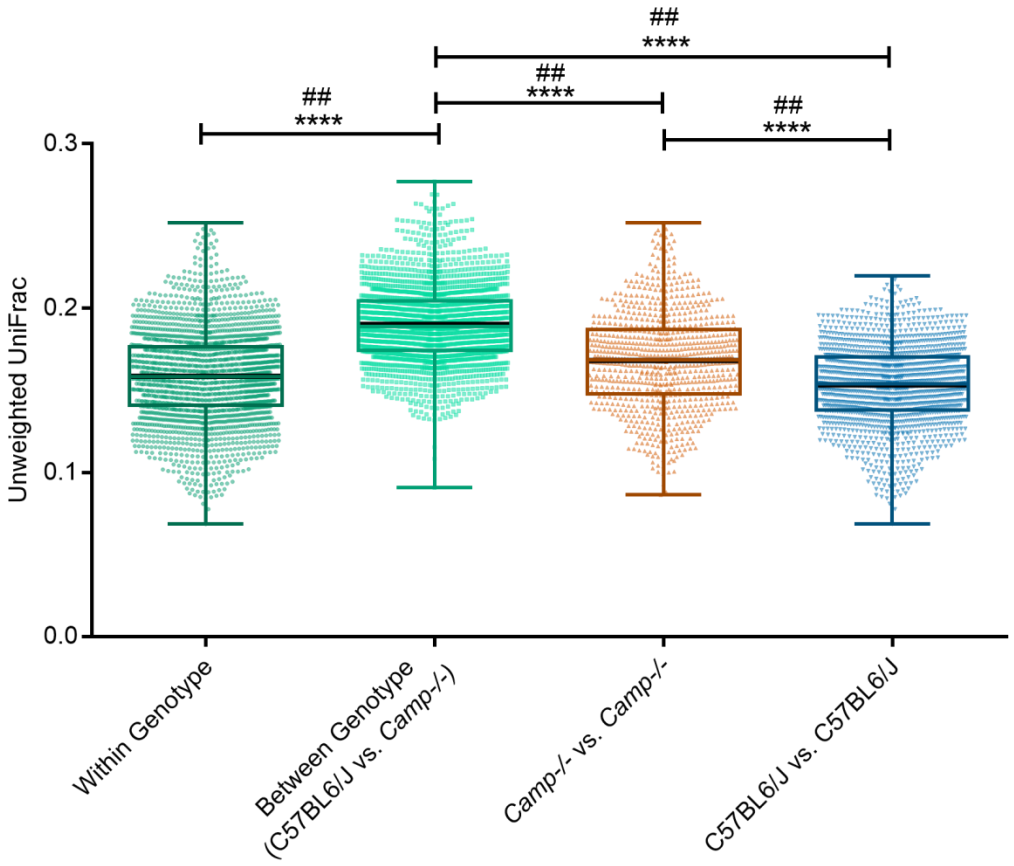

Figure 5.11 Unweighted UniFrac Distance Boxplots comparing C57BL/6J vs. *Camp-/-*

Boxplots representing median, IQR with min, max whisker of pairwise unweighted UniFrac distance within genotypes and between genotypes. (Parametric two sample t-test, Bonferroni-corrected P<0.0001;****) (Nonparametric p-value using 999 Monte Carlo permutations and Bonferroni-corrected P<0.01; ##) C57BL/6J (n=57) and *Camp-/-* (n=42)

The pairwise UniFrac distances were visualised using Principle co-ordinate Analysis (PCoA) (Figure 5.12). Principal coordinate 1 (Axis 1; percent variation explained: 19.6%) of the unweighted UniFrac distances separates the two genotypes, while Principal coordinate 2 (Axis 2; percent variation explained: 9.7%) intercepts the genotypes and appears to be driven partly by cage variation, especially for the wildtype cluster (Figure 5.13). In the weighted UniFrac plot, there is no apparent separation of the samples by genotype or cage, and therefore does not highlight substantial variation in community structure. The clustering of samples by genotype in the unweighted UniFrac suggests a strong relationship in terms of qualitative community membership.

In other terms, it is the presence or absence of certain OTUs that is driving the clustering by genotype, more so than the abundance of the OTUs that are shared.

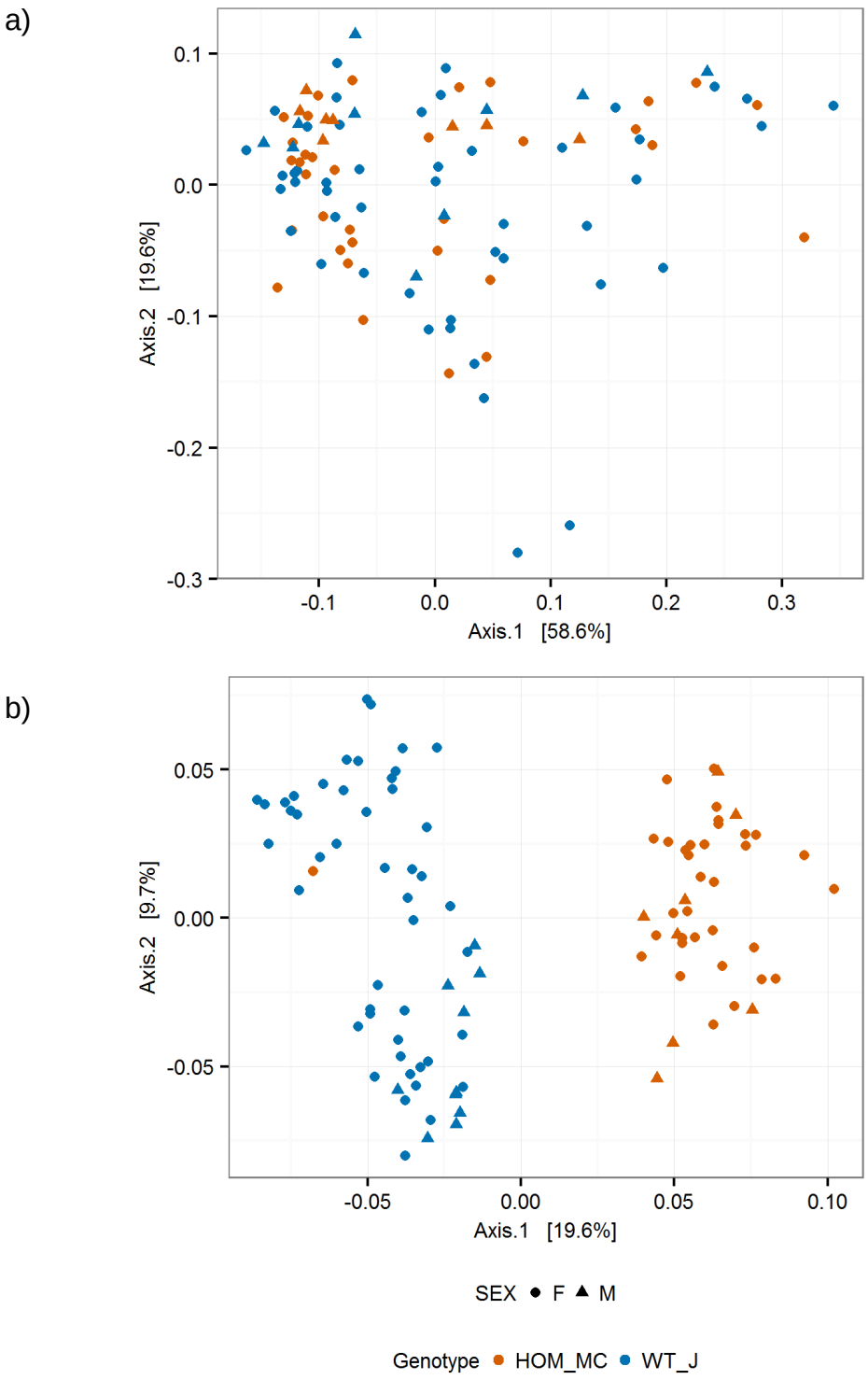

Figure 5.12 UniFrac Distance 2D PCoA plots - Coloured by Genotype
(a) Weighted and (b) Unweighted UniFrac 2D PCoA plots illustrating the relationship between the bacterial diversity of fecal samples from C57BL/6J (n=57) and *Camp-/-* mice (n=42). Points are coloured by genotype and shape by sample sex. Each point represents an individual sample. PCoA axis 1; horizontal separation PCoA axis 2; vertical separation. (HOM_MC = *Camp-/-*, WT_J = C57BL/6J)

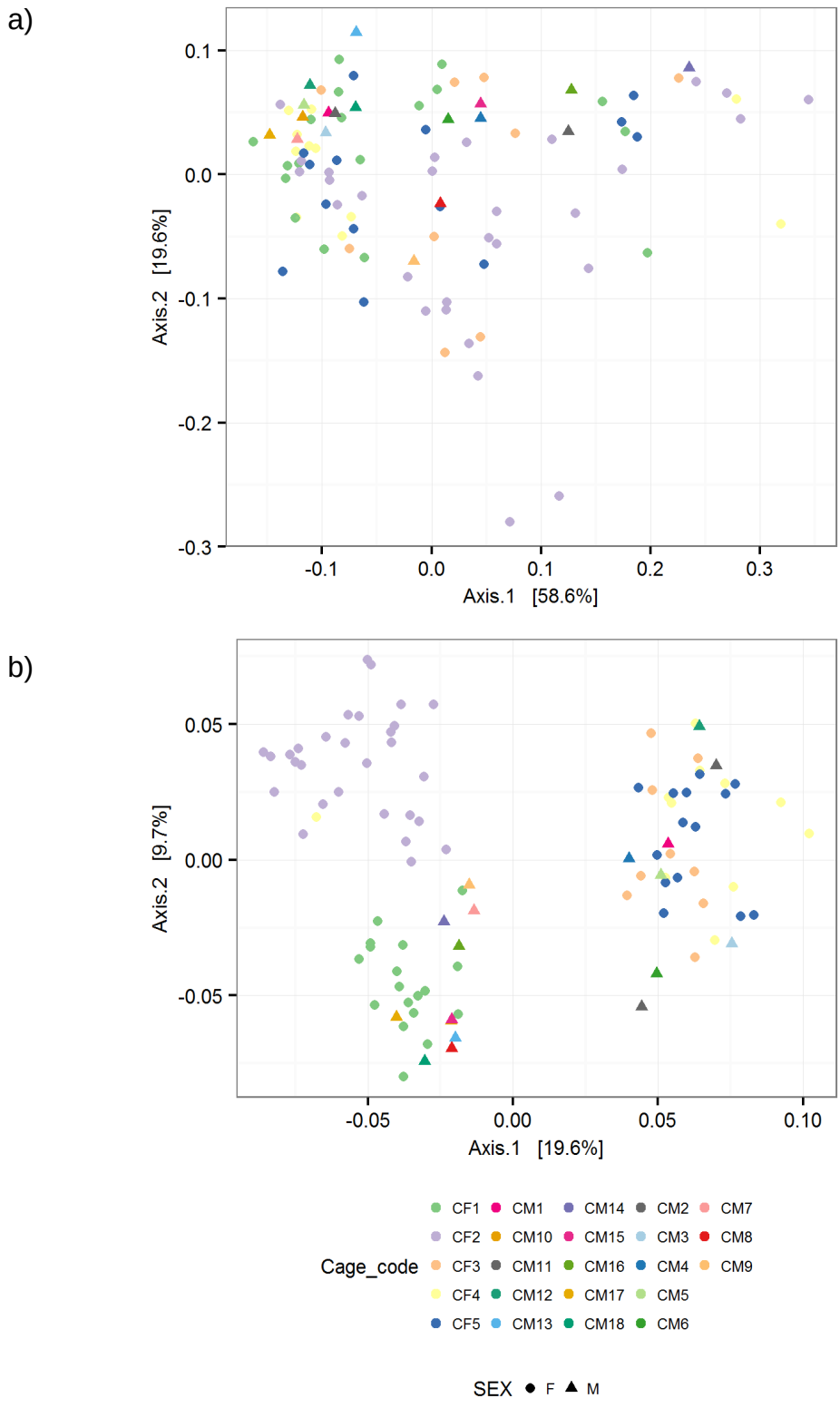

Figure 5.13 UniFrac Distance 2D PCoA plots - Coloured by Cage
(a) Weighted and (b) Unweighted UniFrac 2D PCoA plots illustrating the relationship between the bacterial diversity of fecal samples from C57BL/6J (n=57) and *Camp-/-* (n=42) samples. Points are coloured by breeding cage and shape by sample sex. Each point represents an individual sample.

To determine whether the spatial separations in the PCoA plots associated with genotype were significant, two methods of hypothesis testing were conducted; ANOSIM and Adonis. ANOSIM was conducted on the unweighted UniFrac distance matrix and compared C57BL/6J and *Camp-/-* samples. The difference between genotypes is significant with an *r*-statistic of 0.6345 (P <0.001). Adonis, a permutation approach, gave an r^2 value of 0.16781 (P <0.001). The concordant result of these two hypothesis methods gives weight to the conclusion that the grouping of samples based on genotype is significant. The same hypothesis tests on the weighted UniFrac distances did not show any significant values which backs up the lack of clustering in the PCoA plots (Table 5.5).

Adonis Test Factor	**Df**	**Sums of Sqs**	**Mean Sqs**	**F.Model**	***r*²**	**Pr(>F)**	
Unweighted Genotype	1	0.2564	0.2564	19.5600	0.1678	0.001	***
Weighted Genotype	1	0.0700	0.0700	1.6820	0.0170	0.195	

ANOSIM Test Factor	**Number of permutations**	***r* statistic**	**p-value**	
Unweighted Genotype	999	0.63450	0.00100	***
Weighted Genotype	999	0.00180	0.35700	

Table 5.5 Hypothesis testing comparing C57BL/6J vs. *Camp-/-* Samples
Adonis (top) and ANOSIM (bottom) summary statistics comparing C57BL/6J (n=57) and *Camp-/-* (n=42) samples. Both tests on unweighted UniFrac distance show significant grouping. Weighted UniFrac distance shows no significant grouping by genotype.

As a portion of samples in this study were taken from the same mouse across 4 time-points, this raises the question of whether intra-mouse correlations are artificially increasing the similarity within genotype. To address this question, I examined the average beta-diversity from the same mouse and compared to the beta-diversity between mice, within the same genotype (Figure 5.14). The mean unweighted UniFrac distance within animals is statistically lower than the mean UniFrac distance between animals in both genotypes (P; <0.0001; parametric two sample t-test, Bonferroni-corrected). Overall this suggests the phylogenetic diversity within the same-animal at the different time-points is more similar than between samples at the various time-points. That is to say animals are more similar to themselves than they are to another animal within genotype. This difference suggests no substantial intra-mouse changes in the microbiome composition over the short period of time (17 days). This will however inflate the apparent similarity within genotype; therefore a further subset of the data is required to only include mice that have been sampled once to confirm this separation by genotype is significant. Sub-setting to only include a single time-point (Day 0) will also reduce any confounding signals relating to pregnancy.

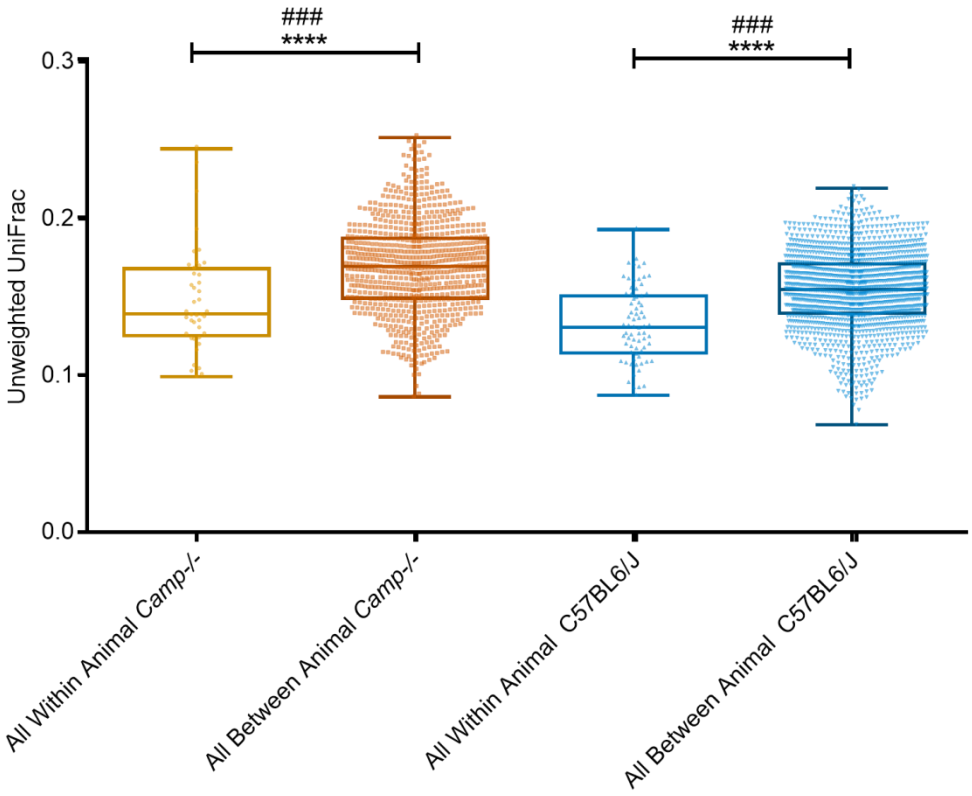

Figure 5.14 Unweighted UniFrac Distance Boxplots - Inter and Intra Animal Variation

Boxplots representing median, IQR with min, max whisker of pairwise unweighted UniFrac distance within genotypes and between genotypes. (Parametric two sample t-test, Bonferroni-corrected P<0.0001;****) (Nonparametric p-value using 999 Monte Carlo permutations and Bonferroni-corrected P<0.01; ##) C57BL/6J (n=57) and *Camp*-/- (n=42)

The pairwise UniFrac distances were recalculated to only include samples from Day 0 and visualised using Principle co-ordinate Analysis (PCoA) as before (Figure 5.15 & Figure 5.16). Axis 1 of the unweighted UniFrac distances separates the two genotypes as was shown previously. In the weighted UniFrac plot, there is no apparent separation of the samples by genotype or cage, and therefore does not highlight substantial variation in community structure, as previous. The clustering of samples by genotype by unweighted UniFrac in the reduced subset suggests the strong relationship in community membership is upheld.

To determine whether the spatial separations in the PCoA plots associated with genotype were still significant after reducing the subset to just Day 0; ANOSIM and Adonis were applied. ANOSIM suggested the difference between genotypes is significant with an *r*-statistic of 0.5856 ($P < 0.001$). Adonis gave an r^2 value of 0.1725 ($P < 0.001$). The concordant result of these two hypothesis methods gives weight to the conclusion that the grouping of samples based on genotype is significant. The same hypothesis tests on the weighted UniFrac distances did not show any significance, which backs up the lack of clustering in the PCoA plots (Figure 5.15).

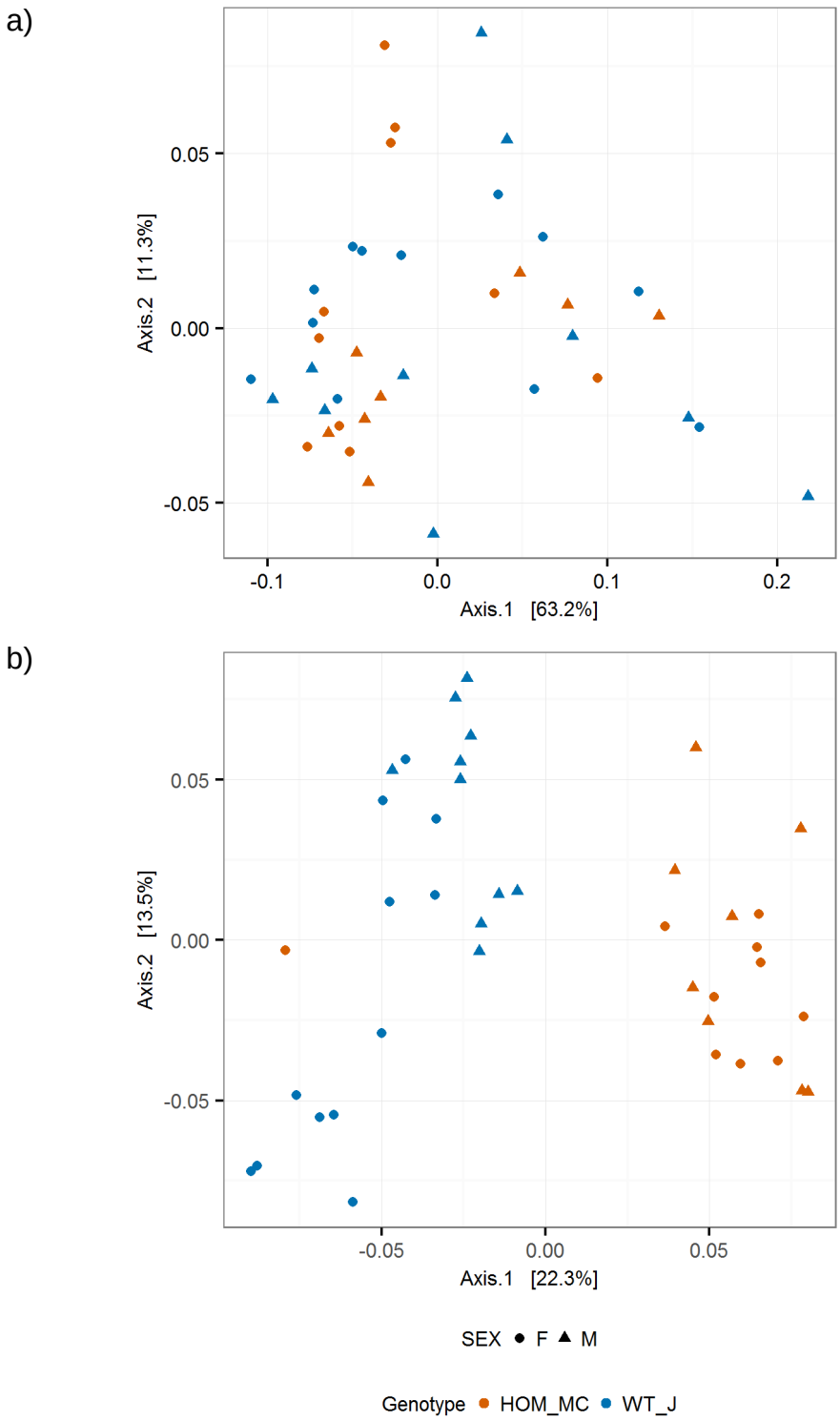

Figure 5.15 UniFrac Distance 2D PCoA plots - Coloured by Genotype; Day 0 Subset

(a) Weighted and (b) Unweighted UniFrac 2D PCoA plots illustrating the relationship between the bacterial diversity of fecal samples from C57BL/6J (n=22) and *Camp-/-* (n=17) animals. Points are coloured by genotype and shape by sample sex. Each point represents an individual animal. (HOM_MC = *Camp-/-*, WT_J = C57BL/6J)

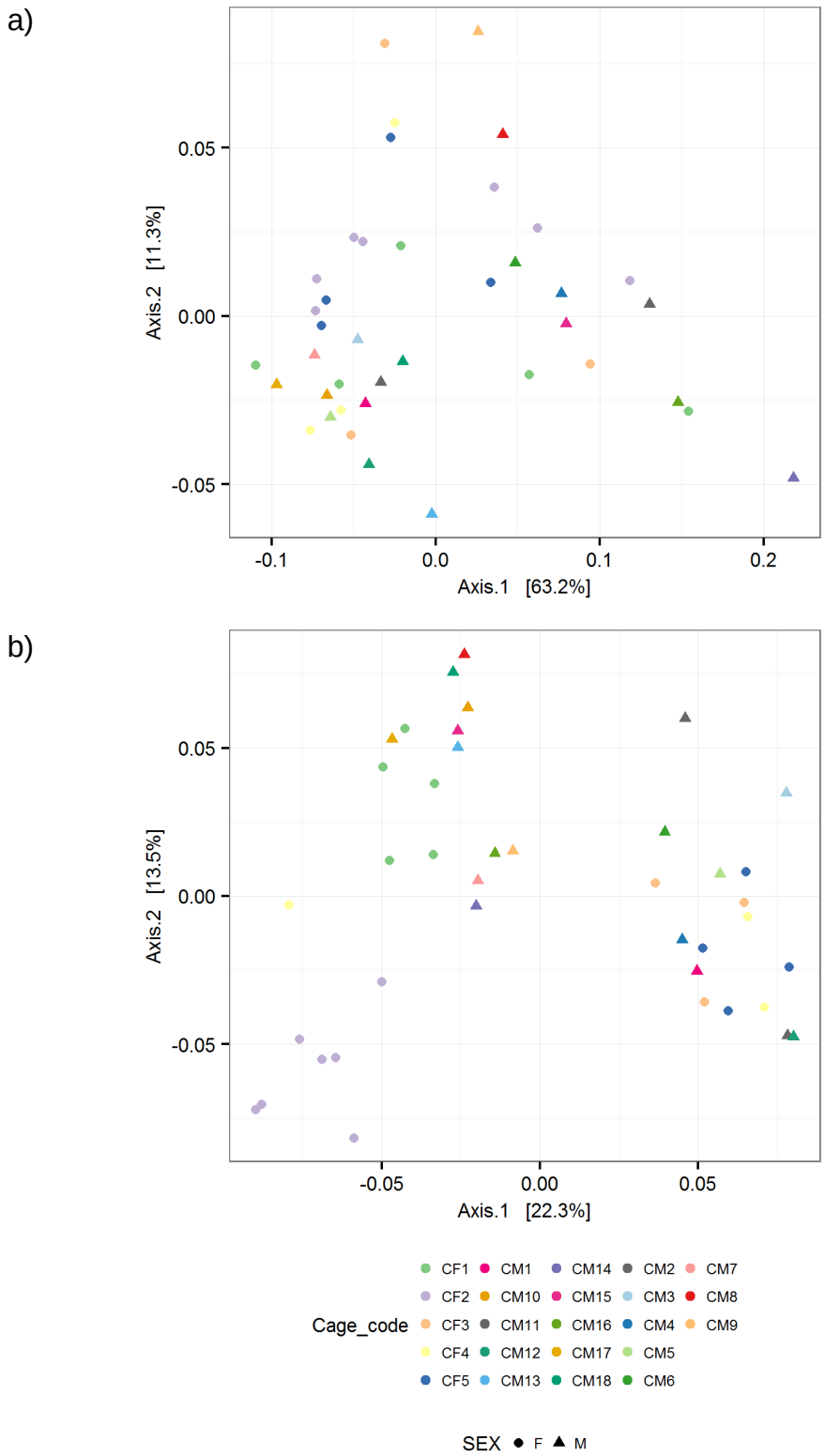

Figure 5.16 UniFrac Distance 2D PCoA plots - Coloured by Cage; Day 0 Subset

(a) Weighted and (b) Unweighted UniFrac 2D PCoA plots illustrating the relationship between the bacterial diversity of fecal samples from C57BL/6J (n=22) and *Camp*-/- (n=17) animals. Points are coloured by breeding cage and shape by sample sex. Each point represents an individual animal.

Adonis Test Factor	Df	Sums of Sqs	Mean Sqs	F.Model	r^2	Pr(>F)	
Unweighted Genotype	1 (38)	0.0983	0.09836	7.9216	0.1725	0.001	***
Weighted Genotype	1 (38)	0.0350	0.03507	1.3028	0.0331	0.233	

ANOSIM Test Factor	Number of permutations	*r* statistic	p-value	
Unweighted Genotype	999	0.5856	0.001	***
Weighted Genotype	999	0.0056	0.310	

Table 5.6 Hypothesis testing comparing C57BL/6J vs. *Camp-/-* Animals; Day 0 subset

Adonis (top) and ANOSIM (bottom) summary statistics comparing C57BL/6J (n=22) and *Camp-/-* (n=17) animals. Both tests on unweighted UniFrac distance show significant grouping. The weighted UniFrac distance shows no significant grouping by genotype in either test.

5.3.7.5 Jack-knife Support; UPMGA bootstrapping

To estimate the uncertainty in the PCoA plots, Jack-knife bootstrapping was performed, whereby samples are hierarchically clustered based on inter-sample variation in UniFrac distances. Specifically, 100 jack-knife replicates at 45,000 sequences were used to generate a bootstrapped Unweighted-Pair Group Method with Arithmetic mean (UPGMA) tree for the unweighted distance matrix (Figure 5.17). Tree generally supports the clustering seen in the PCoA plots; phylogenetic clustering of samples by genotype with the exception of one outlier and root.

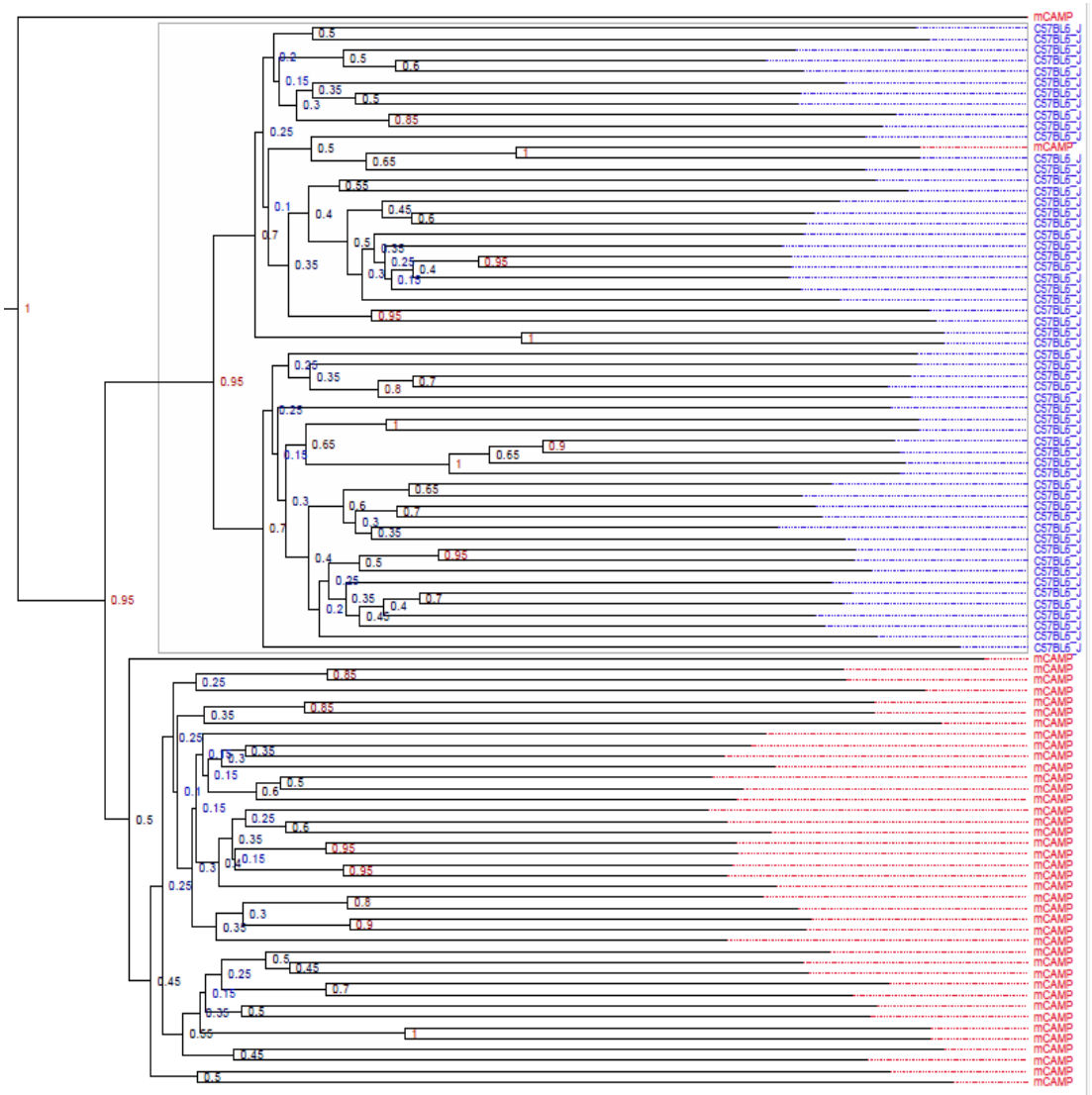

Figure 5.17 Jack-knife Unweighted UniFrac UPGMA Bootstrapped Tree
Unweighted UniFrac pair group method with arithmetic mean (UPGMA) of Jack-knife distance, re-sampling 100 times at 45,000 sequences. Fecal Samples are coloured according to genotype. (mCAMP = *Camp-/-* (red), C57BL6_J (blue))

5.3.7.6 Significant Taxa (LEfSe)

Using Linear Discriminant Analysis with Effect Size (LEfSe), an all-against-all multi-class comparison of C57BL/6J and *Camp-/-* fecal samples was performed (Figure 5.18). This highlighted several taxa were specifically modulated by genotype.

A total of three core microbial groups at the family level were identified with enrichment; *Erysipelotrichaceae, Anaeroplasmataceae* and *Prevotellaceae*. The most notable OTU assigned to be enriched in *Camp-/-* samples was OTU0003, which was classified as S24-7 family of bacteria, having an LDA score of 4.12. At the family level this bacterium is not shown to have significant enrichment in *Camp-/-* samples. OTUs within *Lachnospiraceae* and *Blautia* genera were also enriched in *Camp-/-* animals.

C57BL/6J samples show an enrichment of *Prevotella*, this is very interesting as the *Camp-/-* samples are nearly devoid of *Prevotella* clade. Certain *Blautia* OTUs and *Allobaculum* are also enriched in the C57BL/6J samples.

The only enriched 'class'-level taxa was *Erysipelotrichia* (*p.Firmicutes*), which was mainly attributed to the genera *Allobaculum. Allobaculum* was significantly enriched in C57BL/6J compared to *Camp-/-* samples. The other main genera showing multi-level enrichment were *Anaeroplasma*, which were enriched in *Camp-/-* samples. As one of the few Ten*ericutes* observed in this study, *Anaeroplasma* contributed to the enrichment back to the 'order'-level of classification. *Prevotella* was highlighted as an enriched genera in the C57BL/6J animals, this genus (and family) were also notably absent from the *Camp-/-* samples with the exception of one outlier sample.

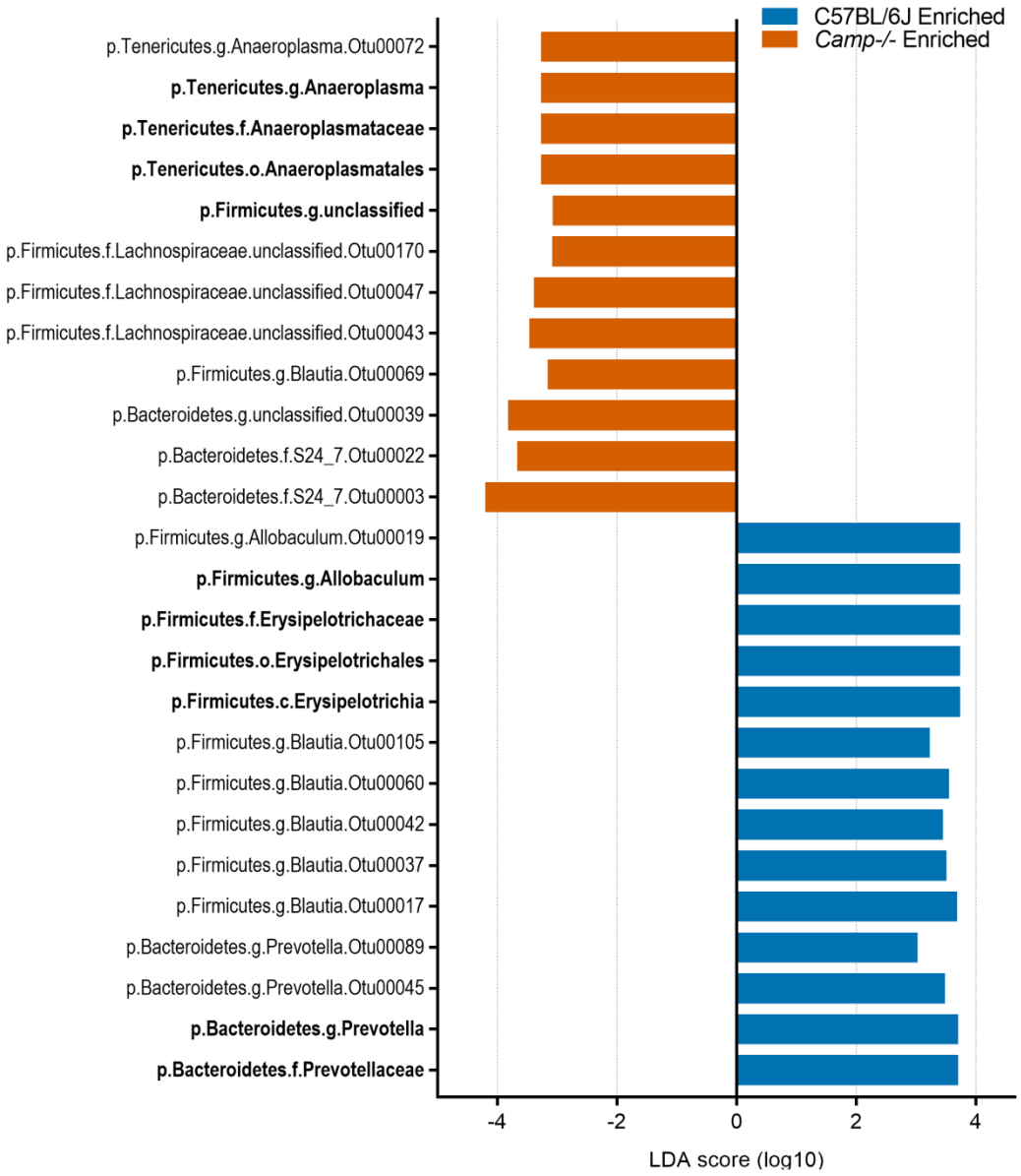

Figure 5.18 Significant Differential Abundant Taxa in C57BL/6J vs. *Camp-/-* Fecal samples

Differential abundant taxa with and LDA cut-off score of >3.0. Enriched taxa in C57BL/6J samples (n=57) are indicated with positive LDA score, while taxa enriched in *Camp-/-* (n=42) have a negative LDA score. 'p', phylum; 'c', class; 'o', order; 'f', family; 'g', genus. For visual clarity, the full classifications of the significant taxa are not annotated. Only the phylum and the significant domain are annotated. Where the significant domain is 'unclassified' the next hierarchical domain with a classification is given. (See appendix for full taxonomic classification)

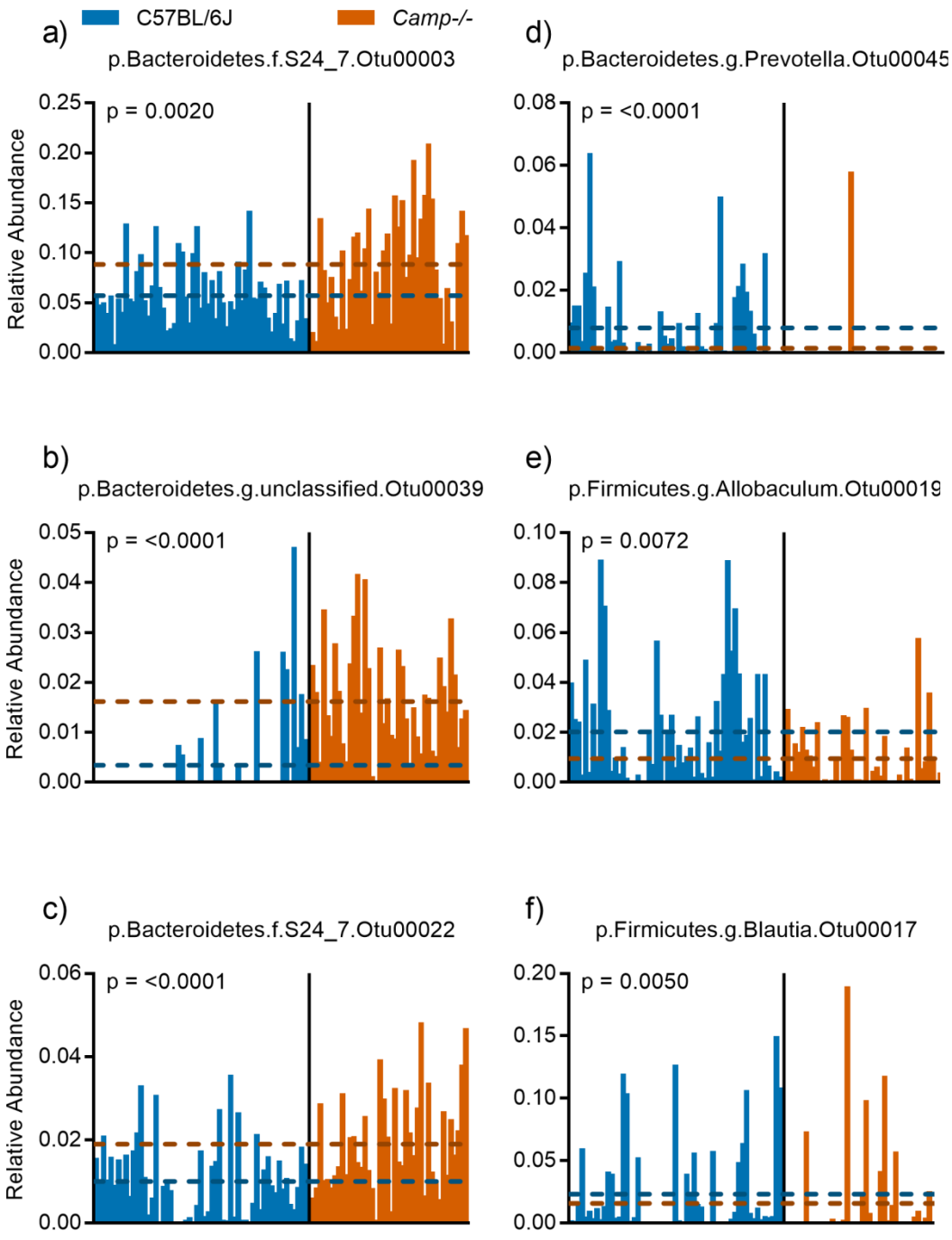

Figure 5.19 Top 6 Differential abundant OTUs
Comparison of relative abundance of top OTUs highlighted as enriched in C57BL/6J (a-c) or *Camp-/-* (d-f) samples. Each bar represents a sample and the mean value within genotype is represented by the dotted line. (P value for each OTU group is reported using Wilcoxon rank sum test). Taxa names are previously described in Figure 5.18.

5.3.8 Pregnancy Modulation of the Microbiome (Subset 3)

To examine whether the fecal microbiome varied longitudinally both in a non-pregnant and pregnant state, samples were partitioned to only include the wildtype C57BL/6J animals which were sampled at 4 time-points over 17 days (n=44 samples; 16 non-pregnant, 28 pregnant).

5.3.8.1 The Stability of the Fecal Microbiome- Non Pregnant

Establishing baseline instability in a population is important when trying to infer microbial shifts that are truly related to pregnancy. It is therefore important to establish the diversity and composition of the bacterial community in a steady sate. To determine the stability of the fecal microbiome over 17 days, longitudinal samples of female C57BL/6J animals (n=4 animals, n=16 samples) were analysed for alpha and beta diversity measures. The 4 mice investigated here (Animal ID: F01, F04, F05, and F12) had very similar bacterial communities, mostly dominated by S24-7 family of bacteria but also high abundances of *Lactobacillus* and *Blautia* spp. (Figure 5.20).

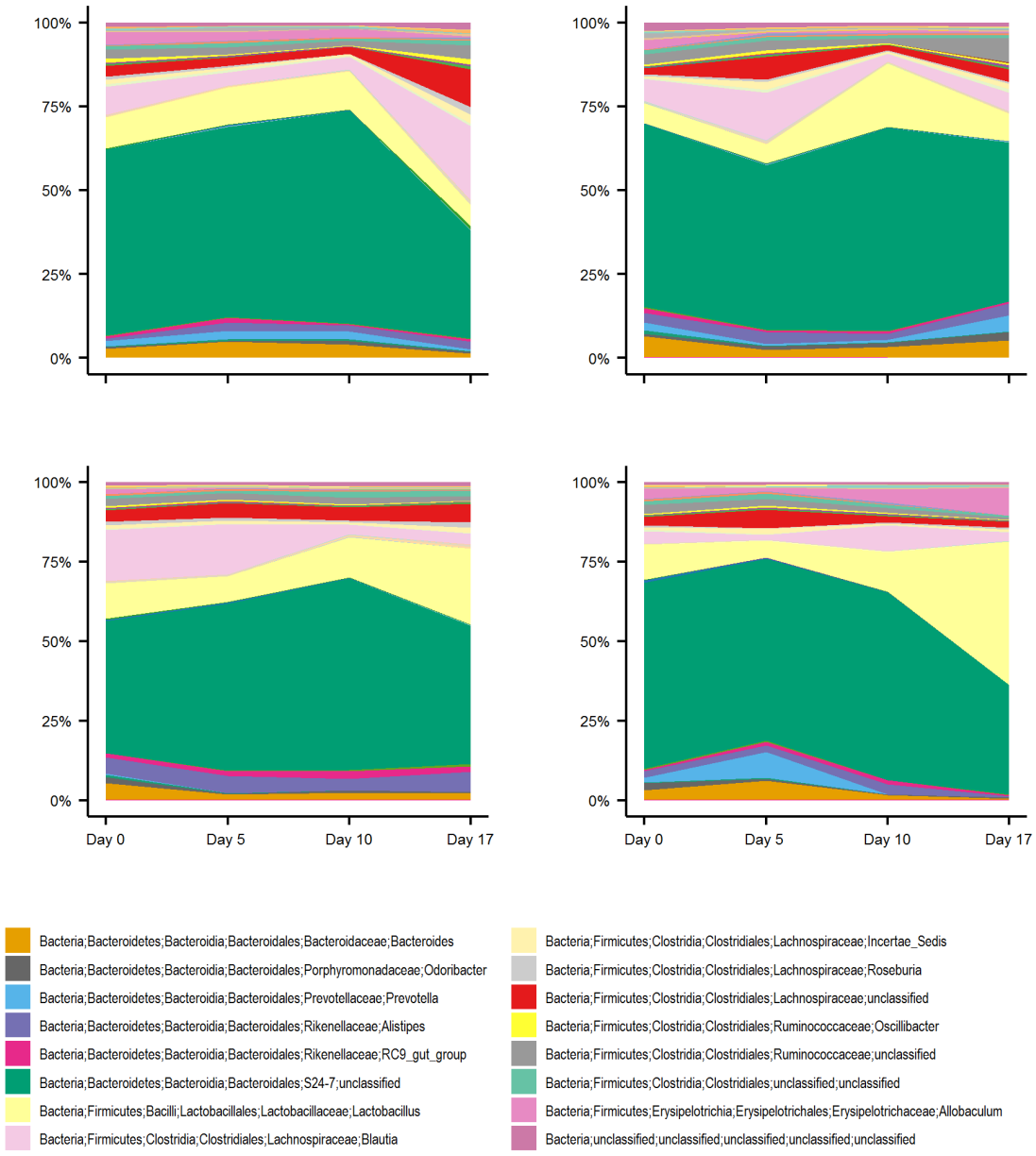

Figure 5.20 Stability of the non-pregnant Fecal Microbiome; Relative Abundance of Genera

Area charts of the relative abundance of taxa at the genus level in n=4 C57BL/6J animals sampled across 4 time-points (Day 0, 4, 10, and 17). For visual clarity, only the 16 most abundant genera are displayed in the key. Animal ID - F01 top left; F04 top right, F05 bottom left and F12 bottom right.

Alpha diversity measures in the longitudinally sampled C57BL/6J animals showed that at day 10 the mean number of observed species (S_{obs}) were significantly lower than that at Day 0 ($P < 0.05$) (Figure 5.21). Although there was a trend for the Shannon Diversity and Inverse Simpson Index to be lower at Day 10, and dispersed at Day 17, neither linear regression analysis nor matched one-way ANOVA suggest this trend was significant. I can therefore conclude that at the community level there is no great difference in bacterial complexity within a mouse across a 17 day period.

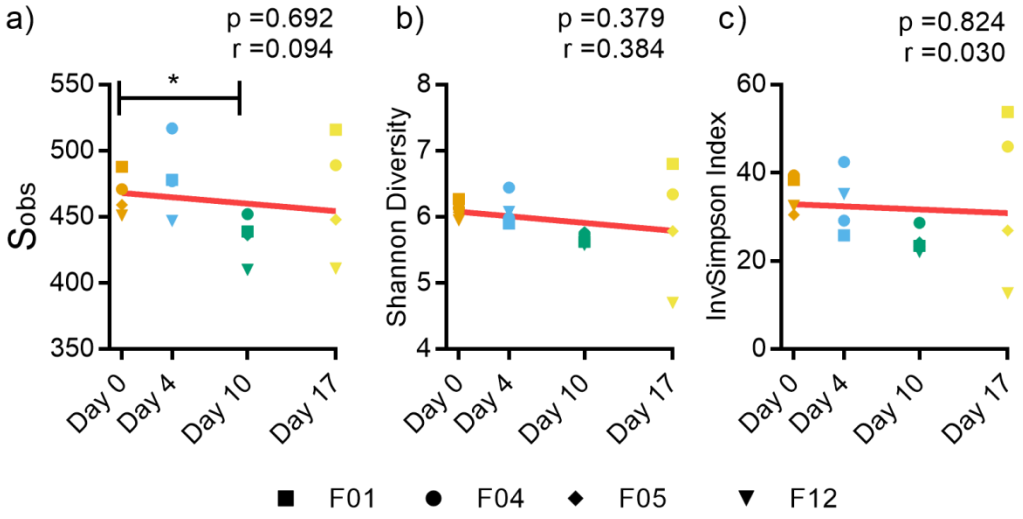

Figure 5.21 Stability of the non-pregnant Fecal Microbiome; Alpha Diversity Measures

(a) Observed species (S_{obs}), (b) Shannon Diversity and (c) Inverse Simpson Index measures of samples from C57BL/6J (n=4) animals collected over 4 time-points (n=16 total samples). Animal ID at each time-point can be identified by the shape of the point. There was no significant linear fit to any of the alpha metrics using a linear regression model. One-way matched ANOVA with Dunnett's post-test compared to Day 0 highlighted a small but significant difference in S_{obs} at Day 10 (*, $P < 0.05$).

No significant trend (P =0.5173) over collection day was observed in the unweighted UniFrac distance between same-animal fecal samples comparing progressive time-points (Figure 5.22). Although the numbers here are low, this suggests the beta diversity across 4 time-points within-animal is mostly stable.

There was no significant difference (P=1.0) in the mean unweighted UniFrac distance within collection day (0.150 ± 0.006) compared to between collection day (0.149 ± 0.0027) (parametric two sample t-test, Bonferroni-corrected), suggesting the between-animal composition of the bacterial species across 17 days is not significantly different (Figure 5.23).

The mean unweighted UniFrac distance within animal is statistically lower than the mean distance between different animals (P; <0.0001; parametric two sample t-test, Bonferroni-corrected) (Figure 5.23). Nonparametric p-values were also calculated using 999 Monte Carlo permutations, (P; < 0.0001) although this significance did not hold once Bonferroni-corrected (P = 0.66). Overall this suggests the phylogenetic diversity within the same-animal at the different time-points is more similar than between samples from different animals at the various time-points. That is to say animals are more similar to themselves than they are to another animal, which is not suggestive of significant community instability within-animal.

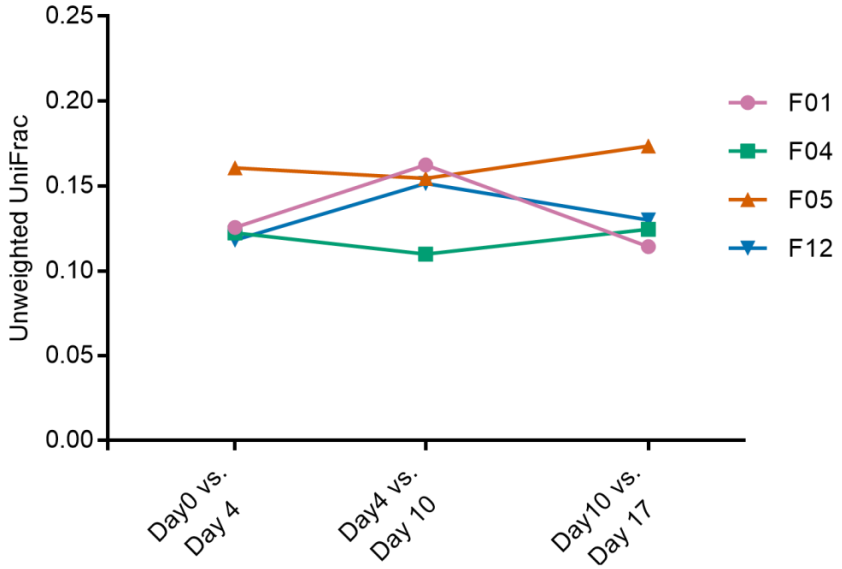

Figure 5.22 Stability of the non-pregnant Fecal Microbiome; Beta Diversity

Unweighted UniFrac distance between same-animal samples comparing progressive time-points. For reference each Animal ID is given and coloured accordingly (NS; RM one-way ANOVA)

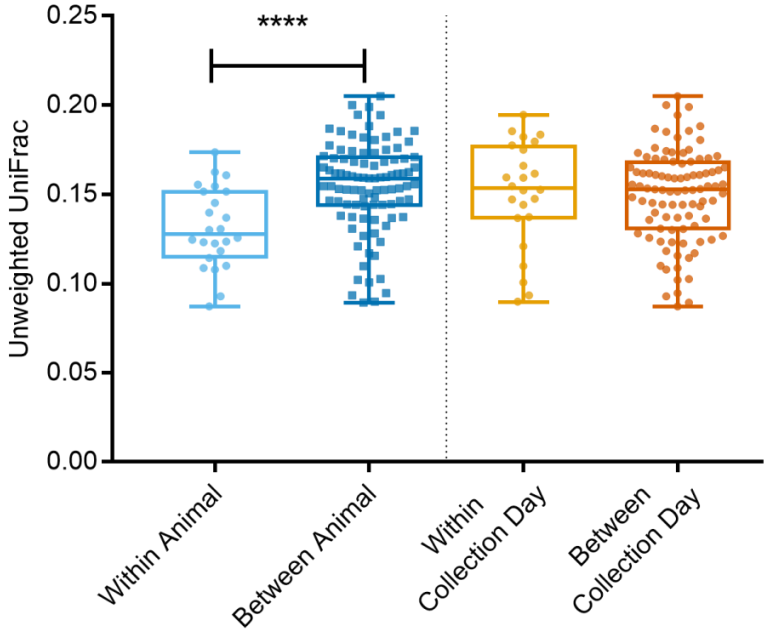

Figure 5.23 Unweighted UniFrac Distance Boxplots - Inter-animal and collection day

Boxplots representing median, IQR with min, max whisker of pairwise unweighted UniFrac distance within genotypes and between genotypes (left) and within and between collection day (right). (Two sample t-test, Bonferroni-corrected P<0.0001;****)

5.3.8.2 Pregnancy Related Microbial Change; Alpha Diversity

To examine whether the fecal microbiome varied longitudinally with gestation, I applied a linear regression to the Observed species, Shannon Diversity and Inverse Simpson Index (Figure 5.24) both in a non-pregnant and pregnant state. The only linear trend was seen in the pregnant Inverse Simpson index ($P = 0.024$, $r = 0.180$) (Figure 5.24.b). However, there is no significant difference in this regression compared to the non-pregnant control slope ($P = 0.192$). In a similar regard, there was no significant difference between the slopes from pregnant and non-pregnant mice in either the S_{obs} ($P = 0.525$; Figure 5.24.a) or Inverse Simpson Index ($P = 0.798$; Figure 5.24.c). This indicates the diversity in microbial community did not progressively change in terms of complexity throughout gestation.

The prior tested hypothesis is that microbial changes in pregnancy are accumulative and progressive with gestation. However this need not be the case; many of the metabolic and immunological changes that could impact the microbiome are temporal during pregnancy. To test a non-linear association between alpha diversity and gestation, a two-way ANOVA was also conducted. The two-way ANOVA showed no significant association with time-point in either the pregnant (i.e. gestation) or non-pregnant samples (i.e. time-point). This gives further support to the conclusion that the complexity of the microbial communities is similar in a pregnant and non-pregnant state.

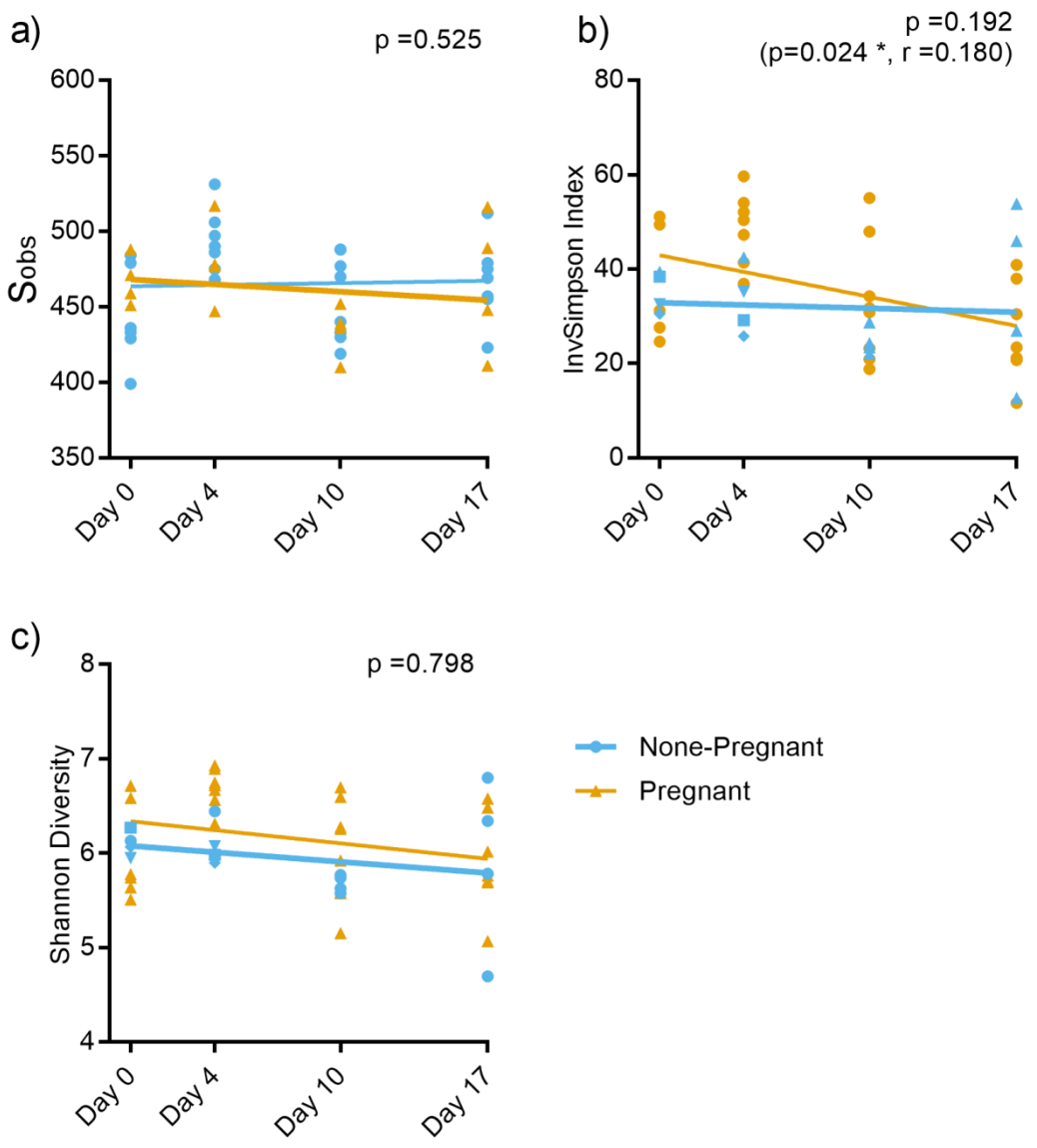

Figure 5.24 Pregnancy Influence on Alpha Diversity Measures
Observed species (a) Shannon Diversity (b) and Inverse Simpson Index (c) measures in samples collected over 4 time-points in pregnant and non-pregnant animals. P-values displayed are for the difference between the Non-Pregnant vs. Pregnant slopes. The only linear trend was seen in the pregnant Inverse Simpson index (b), P-value and slope are given in parentheses. A two-way ANOVA did not highlight any significant association of gestation or pregnancy status with alpha diversity comparing to Day 0 groups.

5.3.8.3 Pregnancy Related Microbial Change; Genera Associated with Progressing Gestation

To determine whether any genera are associated with progressing gestation, linear regression was applied to the absolute abundance of all of the 78 genera classified. Those genera which have a significant (<0.02) linear regression are shown in Figure 5.25. Four genera were increased during pregnancy, *Candidatus saccharimonas*, *Lactobacillus, Candidatus arthromitus*, and *Ralstonia*. *Ralstonia* and *Candidatus saccharimonas* were present at low abundance (<0.5%). Two genera were reduced during pregnancy; *Parabacteroides* and *Bacteroides*.

Linear regression analysis was also applied to the control non-pregnant group to determine differences in abundance that are not due to pregnancy. This group highlighted two of the same genera; *Lactobacillus* and *Parabacteroides* as having a significant linear regression to time-point (Figure 5.26).

As previously suggested, it is important to establish baseline flux in microbial diversity, for this reason, the linear regression slopes of the significant genera between non-pregnant and pregnant samples were compared (Figure 5.27). The majority of the trends seen in pregnancy were also seen in those animals not pregnant collected at the same time-point, with the exception of *Candidatus arthromitus* which significantly increases with gestation compared to non-pregnancy ($p = 0.020$). This is a clear indication that in murine pregnancy there are very little global cumulative or progressive shift in the abundance of taxa at the genera level.

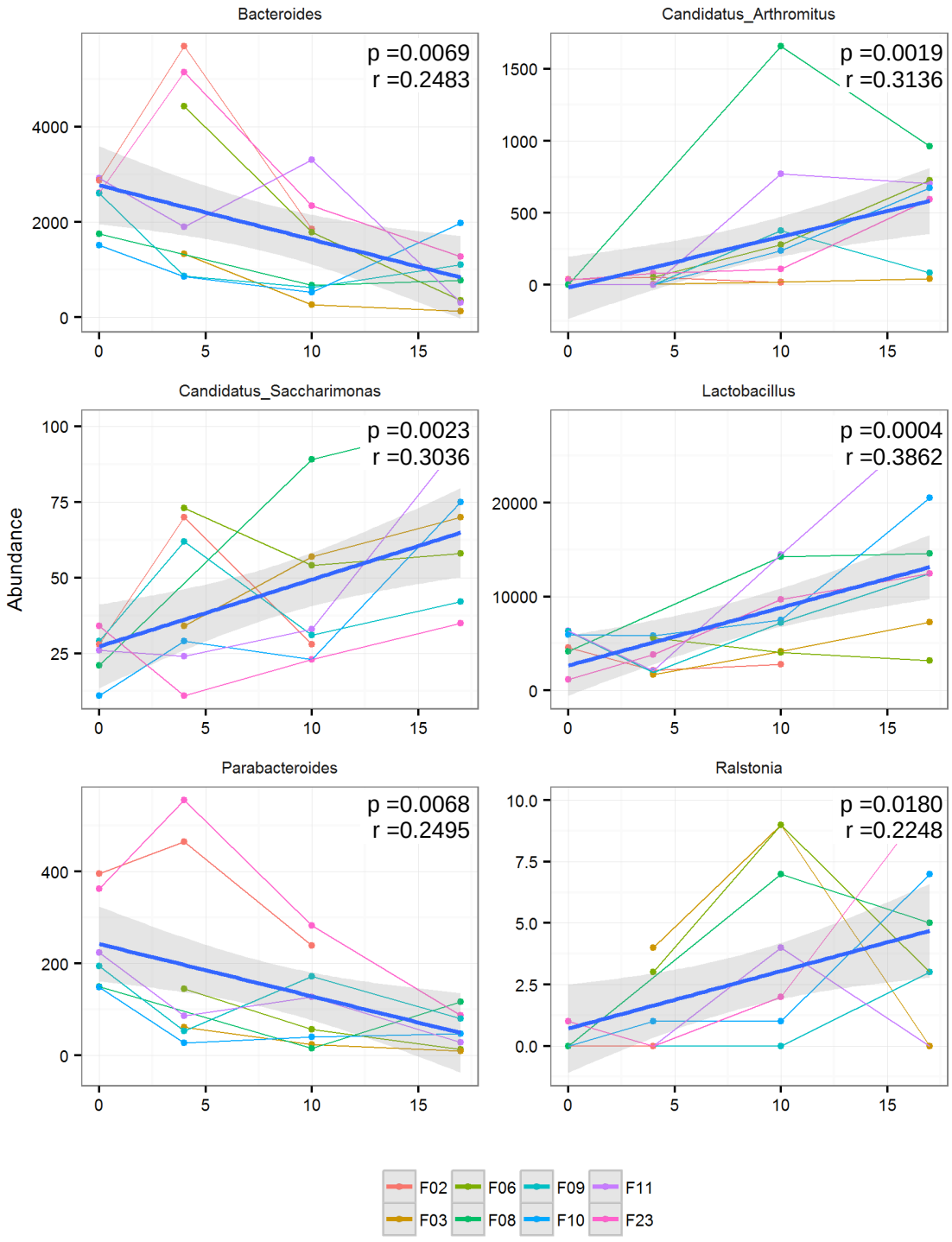

Figure 5.25 Linear Regression of Genera Abundance to Gestation
Linear regression was applied to the absolute abundance of all 78 genera progressive to gestation in pregnant C57BL/6J animals (n=8). Only those linear regressions with a P value of <0.02 are shown. Blue line indicates linear regression with 95% confidence in grey. Animal ID at each time-point can be identified by colour and connecting lines.

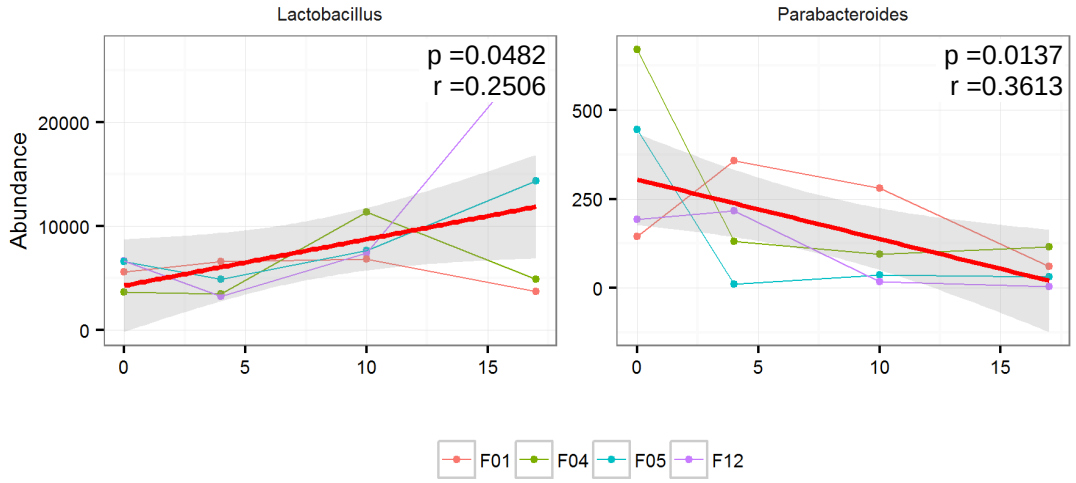

Figure 5.26 Linear Regression of Genera Abundance to Time-point
Linear regression was applied to the absolute abundance of all 78 genera progressive to time-point in non-pregnant C57BL/6J animals (n=4). Only those linear regressions with a P value of <0.05 are shown. Red line indicates linear regression with 95% confidence in grey. Animal ID at each time-point can be identified by colour and connecting lines.

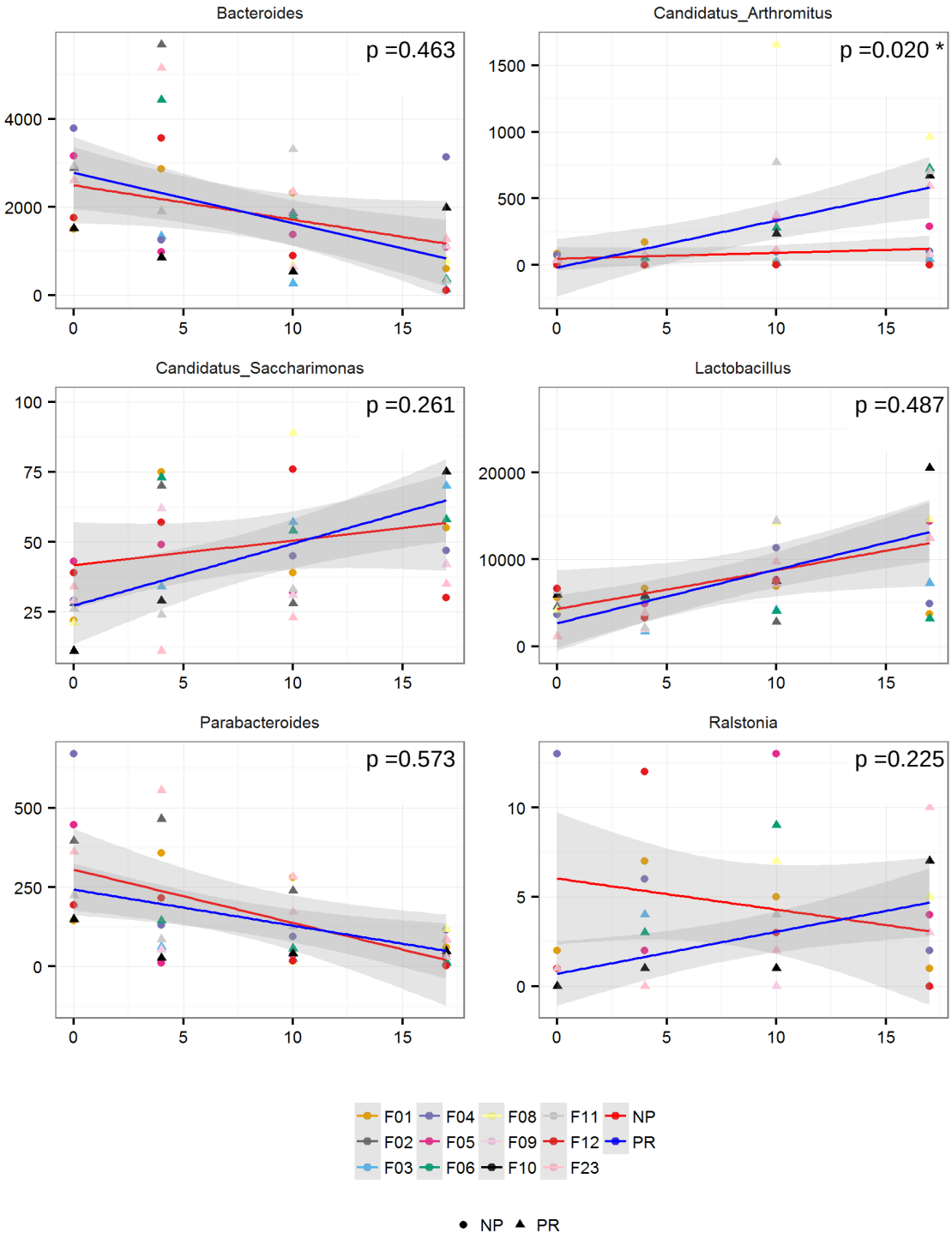

Figure 5.27 Linear Regression of Genera Abundance; Pregnant vs. Non-Pregnant

Linear regression comparison of genera progressive to gestation/time-point in non-pregnant (n=4) and pregnant (n=8) C57BL/6J animals. Only those linear regressions with a P value of <0.05 in either pregnant or non-pregnant group are shown. Red line indicates linear regression in non-pregnant (NP) samples. Blue line indicates linear regression in pregnant samples (PR). Animal ID at each time-point can be identified by colour of point and the shape of point corresponds to pregnancy status.

Candidatus arthromitus significantly increases with gestation compared to non-pregnancy (p =0.020) (Figure 5.27). Furthermore, data from the n=3 mice sampled at 1 day postpartum suggest the maternal increase seen during pregnancy is indeed maintained in to the postpartum period, showing a highly significant linear trend to gestation (P <0.0001) (Figure 5.28).

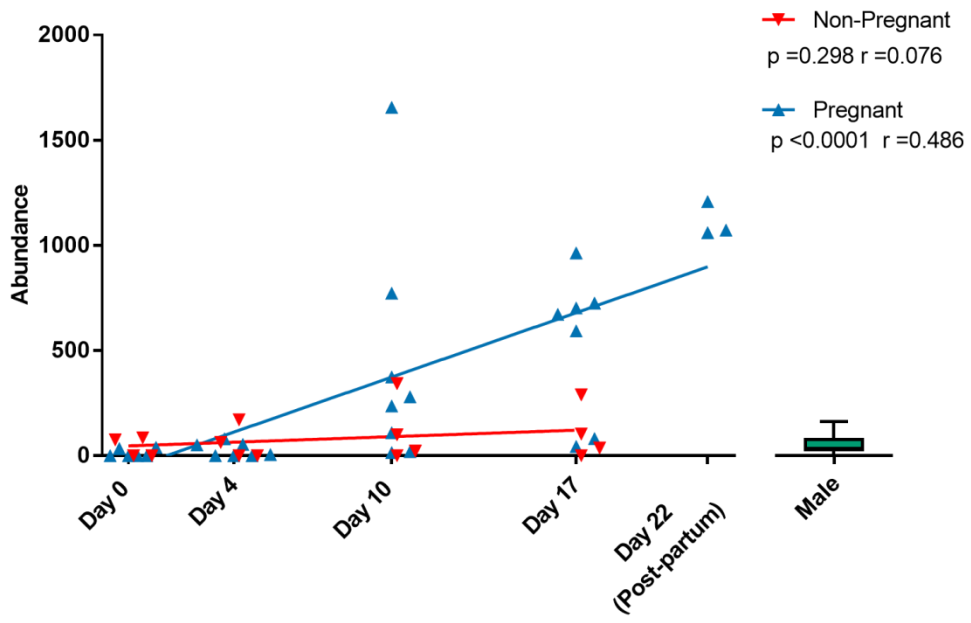

Figure 5.28 Linear Regression of *Candidatus arthromitus*; Pregnant vs. Non-Pregnant

Linear regression comparison of *Candidatus arthromitus* progressive to gestation/time-point in non-pregnant (n=4) and pregnant (n=8) C57BL/6J animals. Red line indicates linear regression in non-pregnant samples. Blue line indicates linear regression in pregnant samples. Postpartum Day 22 samples have been added to the linear fit, in addition a box plot (min-max whiskers) from male fecal samples (n=10) collected on Day 0 is added for reference. Shape and colour of point corresponds to pregnancy status.

As mentioned previously the hypothesis for linear regression analysis is that the community is driven by progressive and accumulative microbial shifts as pregnancy progresses. To test for non-linear association of the gestation/time-point on abundance of genera, a non-parametric Kurskal-Wallis test was used to identify significant genera associated with gestation/time-point in pregnant and non-pregnant animals respectively.

Several genera were highlighted as having a significant association to gestation/time-point, including; *Anaeroplasma, Bacteroides, Blautia, Candidatus arthromitus, Candidatus saccharimonas, Parabacteroides, Prevotella, and Oscillibacter* (Figure 5.29). However, when adjusted for multiple comparisons none of these genera were statistically significant. Moreover, an ANOVA did not show any significant differences between pregnant and non-pregnant abundance of any of these genera across all time-points. This suggests that although there is variation in the relative abundance of genera over time, the majority is not attributed to pregnancy and is most likely normal background community variation.

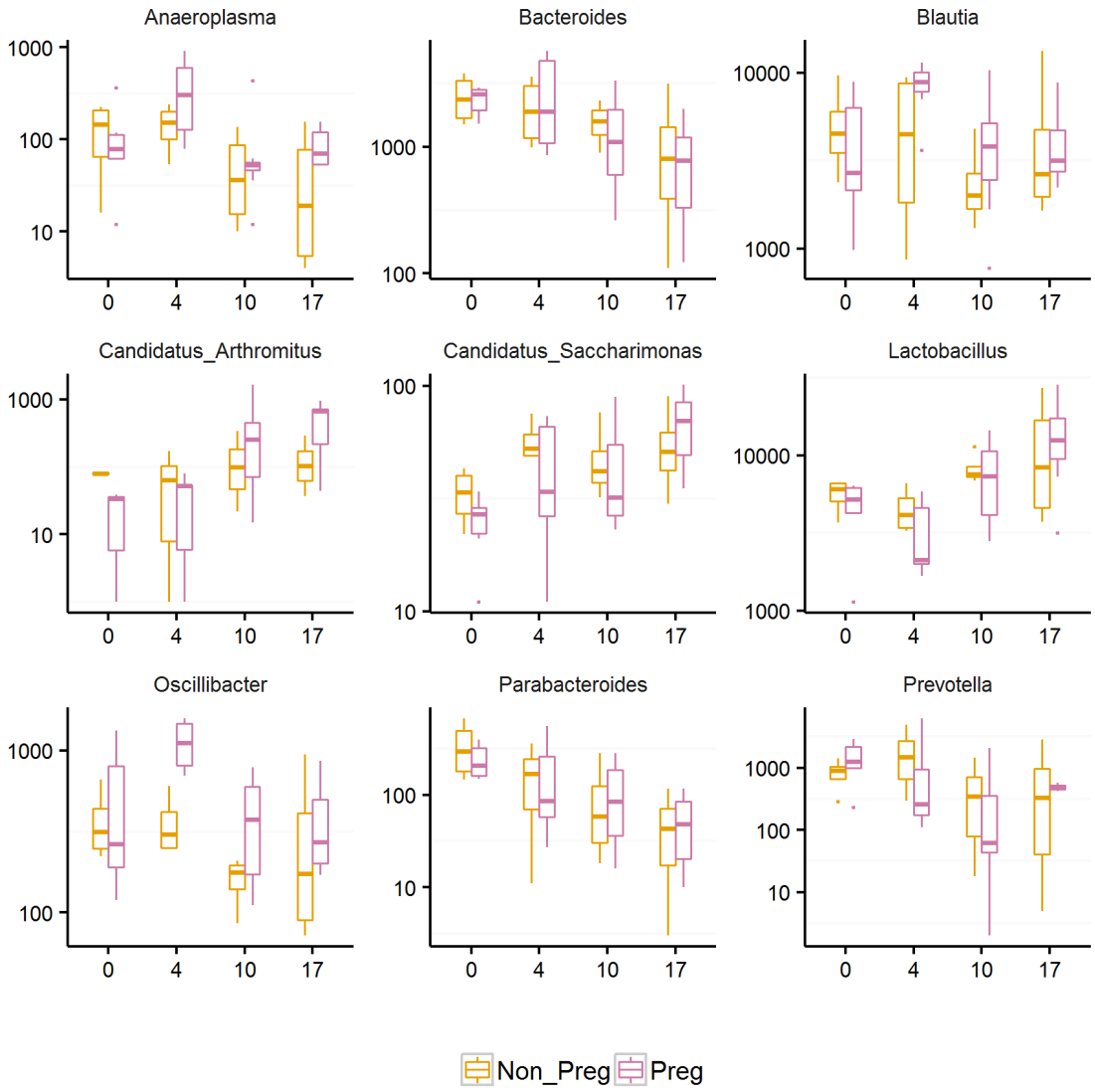

Figure 5.29 Boxplots of Significant Genera Associated with Pregnancy
Boxplots representing median, IQR, whisker length represents 1.5x IQR of the observed sequences for significant genera grouped by genotype. Displaying significant (P <0.05) genera associated with gestation/time-point using non-parametric Kurskal-Wallis test, once adjusted for multiple comparisons NS difference.

5.4 Discussion

Fecal Microbiome of *Camp-/-* Animals

Microbes in the gut are essential for the break down of complex carbohydrates where they can manipulate host metabolism by altering nutrient availability. The presence and abundance of each bacterial group is fundamental since different species differentially metabolise these nutrients. The host antimicrobial defence system has co-evolved with complex communities of bacteria that have sought to create an environment for commensal and mutualistic cohabitation. The mammalian gastrointestinal tract is dominated by two main phyla, *Firmicutes* and *Bacteroidetes.* Shifts in the ratio of these two phyla have been observed in many conditions such as obesity (Ley et al., 2006) and diabetes (Wen et al., 2008). Diet and host genetics can also influence on microbial community composition (Blanton et al., 2016, Ussar et al., 2015). Host Defence Peptides provide the first line of defence against infectious pathogens in the gastrointestinal tract. In the mouse and human colon, cathelicidin is expressed in epithelial cells and immune cells such as macrophages.

In this chapter, I evaluate the direct influence of Cathelicidin on the fecal microbiome by utilising *Camp-/-* knockout animals. The microbiome was interrogated by 16S rRNA gene sequencing for bacterial classification. After subsampling and removal of rare sequences, 908 OTUs were identified, which represent 143 unique genera, 82 unique family level classifications, 50 unique orders, 29 unique classes and 15 different phyla (Figure 5.3).

Direct comparison of the phyla classifications for the *Camp-/-* and C57BL/6J samples showed similar overall compositions; there were no differences in relative abundance at the phylum level (Figure 5.8). As CAMP is a potent broad range antimicrobial which has been shown to modulate mucosal immune responsiveness, it was unexpected that knocking out this gene in mice would not confer shifts in bacteria at the phylum level. Although, cathelicidin is only expressed at moderate levels in the gut without inflammation or infection, moreover it has a higher potency

for pathogenic species; these factors might be responsible for the lack of huge shifts at the phylum level.

At the genera and OTU level of classification, *Camp-/-* and C57BL/6J mice demonstrated disparate gut microbiota as indicated by statistically significant taxonomic differences (Figure 5.18). At the genus level *Allobaculum (*p.*Firmicutes* o.*Erysipelotrichales*), was significantly enriched in C57BL/6J samples, whereas *Anaeroplasma (*p.*Tenericutes* o.*Anaeroplasmatales)* was enriched in samples from *Camp-/-* animals. The most notable OTU assigned to be enriched in *Camp-/-* samples was OTU0003, which was classified as S24-7 family of bacteria. C57BL/6J animals show an enrichment of *Prevotella*, which is interesting as the *Camp-/-* samples are nearly totally devoid of this clade (Figure 5.19).

Allobaculum is a low abundant genera significantly enriched in C57BL/6J animals. On average the sequence contribution of this genus in C57BL/6J samples was 2.02% compared to 0.95% in *Camp-/-* mice. *Allobaculum* is considered beneficial to host physiology; low fat intake has been associated with increases in this genus, compared to high-fat intake where this genus is reduced (Cani et al., 2008, Ravussin et al., 2012). In this study, diet was kept consistent; indicating that innate immune genotype is also able to confer changes in relative abundance of this genus.

As one of the few Ten*ericutes* observed in this study, *Anaeroplasma*, an anaerobic Mycoplasmatales, contributed to the enrichment back to the 'order'-level of classification in *Camp-/-* samples.

S24-7 family, a butyrate-producing bacterium only normally seen in rodents covers the largest component of mouse fecal sequences assigned in the *Bacteroidetes* phylum in this study. Many of the *Bacteroidetes* species in mice do-not fit into existing genera well. The strain reference for S24-7 family (AJ400263), deposited by Salzman et al., (2002a) is distinct but closely related to *Prevotella, Bacteroides*, and *Porphyromonas*. Exercise has been shown to significantly increase the relative proportion of S24-7 in mice, whereas sedentary mice on a high-fat diet had lower levels of S24-7 (Evans et al., 2014). Interestingly antibiotics, and antibiotic prodrug treatments suppresses S24-7 in mice (Yao et al., 2016, Zanvit et al., 2015, Rajpal et

al., 2015). Only one study has found S24-7 in humans (Clemente et al., 2015), S24-7 is however closely related to *Bacteroidetes* which are abundant in humans. Interestingly in humans, *Bacteroidetes* levels in the gut are lower in obese individuals then those of healthy weight (Turnbaugh et al., 2008, Turnbaugh et al., 2009).

The increase in S24-7 in the *Camp-/-* mice could be due to the direct microbicidal activity of CAMP targeted to this genus. As mostly commensals, *Bacteroidetes* have adopted mechanisms of increased resistance to bacterial killing to LL-37 and CAMP (Cullen et al., 2015).

Prevotella was highlighted as an enriched genus in the C57BL/6J animals, this genus (and family) were also notably absent from the *Camp-/-* samples with the exception of one sample. The one outlier sample clusters with the C57BL/6J samples in the PCoA plots (Figure 5.12). This mouse has been sampled multiple times, as all other samples from this animal cluster with the *Camp-/-* samples I would suggest this is a sampling or processing error and can be excluded.

Prevotella spp. have mainly been isolated from the mammalian oral cavity but are also present in the gut, where *Prevotella copri* is generally the more abundant species (Gupta et al., 2015). *Prevotella* has been associated with some beneficial activities but has also been linked with inflammatory conditions (Scher et al., 2013, Dillon et al., 2016). Most *Prevotella* spp. produce succinate and this genus has been positively associated with a Mediterranean diet (De Filippis et al., 2015). This bacterium has also been described to improve glucose metabolism in healthy human individuals (Kovatcheva-Datchary et al., 2015). However, *Prevotella* in the gut has been positively associated with HIV, where exposure of key dendritic cells to *Prevotella copri* boosted cytokine production *in-vitro* (Dillon et al., 2016). Dillon et al., (2016) suggested that increased levels of *Prevotella copri* might contribute to driving the chronic inflammation seen in individuals infected with HIV.

Prevotella copri has been used in many *in-vivo* studies looking at host-microbe interactions. Mice treated with *Prevotella copri* had increased hepatic glycogen storage and showed improved glucose tolerance. On the other hand *Prevotella copri*

post-antibiotic treatment has been shown to increase murine susceptibility to colitis induced by dextran sulfate sodium (DSS). *Camp-/-* animals are also shown to have increased susceptibility to DSS colitis (Tai et al., 2013, Koon et al., 2011), which is interesting as in this study I have shown they have reduced levels of *Prevotella*. This is contradictory to the observation that *Prevotella* increases the host susceptibility to colitis. *Prevotella* is however a very large diverse genus with large genomic diversity between strains. It is most probable that the species of *Prevotella* in this study is not the highly used *in-vivo* strain *Prevotella copri* and therefore can have very different properties. It is also possible that these specific members of the *Prevotella* genus have important anti-inflammatory functions in the gastrointestinal tract; loss of such anti-inflammatory genera could result in exacerbated inflammation during exposure to DSS, conferring the amplified phenotype.

It is not known why removing *Camp* results in a lack of *Prevotella,* it is possible that this decrease is a result of another species inhibiting or out competing for space. As OTUs from the S24-7 family of bacteria are enriched in *Camp-/-* mice I would suggest this genera is an ideal candidate. Another possible reason for the differences in gut microbiome of the *Camp-/-* mice compared to wildtype mice, is the influence of gut architecture.

There are two reports that confer a low-level change in steady state gut morphology in *Camp-/-* mice. While investigating induced inflammation via TLR-9 signalling, Koon et al., (2011) demonstrated that *Camp-/-* mice developed very mild inflammation when given just water. Another study suggested that *Camp-/-* mice have a 32% thinner mucus layer in the colon (Chromek et al., 2012). This is supported by *in-vitro* work on human colon cells which showed LL-37 can directly stimulate mucus synthesis by the increased expression of mucins, MUC1 and MUC2 (Tai et al., 2008). By use of Muc2 knockout mice, this mucin was shown to be essential for limiting the number of pathogenic but also commensal bacteria that can interact with the colonic mucus layer (Bergstrom et al., 2010). The mucus layer is a very dynamic environment, which is rapidly renewing, therefore bacteria need to be tough enough to repopulate at a similar rate while also competing for resources.

The mucus layer development of the *Camp-/-* animals was not investigated in this study. As it has been reported that different animal facilities and background strain can influence mucus development (Jakobsson et al., 2015), it would be essential to establish whether the *Camp-/-* mice which I have shown have an altered microbiome, also have the mucus layer phenotype as described by Chromek et al., (2012).

Jakobsson et al., (2015) showed that two mice colonies within the same animal unit can display different mucus permeability to bacteria. Interestingly, although the authors did not conclude a specific bacteria was responsible for normal mucus development; higher relative abundances of *Bacteroides* were found in mice with less developed mucus. In addition, the authors found that *Erysipelotrichia* was increased in those animals with normal impenetrable mucus. I have shown wildtype mice in this study have enrichment for *Erysipelotrichia* and the *Camp-/-* mice are enriched in S24-7, closely relate to *Bacteroides,* this could be inducing or a result of *Camp-/-* mice having a under developed mucus layer. In addition to histological evidence for mucus layer thickness, it would be of interest to quantify secreted mucus glycoprotein and also transcript levels of key mucins in *Camp-/-* mice to support this theory. Definitive proof of the involvement of these mechanisms would aid understanding of how cathelicidin maintains gut homeostasis by the maintenance of mucus integrity.

It would also be interesting to see whether giving *Camp-/-* mice exogenous *CAMP* peptide could restore the levels of *Prevotella* and *Erysipelotrichia* in the gut. One study has given exogenous LL-37 treatment to wildtype rats and explored gut microbial populations (Pound et al., 2015). Although the authors did not find global alterations in gastrointestinal bacterial communities in response to LL-37 peptide, there were increases in select lineages, including *Adlercreutzia* (p. *Actinobacteria*), but also *Lactobacillus* spp.. These species were not consistently increased in another rat strain suggesting there are possible additional genotypic interactions of LL-37 and the microbiome (Pound et al., 2015).

In this chapter, I compared the alpha diversity (the diversity within samples) and beta diversity (the diversity between samples) in the C57BL/6J and *Camp-/-* animals.

There was no significant difference in any alpha diversity metric between these two genotypes. These alpha diversity measures assume all species are equally related to each other and has no consideration to highly divergent species. UniFrac takes into account the shared species between two groups, their abundance and their phylogenetic relationship. Applying qualitative and quantitative measures allude to different assumptions about the key factors that are driving microbial diversity (Lozupone et al., 2007). It is therefore important to use a variety of distance calculation methods to highlight patterns in the data. Both weighted and unweighted UniFrac measures have specific functions in microbial community analysis. Unweighted UniFrac, a qualitative measure of similarity, is best positioned in revealing communities that predominantly differ by what can sustain growth. Weighted UniFrac distance is a quantitative description of similarity, best suited in revealing community variations that are due to changes in relative abundance of species.

In this study hypothesis tests on the unweighted UniFrac distances, grouping by genotype, was found to be highly significant using multiple methods of hypothesis testing (Table 5.6). Conversely, hypothesis testing on the weighted UniFrac distances did not show any significant trend, which backs up the lack of clustering in the weighted UniFrac PCoA plots (Figure 5.15). The clustering of samples by genotype by unweighted UniFrac suggests a strong relationship in terms of qualitative community membership. Therefore the incidence of particular OTUs is a higher factor separating the samples by genotype as opposed to the flourishment of shared species. Mechanistically this suggests the direct microbicidal activity of *CAMP* could be targeting certain genera more than others.

The unweighted UniFrac pairwise distances show *Camp-/-* knockout animals are significantly more diverse than the wildtype controls ($P<0.0001$). The weighted and unweighted UniFrac UPMGA trees generally support the clustering seen in the PCoA plots (Figure 5.17).

Supplier, housing laboratory, strain, diet, and gender can all affect diversity and be compounding factors in microbial studies (reviewed in Laukens et al., (2016)). The

background animal strain can regulate many experimental phenotypes that also might play a role in mediating microbial communities (Turnbaugh et al., 2006, Hooper and Gordon, 2001). Indeed background strain even within animal facility can all have huge impact on microbial community structure (Friswell et al., 2010, Campbell et al., 2012). Different suppliers of the same strain have also been shown to have different microbial complexity. For this reason, control animals in this study were sourced 'in-house' from backcrossing *Camp*-/- to C57BL/6J animals. Although control C57BL/6J animals here were from backcrosses, they were not littermate controls. It is possible in the few generations the *Camp*-/- and C57BL/6J animals were bred in isolation there has been some amplification of divergent bacterium caused either by mutation or exposure. Looking at littermate controls is also an option in this study, but this too can be complicated by what mice are exposed to dependent upon their parents and grandparents, cage effects can also possibly hide the effects of the genotype. It would be of interest to determine the transmissibility of the microbiome by co-housing wildtype with *Camp*-/- mice and including a larger number of animals.

A strength of this study design was that samples were collected from multiple cages, multiples sexes, and at multiple time-points. Regardless of sex and pregnancy status, the clustering of samples by genotype was robust at every time-point considered. *Camp*-/- and C57BL/6J mice demonstrated disparate gut microbiota. This microbial change, as the data in this chapter suggests, is driven by community-wide effects involving the loss and gain of multiple bacteria. I hypothesise that alteration in relative abundance of these bacterial populations maybe a result of the thinning of the protective mucin layer. Disruption of this mucin layer has been shown to enhance the ability of opportunistic pathogens to invade the mucosa. This could be the attributing factor to why *Camp*-/- mice are more susceptible to DSS colitis and infection with pathogenic organisms. Identifying the mechanisms behind this will be important for addressing how cathelicidin maintains gut homeostasis.

Pregnancy modulation of the microbiome

There are great metabolic changes in pregnancy, especially in late gestation, which could have impact on microbial communities. Late gestation is associated with remodelling of adipose tissue deposits which aid growth of the placenta and fetus (Resi et al., 2012). There has been conflicting reports in humans whether pregnancy is associated with shifts in gut bacteria (Collado et al., 2008, Koren et al., 2012, DiGiulio et al., 2010). It has been reported that the bio-mass of the bacteria in the mother's gut increases during gestation and this was associated with an increase in bacterial diversity (Koren et al., 2012). Koren et al., (2012) went on to suggest that the pregnancy related changes in the gut microbiome are akin to that seen in obesity.

In this chapter, I investigate microbial shifts in murine pregnancy by longitudinally sampling mice throughout gestation and interrogating the microbiome by 16S rRNA gene sequencing.

Akkermenisa and *Bifidobacterium* have been related to pregnancy in mice. Gohir et al., (2015) displayed that these genera were increased after conception. In this study I found no *Akkermenisa* or *Bifidobacterium* in wildtype female C57BL/6J animals. This could obviously be a reflection of the differences in bacteria burden between animal facilities. Gohir et al., (2015) uses the same animal sampled prior to pregnancy as the non-pregnant control group. Indeed in this study I also sample animals prior to conception to account for intra and inter-animal variation. Strength of my study design was that I also collected samples from non-pregnant littermate control mice in parallel, to account for environmental changes that might occur within the time period of the study. In addition, it is not known whether singly housing females for experiment would impact on the microbiome. The majority of the trends seen in pregnancy were also seen in non-pregnant littermate control samples collected at the same time-point, with the exception of *Candidatus arthromitus* which significantly increases with gestation compared to non-pregnancy ($p = 0.020$). This is a clear indication that in murine pregnancy there are very little globally cumulative or progressive shifts at the genera level.

Candidatus arthromitus is an ideal candidate to be a true pregnancy associated bacteria. *Candidatus arthromitus*, also known as segmented filamentous bacteria (SFB), colonises both the gut of human and mice in an age dependent manor (Jiang et al., 2001, Yin et al., 2013). In humans, colonisation occurs within 2 years of age but then disappears by the age of 3 (Yin et al., 2013). In mice, pups are colonised from birth, where SFB peaks at around day 12 then dramatically drops post weaning to adult levels (Jiang et al., 2001). SFB is unique, whereby it is one of the only bacteria that can be in direct contact with intestinal epithelial cells. Its presence and abundance has been correlated with reduced colonisation of many different pathogenic bacteria (Gauguet et al., 2015, Heczko et al., 2000). Most interestingly it has been shown that SFB serves a protective role in shaping adult metabolism. Cox et al., (2014) showed that giving mice low dose antibiotic treatment at birth alters metabolic hormones, expression of immunity genes and adult fat mass. Importantly the authors showed that the mice treated at birth with antibiotics consistently displayed reduced levels of SFB but also *Lactobacillus*. Moreover, young mice populated with SFB developed less severe *Staphylococcus aureus* pneumonia (Gauguet et al., 2015). Co-housing SFB-negative and SFB-positive mice for two weeks transferred the SFB and also this protective phenotype. This SFB mediated resistance to infection was associated with a type 17 innate immune response (Ivanov et al., 2009). It is accepted that the maternal microbiota can be passed onto offspring by direct colonisation at or around the time of birth. Collectively it would therefore be beneficial for the nursing dam to maintain high levels of SFB in their gut for continuous seeding to pups in the critical first few weeks of life. To support this it would be important to establish whether the levels of SFB remain high in the mother's gut postpartum well into the weening stage. The preliminary data I have from n=3 mice sampled at 1 day postpartum suggest the maternal increase seen during pregnancy might be indeed be maintained, but more time-points are needed to establish this.

A slight caveat to this study design is the unequal proportion of non-pregnant (n=4) to pregnant animals (n=8); greater power could also be given to conclusions if the animal numbers were increased.

I have shown that SFB is increased in mid to late gestation, which is fitting that bacteria which occur early in life, and has beneficial activity would be increased in the maternal microbiome. Clearly further studies are required to examine both the causal mechanism for the increase in SFB, and the influence this has on the metabolic function of the offspring. Key candidates for causal mechanisms are sex hormones and preparations for the metabolic demands of lactation. In humans, during the first week of the postpartum period oestrogen levels fall dramatically. Alterations in this postpartum phase have been shown in the vaginal microbiome, where a high proportion of mothers displayed depleted *Lactobacillus* spp. 3 weeks after labour (MacIntyre et al., 2015).

5.5 Summary

In summary, in this chapter I have shown:

- *Camp-/-* and wildtype mice demonstrated disparate gut microbiota as indicated by statistically significant taxonomic differences. This community-wide effect involves the loss and gain of multiple bacteria. Most notably *Camp-/-* mice show an enrichment of S24-7 family of bacteria and a depletion of *Prevotella*.
- *Camp-/-* mice have an altered microbiome and they are more diverse than wildtype controls.
- In murine pregnancy, there are very little globally cumulative or progressive shifts in bacteria, with the exception of *Candidatus arthromitus.*
- *Candidatus arthromitus* significantly increases with gestation compared to non-pregnancy and is maintained at high levels 1 day postpartum.

Chapter 6

Murine Vaginal Microbiome

Chapter 6 Murine Vaginal Microbiome

6.1 Introduction

In contrast to humans it has been proposed only a small percentage of female mice harbour *Lactobacillus* species at the vaginal mucosa (McGrory and Garber, 1992). Bacterial species identified to reside in the murine reproductive tract have mostly been through culture-dependent techniques (Noguchi et al., 2003). Very little is known about the species level richness of bacteria that colonise the murine vaginal mucosa. MacManes (2011) conducted a study looking at two different strains of wild mice, and showed there was a greater degree of diversity in the vaginal bacteria of a promiscuous strain of mice. Only one study has used a bacterial next generation sequencing approach to detail this microbial environment (Barfod et al., 2013).

This chapter investigates microbial change of vaginal bacteria in mice. The first main interest of this chapter was to discover what bacteria are present in the vaginal mucosa, how consistent the communities are and what level of sequencing depth is required to gain insight on microbial diversity. The next progression was to establish whether the vaginal microbiome of animals lacking cathelicidin is altered in pregnancy compared to wildtypes.

6.2 Results

6.2.1 Murine Non-pregnant Vaginal Microbiome

Vaginal lavages were collected from eight wildtype C57BL/6J mice housed in two separate cages. Bacterial DNA was extracted with the PowerSoil® DNA Isolation Kit following the manufactures protocol. Sample processing, multiplexing and library preparation was conducted as described in section 4.8 using the Ion Torrent Protocol. Emulsion PCR was supported on the Ion OneTouch® using the 400 Template Kit (v2) according to the manufacturer's instructions. Sequencing and base calling was conducted on a 314 chip, supported on the Ion Torrent PGM. After base calling, the PGM software filters individual reads to discard sub-threshold and polyclonal sequences. The raw sequence count from this 314 PGM chip was 509,851 reads. Sequences were then binned by sample using the sample-specific barcodes that were incorporated into the fusion primers. Quality filtering was done in Galaxy, using a workflow detailed in the appendix. In brief, reads were quality filtered on the following criteria; i) identical match to a barcode sequence, ii) maximum of 2 mismatches in the complementary primer sequence, iii) average quality score of >=25 in a sliding window of 6bp, iv) read-length after trimming between 150–500bp. This quality filtering reduced the raw read count from 509,851 to 192,888 sequences, which was then used as the input for QIIME analysis. Before OTU picking, reference-based and *de novo* based chimera detection was carried out using USEARCH 6.1. This highlighted 2,632 reference based chimeric reads and 496 *de novo* chimeric reads, which were discarded. OTUs were clustered at 97% similarity using UCLUST, and candidate sequences for each OTU were aligned using PyNAST. The taxonomy was assigned using RDP Classifier with a confidence value threshold of 60%. To exclude potentially contaminating taxa while preserving actual OTUs in the community, singletons were removed (2.9% total reads and 40.3% of clusters). The final resulting OTU count was 2738.

Four phyla; *Firmicutes*, *Bacteroidetes*, *Proteobacteria*, and *Actinobacteria*, dominated the microbiota in most samples (Figure 6.1). At the phylum level sample 001, 002, 004, 006, and 007 were dominated by *Firmicutes* and 003, 005 and 008 had a majority of *Bacteroidetes*.

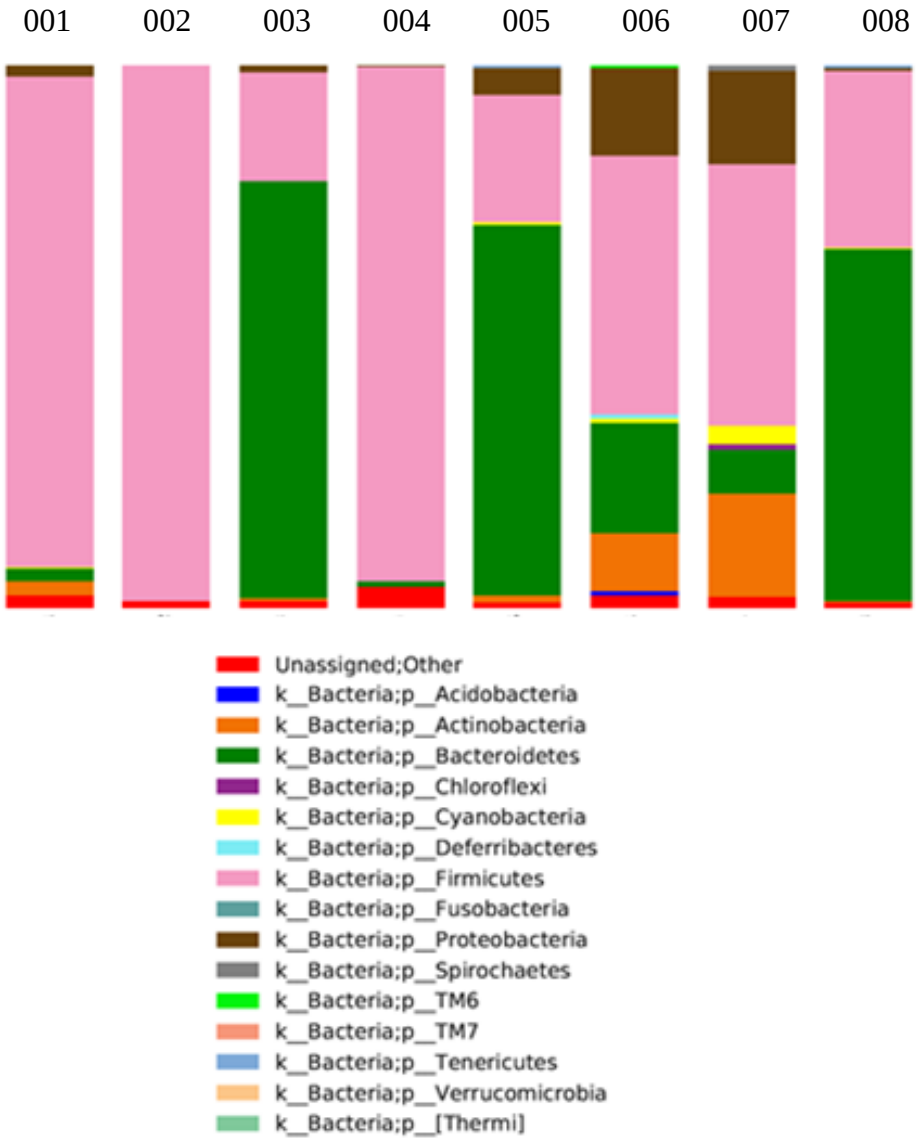

Figure 6.1 Bar Chart of Relative Proportions of Bacteria in Vagina; Phylum Level

Phyla level classification in the vaginal microbiota of non-pregnant C57BL/6J mice. Each bar represents an individual sample. 001-004 were housed in cage 1 and 005-008 were housed in cage 2. Proportions are shown as a percentage of total reads ranging from 17,392 – 25,555 per sample.

At the genus level, four groups dominate the vaginal microbiome; *Lactobacillus, Enterococcus, Planceccacace,* and the S24-7 family of bacteria (Figure 6.2). The S24-7 family of bacteria is a distinct group of *Bacteroidetes* that has been recently identified as a new group that preside in the mouse gastrointestinal tract (Salzman et al., 2002b). It seems that many of the *Bacteroidetes* species in mice such as S24-7 do not fit into existing genera well. While samples 003, 005 and 008 have similar distribution of genera, there is much variability across the other samples. Sample 001 is dominated by *Lactobacillus* while sample 002 is dominated by *Enterococcus*.

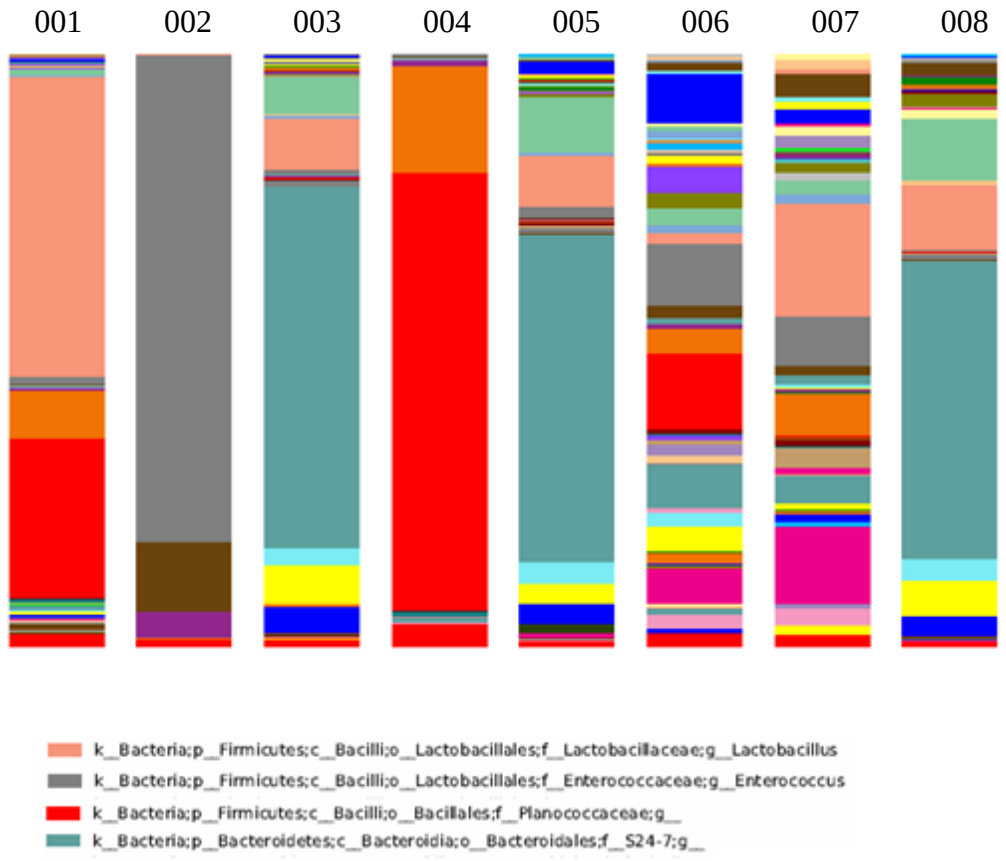

Figure 6.2 Bar Charts of Relative Proportions of Bacteria in Vagina; Genus Level

Genus level classification in the vaginal microbiota of non-pregnant C57BL/6J mice. Each bar represents an individual sample. 001-004 were housed in cage 1 and 005-008 were housed in cage 2. Proportions are shown as a percentage of total reads ranging from 17,392 – 25,555 per sample. For visual clarity, only the top 4 most abundant genera are displayed in the key.

Alpha rarefaction was performed using the number of observed species and Shannon diversity metrics in the QIIME package. The number of species identified across the eight samples is highly variable (Figure 6.3). At 20,000 sequences, sample 001 has well over 1000 OTU clusters, while sample 002 has just 200 OTUs. The plateau in the Shannon refraction plot suggests the sequencing depth is sufficient to capture a true representation of the bacteria in the samples.

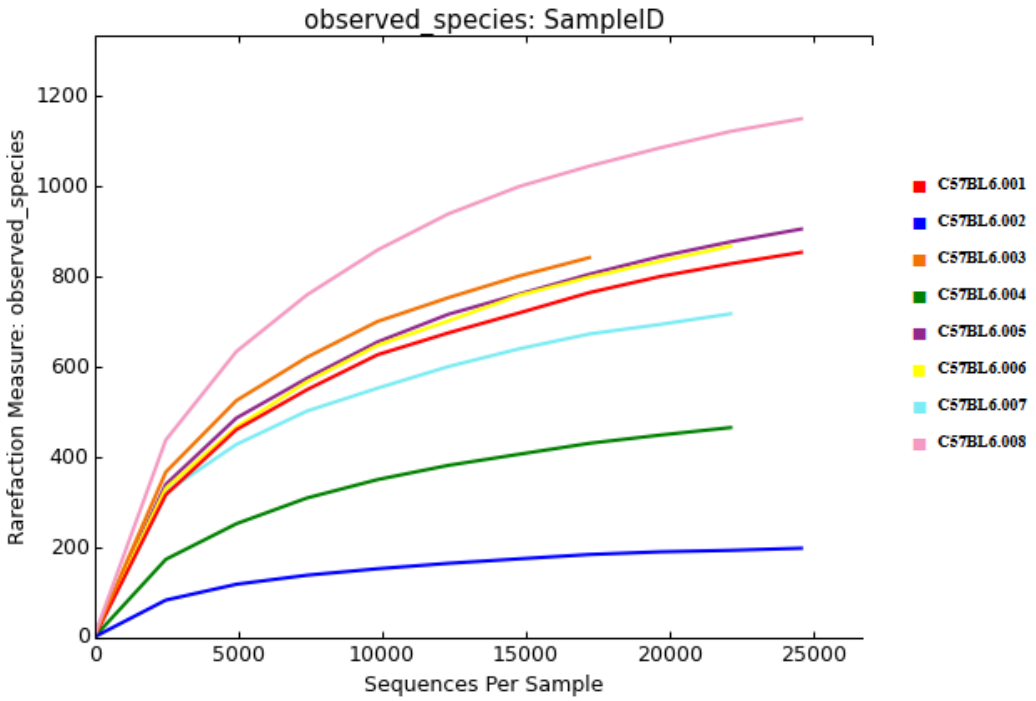

Figure 6.3 Rarefaction Curves; Observed OTUs in Murine Vagina
Rarefaction curves created for observed species (OTUs) plotted against simulated sequencing effort; each line represents an individual sample. Total reads ranging from 17,392 – 25,555 per sample.

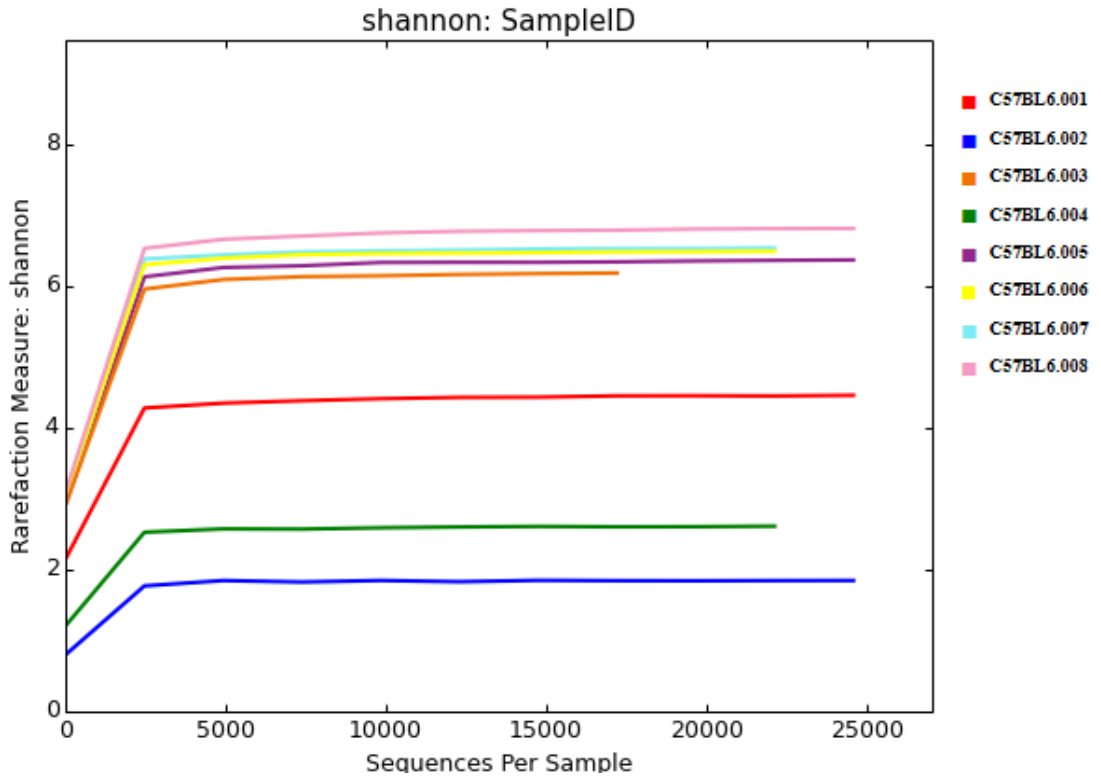

Figure 6.4 Rarefaction Curves; Shannon Index in Murine Vagina
Rarefaction curves created for Shannon Index plotted against simulated sequencing effort. Each line represents an individual sample. Total reads ranging from 17,392 – 25,555 per sample.

6.2.1.1 Conclusion

This first Ion Torrent run, sequencing wildtype non-pregnant vaginal communities, aimed to establish, i) what bacteria are present at the vaginal mucosa ii) what level of sequencing is required to gain insight on microbial diversity.

There was a notable amount of variability in the genera seen across the 8 samples taken from vaginal lavages (Figure 6.2). At the phylum level, 5 of the animals were dominated by *Firmicutes* (001, 002, 004, 006, and 007), whereas 3 animals had a majority of *Bacteroidetes* (003, 005 and 008) (Figure 6.1). In women, the composition in the vagina is mostly dominated by *Firmicutes*, while some women have a dominance of *Actinobacteria* phyla; *Bacteroidetes* are rarely seen. In contrast to humans it has been proposed only a small percentage of female mice harbour *Lactobacillus* species at the vaginal mucosa (McGrory and Garber, 1992). In this study, only 6 of the 8 mice had OTUs classified as *Lactobacillus*, in 5 of these 6 mice *Lactobacillus* was a minor component. *Enterococcus*, *Planceccacace*, and the S24-7 family were other highly abundant species.

The plateau in the Shannon Index prior to 5,000 sequences (Figure 6.4) suggests the sequencing effort in this run has adequately sampled the population. The number of OTUs across the study-set is highly inflated over what I had expected. At the current level of sequencing, the human vaginal microbiome is establishing around 200 bacterial assigned OTUs across study sets (Ravel et al., 2011, Drell et al., 2013, Martin et al., 2013). After chimera checking there were 2738 OTUs in this study, while some of these are true OTUs, many could be spurious clusters from PCR or experimental artefacts. Some of these are likely to be chimeric reads that have not been detected. In addition, the premature truncation of reads on the PGM platform and at quality filtering could be inflating unique clusters. The Ion Torrent chemistry offers the continuous sequencing of reads up to 400bp, which has the potential to span the full 16S rRNA V1-V2 target region. The V1-V2 region was only sequenced in this study in the forward direction. The standard Ion Torrent chemistry does not support paired end sequencing, however, the reverse direction can be sequenced as an independent sequencing run. Premature sequence truncation is specific to

semiconductor sequencing; this can inflate OTUs as the partial sequence fragments may not contain enough taxonomic information for robust classification. In addition, as the base calling quality drops toward the end of the read, many sequences are additionally truncated in the Galaxy workflow (see appendix).

It is well documented that the Ion Torrent platform exhibits a higher rate of sequencing errors than Illumina sequencing technologies. I chose to pursue the Illumina MiSeq platform for subsequent investigations of the vaginal microbiome due to the added benefit of paired end sequencing, in addition to this known advantage in base calling. Illumina sequencing chemistry can sequence 300bp paired-end reads, which covers the majority of the approximately 340-370bp V1-V2 amplicon. The non-overlapping region is proximal on both sequencing reads; where quality is normally the highest.

In addition to using the MiSeq Illumina platform, several other optimisation steps were attempted in aim of reducing the variability in the vaginal community. These optimisation steps included different sampling methods and extraction protocols. These are detailed in section 4.6 and 4.7, but to summarise, whole tissue compared to vaginal lavage provided more consistent bacterial yield. For this reason, post-mortem sampling of whole vaginal tissue for bacterial extraction was adopted. In addition, the FastDNA® SPIN Kit was chosen as it provided more consistency in bacterial yields from vaginal tissue than the PowerSoil® DNA Kit.

6.2.2 *Camp-/-* Pregnant Vaginal Microbiome Study

Virgin female and male mice of either C57BL/6J (n=10♀) or *Camp-/-*(n=8♀) were set-up in mating pairs and females were checked for a copulatory plug over 4 consecutive days. On Day 4 female animals were removed from the mating and singly housed for the remainder of the experiment. Subsequently the majority of the female animals became pregnant; those that did not provided the non-pregnant control group. On Day 17 animals were culled and vaginal tissue collected. All vaginal tissue samples were stored at -20°C within 2-hours of collection, and extracted within 3 weeks. Sample extraction, multiplexing and library preparation was conducted as described in section 4.8 using the MiSeq protocols for nested PCR. Bioinformatics and quality filtering conducted on the raw data are described in section 4.11.

	C57BL6/J		*Camp-/-*	
	Pregnant	Non-Pregnant	Pregnant	Non-Pregnant
Day 17	5 of 8	2 of 4	1 of 6	3 of 4
Post Partum	3 of 3			

Table 6.1 Murine Experimental Numbers - *Camp-/-* Vaginal Pregnancy Microbiome study
This table details the number of samples that had a specific PCR band and the total number collected.

Of the 22 vaginal tissue samples collected, only 14 had a specific band at PCR and passed quality control (Table 6.1). The final data set comprised of 4 *Camp-/-* samples and 10 samples from C57BL/6J mice. As there was only 1 pregnant *Camp-/-* sample in the final data-set, inference of maternal modulation in *Camp-/-* animals has limited power.

Observed species (S_{obs}), Shannon Diversity, and Inverse Simpson Index were calculated for each sample on the rarefied but unfiltered OTU data (Figure 6.5). There was no significant difference between any of the diversity measures between wildtype C57BL/6J and *Camp-/-* animals. The Shannon Diversity and inverse Simpson Index are much lower than was seen in the fecal community (section 5.3.6); this is a result of the vaginal microbiome being dominated by just a few high abundant OTUs.

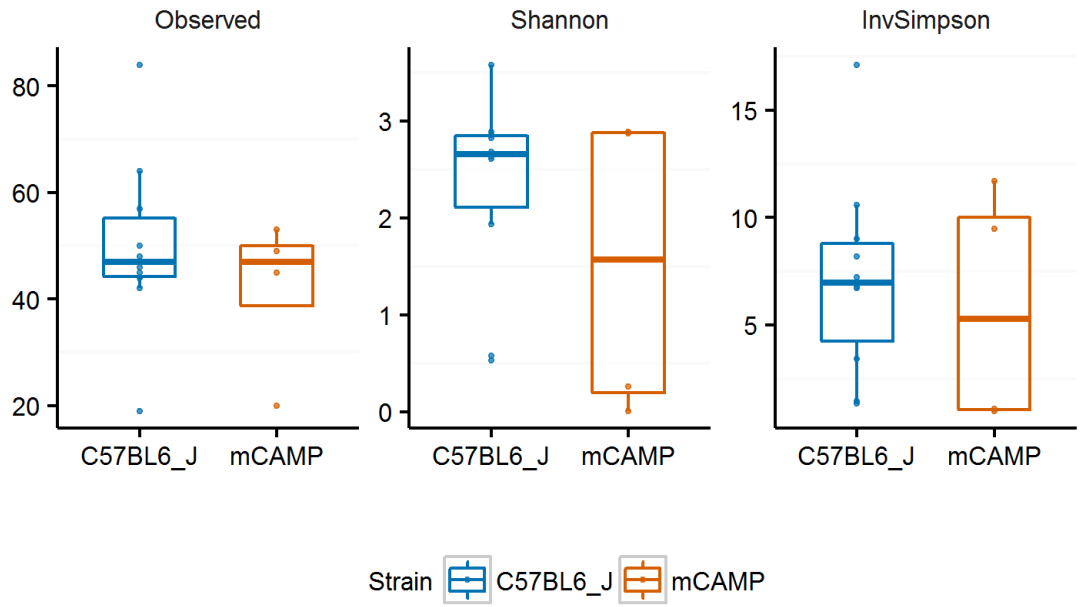

Figure 6.5 Alpha Diversity of *Camp-/-* vs. Wildtype Vaginal Microbiome
Boxplots representing median, IQR, whisker length represents 1.5x IQR of the (a) Observed species, (b) Shannon Diversity, (c) and Inverse Simpson Index measures calculated for all samples and grouped by genotype. (NS difference; unpaired t-test)

Figure 6.6 shows relative abundance of the top 25 most abundant OTUs classified at the genus level. The highest abundant OTU in most samples was classified as *Ralstonia* spp. One *Camp-/-* sample had a dominance of *Staphylococcus*, and two C57BL/6J samples had high proportions of *Streptococcus*.

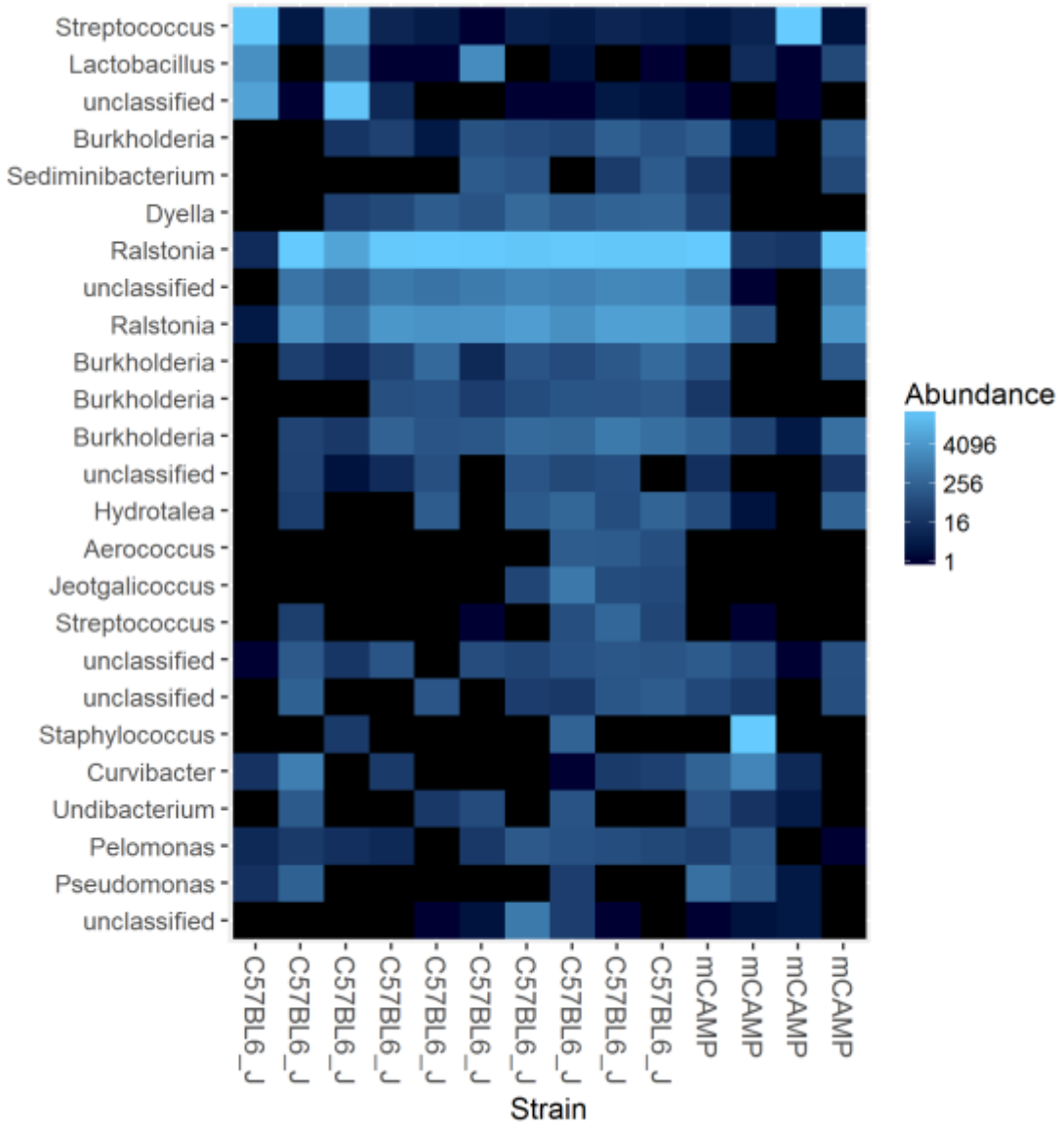

Figure 6.6 Heat map of most Abundant OTUs showing their Genus Level Classification in Vaginal Samples from *Camp-/-* and C57BL/6J mice

Relative abundance of n=14 vaginal samples of the top 25 OTUs, labelled by Genus.

Ralstonia spp. are known contaminants in molecular grade water (Grahn et al., 2003, Barton et al., 2006, Laurence et al., 2014), and I have shown this species is a potential source of contamination by sequencing a mock community (detailed in section 4.18). For this reason, OTUs classified as *Ralstonia* were removed from the data-set prior to beta-diversity distance calculations. The pairwise UniFrac distances were visualised using Principle co-ordinate Analysis (PCoA) (Figure 6.7 and Figure 6.8). In both the weighted and unweighted PCoA plots, there was no clear separation by genotype (Figure 6.7) or pregnancy status (Figure 6.8).

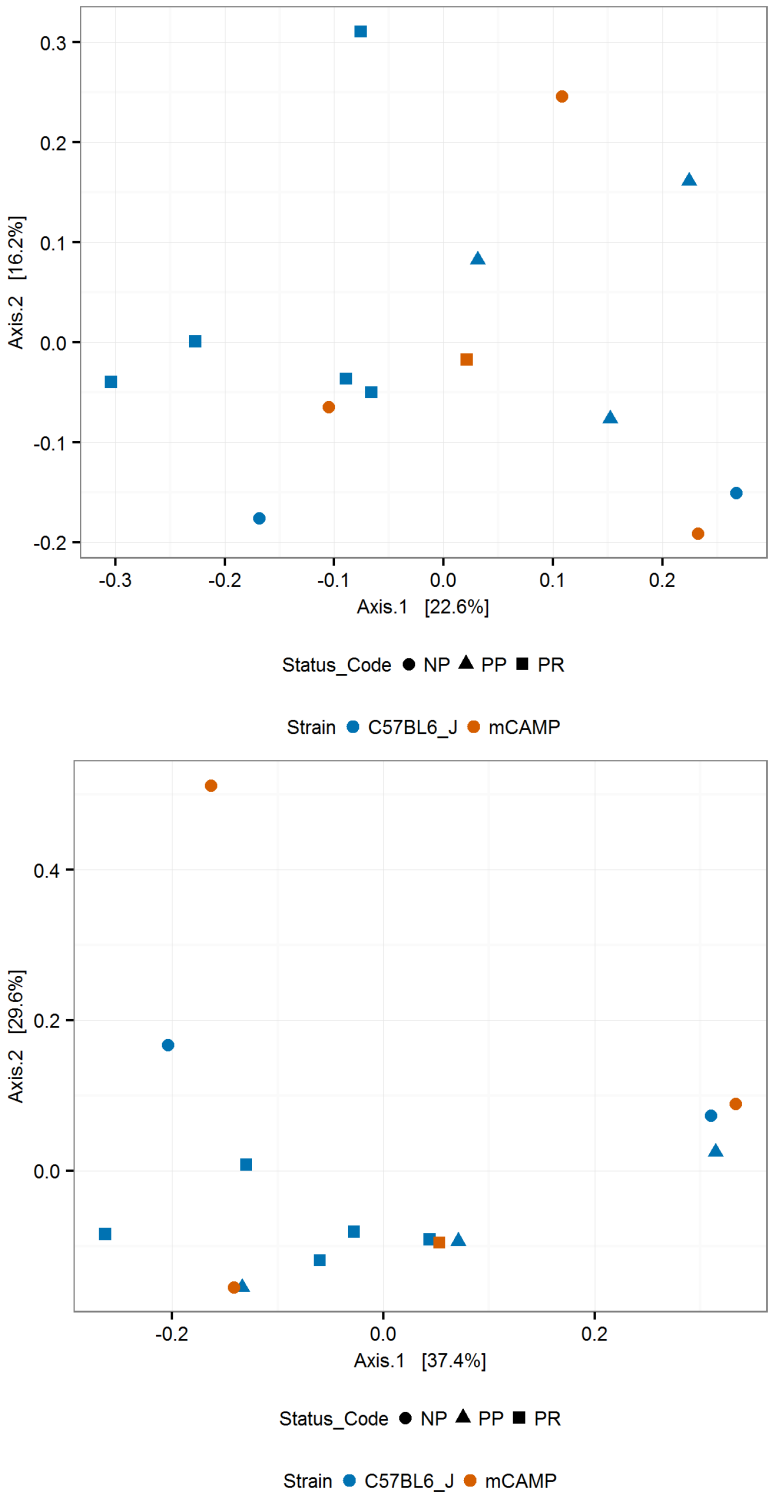

Figure 6.7 UniFrac Distance 2D PCoA plots of Vaginal Community – Colour by Genotype

(a) Unweighted and (b) weighted UniFrac 2D PCoA plots illustrating the relationship between the bacterial diversity of vaginal samples from n=14 mice. Points are coloured by genotype and shape by gestation status. Each point represents an individual mouse. (NP; non-pregnant, PR; pregnant, PP; postpartum, mCAMP = *Camp-/-*)

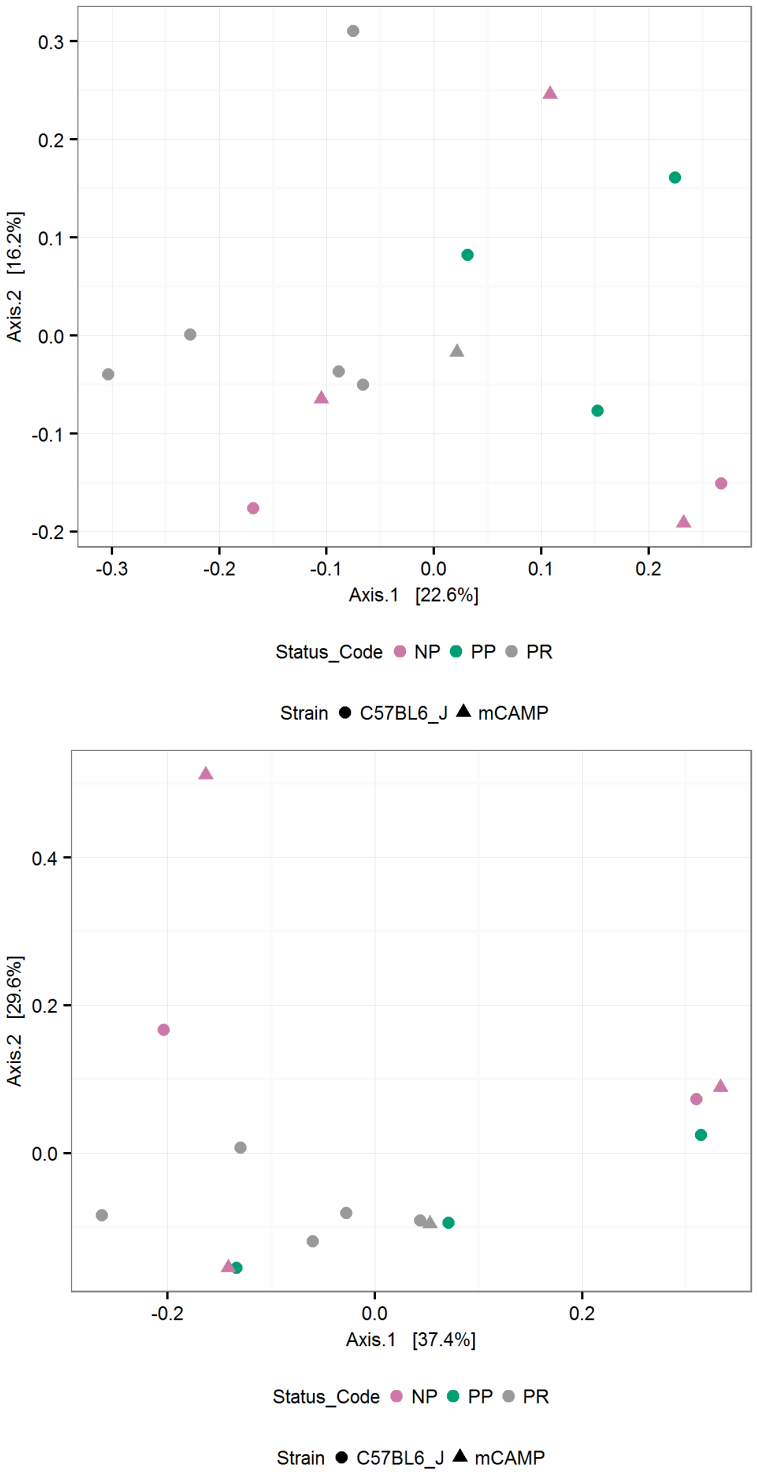

Figure 6.8 UniFrac Distance 2D PCoA plots of Vaginal Community – Colour by Pregnancy Status

(a) Unweighted and (b) weighted UniFrac 2D PCoA plots illustrating the relationship between the bacterial diversity of vaginal samples from n=14 mice. Points are coloured by gestation status and shape by genotype. Each point represents an individual mouse. (NP; non-pregnant, PR; pregnant, PP; postpartum, mCAMP = *Camp-/-*)

6.2.2.1 Conclusion

The vaginal microbiome was problematic due to low bacterial yields. Of the 22 samples collected, only 14 had a specific PCR band and could be carried forward for microbial sequencing. This left n=10 wildtype samples and n=4 *Camp*-/- samples, of which only 1 was from a pregnant animal. Microbial sequencing revealed *Ralstonia* species as the most highly abundant genera in the vaginal samples. *Ralstonia* is a known contaminate of molecular grade water and I have also demonstrated this species is a potential contaminate in the mock community. As both the extraction negative and PCR negative did not display any PCR product, it was surprising to see contaminates in the samples from the vagina. After removal of the contaminating sequences, there is no clear grouping with regard to the genotype of the mouse like there was in the fecal samples. There was also no clear clustering with regards to whether the samples were taken from pregnant or non-pregnant mice, or if they were taken postpartum.

6.3 Discussion

Under normal conditions it is common for female animals caged together to synchronise estrus cycling. The eight non-pregnant mice from experiment detailed in section 6.2.1 were housed in two separate cages but there was no apparent similarity of vaginal community within cage. The estrus stage of the mice used in this experiment was not determined, so it cannot be confirmed that all mice in the same cage were synchronised. It has previously been shown that the total numbers of bacteria are statistically higher during estrus than diestrus or metestrus in the murine vagina (Noguchi et al., 2003). In addition, Noguchi et al., (2003) showed the number of aerobes was higher than the total number of anaerobes during estrus. Synchronising the mice stage of estrus would perhaps result in higher potential bacterial recovery and more uniformity across samples. Hormones could be used in non-pregnant mice to synchronise estrus in aim of reducing this variability.

In section 6.2.2, I collected vaginal samples from animals at the same stage of pregnancy. In addition to gaining insight into the maternal vaginal community, sampling during pregnancy aimed to reduce the potential estrus cycling variability. The pregnant samples did not show any distinct clustering in the UniFrac PCoA plots (Figure 6.8), suggesting the vaginal microbiome while pregnant is also highly variable.

After review of the literature, only one other study attempts to categorise the murine vaginal commensal microbiome using 16S rRNA gene sequencing (Barfod et al., 2013). Similarly, Barfod et al., (2013) highlighted that the vaginal community of BALB/c mice was highly variable. Although the authors only had 8 samples they showed the vaginal community had two sub-clusters. One sub-cluster appeared to be closely related to the lung microbiota, whereas the other sub-cluster did not show similarity to either of the other two sample sites the authors investigated (lung and cecum). Barfod et al., (2013) attributed *Streptococcus* (Gram-positive) as the species driving the separation of the two clusters; the authors also listed *Acinetobacter*, *Sphinogmonas*, *Enterococcus* and *Polaromonas* as genera from the vaginal mucosa. Culture-dependent studies have listed *Streptococci*, gram-negative rods,

Bacteroidaceae and *Staphylococci* as found in the non-pregnant vagina, however, these observations were not consistent and were highly variable (Noguchi et al., 2003).

Further work is needed to refine and understand the commensal vaginal bacteria in mice. Due to the differences in commensal bacteria between women and mice, it is imaginable that an approach inoculating germ-free mice could recreate the human vaginal microbiome, providing a model for testing exogenous disturbances.

Chapter 7

Role of Host Defence Peptides in an Infection/Inflammation Induced Mouse Model of Preterm Labour

Chapter 7 Role of Host Defence Peptides in an Infection/ Inflammation Induced Mouse Model of Preterm Labour

7.1 Introduction

Local inflammation in the decidua and chorion is thought to be important in the initiation of preterm labour (Galinsky et al., 2013, Vrachnis et al., 2010). This inflammation is frequently caused by ascending opportunistic commensal bacteria from the vagina, through the cervix and into the fetal membranes (Allam et al., 2013, DiGiulio et al., 2010). In humans, amniotic fluid cultures from most women with preterm labour are negative for bacterial growth, although amniotic fluid inflammatory cytokines and LPS binding proteins have been shown to be increased (Gardella et al., 2001). This lack of bacterial detection could be due to the limitations of the culture-dependent techniques.

As most women presenting with preterm labour do not have elevated white blood cells or symptoms of illness, exploring a localised model of inflammation at the maternal-fetal interface is used to mimic conditions present in PTL.

Stimulation of the TLR-4 pathway with LPS has been a central method of invoking preterm labour in animal models. Delivery of LPS intrauterine, between two amniotic sacs, in pregnant mice has been reported to induce high rates of preterm labour, resulting in minimum maternal mortality and showing high reproducibility (Rinaldi et al., 2014, Rinaldi et al., 2015, Sykes et al., 2013).

Cells in the female reproductive tract are a major source of multiple microbicides including the defensins and cathelicidin. LL-37 is found at high levels in fetal skin, vaginal epithelial cells, amniotic fluids, vaginal fluid and the vernix caseosa (reviewed in Yarbrough et al., (2015)). Steady state defensin expression is cell specific and compartmentalised in the female reproductive tract in pregnant and non-pregnant women (King et al., 2003b, Fleming et al., 2003, Quayle et al., 1998). Further work on human extra-placental membranes in *ex-vivo* cultures has shown increased levels of hBD2 after exposure to bacteria (Boldenow et al., 2013).

hBD3 and DEFB14 have potent anti-inflammatory effects on human and mouse primary monocyte derived macrophages (Semple et al., 2010). hBD3 and DEFB14 effectively inhibit the LPS-activated TLR4-induced TNF and IL-6 response through both the MyD88 and TRIF pathways, shown both *in-vitro* and *in-vivo* (Semple et al., 2010, Semple et al., 2011). Preliminary unpublished data from Fiona Semple in the Dorin lab indicates that *in-vivo*, *Defb14-/-* mice have an increased sensitivity to LPS when delivered intraperitoneally. Interestingly, hBD3 can act in synergy with LL-37 reducing the LPS-induced secretion of cytokines in gingival cells (Bedran et al., 2014).

LL-37/hCAP18 has numerous immune modulatory properties that can contribute to infection and inflammatory phenotypes (discussed in section 1.2.2). Mice null for *Camp*, the murine orthologue of LL-37/hCAP18, have many inducible phenotypes; showing increased susceptibility to bacterial infections across many body sites, detailed in section 1.2.2.

As hBD3 and LL-37 suppress the inflammatory response of cells to LPS through TLR-4, the hypothesis is that *in-vivo* they might offer protection from preterm birth caused by inflammation.

In this chapter I use LPS, a cell wall component of gram negative bacteria, as the agent to induce inflammation and subsequent preterm labour in mice. Initially this agent was administered intrauterine (between two amniotic sacs) by aid of a laparotomy, but subsequently a more elegant approach of delivering the intrauterine injection guided by ultrasound sonography (USS) was utilised (described in Rinaldi et al.,(2015)). Animals lacking the host defence peptide genes *Defb14* (*Defb14-/-*) or *Camp* (*Camp-/-*) were given LPS intrauterine during late gestation to determine whether these genes are critical in the continuation of pregnancy and timing of delivery.

7.2 Experimental Details

7.2.1 Fertility in Host Defence Peptide Knockout Mice

The fertility of *Camp-/-* (n=46) and *Defb14-/-* mice (n=18) was determined by looking at several pregnancy indices; plug rate, pregnancy rate and first litter size. The plug rate was determined as the fraction of female mice where a copulatory plug was found (within 4-days of being placed with a male), compared to the total number set-up. Subsequent pregnancy rate is the fraction of the plugged females who continued pregnancy to gestational day 17, compared to the total number plugged. First litter sizes are described here as the number of viable fetus found *in-utero* on day 17 of gestation.

7.2.2 Timed Collection Experiment

Detailed experimental method for timed collection experiment is given in section 2.1.5. In brief, at day 17 of murine gestation, 1µg or 20µg of LPS was injected between two fetal-sacs as guided by ultrasound sonography. Animals were then culled 6-hours post treatment where tissue and blood serum were collected for molecular analysis. In parallel non-anaesthetic non-treatment day 17 pregnant females (NTxC) were also culled for control tissue and blood serum for comparison. The number of animals in each treatment group is detailed in Table 7.1.

	C57BL/6J	***Camp-/-***
NTxC	n = 3	n = 3
LPS [1µg]	n = 3	n = 3
LPS [20µg]	n = 6	n = 6

Table 7.1 Timed Collection Experiment - Animal Numbers and Treatment
Treatments and genotype of animals for timed collection experiment using USS guided model of PTL.

7.2.3 Laparotomy Model of PTL Experiment

Detailed experimental method for laparotomy model of PTL experiment is given in section 2.1.2. In brief, at day 17 of murine gestation a laparotomy was performed to expose the uterine horns, 20µg of LPS or sterile physiological saline was then injected between two fetal-sacs. Uterine horns are then returned to the abdominal cavity and the incision was sutured closed. Animals were left to recover and the interval to delivery was recorded in hours. The number of live born pups was also recorded at the first observation after the initiation of labour. Animals that have preterm labour delivered within 36 hours while those that go to term delivered between 36 and 96 hours post-injection. In parallel non-surgery non-treatment control day 17 pregnant females (NTxC) were also set-up to establish normal interval to delivery. The number of animals in each treatment group is detailed in Table 7.2.

	C57BL/6N	***Defb14-/-***
NTxC	n = 3	n = 6
Saline	n = 9	n = 6
LPS [20µg]	n = 8	n = 10

Table 7.2 Laparotomy Model of PTL Experiment Numbers
Treatments and genotype of animals for laparotomy model of PTL experiment.

7.2.4 Ultrasound Sonography guided Model of PTL

Detailed experimental method for USS guided model of PTL experiment is given in section 2.1.3. In brief, at day 17 of murine gestation, 1µg or 20µg of LPS or sterile physiological saline was injected between two fetal-sacs as guided by ultrasound sonography. Animals are left to recover and the interval to delivery is recorded in hours. The number of live born pups is also recorded at the first observation after the initiation of labour. Animals that have preterm labour will deliver within 36 hours while those that go to term will deliver between 36 and 96 hours post-injection. The number of animals in each treatment group is detailed in Table 7.3.

	C57BL/6J	***Camp-/-***
Saline	n = 6	n = 3
LPS [1µg]	n = 10	n = 6
LPS [20µg]	n = 6	n = 6

Table 7.3 USS Model of PTL Experiment Numbers
Treatments and genotype of animals for USS guided model of PTL experiment.

7.2.5 Statistical Analysis

Interval to Delivery

All data is presented as mean ± SEM. Interval to delivery data was log transformed prior to statistical analysis. Two-way ANOVA was used to highlight LPS treatment and genotype effects, significant differences were identified by Dunnett's multiple comparison test compared to the physiological saline injection group.

Number of Live Born Pups

All data is presented as mean ± SEM. Live born pups fractions were ArcSin transformed prior to analysis. Two-way ANOVA was used to highlight LPS treatment and genotype effects, significant differences were identified by Dunnett's multiple comparison test compared to the physiological saline injection group.

RT-qPCR

All data is presented as mean ± SEM normalised to β-Actin and relative to CAL. The calibrator used in this chapter was a cDNA pool from mouse placenta, uterus and fetal membrane from a single animal undergoing no treatment. Data was log transformed prior to analysis.

Where comparing two groups, NTxC and LPS, an unpaired t-test was performed. Two-way ANOVA was used to highlight LPS treatment and genotype effects, significant differences in genotype were identified with Bonferroni's post-test, and significant differences in LPS treatment identified with Tukey's post-test.

Camp mRNA gene expression significance was measured by one-way ANOVA with Tukey's post-test in timed-collection experiment.

Circulating Serum Cytokines

All data is presented as mean ± SEM. Two-way ANOVA was used to highlight LPS treatment and genotype effects, significant differences in genotype were identified with Bonferroni's post-test, and significant differences in LPS treatment identified with Tukey's post-test.

7.3 Results

7.3.1 Fertility of *Camp-/-* and *Defb14-/-* Animals

Camp-/- mice showed a slight but significant decrease in the plug rate (Fisher's exact test, P =0.04) compared to wildtype C57BL/6J mice (Figure 7.1.a). Both *Defb14-/-* and *Camp-/-* mice had comparable subsequent successful pregnancy and litter sizes to that of their wildtype controls (Figure 7.1.b and Figure 7.2). In addition, there is no evidence of spontaneous preterm labour in either *Defb14-/-* (Figure 7.8) or *Camp-/-* (data not shown) animals; the gestational intervals are in line with that widely reported for this background strain.

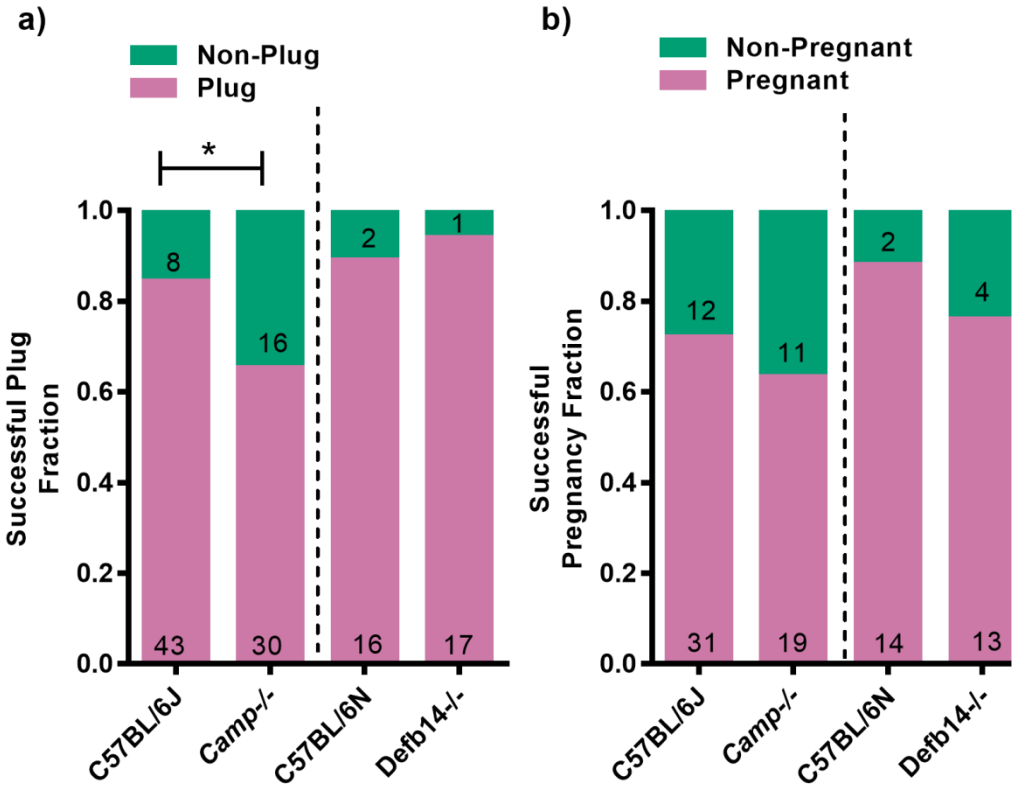

Figure 7.1 Fertility of *Camp-/-* and *Defb14-/-* mice
(a) Plug rate, (b) Pregnancy ratio in *Camp-/-* and *Defb14-/-* mice compared to their wildtype controls; C57BL/6J and C57BL/6N respectively. (Fisher's exact test *, P <0.05)

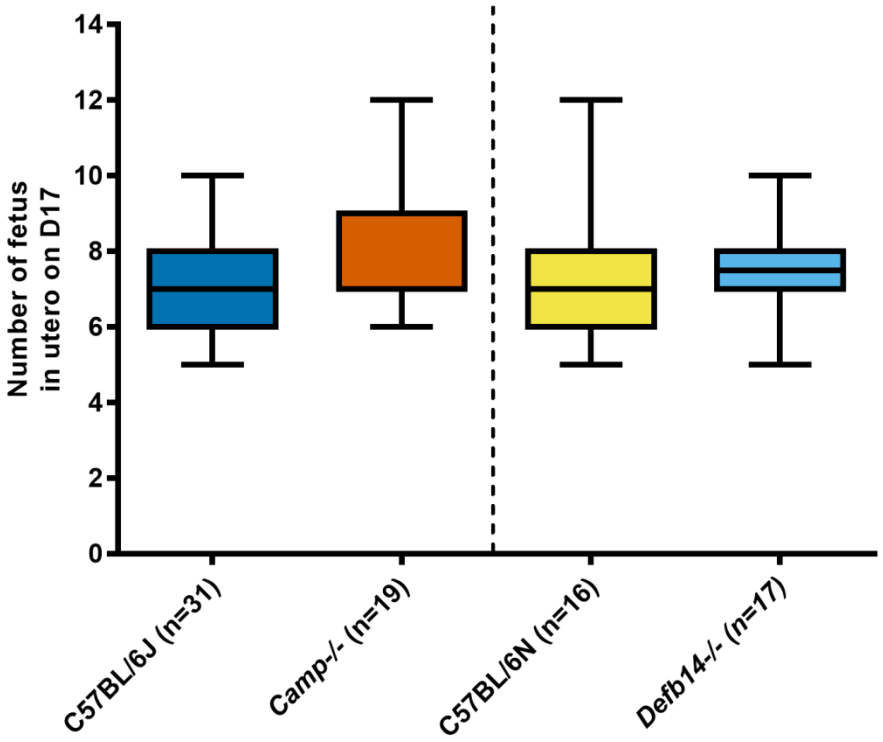

Figure 7.2 Litter Size of *Camp-/-* and *Defb14-/-* mice
Boxplots representing median, IQR with min, max whisker of first litter size in *Camp-/-* and *Defb14-/-* mice compared to their wildtype controls; C57BL/6J and C57BL/6N respectively. (Unpaired t-test; NS difference)

7.3.2 HDPs and Inflammatory Gene Response to LPS-induced model of PTL in C57BL/6J mice - Timed Collection

7.3.2.1 *Defb14* mRNA Expression following PTL model

In C57BL/6J animals, *Defb14* mRNA expression 6-hours post intrauterine LPS [20µg] injection showed no significant increase in the placenta, fetal membrane or uterus as compared to non-treatment control animals by RT-qPCR (Figure 7.3). *Defb14* mRNA levels in the fetal membrane were at the lower limits of detection, and some samples were undetected (Figure 7.3.c)

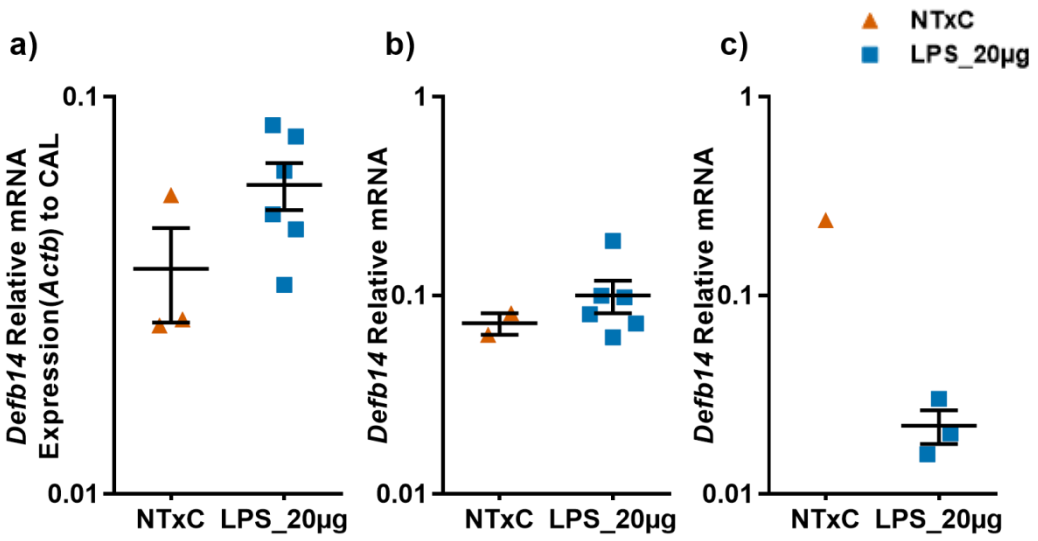

Figure 7.3 Expression of *Defb14* in LPS-induced PTL Model
Relative mRNA expression of *Defb14* in (a) Placenta (b) Uterus, and (c) Fetal Membrane tissues collected in C57BL/6J mice 6-hours post injection of 20µg LPS (n=6) or non-treatment controls (NTxC, n=3). Data presented is mean fold-increase and SEM, normalised to *β-Actin* and relative to CAL. (Unpaired t-test; NS difference)

7.3.2.2 *Camp* mRNA Expression following PTL model

6-hours post intrauterine LPS [20µg] treatment *Camp* mRNA expression levels in wildtype C57BL/6J mice showed a significant increase in the placenta (P <0.05), fetal membrane (P <0.01), and uterus (P <0.01) compared to non-treatment control animals (unpaired-t test) (Figure 7.4).

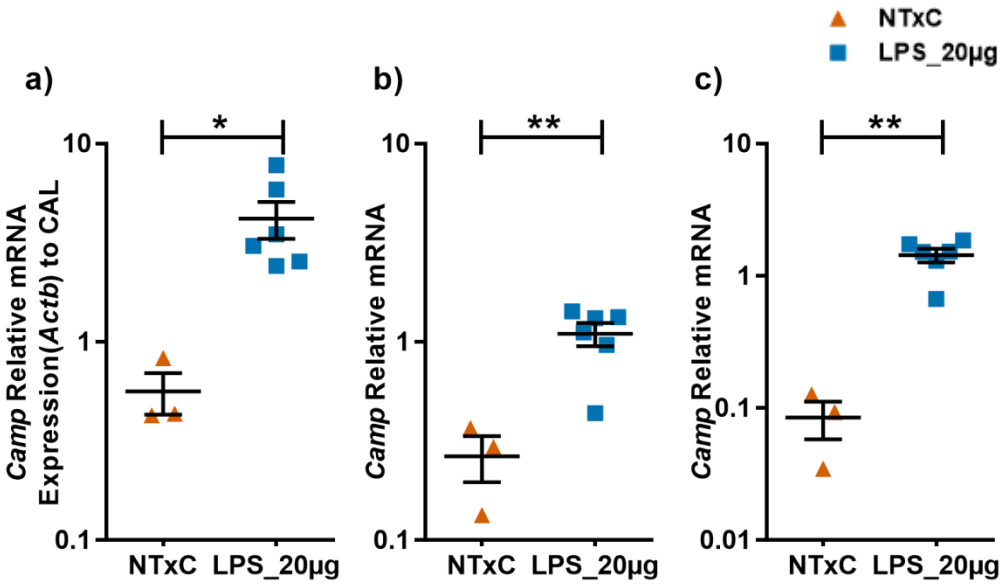

Figure 7.4 Expression of *Camp* in LPS-induced PTL Model
Relative mRNA expression of *Camp* in (a) Placenta, (b) Uterus, and (c) Fetal Membrane tissues collected in C57BL/6J animals 6-hours post LPS [20µg] treatment (n=6) or non-treatment controls (NTxC, n=3). Data presented is mean fold-increase and SEM, normalised to *β-Actin* and relative to CAL. (unpaired t-test; *, P <0.05, **, P <0.01)

7.3.2.3 Inflammatory and Immune Cell Mediators in Placenta

Intrauterine LPS [20µg] injection significantly increased the expression of all investigated inflammatory and immune cell mediators in placental tissues of C57BL/6J mice (Figure 7.5).

The neutrophil chemokines, *Cxcl1* and *Cxcl2,* in placental tissues showed significant increases after LPS [20µg] injection compared to non-treatment controls. *Cxcl1* mRNA expression displayed a mean 45.16 ± 7.06 fold-increase ($P < 0.001$), compared to non-treatment animals. *Cxcl2* mRNA expression increased on average 83.02 ± 20.09 fold, compared to those animals not-treated ($P < 0.01$).

Similarly, the pro-inflammatory cytokines, *Il-1β* and *Tnf*, are also significantly increased in placental tissues following LPS [20µg] treatment; displaying a 14.43 ± 3.15 mean fold-increase ($P < 0.01$) and 6.5 ± 1.46 mean fold-increase ($P < 0.01$) respectively.

Placental mRNA expression of *Ptgs2* (*Cox-2*) showed a 3.61 ± 0.94 fold-increase in the placenta ($P < 0.01$) in response to LPS [20µg] as compared to non-treatment controls.

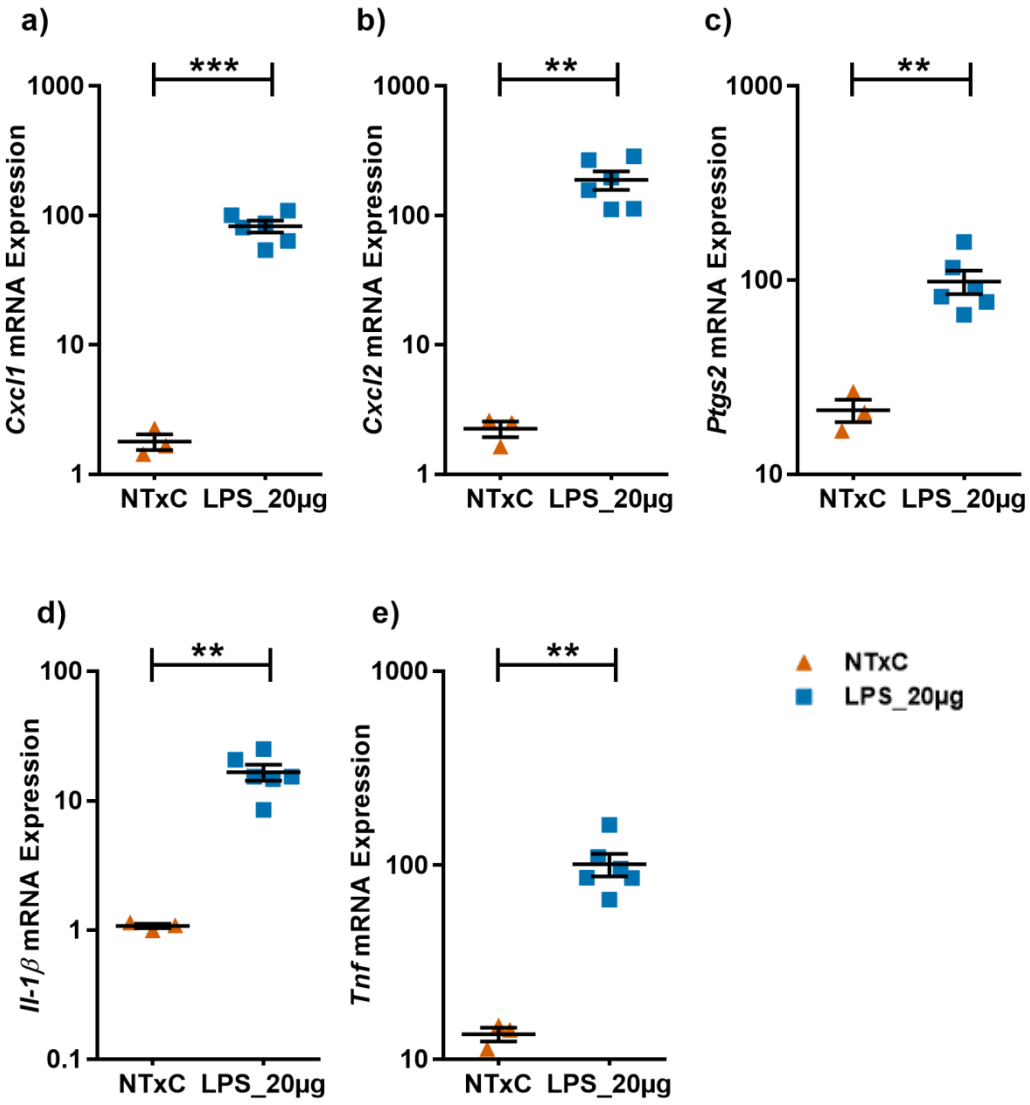

Figure 7.5 Placental Inflammatory and Immune Cell Mediator Response to LPS-induced PTL Model

Relative mRNA expression of (a) *Cxcl1*(b) *Cxcl2* (c) *Ptgs2* (d) *Il-1β* (e) *Tnf* in placenta tissues collected in C57BL/6J mice 6-hours post LPS [20µg] injection (n=6) or NTxC (n=3). Data presented as mean fold-increase and SEM, normalised to *β-Actin* and relative to CAL. (unpaired t-test; *, P <0.05, **, P <0.01, ***, P<0.001)

7.3.2.4 Inflammatory and Immune Cell Mediators in Uterus

Intrauterine LPS [20µg] injection also significantly increased the expression of several inflammatory and immune cell mediators in uterine tissues of C57BL/6J mice compared to those not treated (Figure 7.6).

The neutrophil chemokines, *Cxcl1* and *Cxcl2,* in uterine tissue showed significant increase after LPS [20µg] injection compared to non-treatment controls ($P < 0.0001$ and $P < 0.01$ respectively). mRNA *Cxcl1* expression displayed a mean 443.6 ± 52.89 fold-increase compared to non-treatment animals. *Cxcl2* mRNA expression increased on average 319.1 ± 84.93 fold compared to those animals not-treated

Similarly, the pro-inflammatory cytokines, *Il-1β* and *Tnf*, are also increased in uterine tissues following LPS [20µg] treatment ($P < 0.001$ and $P < 0.0001$ respectively). *Il-β* exhibited a mean fold increase of 49.35 ± 9.14, and on average *Tnf* increased 13.96 ± 1.425 fold compared to the mean of those animals not treated.

Uterine mRNA expression of *Ptgs2* (*Cox-2*) showed a significant ($P < 0.01$) mean 6.18 ± 1.69 fold-increase in the uterus in response to LPS [20µg] compared to non-treatment controls.

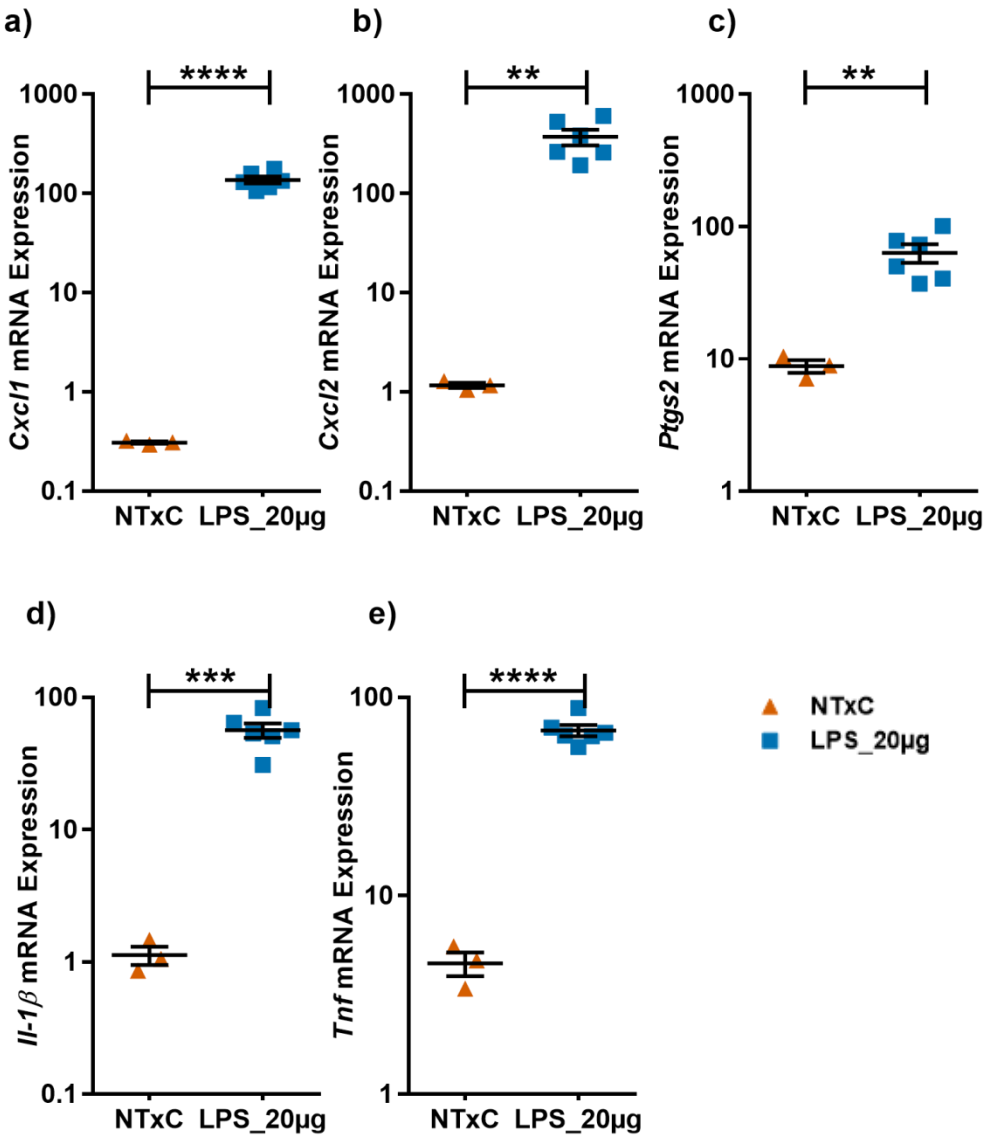

Figure 7.6 Uterine Inflammatory and Immune Cell Mediator Response to LPS-induced PTL Model

Relative mRNA expression of (a) *Cxcl1*(b) *Cxcl2* (c) *Ptgs2* (d) *Il-1β* (e) *Tnf* in uterine tissues collected in C57BL/6J mice 6-hours post LPS [20µg] injection (n=6) or NTxC (n=3). Data is presented as mean fold-increase and SEM, normalised to *β-Actin* and relative to CAL. (unpaired t-test; *, P <0.05, **, P <0.01, ***, P<0.001, ****, P<0.0001)

7.3.2.5 Inflammatory and Immune Cell Mediators in Fetal Membrane

Intrauterine LPS [20µg] injection significantly increased the expression of neutrophil chemokines, *Cxcl1* and *Cxcl2*, and *Ptgs2* in fetal membrane tissues of C57BL/6J mice (Figure 7.7). mRNA *Cxcl1* expression was significantly increased ($P < 0.05$) in fetal membranes, showing a mean 11.32 ± 5.53 fold-increase in LPS treatment compared to non-treatment animals. *Cxcl2* mRNA expression increased 3.22 ± 1.56 -fold, compared to those animals not-treated ($P < 0.05$).

Fetal membrane mRNA expression of *Ptgs2* (*Cox-2*) showed a small but significant ($P < 0.05$) increase of 1.64 ± 0.57 in response to LPS [20µg] treatment as compared to non-treatment animals.

The pro-inflammatory cytokines, *Il-1β* and *Tnf*, did not show a significant increase in the fetal membrane post LPS treatment (Figure 7.7d and Figure 7.7.e).

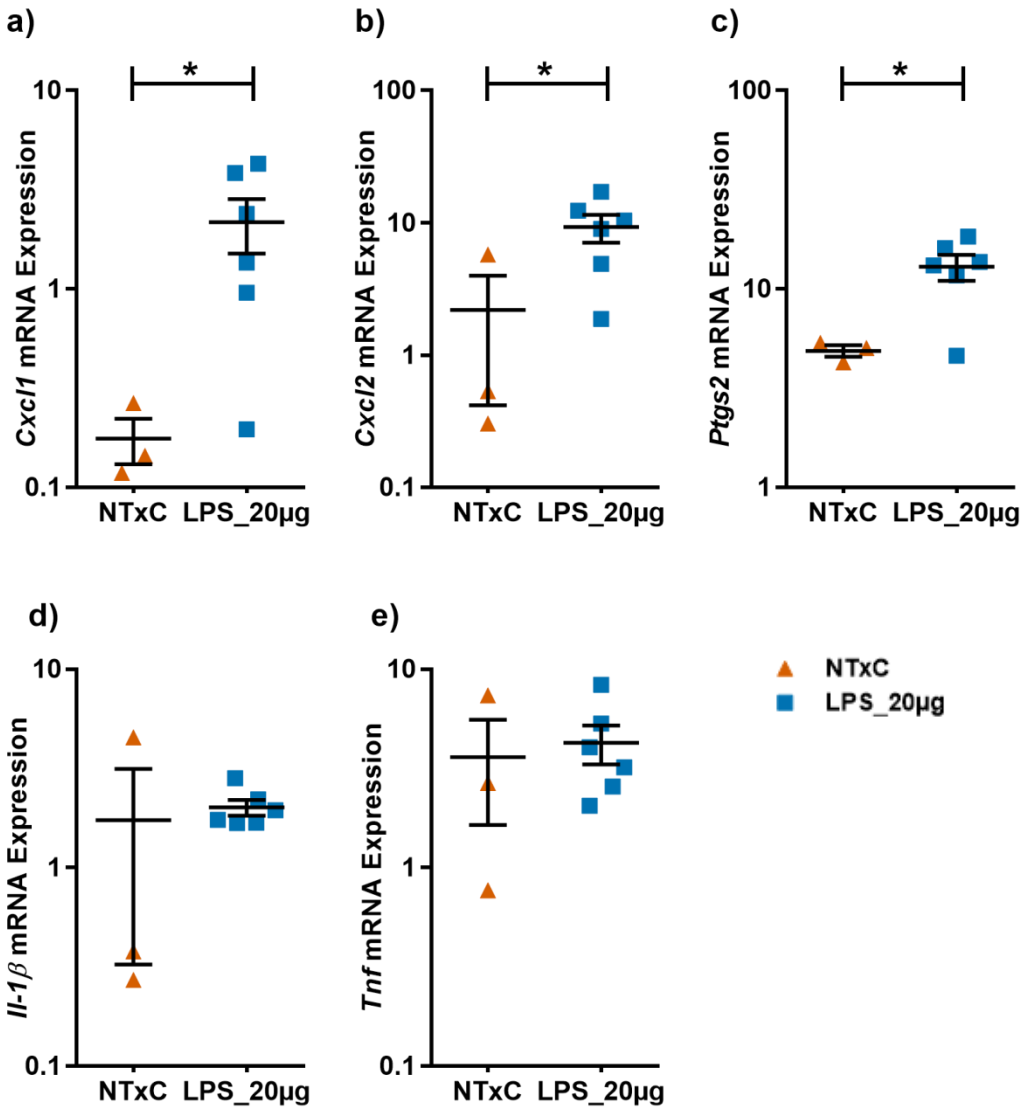

Figure 7.7 Fetal Membrane Inflammatory and Immune Cell Mediator Response to LPS-induced PTL Model

Relative mRNA expression of (a) *Cxcl1*(b) *Cxcl2* (c) *Ptgs2* (d) *Il-1β* (e) *Tnf* in fetal membrane tissues collected in C57BL/6J mice 6-hours post LPS [20µg] injection (n=6) or NTxC (n=3). Data presented is mean fold-increase and SEM, normalised to *β-Actin* and relative to CAL. (Unpaired t-test; *, P <0.05)

7.3.3 *Defb14* in LPS Induced Preterm Labour; Laparotomy Model

7.3.3.1 Interval to Delivery

C57BL/6N and *Defb14-/-* mice received an intrauterine injection of LPS [20µg], physiological sterile saline or no-treatment on day 17 of gestation and the interval to delivery was recorded in hours (Figure 7.8).

The normal gestational interval of C57BL/6N and *Defb14-/-* mice undergoing no-treatment was comparable. C57BL/6N mice deliver on average 62.0 ± 1.5 (n=3) and *Defb14-/-* mice deliver 57.1 ± 3.3 (n=6) hours after being set-up on day 17 with no other intervention. This is equivalent to labour on day 19.5 of gestation, which is in line with what has widely been reported for this background strain.

Intrauterine injection of LPS [20µg] on day 17 of gestation caused preterm labour (defined as delivery within 36 hours) in 17 out of the 18 total animals treated at this dose. LPS [20µg] injection significantly reduces the interval to delivery in C57BL/6N and *Defb14-/-* mice compared to saline injection controls (two-way ANOVA; Dunnett's post-test; $P<0.0001$ at both genotypes). However, there was no significant difference in the interval to delivery between C57BL/6N and *Defb14-/-* mice (two-way ANOVA). C57BL/6N mice deliver on average 14.1 ± 2.0 (n=8) and *Defb14-/-* mice deliver 18.4 ± 6.4 (n=10) hours post LPS [20µg] injection.

Injection of physiological sterile saline by laparotomy induced some variation in the interval to delivery, where 2 of the 10 C57BL/6N mice had preterm labour (defined as delivery within 36 hours). This did not reach statistical significance in C57BL/6N or *Defb14-/-* mice when compared to the respective animals not treated (two-way ANOVA; Dunnett's post-test).

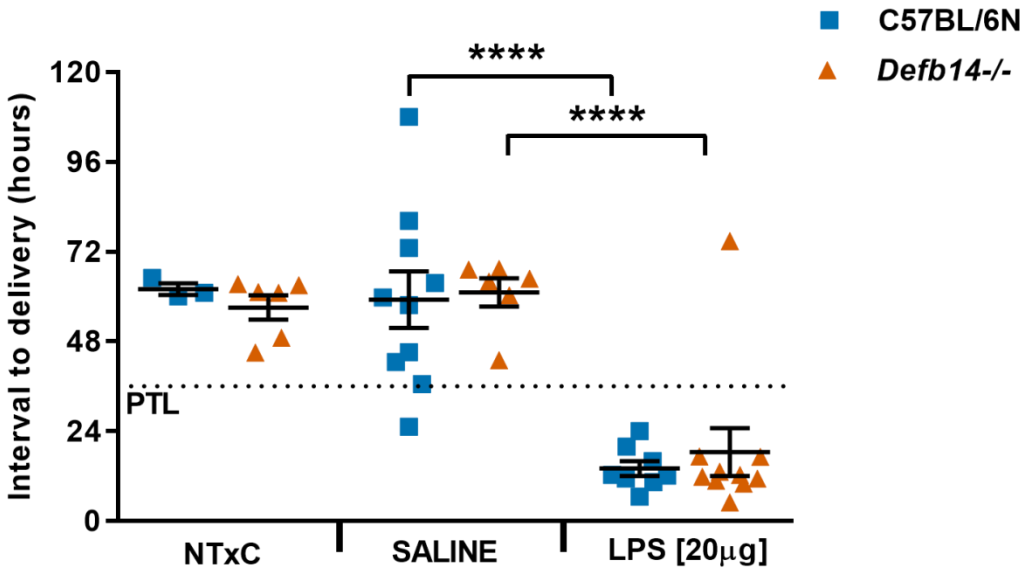

Figure 7.8 Interval to Delivery in *Defb14-/-* mice; LPS-induced PTL Model

Time to delivery in C57BL/6N and *Defb14-/-* mice receiving intrauterine injection of LPS [20µg], physiological sterile saline or non-treatment controls (NTxC). Data presented as mean hours post-treatment on day 17 and SEM. (two-way ANOVA; Dunnett's post-test compared to saline group, ****, P<0.0001)

7.3.3.2 Pup Survival

Post-delivery the number of live born pups in a litter was recorded for C57BL/6N and *Defb14-/-* animals and presented as a ratio to the number of viable fetuses counted at the time of surgery on day 17 of gestation (Figure 7.9). As the number of viable fetuses in NTxC animals is not determined at the time of surgery, the fraction of live born pups presented is calculated against the total number of pups delivered.

Injection of LPS [20µg] by laparotomy resulted in significant amounts of fetal death in both C57BL/6N and *Defb14-/-*mice; where no pups were found born live in this treatment group (Two-way ANOVA; Dunnett's post-test; $P<0.0001$ at both genotypes).

Injection of physiological sterile saline by laparotomy results in an increase in the amount of fetal death seen compared to those animals undergoing no-treatment. This reached significance in just the C57BL/6N animals (two-way ANOVA; Dunnett's post-test compared to saline group; $P <0.01$), where those receiving sterile saline ($n=10$) had on average 0.54 ± 0.13 live born pups compared to those undergoing no-treatment ($n=3$) where 1 ± 0 pups are born live (two-way ANOVA).

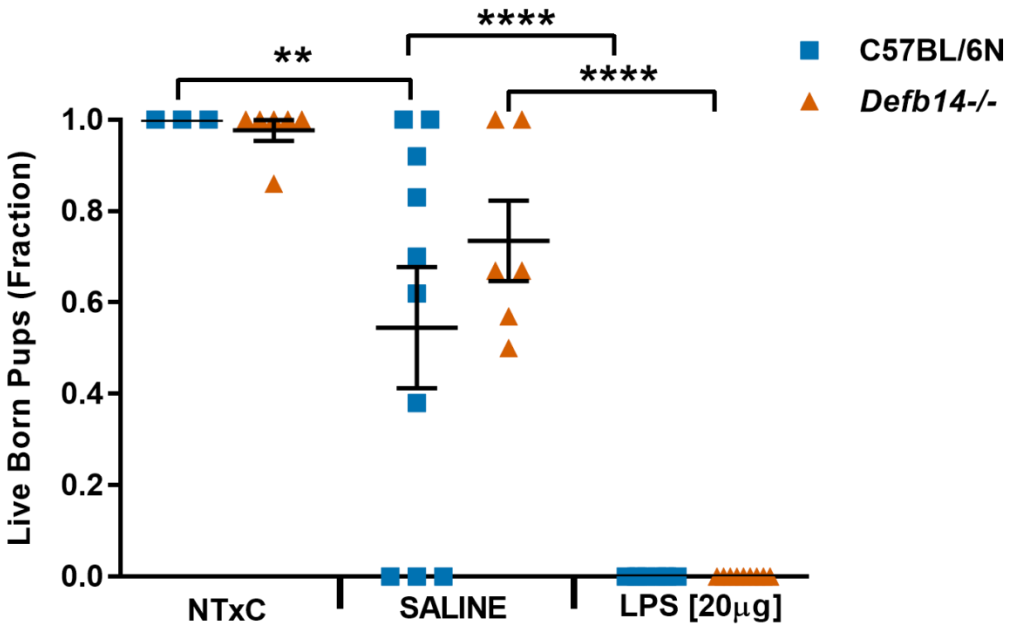

Figure 7.9 Live Born Pup Ratio in *Defb14-/-* mice; LPS-induced PTL Model

Live born pups in C57BL/6N and *Defb14-/-* mice receiving intrauterine injection of LPS [20µg], physiological sterile saline or non-treatment controls (NTxC). Data presented as mean fraction of viable fetuses on day 17 and SEM. (two-way ANOVA; Dunnett's post-test compared to saline group; **, P <0.01, ****, P<0.0001)

7.3.4 *Camp* in LPS Induced Preterm Labour; Ultrasound Model

7.3.4.1 Interval to Delivery

C57BL/6J and *Camp-/-* mice received either, an intrauterine injection of LPS [20µg], LPS [1µg] or physiological sterile saline guided by USS on day 17 of gestation. The interval to delivery was recorded in hours (Figure 7.10). The normal gestational interval of C57BL/6J and *Camp-/-* mice undergoing no-treatment is comparable and in line with that reported for this background strain (data not presented).

Intrauterine injection of LPS [20µg] on day 17 of gestation by USS significantly induces preterm labour in C57BL/6J mice, where the average interval to delivery was 26.8 ± 8.8 (n=6) hours post-LPS injection (two-way ANOVA; Dunnett's post-test compared to saline group; $P<0.001$). *Camp-/-* mice treated in the same way also had significant amounts of preterm labour in response to LPS at 20µg (two-way ANOVA; Dunnett's post-test compared to saline group; $P<0.001$). However, there is no significant difference in the interval to delivery between C57BL/6J and *Camp-/-* mice.

Reducing the dose of LPS to 1µg also robustly induced preterm labour in both C57BL/6J and *Camp-/-* mice. Though like LPS at 20µg, there was no significant difference in the average interval to labour in *Camp-/-* mice (44.4 ± 12.6 hours) compared to C57BL/6J mice (26.1 ± 2.6 hours) at the 1µg dose.

Injection of physiological sterile saline by USS only induced preterm labour in one animal. There is no significant difference in the interval to delivery in C57BL/6J and *Camp-/-* animals when treated with saline alone; C57BL/6J mice deliver on average 65.3 ± 9.0 (n=6) and *Camp-/-* mice deliver 78.1 ± 7.8 (n=3) hours post injection.

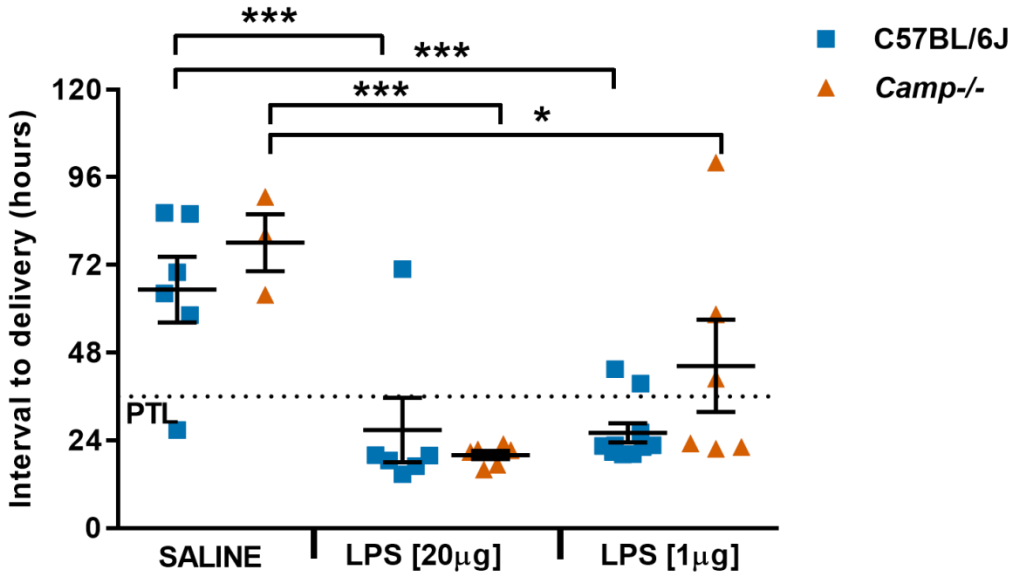

Figure 7.10 Interval to Delivery in *Camp-/-* mice; LPS-induced PTL Model

Time to delivery in C57BL/6J and *Camp-/-* mice receiving intrauterine injection of LPS [20µg], LPS [1µg] or physiological sterile saline. Data presented as mean hours post-treatment on day 17 and SEM. (two-way ANOVA; Dunnett's post-test compared to saline group; *, P<0.05, ***, P<0.001)

7.3.4.2 Pup Survival

Post-delivery the number of live born pups in a litter was recorded for C57BL/6J and *Camp-/-* animals and presented as a ratio to the number of viable fetuses counted at the time of surgery on day 17 (Figure 7.11).

Injection of 20µg LPS resulted in large amounts of fetal death in both C57BL/6J and *Camp-/-* mice. Only one C57BL/6J animal had live pups after 20µg LPS treatment, this animal also delivered at term. LPS at 1µg also resulted in large amounts of fetal death in both genotypes.

Injection of physiological sterile saline by USS results in some fetal death in both C57BL/6J and *Camp-/-* mice. On average C57BL/6J mice have 0.60 ± 0.20 (n=6) live born pups and *Camp-/-* mice have 0.38 ± 0.21 live born pups after saline injection (n=3).

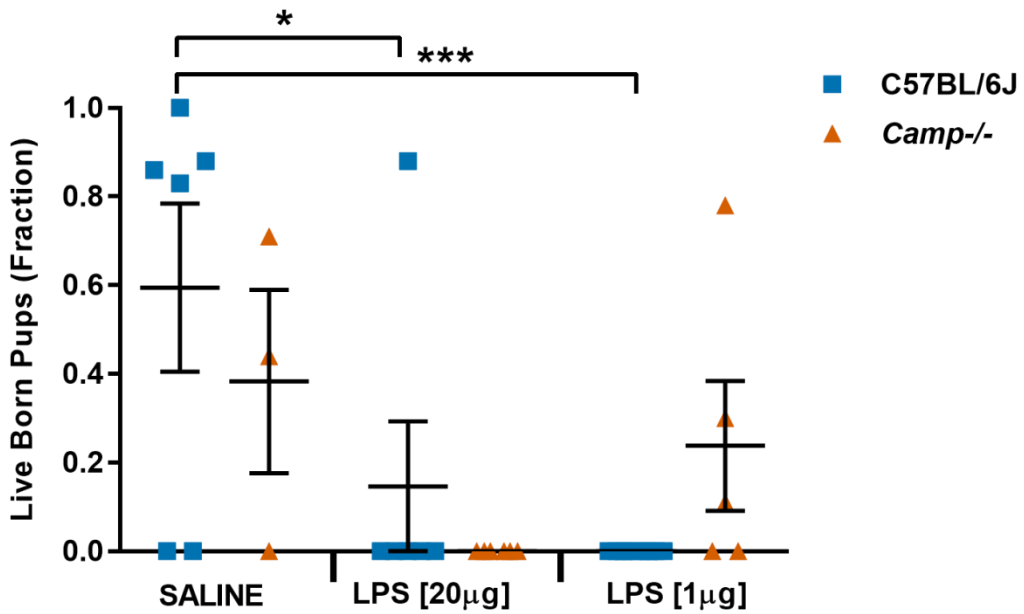

Figure 7.11 Live Born Pup Ratio in *Camp-/-* mice; LPS-induced PTL Model
Live born pups in C57BL/6J and *Camp-/-* mice receiving intrauterine injection of LPS [20µg], LPS [1µg] or physiological sterile saline. Data presented as mean fraction of viable fetuses on day 17 and SEM. (two-way ANOVA; Dunnett's post-test compared to saline group; *, P <0.05, ***, P<0.001)

7.3.4.3 Inflammatory and Immune Cell Mediators in Placenta, Uterus and Fetal Membrane in response to LPS induced PTL

Placental, uterine and fetal membrane tissue were analysed for the mRNA gene expression of several key inflammatory and immune cell mediators in LPS-induced PTL in *Camp-/-* and wildtype animals. The genes investigated were the pro-inflammatory cytokines, *Tnf* and *Il-β,* the strong neutrophil chemoattractants, *Cxcl1* and *Cxcl2, Ptgs2, which* is important in the degradation of prostaglandins, and the Host Defence Peptide, *Camp*.

As expected, placental, uterus and fetal membrane tissue collected 6-hours post treatment in all *Camp-/-* mice showed no expression of the *Camp* gene, confirming these animals are null (Figure 7.13.b, Figure 7.15.b, and Figure 7.17.b)

7.3.4.3.1 Placenta

Chemoattractants

There was a small but significant difference in the expression of the neutrophil chemoattractant *Cxcl1* between C57BL/6J and *Camp-/-* mice following injection of LPS at 1µg (Two-way ANOVA with Bonferroni post-test; P =0.03) (Figure 7.12.a). In response to 1µg of LPS there was 13.6 ± 0.8 fold increase in expression of *Cxcl1* compared to NTxC in C57BL/6J mice. Whereas 1µg of LPS injected *Camp-/-* mice displayed a mean fold increase of 5.5 ± 3.0 in *Cxcl1* compared to NTxC. Sample size in this group is n=3; this genotypic difference in *Cxcl1* was not seen at a dose of 20µg of LPS which has a larger samples size of n=5/6.

In C57BL/6J and *Camp-/-* mice, LPS injection had a significant effect (two-way ANOVA; P <0.0001) on *Cxcl1* expression levels measured by RT-qPCR in placental tissue compared to NTxC. LPS increased *Cxcl1* expression in a dose-responsive manner in both C57BL/6J and *Camp-/-* mice. *Cxcl1* expression level of 20µg LPS injected mice compared to 1µg LPS injection is statistically significant in C57BL/6J animals (two-way ANOVA, with Tukey's post-test; P <0.05). In response to 1µg of LPS there was 13.6 ± 0.8 fold increase in expression of *Cxcl1* compared to NTxC in

C57BL/6J mice. Whereas 20µg of LPS injected in C57BL/6J mice displayed a 42.2 ± 4.8 fold increase in *Cxcl1* compared to NTxC. This significant dose-response was also seen in the *Camp-/-* mice, which had a 5.5 ± 3.0 fold and 31.9 ± 7.4 fold increase in *Cxcl1* gene expression in response to 1µg and 20µg of LPS respectively (two-way ANOVA, with Tukey's post-test; ($P < 0.001$)).

Cxcl2 expression was significantly increased in response to all doses of LPS in both C57BL/6J and *Camp-/-* mice compared to NTxC (two-way ANOVA; $P < 0.0001$ for both 1µg and 20µg) (Figure 7.12.b). The increase in *Cxcl2* expression in 1µg compared to 20µg LPS dose was statistically significant in C57BL/6J ($P < 0.01$) and *Camp-/-* ($P < 0.001$) mouse placental tissue.

Pro-inflammatory Cytokines

There was no difference in the expression of the pro-inflammatory cytokines *Tnf* or *Il-β* between C57BL/6J and *Camp-/-* mice following injection of LPS either at 20µg or 1µg dose (two-way ANOVA) (Figure 7.12c, Figure 7.12.d).

In C57BL/6J and *Camp-/-* mice, LPS injection had a significant effect (two-way ANOVA; $P < 0.0001$) in *Tnf* expression levels measured by RT-qPCR in the placenta. *Tnf* expression in the placenta was significantly elevated in response to LPS in C57BL/6J mice ($P < 0.0001$ at both doses). 20µg of LPS injection in C57BL/6J mice displayed an 84.0 ± 13.0 fold increase in *Tnf* levels compared to NTxC. This significant increase in *Tnf* gene expression was also seen in the *Camp-/-* mice, ($P < 0.0001$ at both doses) where 20µg of LPS increase *Tnf* gene expression 60.1 ± 8.1 fold compared to the NTxC group.

Similarly in C57BL/6J and *Camp-/-* mice, LPS injection had a significant effect (two-way ANOVA; $P < 0.0001$) in *Il-1β* expression levels measured by RT-qPCR in the placenta. *Il-1β* expression in the placenta was significantly elevated in response to LPS in C57BL/6J mice ($P < 0.05$ at 1µg dose, $P < 0.0001$ at 20µg). 20µg of LPS in C57BL/6J mice displayed a 15.4 ± 2.2 fold increase in *Il-1β* compared to NTxC. This significant increase in *Il-1β* gene expression was also seen in the *Camp-/-* mice, (P

<0.0001 at 1µg, P <0.001 at 20µg) where at 20µg there was a 20.4 ± 2.7 fold increase (Two-way ANOVA, with Tukey's post-test).

Ptgs2 (Cox-2)

In C57BL/6J and *Camp-/-* mice, LPS injection had a significant effect (two-way ANOVA; P <0.0001) on *Ptgs2* expression levels measured by RT-qPCR in placental tissue (Figure 7.13.a). There was a small but significant interaction between LPS and genotype (Two-way ANOVA; P = 0.02). *Ptgs2* expression in the placenta was significantly elevated in response to LPS in C57BL/6J mice (P <0.01 at 1 µg, P <0.0001 at 20 µg). 20µg of LPS injected in C57BL/6J mice displayed a 4.6 ± 0.3 fold increase in *Ptgs2* compared to the NTxC group. A significant increase in *Ptgs2* gene expression was only seen in the *Camp-/-* mice treated with 20µg of LPS (P <0.001), where 20µg of LPS increases *Ptgs2* gene expression 4.8 ± 0.7 fold compared to NTxC.

Given the significant interaction effect of LPS and Genotype a two-way ANOVA with Tukey's post-test indicated a significant dose-responsive LPS effect in only *Camp-/-* mice (two-way ANOVA, with Tukey's post-test, P <0.001). *Camp-/-* mice had a 1.4 ± 0.5 fold and 4.8 ± 0.7 fold increase in *Ptgs2* gene expression in response to 1µg and 20µg of LPS respectively.

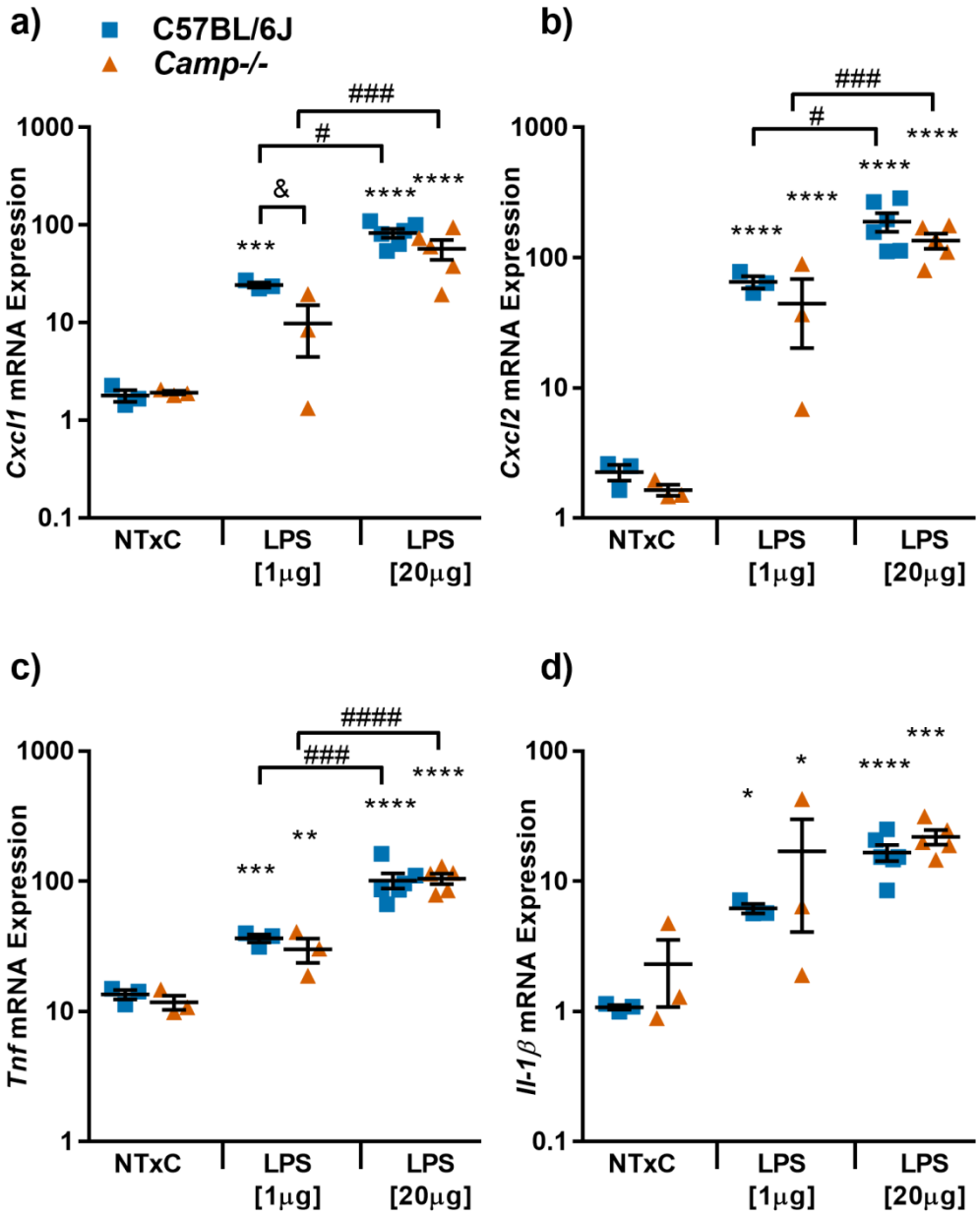

Figure 7.12 Placental Inflammatory and Immune Cell Mediator Response in *Camp-/-* LPS-induced PTL Model

Relative mRNA expression of (a) *Cxcl1* (b) *Cxcl2* (c) *Tnf* (d) *Il-1β* in placenta tissues collected in C57BL/6J and *Camp-/-* mice 6-hours post injection of LPS [20µg], LPS [1µg] or no-treatment controls (NTxC). Data presented is mean fold-increase and SEM, normalised to *β-Actin* and relative to CAL. (Two-way ANOVA with Tukey's post-test; *, P <0.05, **, P <0.01, ***, P<0.001, ****, P<0.0001 compared to NTxC, #, P <0.05, ###, P<0.001, ####, P<0.0001 1µg compared to 20µg. Two-way ANOVA with Bonferroni post-test; &, P<0.05 C57BL/6J compared to *Camp-/-* mice)

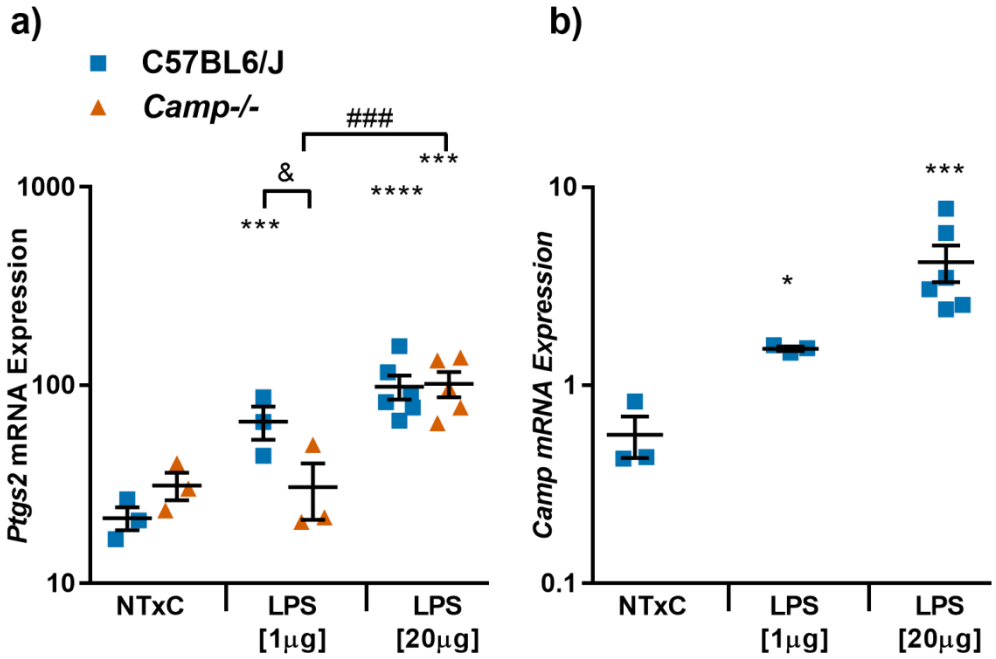

Figure 7.13 Placental *Ptgs2* and *Camp* Response in *Camp-/-* LPS-induced PTL Model

Relative mRNA expression of (a) P*tgs2* and (b) *Camp* in placenta tissues collected in C57BL/6J and *Camp-/-* mice 6-hours post injection of LPS [20µg], LPS [1µg] or no-treatment controls (NTxC). Data presented is mean fold-increase and SEM, normalised to *β-Actin* and relative to CAL. (Two-way ANOVA with Tukey's post-test; ***, P<0.001, ****, P<0.0001 compared to NTxC, ###, P<0.001 1µg compared to 20µg. Two-way ANOVA with Bonferroni post-test; &, P<0.05 C57BL/6J compared to *Camp-/-* mice. For figure (b) *Camp* expression one-way ANOVA with Tukey's post-test; *, P <0.05, ***, P<0.001 compared to NTxC)

7.3.4.3.2 Uterus

Chemoattractants

There was no difference in the expression of the neutrophil chemoattractants *Cxcl1* or *Cxcl2* between C57BL/6J and *Camp-/-* mice following injection of LPS at either 20µg or 1µg dose (two-way ANOVA) (Figure 7.14.a, Figure 7.14,b).

In C57BL/6J and *Camp-/-* mice, LPS injection had a significant effect (two-way ANOVA; P <0.0001) on *Cxcl1* expression levels measured by RT-qPCR in uterine tissue compared to NTxC. LPS increased *Cxcl1* expression in a dose-responsive manner in both C57BL/6J and *Camp-/-* mice. *Cxcl1* expression level of 20µg LPS injected mice compared to 1µg LPS injection is statistically significant in C57BL/6J animals (two-way ANOVA, with Tukey's post-test; P <0.05). In response to 1µg of LPS there was 57.5 ± 22 fold increase in expression of *Cxcl1* compared to NTxC in C57BL/6J mice. Whereas 20µg of LPS injected in C57BL/6J mice displayed a 444.6 ± 36.1 fold increase in *Cxcl1* compared to NTxC. This significant dose-response was also seen in the *Camp-/-* mice, which had a 91.9 ± 47.9 fold and 420.2 ± 121.6 fold increase in *Cxcl1* gene expression in response to 1µg and 20µg of LPS respectively (two-way ANOVA, with Tukey's post-test; P <0.05).

Cxcl2 expression was significantly increased in response to all doses of LPS in both C57BL/6J and *Camp-/-* mice compared to NTxC (two-way ANOVA; P <0.0001 for both 1µg and 20µg). The dose-responsive manner of LPS in *Cxcl2* response did not reach statistical significance in either, C57BL/6J or *Camp-/-* mice.

Pro-inflammatory cytokines

There was no difference in the expression of the pro-inflammatory cytokines *Tnf* or *Il-β* between C57BL/6J and *Camp-/-* mice following injection of LPS at either 20µg or 1µg dose (two-way ANOVA) (Figure 7.14.c, Figure 7.14.d).

In C57BL/6J and *Camp-/-* mice, LPS injection had a significant effect (two-way ANOVA; P <0.0001) in *Tnf* expression levels measured by RT-qPCR in the uterus. *Tnf* expression in the uterus was significantly elevated in response to LPS in

C57BL/6J mice (P <0.001 at 1µg and P <0.0001 at 20µg). 20µg of LPS in C57BL/6J mice displayed a 15.0 ± 1.0 fold increase in *Tnf* compared to NTxC. This significant increase in *Tnf* gene expression was also seen in the *Camp-/-* mice, (P <0.0001 at both doses) where 20µg LPS injection increase *Tnf* gene expression 15.0 ± 2.6 fold compared to NTxC. Similarly in C57BL/6J and *Camp-/-* mice, LPS injection had a significant effect (two-way ANOVA; P <0.0001) in *Il-1β* expression levels measured by RT-qPCR in the uterus.

Il-1β expression in the uterus was significantly elevated in response to LPS in C57BL/6J mice (P <0.001 both doses). 20µg of LPS injection in C57BL/6J mice displayed a 50.3 ± 6.2 fold increase in *Il-1β* compared to NTxC. This significant increase in *Il-1β* gene expression was also seen in the *Camp-/-* mice, (P <0.0001) given 20µg of LPS (Two-way ANOVA, with Tukey's post-test).

Ptgs2 (Cox-2)

In C57BL/6J and *Camp-/-* mice, LPS injection had a significant effect (two-way ANOVA; P <0.01) on *Ptgs2* expression levels measured by RT-qPCR in uterine tissue. A significant increase in *Ptgs2* was only seen at the 20µg LPS dose in C57BL/6J and *Camp-/-* mice (P <0.05 for both genotypes) compared to NTxC (two-way ANOVA, with Tukey's post-test; P <0.05). In response to 20µg of LPS in C57BL/6J and *Camp-/-* mice there was a 7.2 ± 1.2 fold increase and 9.6 ± 3.1 fold increase in *Ptgs2* respectively compared to NTxC. Two-way ANOVA with Tukey's post-test indicated a small (P = 0.41) but significant difference in Ptgs2 expression between 1µg and 20µg treated C57BL/6J mice.

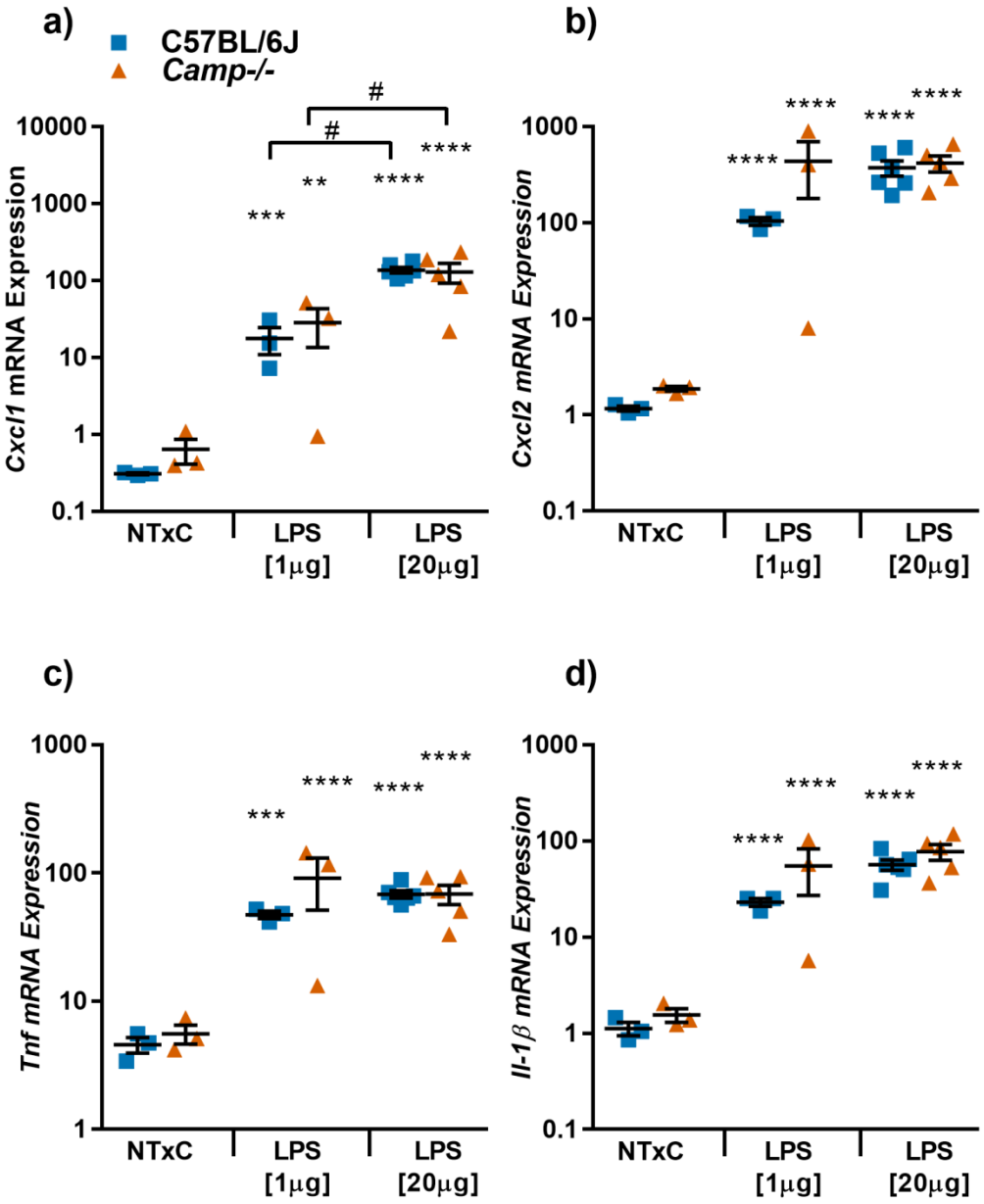

Figure 7.14 Uterine Inflammatory and Immune Cell Mediator Response in *Camp-/-* LPS-induced PTL Model

Relative mRNA expression of (a) *Cxcl1* (b) *Cxcl2* (c) *Tnf* and (d) *Il-1β* in uterus tissues collected in C57BL/6J and *Camp-/-* mice 6-hours post injection of LPS [20µg], LPS [1µg] or no-treatment controls (NTxC). Data presented is mean fold-increase and SEM, normalised to *β-Actin* and relative to CAL. (two-way ANOVA with Tukey's post-test; *, P <0.05, **, P <0.01, ***, P<0.001, ****, P<0.0001 compared to NTxC, #, P <0.05 1µg compared to 20µg).

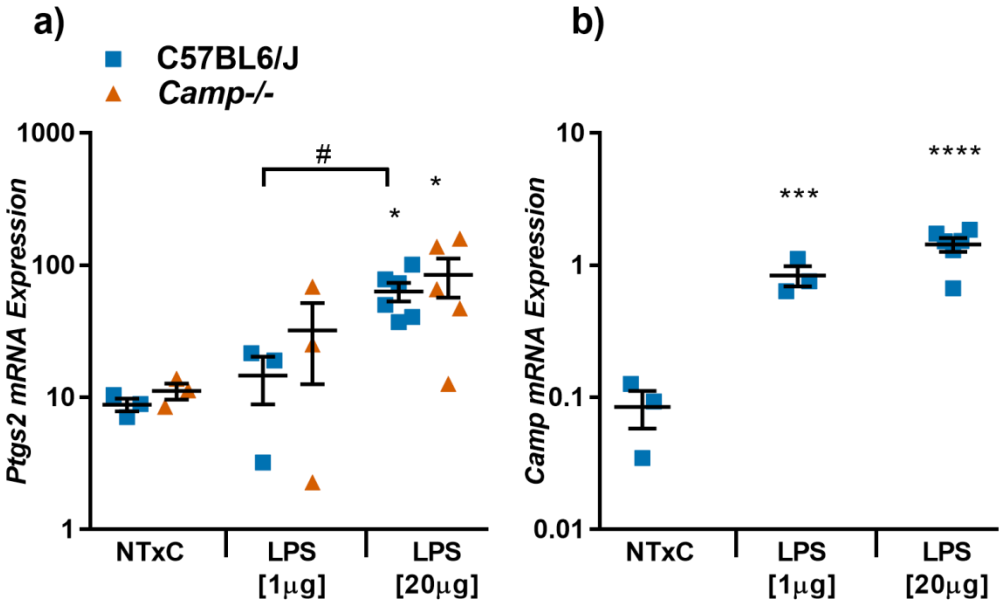

Figure 7.15 Uterine *Ptgs2* and *Camp* Response in *Camp-/-* LPS-induced PTL Model

Relative mRNA expression of (a) P*tgs2* (b) *Camp* in uterus tissues collected in C57BL/6J and *Camp-/-* mice 6-hours post injection of LPS [20µg], LPS [1µg] or no-treatment controls (NTxC). Data presented is mean fold-increase and SEM, normalised to *β-Actin* and relative to CAL. (two-way ANOVA with Tukey's post-test; *, P <0.05, **, P <0.01, ***, P<0.001, ****, P<0.0001 compared to NTxC, #, P <0.05 1µg compared to 20µg. For figure (b) *Camp* expression one-way ANOVA with Tukey's post-test; ***, P<0.001, ****, P<0.0001 compared to NTxC)

7.3.4.3.3 Fetal Membrane

Chemoattractants

There was no difference in the expression of the neutrophil chemoattractants *Cxcl1* or *Cxxl2* between C57BL/6J and *Camp-/-* mice following injection of LPS at either 20µg or 1µg dose (two-way ANOVA) in fetal membrane tissue (Figure 7.16.a, Figure 7.16.b).

In C57BL/6J and *Camp-/-* mice, LPS injection had a significant effect (two-way ANOVA; $P < 0.0001$) on *Cxcl1* expression levels measured by RT-qPCR in fetal membrane tissue compared to NTxC. Cxcl1 expression was only significantly increased in the 20µg treated animals ($P < 0.05$ in C57BL/6J, $P < 0.001$ in *Camp-/-*)

In response to 20µg of LPS there was a 12.3 ± 3.8 fold increase in expression of *Cxcl1* compared to NTxC in C57BL/6J mice. 20µg of LPS injected *Camp-/-* mice displayed a mean fold increase of 65.9 ± 26.6 in *Cxcl1* compared to NTxC.

LPS injection had a significant effect (two-way ANOVA; $P < 0.001$) on *Cxcl2* expression levels measured by RT-qPCR in fetal membrane tissue compared to NTxC. *Cxcl2* expression was only significantly increased in response to 20 µg LPS in *Camp-/-* mice compared to NTxC ($P < 0.01$).

Pro-inflammatory Cytokines

LPS injection had no significant effect (two-way ANOVA) in *Tnf* expression levels measured by RT-qPCR in the fetal membrane (Figure 7.16.c).

Il-1β expression levels measured by RT-qPCR in the fetal membrane only showed a modest response to LPS (two-way ANOVA; $P < 0.05$) (Figure 7.16.d). *Il-1β* expression in the fetal membrane was only significantly elevated in response to 20 µg of LPS in *Camp-/-* mice ($P < 0.01$).

Ptgs2 (Cox-2)

LPS injection had a significant effect (two-way ANOVA; P <0.0001) on *Ptgs2* expression levels measured by RT-qPCR in fetal membrane tissue (Figure 7.17.a). *Il-1β* expression in the fetal membrane was only significantly elevated in response to 20 µg of LPS in C57BL/6J (P <0.05) and *Camp-/-* mice (P <0.01). 20µg of LPS in C57BL/6J mice displayed a 2.6 ± 0.4 fold increase in *Ptgs2* compared to NTxC. *Camp-/-* mice treated with 20 µg LPS increase *Ptgs2* gene expression 5.6 ± 1.5 fold compared to NTxC.

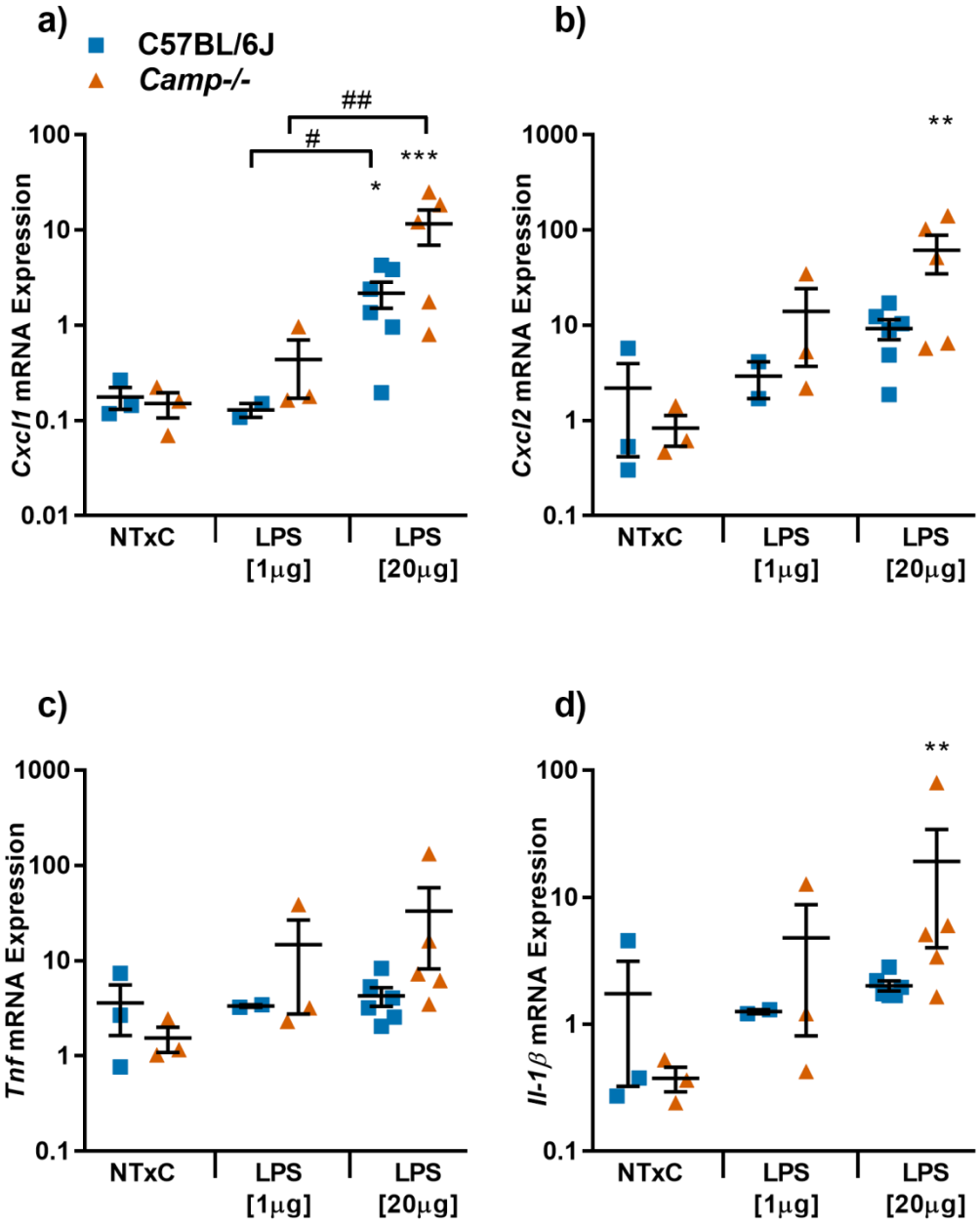

Figure 7.16 Fetal Membrane Inflammatory and Immune Cell Mediator Response in *Camp-/-* LPS-induced PTL Model

Relative mRNA expression of (a) *Cxcl1* (b) *Cxcl2* (c) *Tnf* and (d) *Il-1β* in fetal membrane tissues collected in C57BL/6J and *Camp-/-* mice 6-hours post injection of LPS [20µg], LPS [1µg] or no-treatment controls (NTxC). Data presented is mean fold-increase and SEM, normalised to *β-Actin* and relative to CAL. (two-way ANOVA with Tukey's post-test; *, P <0.05, **, P <0.01, ***, P<0.001, ****, P<0.0001 compared to NTxC, #, P <0.05, ##, P<0.01 1µg compared to 20µg)

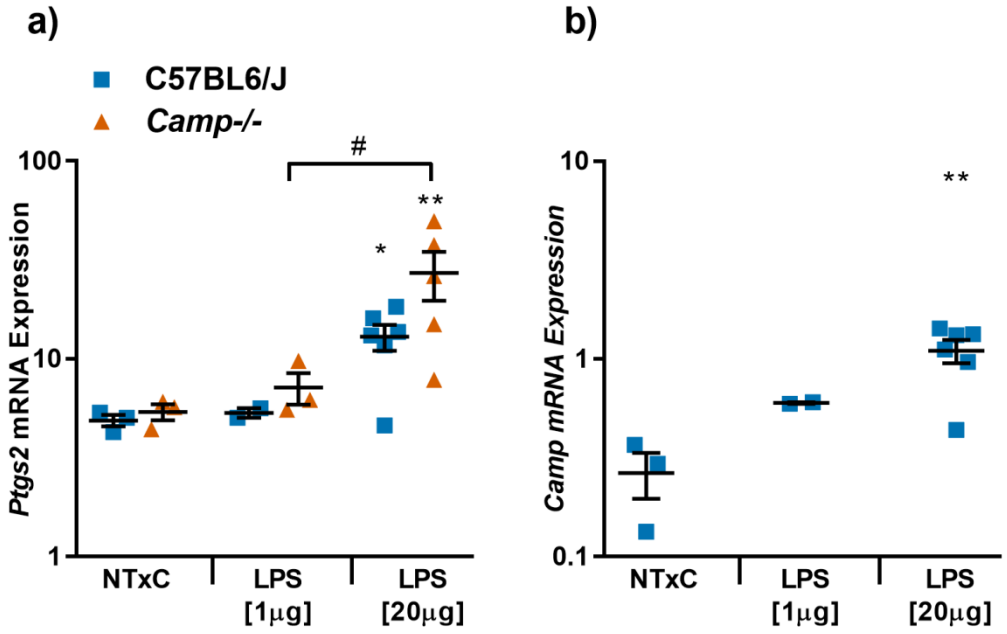

Figure 7.17 Fetal Membrane *Ptgs2* and *Camp* Response in *Camp-/-* LPS-induced PTL Model

Relative mRNA expression of (a) P*tgs2* and (b) *Camp* in fetal membrane tissues collected in C57BL/6J and *Camp-/-* mice 6-hours post injection of LPS [20µg], LPS [1µg] or no-treatment controls (NTxC). Data presented is mean fold-increase and SEM, normalised to *β-Actin* and relative to CAL. (two-way ANOVA with Tukey's post-test; *, P <0.05, **, P <0.01 compared to NTxC, #, P <0.05 1µg compared to 20µg. For figure (b) *Camp* expression one-way ANOVA with Tukey's post-test; **, P <0.01 compared to NTxC)

7.3.4.4 Circulating Serum IL-6 and TNF levels in response to LPS induced PTL

6-hours post-injection of LPS or saline, TNF and IL-6 were measured in maternal circulating serum in LPS-induced PTL by ELISA (Figure 7.18).

Both circulating TNF and Il-6 protein levels were increased in response to LPS (Figure 7.18). However, there was no difference in the level of these cytokines between C57BL/6J and *Camp-/-* mice following injection of LPS at either 20µg or 1µg dose (two-way ANOVA).

In C57BL/6J and *Camp-/-* mice, LPS injection had a significant effect (two-way ANOVA; $P < 0.0001$) in circulating TNF levels. TNF was significantly elevated in response to LPS in C57BL/6J mice ($P < 0.05$ at 1µg and $P < 0.0001$ at 20µg). This significant increase in TNF level was only seen in the *Camp-/-* mice when given 20µg of LPS ($P < 0.001$).

Similarly LPS injection had a significant effect (two-way ANOVA; $P < 0.0001$) in circulating IL-6 levels measured by ELISA in the serum. IL-6 was significantly elevated in response to LPS in C57BL/6J mice ($P < 0.01$ at 1µg and $P < 0.001$ at 20µg). This significant increase in IL-6 level was only seen in the *Camp-/-* mice when given 20µg of LPS ($P < 0.01$).

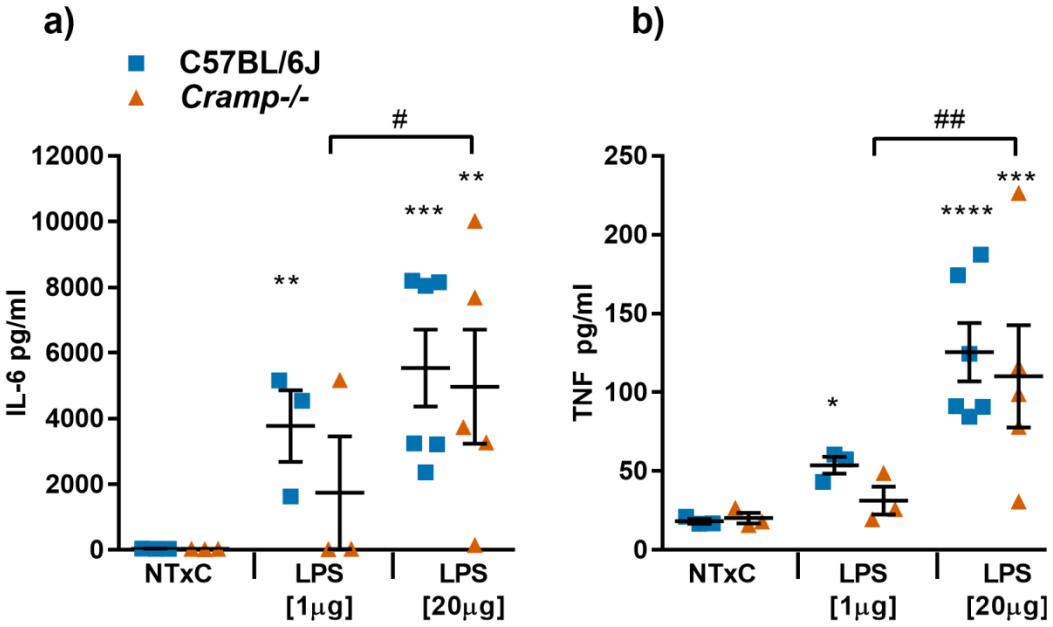

Figure 7.18 IL-6 and TNF in Circulating Serum in *Camp-/-* LPS-induced PTL Model

(a) IL-6 and (b) TNF protein levels in circulating serum collected in C57BL/6J and *Camp-/-* mice 6-hours post injection of LPS [20µg], LPS [1µg] or non-treatment controls (NTxC) and measured by ELISA. Data presented is mean pg/ml and SEM (two-way ANOVA with Tukey's post-test; *, P <0.05, **, P <0.01, ***, P<0.001, ****, P<0.0001 compared to NTxC, #, P <0.05, ##, P<0.01 1µg compared to 20µg)

7.4 Discussion

Interval to Delivery and Pup Survival

In this chapter, I have addressed the murine expression of the HDPs, *Defb14* and *Camp,* in the reproductive tract and whether they have a role modulating the inflammation that maybe the inducing factor of preterm labour. *Defb14-/-* and *Camp-/-* mice have no marked reduction in fertility neither do they display any evidence of spontaneous PTL. I found that a dose of 20µg LPS injected intrauterine on day 17 of gestation by laparotomy significantly and robustly induces preterm labour in C57BL/6N mice. The *Defb14-/-* mice that were treated the same way showed no significant difference from the C57BL/6N mice in the interval to delivery (Figure 7.8), or in the number of live born pups (Figure 7.9). Thus at this concentration of LPS delivered by the laparotomy technique there was no evidence for an influence of *Defb14* on preterm labour in mice.

Injection of 20µg and 1µg of LPS intrauterine on day 17 of gestation by USS significantly induces preterm labour in C57BL/6J animals. *Camp-/-* mice receiving the same treatment displayed no significant difference in the interval to delivery or the number of live born pups to that of C57BL/6J mice (Figure 7.10; Figure 7.11). At 20µg and 1µg LPS dose, delivered by the ultrasound technique, there was no evidence for an influence of *Camp* on preterm labour in mice. Some of the *Camp-/-* animals given 1µg of LPS went on to deliver at term and had associated increase in pup survival. However there was no significant difference in pup survival in *Camp-/-* animals between the Saline and LPS treatment group; more animal numbers are needed here to fully exclude effect.

Pup Survival and Model Refinement

Some of the physiological saline injection control mice delivered preterm and showed a large number of fetal deaths when treatment was given by laparotomy. This model of preterm labour was refined for subsequent experiments where injection of treatments was adapted to be guided by ultrasound sonography. This refined method is less invasive and reported to negate the laparotomy induced

neutrophil influx to the uterus (Rinaldi et al., 2015, Rinaldi et al., 2014). This model displayed a small improvement in the number of live-born pups in the saline injection group of *Camp-/-* and C57BL/6J control mice. Due to the slight difference in background strain of the *Defb14-/-* and *Camp-/-* animals (C57BL/6N and C57BL/6J respectively), direct comparisons between modes of treatment delivery would not be valid here (see Rinaldi et al., (2015) for a direct and robust comparison). Moreover, the laparotomy and USS model experiments in this chapter had been conducted in different SPF animal facilities. The effect of differential bacterial burden between animal facilities on steady state immune profiles remains to be established.

hBD3 and Defb14

hBD3 expression is known to be upregulated in many cell types when treated with bacterial stimuli. Oral squamous cells (Shuyi et al., 2011), gingival epithelial cells and dendritic cells (Yin et al., 2010) all show a marked increase in hBD3 in response to LPS treatment *in-vitro*. Garcia-Lopez et al., (2010) displayed that hBD3 secretion was increased in fetal membranes in a tissue-specific manner; application of *E.coli* to the choriodecidua increased both gene and protein expression. Mouse bone marrow dendritic cells (BMDCs) treated with LPS *in-vitro* increase the expression of *Defb14* gene and protein (Semple et al., 2010). Mouse lung epithelial cells also increase *Defb14* expression in response to TLR stimuli (Rohrl et al., 2008). It is therefore unexpected that in this chapter LPS treatment intrauterine did not result in increased endogenous gene expression of *Defb14* in response to PTL.

Gene level mRNA for *Defb14* can also be stimulated by the pro-inflammatory cytokines TNF and INF-γ (Rohrl et al., 2008). In this chapter, mice treated with LPS had increases in circulating TNF protein level and local *Tnf* mRNA expression in utero-placenta tissues, nonetheless this had no effect on *Defb14* gene expression in tissues collected 6-hours post injection. It is possible that increase in transcription of *Defb14* comes into effect later than the 6-hours investigated here. Yin et al., (2010) had shown that LPS was not effective in upregulating hBD3 gene expression in

epithelial cells at 24-hours post treatment *in-vitro,* but showed an increase at 48-hours at the protein level.

Defb14 in mouse pregnancy has not been well studied. Hickey et al., (2013) found that in non-pregnant animals *Defb14* had specific estrus cycle mRNA expression profiles and the level in the vagina was much higher than that in the uterus. Indeed, in Chapter 2, I show mRNA level of *Defb14* to be 1368 fold higher in the vagina than in the uterus. It is therefore possible that *Defb14* has a greater importance in the lower reproductive tract, which has constant exposure to bacteria.

Dose of LPS in PTL

The hypothesis of this chapter was that mice null for *Defb14* or *Camp* would have increased rates of preterm labour and the interval to delivery would be shorter than wildtype animals. However, it is possible that 20µg of LPS is excessive in this system and any effects of the host defence peptides might be masked by this bolus of endotoxin. Rinaldi et al., (2014) had previously shown that reducing the LPS concentration below 15µg delivered by laparotomy caused no-significant increase in the rate of animals delivering preterm. In the less invasive USS mode of LPS delivery the lower dose threshold for causing preterm labour has yet to be established.

Given the published dose response data from the laparotomy model the experiments conducted in this chapter, using a lower dose of 1µg of LPS induced preterm labour rates higher than expected in the C57BL/6J animals. Eight out of 10 C57BL/6J animals delivered preterm, and three out of five of the *Camp-/-* animals had PTL in response to 1µg of LPS (Figure 7.10).

To further refine this model it would have been ideal to use LPS at a dose sufficient to only induce preterm labour in 50% of the wildtype animals, thus highlighting whether the rates of preterm labour in the HDP knockout mice are higher. I sought to achieve this by lowering the dose to 1µg of LPS but in this system eight out of 10 wildtype animals delivered preterm (80%), thus conducting a dose response lower than 1µg would be needed.

Inflammatory and Immune Cell Mediators in *Camp-/-* PTL

Given the anti-inflammatory effects of human LL-37 on placental explants I have shown in Chapter 2, and the known ability of CAMP to bind to LPS, I investigated differences in immune response of *Camp-/-* mice compared to wildtype in LPS-induced PTL model. Placental, uterine and fetal membrane tissue were analysed for the mRNA gene expression of several key inflammatory and immune cell mediators; *Tnf*, *Il-β*, *Cxcl1*, *Cxcl2* and *Ptgs2*. Broadly most of these mediators showed no difference in expression between *Camp-/-* and wildtype animals at either the 1µg or 20µg dose in utero-placental tissue. *Cxcl1* and *Ptgs2* expression in the placenta at 1µg LPS injection showed a small but significant ($P<0.05$) difference in the mRNA expression level between *Camp-/-* and wildtype animals, although the sample sizes here are small (n=3 per group).

A 6-hour post-injection time-point was chosen for tissue and blood serum collection to highlight effects of LPS on inflammatory and immune cell mediators in pregnancy tissues and circulating serum. This was an intermediate stage between treatment and the initiation of labour, which would be variable between mice. As many cytokines and immune cell mediators have unique temporal and presumably spatial patterning in response to endotoxin, a single time-point is a limiting factor in this study.

Rinaldi et al., (unpublished) had previously shown that saline injection by USS in C57BL/6J mice did not result in any significant increase in key immune markers when compared to non-treated animals of the same gestation. Therefore, in this chapter, the immune marker levels of LPS [20µg/1µg] treatment was compared to non-treatment animals.

In humans, labour at term and preterm has been associated with pro-inflammatory mediators in amniotic fluid and at the local maternal fetal interface (Gardella et al., 2001, Galinsky et al., 2013, Vrachnis et al., 2010). These inflammatory cytokines can stimulate prostaglandin production and propagate neutrophil chemotaxis, infiltration, and activation, resulting in metalloproteases (MMPs) synthesis and release. Prostaglandins can directly stimulate myometrial contractions, in addition to indirect stimulation by the up regulation of the oxytocin receptor (COX-2) (Liggins, 1989,

Crankshaw and Dyal, 1994). COX-2 is an inducible labour associated gene, which is expressed at term in the human myometrium; while MMPs can aid tissue remodelling in the cervix and fetal membrane (Heng et al., 2012)

Chemokines in term labour in both humans (Hamilton et al., 2013) and mice (Shynlova et al., 2013a) have shown increased production. To investigate the role of these immune mediators in the mouse model of preterm labour I looked at *Cxcl1* and *Cxcl2* the strong neutrophil chemoattractants in response to different doses of LPS. These chemokines increased in utero-placental tissue in a mostly dose-responsive manner, the consequences of this are likely to include neutrophil influx. Leucocytes are a large source of pro-inflammatory cytokines and prostaglandins thus are capable of initiating or strengthening an inflammatory cascade and triggering labour by activating the fetal membrane tissues and uterine epithelia. However, Rinaldi et al (2014) showed that neutrophil influx to the decidua is not necessary for initiation of preterm labour in an animal model of PTL.

Many chemokines are reported to be increased in normal mouse labour (Shynlova et al., 2013a), but how the levels in response to LPS-induced PTL compares to spontaneous term-labour was not studied in this chapter.

Prostaglandins are important inflammatory mediators involved in parturition. PTGS2 (COX-2) is expressed at term in the human myometrium and also in animal cervical fibroblasts (Sato et al., 2001); there is also some evidence that low expression may be protective against preterm labour (Hirsch et al., 2006). To investigate the role of *Ptgs2* in the mouse model of preterm labour I looked at *Ptgs2* gene expression in utero-placental tissues; this mediator increased in a mostly dose-responsive manner to LPS.

Cytokines in Blood Serum

6-hours post-injection of LPS or saline, TNF and IL-6 were measured in maternal circulating serum in LPS-induced PTL by ELISA. Elevated serum cytokines have been associated with PTL, although most women with utero-placental infection do not present with symptoms of systemic illness. It is often reported that LPS induces a

rapid induction of pro-inflammatory cytokines after intraperitoneal injection in non-pregnant mice. In one study, IL-6 and TNF in the serum increased sharply, peaking at 2-hours and returned to baseline levels by 6-hours post injection (Copeland et al., 2005). In this chapter, I found that the increase of TNF and IL-6 in maternal serum was still detectable 6-hours post LPS-treatment. The timing of peak response and duration before returning to baseline of these cytokines in LPS-induced PTL remains to be established.

Mice as a model for PTL

There is known variability in the maternal and fetal inflammatory response to different serotypes of LPS used to induce preterm labour (Migale et al., 2015). In this study the serotype of LPS (O111:B4) was kept constant, nonetheless cross-study comparisons will be problematic. There are limitations of using mouse as a model for preterm labour, due to the physiological differences to human pregnancy. One main difference between humans and mice is progesterone production. Humans first maintain pregnancy by the production of progesterone in the corpus lutum; this is then superseded by placental progesterone production. In humans, labour is not associated with a systemic withdrawal of progesterone (Elovitz and Mrinalini, 2004), however emerging evidence suggests there may be local functional progesterone withdrawal prior to the onset of labour (Mesiano et al., 2002, Pieber et al., 2001). In mice however, the contribution of placental progesterone is not thought to supersede that of the corpus lutum, and removing the ovaries during pregnancy induces labour (Condon et al., 2004). It has been proposed that Surfactant Protein A (SP-A) released from the pup lung initiates labour in mice as it causes activation and migration of amniotic fluid macrophages into the serum, leading to activation of pro-inflammatory factors such as NF-κB and IL-1β (Condon et al., 2004, Mendelson and Condon, 2005). However, the causative factor that initiates the inflammatory cascade in human term labour still remains unclear.

7.5 Summary

In this chapter, I have shown that:

- Intrauterine injection of LPS induces preterm labour in wildtype C57BL/6J and C57BL/6N mice.
- *Defb14-/-* and *Camp-/-* mice do not have an increased rate of preterm labour in a LPS induced inflammatory model.
- *Camp* but not *Defb14* is upregulated in utero-placental tissues in response to intrauterine LPS injection.
- The inflammatory mediators; *Cxcl1*, *Cxcl2*, *Tnf*, and *Il-1β* are increased in response to LPS-induced PTL, some in a dose-responsive manner.
- *Camp-/-* animals have a similar inflammatory response as wildtypes C57BL/6J mice when given LPS at 20µg or 1µg during pregnancy.

In this model of preterm labour, it is not clear whether the HDPs, *Defb14* and *Camp* are fundamental to immune defence of the reproductive tract in pregnancy, preventing excessive inflammation that can cause preterm labour.

Chapter 8

Discussion

Chapter 8 Discussion

Summary of Findings

In a pregnant state, the hypothesis of this thesis is that HDPs have a dual role in preventing ascending infection, but also preventing an exacerbated inflammatory response that can cause preterm birth by initiation of the labour cascade.

To explore this I determine whether bacterial stimuli can regulate HDPs expression in pregnancy tissues. I also explore what interactions HDPs have on the production/induction of important cytokines, which are vital to the inflammatory response. As hBD3 and LL-37 suppress the inflammatory response of cells to LPS through TLR-4, the hypothesis is that *in-vivo* they might offer protection from preterm birth caused by inflammation. With the aid of HDP knockout mice, the role of these peptides in infection/inflammation and continuation of pregnancy is investigated in a mouse-model of induced preterm-labour. Infection-induced preterm labour in women is associated with vaginal disruption of commensal bacteria as well as invading pathogens. To understand how ascending infection might be controlled by HDPs in pregnancy, I explore how HDPs regulate commensal bacteria. This is achieved by interrogating the maternal microbiome at mucosal sites in HDP knockout mice, utilising the bacterial 16S rRNA gene and next generation sequencing.

In summary, in this thesis I have shown:

- *DEFB103* and *CAMP* are expressed in myometrium, placenta and amnion/chorion tissues in term human pregnancy.

- Human placental explants respond to LPS challenge by increasing the production of pro-inflammatory cytokines.

- LL-37 but not hBD3 peptide was able to modulate LPS induced inflammatory response by inhibiting the release of pro-inflammatory cytokines in the placenta.

- Beta-defensins; *Defb1*, *Defb4*, *Defb6*, *Defb14*, and the cathelicidin, *Camp*, show spatial expression patterns along the female reproductive tract in mice.

- *Camp-/-* and wildtype mice demonstrated disparate gut microbiota as indicated by statistically significant taxonomic differences. This community-wide effect involves the loss and gain of multiple bacteria.

- *Camp-/-* mice have a more diverse gut microbiome than wildtype controls.

- In murine pregnancy, there are very little global cumulative or progressive shifts in bacteria, with the exception of *Candidatus arthromitus*.

- *Candidatus arthromitus* significantly increases with gestation compared to non-pregnancy and is maintained at high levels 1 day postpartum.

- *Defb14-/-* and *Camp-/-* mice do not have an increased rate of preterm labour in a LPS induced inflammatory model.

- *Camp-/-* animals have a similar inflammatory response as wildtype mice when given LPS at 20µg or 1µg during pregnancy.

Preterm Birth

Preterm birth (<37 weeks gestation) is the main cause of morbidity and mortality in newborn infants, resulting in a multitude of developmental, neurological and cognitive problems (Galinsky et al., 2013). Although research into preterm labour has vastly increased in the last decade, this has not translated into a reduction in the incidence of preterm labour and improved neonatal outcomes. Preterm labour is complex and has multifactorial aetiologies; while some preterm labours are idiopathic, others can be brought on by rupture of the fetal membranes, cervical insufficiency, infection or medically indicated delivery (iatrogenic).

The upper genital tract was generally considered sterile prior to the onset of labour (Jones et al., 2009). However, studies investigating bacterial DNA in placenta and fetal membranes discovered that women who present with preterm labour had a greater diversity of bacteria in these tissues (Prince et al., 2016, Aagaard et al., 2014). Indeed, nearly 40% of preterm deliveries are associated with intrauterine infection and/or clinical inflammation (Romero et al., 2006). The proposed mechanisms by which infectious agents can transfer to the fetus is either by systemic maternal-fetal transfer, or more likely initiated by ascending opportunistic commensal or pathogenic bacteria from the vagina, through the cervix and into the fetal membrane (Allam et al., 2013, DiGiulio et al., 2010). Cells in the female reproductive tract, including vaginal epithelial cells, cervical glands, and neutrophils, are a major source of multiple microbicides including HDPs. Evidence of their importance has come from many animal and *in-vitro* studies. For example, mice null for *Camp*, the murine orthologue of LL-37/hCAP18 have increased susceptibility to bacterial urinary tract infections (Chromek et al., 2006). *Defb1* homozygous knockout mice also have increased susceptibility to urinary tract infections whereby they were shown to retain *Staphylococcus* spp. in the bladder longer than wildtype mice (Morrison et al., 2002). In Chapter 3, I show *DEFB103,* which encodes hBD3, and *CAMP*, which encodes LL-37, are expressed in human term myometrium, placenta and amnion/chorion and there are tissue-specific increases during normal term labour without signs of infection. This suggests these HDPs could be having a role in processes of parturition not induced by infection. It is possible their role is

providing additional microbicidal protection at this vulnerable phase of pregnancy or in the case of the myometrium; HDPs could be involved in tissue remodelling and repair.

Steady state HDP expression is cell specific and compartmentalised in the female reproductive tract in pregnant and non-pregnant women. hBD1-4 and human alpha defensin 5 (HD5) have all been reported to be expressed with distinctive temporal profiles in the endometrial epithelium, vagina and cervix (King et al., 2003a, Fleming et al., 2003, Quayle et al., 1998). Similarly, in Chapter 3 I have shown that many mouse HDPs, specifically, *Defb1*, *Defb4*, *Defb6*, *Defb14* and *Camp* are not uniformly expressed in the reproductive tract and show spatial patterns. The kinetics of this differential expression most likely reflects the differing immunological requirements along the length of the female reproductive tract. This confirms what Hickey et al., (2013) found in defensin mRNA expression profiles in the vagina and uterus of lab mice.

In a steady state, I have shown *Defb14* is highly expressed in the vagina, which suggests that this peptide is having a continuous role here, possibly in the maintenance of commensal microbiota and pathogen clearance. Indeed, lower levels of the human orthologue, hBD3 have been shown in women with vaginal microbiota dysbiosis (bacterial vaginosis) and colonisation with BV associated bacteria (Mitchell et al., 2013). At other mucosal sites, lower hBD3 levels have also been associated with infection, for example in periodontitis patients. hBD3 levels in gingival fluid in periodontitis patients were found to be lower than the levels in normal control individuals (Brancatisano et al., 2011). Interestingly, periodontitis is a risk factor for preterm birth and having a low birthweight baby. The causality of this is still unclear but systemic and fetomaternal increases in pro-inflammatory cytokines, which are deleterious to the fetus, are thought to be involved (Walia and Saini, 2015). It is not known what causes the reduction in hBD3 levels seen in mucosal dysbiosis; this could be due to host genetic variation or possible bacterial inhibition or degradation. *Klebsiella pneumoniae* is known to inhibit the production of hBD3 and cysteine proteases can directly degrade hBD3 peptide (Cogen et al., 2010). hBD3 is copy number variable and the copy number of this loci has been

linked to the inflammatory disease psoriasis (Hollox et al., 2008). An interesting study looking at the beta-defensin copy number and the nasopharynx microbiota from otitis media prone children showed that copy number was associated with the composition of specific pathogens in these children (Jones et al., 2014). Collectively, it would therefore be valid to investigate beta-defensin copy number in association with the vaginal microbiome in women. It is possible that pregnancy modifies the interaction between bacteria and the host mucosa. Therefore correlating the CNV of the beta-defensin loci and vagina microbiome in pregnancy would provide insight into maternal microbiome modulation. The commensal vaginal microbiome of *Defb14* null mice was not studied in this thesis; this could well be an avenue for investigation. Due to concerns with low bacterial yield and variability, an equally valid approach would be looking at *in-vivo* vaginal pathogen clearance and *in-vitro* bacterial killing from vaginal lavages. Given the impact on outcomes of pregnancy caused by vaginal bacteria, it is fundamentally essential that we continue to research vaginal microbiome modulation and dysbiosis to improve female reproductive health.

Although in Chapter 7 I show *Defb14*-/- mice do not have an increased rate of PTL using an LPS-induced model, it would be interesting to investigate the role of *Defb14* in the lower reproductive tract in response to pathogens during pregnancy by using a model of ascending infection. *In-vivo* inoculation of pathogenic organisms into the vagina of *Defb14* null mice while pregnant would be a valid investigation. It has been demonstrated that during murine pregnancy the cervical plug prevents from ascending infection of *E.coli* (Racicot et al., 2013). It is highly plausible that *Defb14* null animals would have defective bacterial killing that could allow bacteria to colonise in the vagina, transverse the cervix, influencing the continuation of pregnancy. This would allow for a better understanding in the role *Defb14*/hBD3 plays in protecting the genital tract during pregnancy. Defensins are however a multigene family and they may well have redundant compensatory roles in the vagina mucosa. Indeed, in Chapter 3 I found *Defb4*, mouse orthologue of hBD2, was also highly expressed in the vagina in a steady state. To determine the collective role of these peptides it would be appropriate to knockout multiple highly expressed defensin genes. The Dorin lab has a genetically modified mouse with a complete

deletion of the beta-defensin region on chromosome 8 that would be suited for such an investigation. The female mice are sub-fertile but further investigation has not been carried out.

Some HDPs are inducible upon stimulation with pathogenic agents, which is when they are most likely to be expressed. It was surprising that *Defb14*, the murine orthologue of *DEFB103*, was not increased in the placenta and uterus 6 hours after LPS exposure in wildtype pregnant mice. In humans, hBD3 is known to be inducible upon stimulation. In gingival fibroblasts, hBD3 expression increases in response to bacterial infection with *Candida albicans* (Gursoy and Kononen, 2012). Oral squamous cells (Shuyi et al., 2011), gingival epithelial cells and dendritic cells (Yin et al., 2010) all show a marked increase in hBD3 in response to LPS treatment *in-vitro*. The lack of *Defb14* increase in response to LPS in this thesis could be a factor of the time-point that the tissues were collected in the experiment. A 6-hour post-injection time-point was chosen for tissue and blood serum collection. This was an intermediate stage between treatment and the initiation of labour, which would be variable between mice. As many cytokines and immune cell mediators have unique temporal and presumably spatial patterning in response to endotoxin, a single time-point is a limiting factor in this study.

Although inflammation is a crucial mechanism in response to injury and pathogen clearance, inappropriate or excessive induction of the inflammatory response in pregnancy can cause initiation of the labour cascade and subsequent preterm delivery. There is therefore a great need to understand the pathophysiology of infection/inflammation in the context of preterm labour concerning both host-genetic and environmental risk factors. The immunomodulatory effect of HDPs in reproductive tissues in response to infection/inflammation has not been well studied. In a pregnant state, the hypothesis of this thesis is that HDPs prevent an exacerbated inflammatory response that can cause preterm birth by initiation of the labour cascade. To explore this I determine whether bacterial stimuli can regulate HDPs expression in pregnancy tissues. I also explore what interactions HDPs have on the production/induction of important cytokines, which are vital to the inflammatory response. Placental explants respond to LPS challenge by increasing production of

pro-inflammatory cytokines. LL-37 but not hBD3 peptide was able to modulate this inflammation by inhibiting the release of these pro-inflammatory cytokines. It is of importance to understand how the inflammatory process leads to preterm labour with the end goal of delaying or preventing this process in women. Further study could lead to the development of new antimicrobial therapies for infection and threatened preterm birth.

Mouse Model of PTL

Ethically and practically the number of samples that can be obtained from women during pregnancy is limited. In addition, there are multiple compounding factors concerning ethnicity, BMI, smoking status and the multifactorial aetiologies of preterm labour. Many different animals have been used to understand the mechanisms of labour and to search for therapeutics that might have benefit to both the mother and neonate. Each animal has associated limitations and benefits as a model for parturition, concerning the correlation to human reproductive biology (reviewed in Elovitz and Mrinalini, (2004) and Bezold et al., (2013)). Mice have extensively been used in labour studies as they have the advantage that tissue can be collected at multiple time-points, in addition to the advantage of their short gestational period. The immune profile of mice is reasonably well annotated and the relative ease of genetic modification makes it possible to elude causative effects. There are some notable differences in mouse physiology that are limitations in using mouse as a model for parturition; one main feature being the production of progesterone. Humans first maintain pregnancy by the production of progesterone in the corpus lutum; this is then superseded by placental progesterone production (Elovitz and Mrinalini, 2004). In contrast, in mice, placental progesterone is not thought to supersede that of the corpus lutum and so removal of the ovaries during pregnancy induces labour (Condon et al., 2004). That said, there is emerging evidence in humans that suggests there may be local functional progesterone withdrawal prior to the onset of labour (Pieber et al., 2001, Mesiano et al., 2002). Mice also have multiple pregnancies and deliver fetus still in their gestational sac, which is not always ruptured at labour. Contrastingly, in women, the fetal membranes and placenta are retained for a short duration after labour. Mouse preterm

labour models have focused on stimulation with agents to create an infection and/or inflammatory state. Stimulation of the TLR4 pathways with LPS has been the central method of invoking preterm labour in animal models. To establish whether HDPs are critical in the continuation of pregnancy I used a LPS induced mouse–model of preterm labour. The initial model of PTL adopted in this thesis was highly invasive in nature; involving a laparotomy to expose the uterine horns for intrauterine injection. This was a limitation of this model as some mice receiving only saline control went on to have preterm labour. An approach established by Sara Rinaldi and Sarah Stock at the University of Edinburgh, used ultrasound sonography to guide intrauterine injection. This refined model was adopted in the later experiments in this thesis, reducing the need for invasive surgery. This is in keeping with the "3Rs" which is a framework aiming to 'refine, reduce and replace' animals used in research.

Intrauterine injection of LPS induced preterm labour in wildtype mice but the *Defb14-/-* and *Camp-/-* mice did not have an increased rate of preterm labour. Key inflammatory mediators are increased in response to LPS-induced PTL, some in a dose-responsive manner, but knockout animals have a similar inflammatory response as wildtype mice when given LPS during pregnancy. At this dose of LPS in this model of preterm labour, is not clear whether the HDPs, *Defb14* and *Camp* are fundamental to immune defence of the reproductive tract in pregnancy, preventing excessive inflammation that can cause preterm labour. As previously discussed, additional studies with lower doses of LPS are needed to fully establish the role of HDP in LPS-induced PTL.

Microbiome

Being able to survey all the microbes in a community is important especially for applications looking at low abundant species, slow-growing bacteria or bacteria that cannot easily be cultured. The use of 16S rRNA gene sequencing is becoming a more popular method for species identification in research, but also in clinical settings for the discovery of novel bacteria in culture-negative infections (reviewed in Woo et al., (2008)). Animals offer researchers a tool to study the role and function of the

microbiome under controlled conditions. Understanding host-microbiome interaction is vital when looking at disease causality. The advantage of the mouse is that we can manipulate host genetics to elude gene function. In addition, animals allow for select colonisation and perturbations such as antibiotics and dietary changes. As the number and diversity of species we can identify is expanding, there needs to be a parallel advancement of annotation of bacterial genome databases. The microbiome field has yet to establish a gold standard for looking at microbial communities. This thesis has put into place a number of techniques and experimental protocols for 16S rRNA gene sequencing on next-generation sequencing platforms. Using this approach I was able to show the mucosal microbiome of *Camp-/-* animals were significantly different to that of wildtype controls, showing increased diversity in the microbes present. While this thesis has displayed a relatively comprehensive understanding of the major players present in the microbiome in *Camp-/-* mice, it has not addressed what these genotype related bacteria are doing. Metagenomics will help to understand the interactions between the gene of the bacteria and the microbiota. It would be of interest to study the metabolome in combination with transcriptomics to gain insight into how these differences in bacterial populations maybe interacting with the host. Determining the transmissibility of the microbiome is also a key avenue for investigation. This can be achieved by co-housing wildtype with *Camp-/-* mice and interrogating the microbiome. As *Camp-/-* animals are known to have increased susceptibility to DSS colitis (Tai et al., 2013, Koon et al., 2011) it is possible that this could be a result of having an altered microbiome as has been demonstrated in Chapter 5. Testing the susceptibility to DSS of animals that have been co-housed would highlight whether this susceptibility phenotype can be transferred by the transfer of microbes.

There has been much interest on the maternal microbiome during pregnancy and in the preconception period, but little is known about the postpartum microbiome and the effects of diet during the lactation stage. As baby's first colonisation and re-seeding in the first few weeks of life comes from the mother, promoting postpartum microbial health could improve the metabolic functions in offspring later in life. In murine pregnancy, there were very little global cumulative or progressive shifts in bacteria, with the exception of *Candidatus arthromitus*, which significantly increases

with gestation compared to non-pregnancy. *Candidatus arthromitus*, also known as segmented filamentous bacteria has been shown to serve a protective role in shaping adult metabolism (Jiang et al., 2001). I have shown that SFB is increased in mid to late gestation, which is fitting that bacteria which occur early in life and has beneficial activity would be increased in the maternal microbiome. Clearly further studies are required to examine both the causal mechanism for the increase in SFB, and the influence this has on the metabolic function of the offspring.

Apart from primates, which are expensive to work with, there are very few animal models to test the effects of exogenous perturbation on commensal vaginal communities. Mice could provide a useful tool to develop and test concepts although there are clear differences in physiology that make this challenging. In contrast to humans it has been proposed only a small percentage of female mice harbour *Lactobacillus* species at the vaginal mucosa (McGrory and Garber, 1992). In Chapter 6, I have shown that the commensal vaginal microbiome in mice is highly variable. After review of the literature, this is only the second study to look at laboratory murine vaginal microbiome by high throughput sequencing (Barfod et al., 2013). Concordantly Barfod et al., (2013) also concluded there was high variability in vaginal communities. Collectively this suggests that the murine vagina is perhaps not an ideal fit for looking at commensal bacterial disturbances in small sample sizes.

Treatments for Infection Associated PTL

In the context of infection, delaying myometrial contractions by the use of anti-inflammatory agents to target inflammatory signalling pathways might actually be doing more harm. Initiation of the labour cascade could be a conserved mechanism to deliver the fetus out of the inflamed *in-utero* environment. That said, anti-inflammatory agents could also resolve the intrauterine inflammation that threatens a preterm delivery. There is therefore a delicate balance in the treatment of PTL, between dampening the inflammatory environment enough that any negative effects of retaining pregnancy improve neonatal outcome. Preventing infection in the first instance is going to be a vital mode for improving neonatal outcome. As it are commonly bacteria from the vagina that cause infection during pregnancy, vaginal

microbial health even prior to conception will be paramount. The combination of antimicrobial and anti-inflammatory properties of HDPs make these peptides attractive as a treatment. The biphasic pro- and anti-inflammatory properties of HDPs are a benefit, but could also be a concern for therapeutic use. Further studies are needed to investigate HDP and pro-inflammatory processes such as chemotaxis in pregnancy.

Conclusion

The development of preventative therapies for preterm labour requires a mechanistic understanding of how the pro-inflammatory profile is induced. HDPs have been shown to have multiple roles in this pro-inflammatory process. This thesis has demonstrated that Host Defence Peptides are expressed in pregnancy tissues and have anti-inflammatory properties in response to bacterial stimuli. It is not clear whether the HDP, hBD3 and LL-37 are fundamental to the immune defence in pregnancy by preventing excessive inflammation. I have shown LL-37 may have a role in modulation of the maternal microbiota. Given the deleterious impact on outcomes of pregnancy caused by the vaginal bacteria, it is fundamentally essential that we continue to apply the findings of this thesis to improve female reproductive health

References

AAGAARD, K., MA, J., ANTONY, K. M., GANU, R., PETROSINO, J. & VERSALOVIC, J. 2014. The placenta harbors a unique microbiome. *Sci Transl Med,* 6**,** 237ra65.

AAGAARD, K., RIEHLE, K., MA, J., SEGATA, N., MISTRETTA, T. A., COARFA, C., RAZA, S., ROSENBAUM, S., VAN DEN VEYVER, I., MILOSAVLJEVIC, A., GEVERS, D., HUTTENHOWER, C., PETROSINO, J. & VERSALOVIC, J. 2012. A metagenomic approach to characterization of the vaginal microbiome signature in pregnancy. *PLoS One,* 7**,** e36466.

ABOU ALAIWA, M. H., REZNIKOV, L. R., GANSEMER, N. D., SHEETS, K. A., HORSWILL, A. R., STOLTZ, D. A., ZABNER, J. & WELSH, M. J. 2014. pH modulates the activity and synergism of the airway surface liquid antimicrobials beta-defensin-3 and LL-37. *Proc Natl Acad Sci U S A,* 111**,** 18703-8.

ACINAS, S. G., SARMA-RUPAVTARM, R., KLEPAC-CERAJ, V. & POLZ, M. F. 2005. PCR-induced sequence artifacts and bias: insights from comparison of two 16S rRNA clone libraries constructed from the same sample. *Appl Environ Microbiol,* 71**,** 8966-9.

AHN, J. H., KIM, B. Y., SONG, J. & WEON, H. Y. 2012. Effects of PCR cycle number and DNA polymerase type on the 16S rRNA gene pyrosequencing analysis of bacterial communities. *J Microbiol,* 50**,** 1071-4.

AISEMBERG, J., VERCELLI, C. A., BARIANI, M. V., BILLI, S. C., WOLFSON, M. L. & FRANCHI, A. M. 2013. Progesterone is essential for protecting against LPS-induced pregnancy loss. LIF as a potential mediator of the anti-inflammatory effect of progesterone. *PLoS ONE,* 8**,** e56161-e56161.

AKIRA, S. & TAKEDA, K. 2004. Toll-like receptor signalling. *Nat Rev Immunol,* 4**,** 499-511.

ALDUNATE, M., SRBINOVSKI, D., HEARPS, A. C., LATHAM, C. F., RAMSLAND, P. A., GUGASYAN, R., CONE, R. A. & TACHEDJIAN, G. 2015. Antimicrobial and immune modulatory effects of lactic acid and short chain fatty acids produced by vaginal microbiota associated with eubiosis and bacterial vaginosis. *Front Physiol,* 6**,** 164.

ALLAM, A. B., VON CHAMIER, M., BROWN, M. B. & REYES, L. 2013. Immune Profiling of BALB/C and C57BL/6 Mice Reveals a Correlation Between Ureaplasma parvum-Induced Fetal Inflammatory Response Syndrome-Like Pathology and Increased Placental Expression of TLR2 and CD14. *American journal of reproductive immunology (New York, N.Y. : 1989)***,** 1-11.

ALVAREZ-OLMOS, M. I., BAROUSSE, M. M., RAJAN, L., VAN DER POL, B. J., FORTENBERRY, D., ORR, D. & FIDEL, P. L., JR. 2004. Vaginal lactobacilli in adolescents: presence and relationship to local and systemic immunity, and to bacterial vaginosis. *Sex Transm Dis,* 31**,** 393-400.

ARAKI, A., KANAI, T., ISHIKURA, T., MAKITA, S., URAUSHIHARA, K., IIYAMA, R., TOTSUKA, T., TAKEDA, K., AKIRA, S. & WATANABE, M. 2005. MyD88-deficient mice develop severe intestinal inflammation in dextran sodium sulfate colitis. *J Gastroenterol,* 40**,** 16-23.

ARCURI, F., TOTI, P., BUCHWALDER, L., CASCIARO, A., CINTORINO, M., SCHATZ, F., RYBALOV, B. & LOCKWOOD, C. J. 2009. Mechanisms of leukocyte accumulation and activation in chorioamnionitis: interleukin 1 beta and tumor necrosis factor alpha enhance colony stimulating factor 2 expression in term decidua. *Reprod Sci,* 16**,** 453-61.

ARON-WISNEWSKY, J. & CLEMENT, K. 2016. The gut microbiome, diet, and links to cardiometabolic and chronic disorders. *Nat Rev Nephrol,* 12**,** 169-81.

BACH, J. F. 2002. The effect of infections on susceptibility to autoimmune and allergic diseases. *N Engl J Med,* 347**,** 911-20.

BALS, R., WANG, X., MEEGALLA, R. L., WATTLER, S., WEINER, D. J., NEHLS, M. C. & WILSON, J. M. 1999. Mouse beta-defensin 3 is an inducible antimicrobial peptide expressed in the epithelia of multiple organs. *Infection and immunity,* 67**,** 3542-7.

BALU, R. B., SAVITZ, D. A., ANANTH, C. V., HARTMANN, K. E., MILLER, W. C., THORP, J. M. & HEINE, R. P. 2003. Bacterial vaginosis, vaginal fluid neutrophil defensins, and preterm birth. *Obstetrics and gynecology,* 101**,** 862-8.

BARFOD, K. K., ROGGENBUCK, M., HANSEN, L. H., SCHJORRING, S., LARSEN, S. T., SORENSEN, S. J. & KROGFELT, K. A. 2013. The murine lung microbiome in relation to the intestinal and vaginal bacterial communities. *BMC Microbiol,* 13**,** 303.

BARLOW, P. G., LI, Y., WILKINSON, T. S., BOWDISH, D. M., LAU, Y. E., COSSEAU, C., HASLETT, C., SIMPSON, A. J., HANCOCK, R. E. & DAVIDSON, D. J. 2006. The human cationic host defense peptide LL-37 mediates contrasting effects on apoptotic pathways in different primary cells of the innate immune system. *J Leukoc Biol,* 80**,** 509-20.

BARNES, P. J. 2006. How corticosteroids control inflammation: Quintiles Prize Lecture 2005. *Br J Pharmacol.*

BARTON, H. A., TAYLOR, N. M., LUBBERS, B. R. & PEMBERTON, A. C. 2006. DNA extraction from low-biomass carbonate rock: an improved method with reduced contamination and the low-biomass contaminant database. *J Microbiol Methods,* 66**,** 21-31.

BAUER, F., SCHWEIMER, K., KLUVER, E., CONEJO-GARCIA, J. R., FORSSMANN, W. G., ROSCH, P., ADERMANN, K. & STICHT, H. 2001. Structure determination of human and murine beta-defensins reveals structural conservation in the absence of significant sequence similarity. *Protein Sci,* 10**,** 2470-9.

BAUMANN, P., ROMERO, R., BERRY, S., GOMEZ, R., MCFARLIN, B., ARANEDA, H., COTTON, D. B. & FIDEL, P. 1993. Evidence of participation of the soluble tumor necrosis factor receptor I in the host response to intrauterine infection in preterm labor. *American journal of reproductive immunology (New York, N.Y. : 1989),* 30**,** 184-93.

BEDRAN, T. B., MAYER, M. P., SPOLIDORIO, D. P. & GRENIER, D. 2014. Synergistic anti-inflammatory activity of the antimicrobial peptides human beta-defensin-3 (hBD-3) and cathelicidin (LL-37) in a three-dimensional co-culture model of gingival epithelial cells and fibroblasts. *PLoS One,* 9**,** e106766.

BERGMAN, P., WALTER-JALLOW, L., BROLIDEN, K., AGERBERTH, B. & SODERLUND, J. 2007. The antimicrobial peptide LL-37 inhibits HIV-1 replication. *Curr HIV Res,* 5**,** 410-5.

BERGSTROM, K. S. B., KISSOON-SINGH, V., GIBSON, D. L., MA, C., MONTERO, M., SHAM, H. P., RYZ, N., HUANG, T., VELCICH, A., FINLAY, B. B., CHADEE, K. & VALLANCE, B. A. 2010. Muc2 Protects against Lethal Infectious Colitis by Disassociating Pathogenic and Commensal Bacteria from the Colonic Mucosa. *PLoS Pathog.*

BETHEA, C. L., GRAVETT, M. G., SADOWSKY, D. W., HALUSKA, G. J., AXTHELM, M. K. & NOVY, M. J. 1998. Amniotic fluid prolactin is decreased by experimental intrauterine infection or interleukin-1beta infusion but not via prostaglandins in pregnant rhesus macaques. *Biol Reprod,* 58**,** 1385-93.

BEZOLD, K. Y., KARJALAINEN, M. K., HALLMAN, M., TERAMO, K. & MUGLIA, L. J. 2013. The genomics of preterm birth: from animal models to human studies. *Genome Med,* 5**,** 34.

BISCHOFF, F. Z., LEWIS, D. E. & SIMPSON, J. L. 2005. Cell-free fetal DNA in maternal blood: kinetics, source and structure. *Human reproduction update,* 11**,** 59-67.

BLANTON, L. V., CHARBONNEAU, M. R., SALIH, T., BARRATT, M. J., VENKATESH, S., ILKAVEYA, O., SUBRAMANIAN, S., MANARY, M. J., TREHAN, I., JORGENSEN, J. M., FAN, Y. M., HENRISSAT, B., LEYN, S. A., RODIONOV, D. A., OSTERMAN, A. L.,

MALETA, K. M., NEWGARD, C. B., ASHORN, P., DEWEY, K. G. & GORDON, J. I. 2016. Gut bacteria that prevent growth impairments transmitted by microbiota from malnourished children. *Science,* 351.

BOLDENOW, E., JONES, S., LIEBERMAN, R. W., CHAMES, M. C., ARONOFF, D. M., XI, C. & LOCH-CARUSO, R. 2013. Antimicrobial peptide response to group B Streptococcus in human extraplacental membranes in culture. *Placenta,* 34**,** 480-5.

BOLGER, A. M., LOHSE, M. & USADEL, B. 2014. Trimmomatic: a flexible trimmer for Illumina sequence data. *Bioinformatics,* 30**,** 2114-20.

BOLLAPRAGADA, S., YOUSSEF, R., JORDAN, F., GREER, I., NORMAN, J. & NELSON, S. 2009. Term labor is associated with a core inflammatory response in human fetal membranes, myometrium, and cervix. *Am J Obstet Gynecol,* 200**,** 104 e1-11.

BOWDISH, D. M., DAVIDSON, D. J., SPEERT, D. P. & HANCOCK, R. E. 2004. The human cationic peptide LL-37 induces activation of the extracellular signal-regulated kinase and p38 kinase pathways in primary human monocytes. *J Immunol,* 172**,** 3758-65.

BRADSHAW, C. S. & BROTMAN, R. M. 2015. Making inroads into improving treatment of bacterial vaginosis - striving for long-term cure. *BMC Infect Dis,* 15**,** 292.

BRANCATISANO, F. L., MAISETTA, G., BARSOTTI, F., ESIN, S., MICELI, M., GABRIELE, M., GIUCA, M. R., CAMPA, M. & BATONI, G. 2011. Reduced human beta defensin 3 in individuals with periodontal disease. *J Dent Res,* 90**,** 241-5.

BRAVO, J. A., FORSYTHE, P., CHEW, M. V., ESCARAVAGE, E., SAVIGNAC, H. M., DINAN, T. G., BIENENSTOCK, J. & CRYAN, J. F. 2011. Ingestion of Lactobacillus strain regulates emotional behavior and central GABA receptor expression in a mouse via the vagus nerve. *Proc Natl Acad Sci U S A,* 108**,** 16050-5.

BRIERY, C. M., VEILLON, E. W., KLAUSER, C. K., MARTIN, R. W., MAGANN, E. F., CHAUHAN, S. P. & MORRISON, J. C. 2011. Women with preterm premature rupture of the membranes do not benefit from weekly progesterone. *Am J Obstet Gynecol,* 204**,** 54.e1-5.

BUFFINGTON, S. A., DI PRISCO, G. V., AUCHTUNG, T. A., AJAMI, N. J., PETROSINO, J. F. & COSTA-MATTIOLI, M. 2016. Microbial Reconstitution Reverses Maternal Diet-Induced Social and Synaptic Deficits in Offspring. *Cell,* 165**,** 1762-75.

BUHIMSCHI, I., ALI, M., JAIN, V., CHWALISZ, K. & GARFIELD, R. E. 1996. Differential regulation of nitric oxide in the rat uterus and cervix during pregnancy and labour. *Hum Reprod,* 11**,** 1755-66.

BURD, I., BROWN, A., GONZALEZ, J. M., CHAI, J. & ELOVITZ, M. A. 2011. A mouse model of term chorioamnionitis: unraveling causes of adverse neurological outcomes. *Reproductive sciences (Thousand Oaks, Calif.),* 18**,** 900-7.

BURRIS, H. H., COLLINS, J. W. & WRIGHT, R. O. 2011. Racial/ethnic disparities in preterm birth: clues from environmental exposures. *Curr Opin Pediatr,* 23**,** 227-32.

BYERS, S. L., WILES, M. V., DUNN, S. L. & TAFT, R. A. 2012. Mouse estrous cycle identification tool and images. *PLoS ONE,* 7**,** e35538-e35538.

CAMPBELL, J. H., FOSTER, C. M., VISHNIVETSKAYA, T., CAMPBELL, A. G., YANG, Z. K., WYMORE, A., PALUMBO, A. V., CHESLER, E. J. & PODAR, M. 2012. Host genetic and environmental effects on mouse intestinal microbiota. *Isme j,* 6**,** 2033-44.

CANI, P. D., BIBILONI, R., KNAUF, C., WAGET, A., NEYRINCK, A. M., DELZENNE, N. M. & BURCELIN, R. 2008. Changes in gut microbiota control metabolic endotoxemia-induced inflammation in high-fat diet-induced obesity and diabetes in mice. *Diabetes,* 57**,** 1470-81.

CAPORASO, J. G., BITTINGER, K., BUSHMAN, F. D., DESANTIS, T. Z., ANDERSEN, G. L. & KNIGHT, R. 2010a. PyNAST: a flexible tool for aligning sequences to a template alignment. *Bioinformatics,* 26**,** 266-7.

CAPORASO, J. G., KUCZYNSKI, J., STOMBAUGH, J., BITTINGER, K., BUSHMAN, F. D., COSTELLO, E. K., FIERER, N., PEÑA, A. G., GOODRICH, J. K., GORDON, J. I., HUTTLEY, G. A., KELLEY, S. T., KNIGHTS, D., KOENIG, J. E., LEY, R. E., LOZUPONE, C. A., MCDONALD, D., MUEGGE, B. D., PIRRUNG, M., REEDER, J., SEVINSKY, J. R., TURNBAUGH, P. J., WALTERS, W. A., WIDMANN, J., YATSUNENKO, T., ZANEVELD, J. & KNIGHT, R. 2010b. QIIME allows analysis of high-throughput community sequencing data. *Nat Methods,* 7**,** 335-6.

CARDING, S., VERBEKE, K., VIPOND, D. T., CORFE, B. M. & OWEN, L. J. 2015. Dysbiosis of the gut microbiota in disease. *Microb Ecol Health Dis.*

CARRETERO, M., ESCAMEZ, M. J., GARCIA, M., DUARTE, B., HOLGUIN, A., RETAMOSA, L., JORCANO, J. L., RIO, M. D. & LARCHER, F. 2008. In vitro and in vivo wound healing-promoting activities of human cathelicidin LL-37. *J Invest Dermatol,* 128**,** 223-36.

CATALANO, R. D., LANNAGAN, T. R. M., GOROWIEC, M., DENISON, F. C., NORMAN, J. E. & JABBOUR, H. N. 2010. Prokineticins: novel mediators of inflammatory and contractile pathways at parturition? *Molecular human reproduction,* 16**,** 311-9.

CDC 2006. Community-associated methicillin-resistant Staphylococcus aureus infection among healthy newborns--Chicago and Los Angeles County, 2004. *MMWR Morb Mortal Wkly Rep,* 55**,** 329-32.

CHAKRAVORTY, S., HELB, D., BURDAY, M., CONNELL, N. & ALLAND, D. 2007. A detailed analysis of 16S ribosomal RNA gene segments for the diagnosis of pathogenic bacteria. *Journal of microbiological methods,* 69**,** 330-9.

CHAMORRO, C. I., WEBER, G., GRONBERG, A., PIVARCSI, A. & STAHLE, M. 2009. The human antimicrobial peptide LL-37 suppresses apoptosis in keratinocytes. *J Invest Dermatol,* 129**,** 937-44.

CHAO, A. 1987. Estimating the population size for capture-recapture data with unequal catchability. *Biometrics,* 43**,** 783-91.

CHERTOV, O., UEDA, H., XU, L. L., TANI, K., MURPHY, W. J., WANG, J. M., HOWARD, O. M., SAYERS, T. J. & OPPENHEIM, J. J. 1997. Identification of human neutrophil-derived cathepsin G and azurocidin/CAP37 as chemoattractants for mononuclear cells and neutrophils. *J Exp Med,* 186**,** 739-47.

CHEUNG, P. Y., WALTON, J. C., TAI, H. H., RILEY, S. C. & CHALLIS, J. R. 1992. Localization of 15-hydroxy prostaglandin dehydrogenase in human fetal membranes, decidua, and placenta during pregnancy. *Gynecol Obstet Invest,* 33**,** 142-6.

CHO, I. & BLASER, M. J. 2012. The human microbiome: at the interface of health and disease. *Nat Rev Genet,* 13**,** 260-70.

CHOI, K. Y., CHOW, L. N. & MOOKHERJEE, N. 2012. Cationic host defence peptides: multifaceted role in immune modulation and inflammation. *J Innate Immun,* 4**,** 361-70.

CHROMEK, M., ARVIDSSON, I. & KARPMAN, D. 2012. The antimicrobial peptide cathelicidin protects mice from Escherichia coli O157:H7-mediated disease. *PLoS One,* 7**,** e46476.

CHROMEK, M., SLAMOVA, Z., BERGMAN, P., KOVACS, L., PODRACKA, L., EHREN, I., HOKFELT, T., GUDMUNDSSON, G. H., GALLO, R. L., AGERBERTH, B. & BRAUNER, A. 2006. The antimicrobial peptide cathelicidin protects the urinary tract against invasive bacterial infection. *Nat Med,* 12**,** 636-41.

CHU, H., PAZGIER, M., JUNG, G., NUCCIO, S. P., CASTILLO, P. A., DE JONG, M. F., WINTER, M. G., WINTER, S. E., WEHKAMP, J., SHEN, B., SALZMAN, N. H., UNDERWOOD, M. A., TSOLIS, R. M., YOUNG, G. M., LU, W., LEHRER, R. I., BAUMLER, A. J. & BEVINS, C. L. 2012. Human alpha-defensin 6 promotes mucosal innate immunity through self-assembled peptide nanonets. *Science,* 337**,** 477-81.

CIORNEI, C. D., SIGURDARDOTTIR, T., SCHMIDTCHEN, A. & BODELSSON, M. 2005. Antimicrobial and chemoattractant activity, lipopolysaccharide neutralization, cytotoxicity, and inhibition by serum of analogs of human cathelicidin LL-37. *Antimicrob Agents Chemother,* 49**,** 2845-50.

CLAESSON, M. J., JEFFERY, I. B., CONDE, S., POWER, S. E., O'CONNOR, E. M., CUSACK, S., HARRIS, H. M., COAKLEY, M., LAKSHMINARAYANAN, B., O'SULLIVAN, O., FITZGERALD, G. F., DEANE, J., O'CONNOR, M., HARNEDY, N., O'CONNOR, K., O'MAHONY, D., VAN SINDEREN, D., WALLACE, M., BRENNAN, L., STANTON, C., MARCHESI, J. R., FITZGERALD, A. P., SHANAHAN, F., HILL, C., ROSS, R. P. & O'TOOLE, P. W. 2012. Gut microbiota composition correlates with diet and health in the elderly. *Nature,* 488**,** 178-84.

CLAESSON, M. J., WANG, Q., O'SULLIVAN, O., GREENE-DINIZ, R., COLE, J. R., ROSS, R. P. & O'TOOLE, P. W. 2010. Comparison of two next-generation sequencing technologies for resolving highly complex microbiota composition using tandem variable 16S rRNA gene regions. *Nucleic Acids Res,* 38**,** e200.

CLEMENTE, J. C., PEHRSSON, E. C., BLASER, M. J., SANDHU, K., GAO, Z., WANG, B., MAGRIS, M., HIDALGO, G., CONTRERAS, M., NOYA-ALARCON, O., LANDER, O., MCDONALD, J., COX, M., WALTER, J., OH, P. L., RUIZ, J. F., RODRIGUEZ, S., SHEN, N., SONG, S. J., METCALF, J., KNIGHT, R., DANTAS, G. & DOMINGUEZ-BELLO, M. G. 2015. The microbiome of uncontacted Amerindians. *Sci Adv,* 1.

COGEN, A. L., YAMASAKI, K., MUTO, J., SANCHEZ, K. M., CROTTY ALEXANDER, L., TANIOS, J., LAI, Y., KIM, J. E., NIZET, V. & GALLO, R. L. 2010. Staphylococcus epidermidis antimicrobial delta-toxin (phenol-soluble modulin-gamma) cooperates with host antimicrobial peptides to kill group A Streptococcus. *PLoS One,* 5**,** e8557.

COLE, J. R., WANG, Q., CARDENAS, E., FISH, J., CHAI, B., FARRIS, R. J., KULAM-SYED-MOHIDEEN, A. S., MCGARRELL, D. M., MARSH, T., GARRITY, G. M. & TIEDJE, J. M. 2009. The Ribosomal Database Project: improved alignments and new tools for rRNA analysis. *Nucleic Acids Res.*

COLLADO, M. C., ISOLAURI, E., LAITINEN, K. & SALMINEN, S. 2008. Distinct composition of gut microbiota during pregnancy in overweight and normal-weight women. *Am J Clin Nutr,* 88**,** 894-9.

COMSTOCK, L. E. 2009. Importance of glycans to the host-bacteroides mutualism in the mammalian intestine. *Cell Host Microbe,* 5**,** 522-6.

CONDON, J. C., JEYASURIA, P., FAUST, J. M. & MENDELSON, C. R. 2004. Surfactant protein secreted by the maturing mouse fetal lung acts as a hormone that signals the initiation of parturition. *Proc Natl Acad Sci U S A,* 101**,** 4978-83.

COPELAND, S., WARREN, H. S., LOWRY, S. F., CALVANO, S. E., REMICK, D. & INVESTIGATORS, T. I. A. T. H. R. T. I. 2005. Acute Inflammatory Response to Endotoxin in Mice and Humans.

COX, L. M., YAMANISHI, S., SOHN, J., ALEKSEYENKO, A. V., LEUNG, J. M., CHO, I., KIM, S. G., LI, H., GAO, Z., MAHANA, D., ZARATE RODRIGUEZ, J. G., ROGERS, A. B., ROBINE, N., LOKE, P. & BLASER, M. J. 2014. Altering the intestinal microbiota during a critical developmental window has lasting metabolic consequences. *Cell,* 158**,** 705-21.

CRANKSHAW, D. J. & DYAL, R. 1994. Effects of some naturally occurring prostanoids and some cyclooxygenase inhibitors on the contractility of the human lower uterine segment in vitro. *Can J Physiol Pharmacol,* 72**,** 870-4.

CULLEN, T. W., SCHOFIELD, W. B., BARRY, N. A., PUTNAM, E. E., RUNDELL, E. A., TRENT, M. S., DEGNAN, P. H., BOOTH, C. J., YU, H. & GOODMAN, A. L. 2015. Gut microbiota. Antimicrobial peptide resistance mediates resilience of prominent gut commensals during inflammation. *Science,* 347**,** 170-5.

CURRIE, S. M., GWYER FINDLAY, E., MCFARLANE, A. J., FITCH, P. M., BÖTTCHER, B., COLEGRAVE, N., PARAS, A., JOZWIK, A., CHIU, C., SCHWARZE, J. & DAVIDSON, D. J. 2016. Cathelicidins Have Direct Antiviral Activity against Respiratory Syncytial Virus In Vitro and Protective Function In Vivo in Mice and Humans. *J Immunol.*

DA FONSECA, E. B., BITTAR, R. E., CARVALHO, M. H. & ZUGAIB, M. 2003. Prophylactic administration of progesterone by vaginal suppository to reduce the incidence of spontaneous preterm birth in women at increased risk: a randomized placebo-controlled double-blind study. *Am J Obstet Gynecol,* 188**,** 419-24.

DAS, S., VINCE, G. S., LEWIS-JONES, I., BATES, M. D. & GAZVANI, R. 2007. The expression of human alpha and beta defensin in the endometrium and their effect on implantation. *J Assist Reprod Genet,* 24**,** 533-9.

DAVIDSON, D. J., CURRIE, A. J., REID, G. S., BOWDISH, D. M., MACDONALD, K. L., MA, R. C., HANCOCK, R. E. & SPEERT, D. P. 2004. The cationic antimicrobial peptide LL-37 modulates dendritic cell differentiation and dendritic cell-induced T cell polarization. *J Immunol,* 172**,** 1146-56.

DE FILIPPIS, F., PELLEGRINI, N., VANNINI, L., JEFFERY, I. B., LA STORIA, A., LAGHI, L., SERRAZANETTI, D. I., DI CAGNO, R., FERROCINO, I., LAZZI, C., TURRONI, S., COCOLIN, L., BRIGIDI, P., NEVIANI, E., GOBBETTI, M., O'TOOLE, P. W. & ERCOLINI, D. 2015. High-level adherence to a Mediterranean diet beneficially impacts the gut microbiota and associated metabolome. *Gut*.

DE, Y., CHEN, Q., SCHMIDT, A. P., ANDERSON, G. M., WANG, J. M., WOOTERS, J., OPPENHEIM, J. J. & CHERTOV, O. 2000. LI-37, the Neutrophil Granule–And Epithelial Cell–Derived Cathelicidin, Utilizes Formyl Peptide Receptor–Like 1 (Fprl1) as a Receptor to Chemoattract Human Peripheral Blood Neutrophils, Monocytes, and T Cells. *J Exp Med.*

DEAN, S. N., BISHOP, B. M. & VAN HOEK, M. L. 2011. Natural and synthetic cathelicidin peptides with anti-microbial and anti-biofilm activity against Staphylococcus aureus. *BMC Microbiol,* 11**,** 114.

DERUAZ, M. & LUSTER, A. D. 2013. BLT humanized mice as model to study HIV vaginal transmission. *J Infect Dis,* 208 Suppl 2**,** S131-6.

DESANTIS, T. Z., HUGENHOLTZ, P., KELLER, K., BRODIE, E. L., LARSEN, N., PICENO, Y. M., PHAN, R. & ANDERSEN, G. L. 2006a. NAST: a multiple sequence alignment server for comparative analysis of 16S rRNA genes. *Nucleic Acids Res,* 34**,** W394-9.

DESANTIS, T. Z., HUGENHOLTZ, P., LARSEN, N., ROJAS, M., BRODIE, E. L., KELLER, K., HUBER, T., DALEVI, D., HU, P. & ANDERSEN, G. L. 2006b. Greengenes, a Chimera-Checked 16S rRNA Gene Database and Workbench Compatible with ARB. *Appl Environ Microbiol.*

DETHLEFSEN, L., MCFALL-NGAI, M. & RELMAN, D. A. 2007. An ecological and evolutionary perspective on human-microbe mutualism and disease. *Nature,* 449**,** 811-8.

DHOPLE, V., KRUKEMEYER, A. & RAMAMOORTHY, A. 2006. The human beta-defensin-3, an antibacterial peptide with multiple biological functions. *Biochim Biophys Acta,* 1758**,** 1499-512.

DIGIULIO, D. B., CALLAHAN, B. J., MCMURDIE, P. J., COSTELLO, E. K., LYELL, D. J., ROBACZEWSKA, A., SUN, C. L., GOLTSMAN, D. S., WONG, R. J., SHAW, G., STEVENSON, D. K., HOLMES, S. P. & RELMAN, D. A. 2015. Temporal and spatial variation of the human microbiota during pregnancy. *Proc Natl Acad Sci U S A,* 112**,** 11060-5.

DIGIULIO, D. B., ROMERO, R., KUSANOVIC, J. P., GÓMEZ, R., KIM, C. J., SEOK, K. S., GOTSCH, F., MAZAKI-TOVI, S., VAISBUCH, E., SANDERS, K., BIK, E. M., CHAIWORAPONGSA, T., OYARZÚN, E. & RELMAN, D. A. 2010. Prevalence and diversity of microbes in the amniotic fluid, the fetal inflammatory response, and

pregnancy outcome in women with preterm pre-labor rupture of membranes. *American journal of reproductive immunology (New York, N.Y. : 1989),* 64**,** 38-57.

DILLON, S. M., LEE, E. J., KOTTER, C. V., AUSTIN, G. L., GIANELLA, S., SIEWE, B., SMITH, D. M., LANDAY, A. L., MCMANUS, M. C., ROBERTSON, C. E., FRANK, D. N., MCCARTER, M. D. & WILSON, C. C. 2016. Gut dendritic cell activation links an altered colonic microbiome to mucosal and systemic T-cell activation in untreated HIV-1 infection. *Mucosal Immunol,* 9**,** 24-37.

DOMINGUEZ-BELLO, M. G., COSTELLO, E. K., CONTRERAS, M., MAGRIS, M., HIDALGO, G., FIERER, N. & KNIGHT, R. 2010. Delivery mode shapes the acquisition and structure of the initial microbiota across multiple body habitats in newborns. *Proceedings of the National Academy of Sciences of the United States of America,* 107**,** 11971-5.

DONG, W. & YIN, L. 2014. Expression of lipoxin A4, TNFalpha and IL-1beta in maternal peripheral blood, umbilical cord blood and placenta, and their significance in pre-eclampsia. *Hypertens Pregnancy,* 33**,** 449-56.

DRELL, T., LILLSAAR, T., TUMMELEHT, L., SIMM, J., AASPÕLLU, A., VÄIN, E., SAARMA, I., SALUMETS, A., DONDERS, G. G. G. & METSIS, M. 2013. Characterization of the Vaginal Micro- and Mycobiome in Asymptomatic Reproductive-Age Estonian Women. *PLoS ONE,* 8**,** e54379-e54379.

DUITS, L. A., RADEMAKER, M., RAVENSBERGEN, B., VAN STERKENBURG, M. A., VAN STRIJEN, E., HIEMSTRA, P. S. & NIBBERING, P. H. 2001. Inhibition of hBD-3, but not hBD-1 and hBD-2, mRNA expression by corticosteroids. *Biochem Biophys Res Commun,* 280**,** 522-5.

DURNWALD, C. P., MOMIROVA, V., ROUSE, D. J., CARITIS, S. N., PEACEMAN, A. M., SCISCIONE, A., VARNER, M. W., MALONE, F. D., MERCER, B. M., THORP, J. M., JR., SOROKIN, Y., CARPENTER, M. W., LO, J., RAMIN, S. M., HARPER, M. & SPONG, C. Y. 2010. Second trimester cervical length and risk of preterm birth in women with twin gestations treated with 17-alpha hydroxyprogesterone caproate. *J Matern Fetal Neonatal Med,* 23**,** 1360-4.

DURR, U. H., SUDHEENDRA, U. S. & RAMAMOORTHY, A. 2006. LL-37, the only human member of the cathelicidin family of antimicrobial peptides. *Biochim Biophys Acta,* 1758**,** 1408-25.

ECKBURG, P. B., BIK, E. M., BERNSTEIN, C. N., PURDOM, E., DETHLEFSEN, L., SARGENT, M., GILL, S. R., NELSON, K. E. & RELMAN, D. A. 2005. Diversity of the Human Intestinal Microbial Flora. *Science,* 308**,** 1635-8.

EDGAR, R. C. 2010. Search and clustering orders of magnitude faster than BLAST. *Bioinformatics,* 26**,** 2460-1.

EDGAR, R. C., HAAS, B. J., CLEMENTE, J. C., QUINCE, C. & KNIGHT, R. 2011. UCHIME improves sensitivity and speed of chimera detection. *Bioinformatics.*

ELLIOTT, C. L., ALLPORT, V. C., LOUDON, J. A., WU, G. D. & BENNETT, P. R. 2001. Nuclear factor-kappa B is essential for up-regulation of interleukin-8 expression in human amnion and cervical epithelial cells. *Mol Hum Reprod,* 7**,** 787-90.

ELOVITZ, M. A. & MRINALINI, C. 2004. Animal models of preterm birth. *Trends in endocrinology and metabolism: TEM,* 15**,** 479-87.

ELOVITZ, M. A., WANG, Z., CHIEN, E. K., RYCHLIK, D. F. & PHILLIPPE, M. 2003. A New Model for Inflammation-Induced Preterm Birth: The Role of Platelet-Activating Factor and Toll-Like Receptor-4. *Am J Pathol.*

ERIGUCHI, Y., TAKASHIMA, S., OKA, H., SHIMOJI, S., NAKAMURA, K., URYU, H., SHIMODA, S., IWASAKI, H., SHIMONO, N., AYABE, T., AKASHI, K. & TESHIMA, T. 2012. Graft-versus-host disease disrupts intestinal microbial ecology by inhibiting Paneth cell production of alpha-defensins. *Blood,* 120**,** 223-31.

EVANS, C. C., LEPARD, K. J., KWAK, J. W., STANCUKAS, M. C., LASKOWSKI, S., DOUGHERTY, J., MOULTON, L., GLAWE, A., WANG, Y., LEONE, V., ANTONOPOULOS, D. A., SMITH, D., CHANG, E. B. & CIANCIO, M. J. 2014. Exercise prevents weight gain and alters the gut microbiota in a mouse model of high fat diet-induced obesity. *PLoS One,* 9**,** e92193.

FAN, S. R., LIU, X. P. & LIAO, Q. P. 2008. Human defensins and cytokines in vaginal lavage fluid of women with bacterial vaginosis. *International journal of gynaecology and obstetrics: the official organ of the International Federation of Gynaecology and Obstetrics,* 103**,** 50-4.

FARINA, A., LESHANE, E. S., ROMERO, R., GOMEZ, R., CHAIWORAPONGSA, T., RIZZO, N. & BIANCHI, D. W. 2005. High levels of fetal cell-free DNA in maternal serum: a risk factor for spontaneous preterm delivery. *American journal of obstetrics and gynecology,* 193**,** 421-5.

FELLERMANN, K., STANGE, D. E., SCHAEFFELER, E., SCHMALZL, H., WEHKAMP, J., BEVINS, C. L., REINISCH, W., TEML, A., SCHWAB, M., LICHTER, P., RADLWIMMER, B. & STANGE, E. F. 2006. A chromosome 8 gene-cluster polymorphism with low human beta-defensin 2 gene copy number predisposes to Crohn disease of the colon. *Am J Hum Genet,* 79**,** 439-48.

FIDEL, P. L., ROMERO, R., WOLF, N., CUTRIGHT, J., RAMIREZ, M., ARANEDA, H. & COTTON, D. B. 1994. Systemic and local cytokine profiles in endotoxin-induced preterm parturition in mice. *American journal of obstetrics and gynecology,* 170**,** 1467-75.

FLEMING, D. C., KING, A. E., WILLIAMS, A. R. W., CRITCHLEY, H. O. D. & KELLY, R. W. 2003. Hormonal contraception can suppress natural antimicrobial gene transcription in human endometrium. *Fertility and sterility,* 79**,** 856-63.

FRANK, J. A., REICH, C. I., SHARMA, S., WEISBAUM, J. S., WILSON, B. A. & OLSEN, G. J. 2008. Critical evaluation of two primers commonly used for amplification of bacterial 16S rRNA genes. *Applied and environmental microbiology,* 74**,** 2461-70.

FRANTZ, A. L., ROGIER, E. W., WEBER, C. R., SHEN, L., COHEN, D. A., FENTON, L. A., BRUNO, M. E. C. & KAETZEL, C. S. 2012. Targeted deletion of MyD88 in intestinal epithelial cells results in compromised antibacterial immunity associated with downregulation of polymeric immunoglobulin receptor, mucin-2, and antibacterial peptides. *Mucosal Immunol.*

FREW, L. 2013. *The production and function of cervical hCAP18/LL-37 in pregnancy.* PhD, University of Edinburgh.

FREW, L., MAKIEVA, S., MCKINLAY, A. T., MCHUGH, B. J., DOUST, A., NORMAN, J. E., DAVIDSON, D. J. & STOCK, S. J. 2014. Human cathelicidin production by the cervix. *PLoS One,* 9**,** e103434.

FRISWELL, M. K., GIKA, H., STRATFORD, I. J., THEODORIDIS, G., TELFER, B., WILSON, I. D. & MCBAIN, A. J. 2010. Site and strain-specific variation in gut microbiota profiles and metabolism in experimental mice. *PLoS One,* 5**,** e8584.

FUNDERBURG, N., LEDERMAN, M. M., FENG, Z., DRAGE, M. G., JADLOWSKY, J., HARDING, C. V., WEINBERG, A. & SIEG, S. F. 2007. Human -defensin-3 activates professional antigen-presenting cells via Toll-like receptors 1 and 2. *Proc Natl Acad Sci U S A,* 104**,** 18631-5.

GAJER, P., BROTMAN, R. M., BAI, G., SAKAMOTO, J., SCHÜTTE, U. M. E., ZHONG, X., KOENIG, S. S. K., FU, L., MA, Z. S., ZHOU, X., ABDO, Z., FORNEY, L. J. & RAVEL, J. 2012. Temporal dynamics of the human vaginal microbiota. *Science translational medicine,* 4**,** 132ra52-132ra52.

GALINSKY, R., POLGLASE, G. R., HOOPER, S. B., BLACK, M. J. & MOSS, T. J. M. 2013. The consequences of chorioamnionitis: preterm birth and effects on development. *Journal of pregnancy,* 2013**,** 412831-412831.

GARCIA-LOPEZ, G., FLORES-ESPINOSA, P. & ZAGA-CLAVELLINA, V. 2010. HBD2 , and HBD3 secretion from human extra-placental membranes stimulated with Escherichia coli. 1-9.

GARCIA-LOPEZ, G., FLORES-ESPINOSA, P. & ZAGA-CLAVELLINA, V. 2010. Tissue-specific human beta-defensins (HBD)1, HBD2, and HBD3 secretion from human extra-placental membranes stimulated with Escherichia coli. *Reproductive biology and endocrinology : RB&E,* 8**,** 146-146.

GARDELLA, C., HITTI, J., MARTIN, T. R., RUZINSKI, J. T. & ESCHENBACH, D. 2001. Amniotic fluid lipopolysaccharide-binding protein and soluble CD14 as mediators of the inflammatory response in preterm labor. *Am J Obstet Gynecol,* 184**,** 1241-8.

GARNIER, Y., KADYROV, M., GANTERT, M., EINIG, A., RATH, W. & HUPPERTZ, B. 2008. Proliferative responses in the placenta after endotoxin exposure in preterm fetal sheep. *Eur J Obstet Gynecol Reprod Biol,* 138**,** 152-7.

GAUGUET, S., D'ORTONA, S., AHNGER-PIER, K., DUAN, B., SURANA, N. K., LU, R., CYWES-BENTLEY, C., GADJEVA, M., SHAN, Q., PRIEBE, G. P. & PIER, G. B. 2015. Intestinal Microbiota of Mice Influences Resistance to Staphylococcus aureus Pneumonia. *Infect Immun,* 83**,** 4003-14.

GHOSH, S. & BALTIMORE, D. 1990. Activation in vitro of NF-kappa B by phosphorylation of its inhibitor I kappa B. *Nature,* 344**,** 678-82.

GILBERT, N. M., LEWIS, W. G. & LEWIS, A. L. 2013. Clinical Features of Bacterial Vaginosis in a Murine Model of Vaginal Infection with Gardnerella vaginalis. *PLoS ONE,* 8**,** e59539-e59539.

GILLIET, M. & LANDE, R. 2008. Antimicrobial peptides and self-DNA in autoimmune skin inflammation. *Curr Opin Immunol,* 20**,** 401-7.

GOHIR, W., WHELAN, F. J., SURETTE, M. G., MOORE, C., SCHERTZER, J. D. & SLOBODA, D. M. 2015. Pregnancy-related changes in the maternal gut microbiota are dependent upon the mother's periconceptional diet. *Gut Microbes,* 6**,** 310-20.

GOLDENBERG, R. L., HAUTH, J. C. & ANDREWS, W. W. 2000. Intrauterine infection and preterm delivery. *N Engl J Med,* 342**,** 1500-7.

GOMEZ-LOPEZ, N., GUILBERT, L. J. & OLSON, D. M. 2010. Invasion of the leukocytes into the fetal-maternal interface during pregnancy. *J Leukoc Biol,* 88**,** 625-33.

GOMEZ-LOPEZ, N., STLOUIS, D., LEHR, M. A., SANCHEZ-RODRIGUEZ, E. N. & ARENAS-HERNANDEZ, M. 2014. Immune cells in term and preterm labor. *Cell Mol Immunol,* 11**,** 571-81.

GONZALEZ, J. M., DONG, Z., ROMERO, R. & GIRARDI, G. 2011a. Cervical remodeling/ripening at term and preterm delivery: the same mechanism initiated by different mediators and different effector cells. *PloS one,* 6**,** e26877-e26877.

GONZALEZ, J. M., FRANZKE, C.-W., YANG, F., ROMERO, R. & GIRARDI, G. 2011b. Complement activation triggers metalloproteinases release inducing cervical remodeling and preterm birth in mice. *The American journal of pathology,* 179**,** 838-49.

GRAHN, N., OLOFSSON, M., ELLNEBO-SVEDLUND, K., MONSTEIN, H. J. & JONASSON, J. 2003. Identification of mixed bacterial DNA contamination in broad-range PCR amplification of 16S rDNA V1 and V3 variable regions by pyrosequencing of cloned amplicons. *FEMS Microbiol Lett,* 219**,** 87-91.

GRASSO, E., PAPARINI, D., HAUK, V., SALAMONE, G., LEIROS, C. P. & RAMHORST, R. 2014. Differential Migration and Activation Profile of Monocytes after Trophoblast Interaction. *PLoS One.*

GRAVETT, M. G., HUMMEL, D., ESCHENBACH, D. A. & HOLMES, K. K. 1986. Preterm labor associated with subclinical amniotic fluid infection and with bacterial vaginosis. *Obstet Gynecol,* 67**,** 229-37.

GUO, C., SINNOTT, B., NIU, B., LOWRY, M. B., FANTACONE, M. L. & GOMBART, A. F. 2013. Synergistic induction of human cathelicidin antimicrobial peptide gene expression by vitamin D and stilbenoids. *Molecular nutrition & food research,* 3**,** 1-9.

GUPTA, V. K., CHAUDHARI, N. M., ISKEPALLI, S. & DUTTA, C. 2015. Divergences in gene repertoire among the reference Prevotella genomes derived from distinct body sites of human. *BMC Genomics.*

GURSOY, U. K. & KONONEN, E. 2012. Understanding the roles of gingival beta-defensins. *J Oral Microbiol,* 4.

HAMILTON, S., OOMOMIAN, Y., STEPHEN, G., SHYNLOVA, O., TOWER, C. L., GARROD, A., LYE, S. J. & JONES, R. L. 2012. Macrophages infiltrate the human and rat decidua during term and preterm labor: evidence that decidual inflammation precedes labor. *Biol Reprod,* 86**,** 39.

HAMILTON, S. A., TOWER, C. L. & JONES, R. L. 2013. Identification of Chemokines Associated with the Recruitment of Decidual Leukocytes in Human Labour: Potential Novel Targets for Preterm Labour. *PLoS One.*

HAMMERSCHLAG, M. R., ALPERT, S., ONDERDONK, A. B., THURSTON, P., DRUDE, E., MCCORMACK, W. M. & BARTLETT, J. G. 1978. Anaerobic microflora of the vagina in children. *Am J Obstet Gynecol,* 131**,** 853-6.

HAN, Y. W., REDLINE, R. W., LI, M. & YIN, L. 2004. Fusobacterium nucleatum induces premature and term stillbirths in pregnant mice: implication of oral bacteria in preterm birth. *Infection and …,* 72**,** 2272-2279.

HARDER, J., BARTELS, J., CHRISTOPHERS, E. & SCHRODER, J. M. 2001. Isolation and characterization of human beta -defensin-3, a novel human inducible peptide antibiotic. *J Biol Chem,* 276**,** 5707-13.

HARDER, J., MEYER-HOFFERT, U., WEHKAMP, K., SCHWICHTENBERG, L. & SCHRODER, J. M. 2004. Differential gene induction of human beta-defensins (hBD-1, -2, -3, and -4) in keratinocytes is inhibited by retinoic acid. *J Invest Dermatol,* 123**,** 522-9.

HART, K. M., MURPHY, A. J., BARRETT, K. T., WIRA, C. R., GUYRE, P. M. & PIOLI, P. A. 2009. Functional Expression of Pattern Recognition Receptors in Tissues of the Human Female Reproductive Tract. *J Reprod Immunol,* 80**,** 33-40.

HAYDEN, M. S. & GHOSH, S. 2004. Signaling to NF-kappaB. *Genes Dev,* 18**,** 2195-224.

HAZRATI, E., GALEN, B., LU, W., WANG, W., OUYANG, Y., KELLER, M. J., LEHRER, R. I. & HEROLD, B. C. 2006. Human alpha- and beta-defensins block multiple steps in herpes simplex virus infection. *J Immunol,* 177**,** 8658-66.

HECZKO, U., ABE, A. & FINLAY, B. B. 2000. Segmented filamentous bacteria prevent colonization of enteropathogenic Escherichia coli O103 in rabbits. *J Infect Dis,* 181**,** 1027-33.

HELL, E., GISKE, C. G., NELSON, A., ROMLING, U. & MARCHINI, G. 2010. Human cathelicidin peptide LL37 inhibits both attachment capability and biofilm formation of Staphylococcus epidermidis. *Lett Appl Microbiol,* 50**,** 211-5.

HENG, Y. J., DI QUINZIO, M. K. W., LIONG, S., PERMEZEL, M., RICE, G. E. & GEORGIOU, H. M. 2012. Temporal investigation of matrix metalloproteinases and their inhibitors in human cervicovaginal fluid in late pregnancy and labor. *Reproductive sciences (Thousand Oaks, Calif.),* 19**,** 55-63.

HENZLER WILDMAN, K. A., LEE, D. K. & RAMAMOORTHY, A. 2003. Mechanism of lipid bilayer disruption by the human antimicrobial peptide, LL-37. *Biochemistry,* 42**,** 6545-58.

HICKEY, D. K., FAHEY, J. V. & WIRA, C. R. 2013. Mouse estrous cycle regulation of vaginal versus uterine cytokines, chemokines, α-/β-defensins and TLRs. *Innate immunity,* 19**,** 121-31.

HILL, G. B., ST CLAIRE, K. K. & GUTMAN, L. T. 1995. Anaerobes predominate among the vaginal microflora of prepubertal girls. *Clin Infect Dis,* 20 Suppl 2**,** S269-70.

HING, T. C., HO, S., SHIH, D. Q., ICHIKAWA, R., CHENG, M., CHEN, J., CHEN, X., LAW, I., NAJARIAN, R., KELLY, C. P., GALLO, R. L., TARGAN, S. R., POTHOULAKIS, C. & KOON, H. W. 2013. The antimicrobial peptide cathelicidin modulates Clostridium difficile-associated colitis and toxin A-mediated enteritis in mice. *Gut,* 62**,** 1295-305.

HINRICHSEN, K., PODSCHUN, R., SCHUBERT, S., SCHRÖDER, J. M., HARDER, J. & PROKSCH, E. 2008. Mouse beta-defensin-14, an antimicrobial ortholog of human beta-defensin-3. *Antimicrobial agents and chemotherapy,* 52**,** 1876-9.

HIRATA, T., OSUGA, Y., HAMASAKI, K., HIROTA, Y., NOSE, E., MORIMOTO, C., HARADA, M., TAKEMURA, Y., KOGA, K., YOSHINO, O., TAJIMA, T., HASEGAWA, A., YANO, T. & TAKETANI, Y. 2007. Expression of toll-like receptors 2, 3, 4, and 9 genes in the human endometrium during the menstrual cycle. *J Reprod Immunol,* 74**,** 53-60.

HIRSCH, E., FILIPOVICH, Y. & MAHENDROO, M. 2006. Signaling via the type I IL-1 and TNF receptors is necessary for bacterially induced preterm labor in a murine model. *American journal of obstetrics and gynecology,* 194**,** 1334-40.

HOLLOX, E. J., HUFFMEIER, U., ZEEUWEN, P. L., PALLA, R., LASCORZ, J., RODIJK-OLTHUIS, D., VAN DE KERKHOF, P. C., TRAUPE, H., DE JONGH, G., DEN HEIJER, M., REIS, A., ARMOUR, J. A. & SCHALKWIJK, J. 2008. Psoriasis is associated with increased beta-defensin genomic copy number. *Nat Genet,* 40**,** 23-5.

HOOPER, L. V. & GORDON, J. I. 2001. Commensal host-bacterial relationships in the gut. *Science,* 292**,** 1115-8.

HOOPER, L. V., WONG, M. H., THELIN, A., HANSSON, L., FALK, P. G. & GORDON, J. I. 2001. Molecular analysis of commensal host-microbial relationships in the intestine. *Science,* 291**,** 881-4.

HOOVER, D. M., BOULEGUE, C., YANG, D., OPPENHEIM, J. J., TUCKER, K., LU, W. & LUBKOWSKI, J. 2002. The structure of human macrophage inflammatory protein-3alpha /CCL20. Linking antimicrobial and CC chemokine receptor-6-binding activities with human beta-defensins. *J Biol Chem,* 277**,** 37647-54.

HUANG, L. C., REINS, R. Y., GALLO, R. L. & MCDERMOTT, A. M. 2007. Cathelicidin-deficient (Cnlp -/-) mice show increased susceptibility to Pseudomonas aeruginosa keratitis. *Invest Ophthalmol Vis Sci,* 48**,** 4498-508.

HUMAN MICROBIOME, P. 2010. Human Microbiome Project.

HURTADO, P. & PEH, C. A. 2010. LL-37 promotes rapid sensing of CpG oligodeoxynucleotides by B lymphocytes and plasmacytoid dendritic cells. *J Immunol,* 184**,** 1425-35.

HYMAN, R. W., FUKUSHIMA, M., JIANG, H., FUNG, E., RAND, L., JOHNSON, B., VO, K. C., CAUGHEY, A. B., HILTON, J. F., DAVIS, R. W. & GIUDICE, L. C. 2014. Diversity of the vaginal microbiome correlates with preterm birth. *Reprod Sci,* 21**,** 32-40.

IVANOV, II, ATARASHI, K., MANEL, N., BRODIE, E. L., SHIMA, T., KARAOZ, U., WEI, D., GOLDFARB, K. C., SANTEE, C. A., LYNCH, S. V., TANOUE, T., IMAOKA, A., ITOH, K., TAKEDA, K., UMESAKI, Y., HONDA, K. & LITTMAN, D. R. 2009. Induction of intestinal Th17 cells by segmented filamentous bacteria. *Cell,* 139**,** 485-98.

JAKOBSEN, T. R., CLAUSEN, F. B., RODE, L., DZIEGIEL, M. H. & TABOR, A. 2012. High levels of fetal DNA are associated with increased risk of spontaneous preterm delivery. *Prenatal diagnosis,* 32**,** 840-5.

JAKOBSSON, H. E., RODRÍGUEZ-PIÑEIRO, A. M., SCHÜTTE, A., ERMUND, A., BOYSEN, P., BEMARK, M., SOMMER, F., BÄCKHED, F., HANSSON, G. C. & JOHANSSON, M. E. 2015. The composition of the gut microbiota shapes the colon mucus barrier. *EMBO Rep,* 16**,** 164-77.

JAMES, C., BAJAJ-ELLIOTT, M., SYNGELAKI, A., KLEIN, N., NICOLAIDES, K. & PEEBLES, D. 2013. Variation in Beta Defensin 1 Genotype is Associated with Preterm Birth. *Archives of Disease in Childhood - Fetal and Neonatal Edition,* 98**,** A4-A4.

JANSEN, P. A., RODIJK-OLTHUIS, D., HOLLOX, E. J., KAMSTEEG, M., TJABRINGA, G. S., DE JONGH, G. J., VAN VLIJMEN-WILLEMS, I. M., BERGBOER, J. G., VAN ROSSUM, M. M., DE JONG, E. M., DEN HEIJER, M., EVERS, A. W., BERGERS, M., ARMOUR, J. A., ZEEUWEN, P. L. & SCHALKWIJK, J. 2009. Beta-defensin-2 protein is a serum biomarker for disease activity in psoriasis and reaches biologically relevant concentrations in lesional skin. *PLoS One,* 4**,** e4725.

JENQ, R. R., TAUR, Y., DEVLIN, S. M., PONCE, D. M., GOLDBERG, J. D., AHR, K. F., LITTMANN, E. R., LING, L., GOBOURNE, A. C., MILLER, L. C., DOCAMPO, M. D., PELED, J. U., ARPAIA, N., CROSS, J. R., PEETS, T. K., LUMISH, M. A., SHONO, Y., DUDAKOV, J. A., POECK, H., HANASH, A. M., BARKER, J. N., PERALES, M. A., GIRALT, S. A., PAMER, E. G. & VAN DEN BRINK, M. R. 2015. Intestinal Blautia Is Associated with Reduced Death from Graft-versus-Host Disease. *Biol Blood Marrow Transplant,* 21**,** 1373-83.

JIANG, H. Q., BOS, N. A. & CEBRA, J. J. 2001. Timing, Localization, and Persistence of Colonization by Segmented Filamentous Bacteria in the Neonatal Mouse Gut Depend on Immune Status of Mothers and Pups. *Infect Immun.*

JONES, E. A., KANANURAK, A., BEVINS, C. L., HOLLOX, E. J. & BAKALETZ, L. O. 2014. Copy number variation of the beta defensin gene cluster on chromosome 8p influences the bacterial microbiota within the nasopharynx of otitis-prone children. *PLoS One,* 9**,** e98269.

JONES, H. E., HARRIS, K. A., AZIZIA, M., BANK, L., CARPENTER, B., HARTLEY, J. C., KLEIN, N. & PEEBLES, D. 2009. Differing prevalence and diversity of bacterial species in fetal membranes from very preterm and term labor. *PLoS One,* 4**,** e8205.

KAI-LARSEN, Y., LUTHJE, P., CHROMEK, M., PETERS, V., WANG, X., HOLM, A., KADAS, L., HEDLUND, K. O., JOHANSSON, J., CHAPMAN, M. R., JACOBSON, S. H., ROMLING, U., AGERBERTH, B. & BRAUNER, A. 2010. Uropathogenic Escherichia coli modulates immune responses and its curli fimbriae interact with the antimicrobial peptide LL-37. *PLoS Pathog,* 6**,** e1001010.

KAUSHIC, C., ASHKAR, A. A., REID, L. A. & ROSENTHAL, K. L. 2003. Progesterone Increases Susceptibility and Decreases Immune Responses to Genital Herpes Infection. *J Virol.*

KAUSHIC, C., ZHOU, F., MURDIN, A. D. & WIRA, C. R. 2000. Effects of estradiol and progesterone on susceptibility and early immune responses to Chlamydia trachomatis infection in the female reproductive tract. *Infect Immun,* 68**,** 4207-16.

KIDA, Y., SHIMIZU, T. & KUWANO, K. 2006. Sodium butyrate up-regulates cathelicidin gene expression via activator protein-1 and histone acetylation at the promoter region in a human lung epithelial cell line, EBC-1. *Mol Immunol,* 43**,** 1972-81.

KIM, M., MORRISON, M. & YU, Z. 2011. Evaluation of different partial 16S rRNA gene sequence regions for phylogenetic analysis of microbiomes. *J Microbiol Methods,* 84**,** 81-7.

KIM, Y. M., ROMERO, R., CHAIWORAPONGSA, T., KIM, G. J., KIM, M. R., KUIVANIEMI, H., TROMP, G., ESPINOZA, J., BUJOLD, E., ABRAHAMS, V. M. & MOR, G. 2004. Toll-like receptor-2 and -4 in the chorioamniotic membranes in spontaneous labor at term and in preterm parturition that are associated with chorioamnionitis. *Am J Obstet Gynecol,* 191**,** 1346-55.

KINDINGER, L. M., MACINTYRE, D. A., LEE, Y. S., MARCHESI, J. R., SMITH, A., MCDONALD, J. A., TERZIDOU, V., COOK, J. R., LEES, C., ISRAFIL-BAYLI, F., FAIZA, Y., TOOZS-HOBSON, P., SLACK, M., CACCIATORE, S., HOLMES, E., NICHOLSON, J. K., TEOH, T. G. & BENNETT, P. R. 2016. Relationship between vaginal microbial

dysbiosis, inflammation, and pregnancy outcomes in cervical cerclage. *Sci Transl Med,* 8**,** 350ra102.

KING, A. E., CRITCHLEY, H. O. & KELLY, R. W. 2003a. Innate immune defences in the human endometrium. *Reprod Biol Endocrinol,* 1**,** 116.

KING, A. E., FLEMING, D. C., CRITCHLEY, H. O. D. & KELLY, R. W. 2003b. Differential expression of the natural antimicrobials, beta-defensins 3 and 4, in human endometrium. *Journal of reproductive immunology,* 59**,** 1-16.

KING, J. & FLENADY, V. 2002. Prophylactic antibiotics for inhibiting preterm labour with intact membranes. *Cochrane Database Syst Rev***,** CD000246.

KLINDWORTH, A., PRUESSE, E., SCHWEER, T., PEPLIES, J., QUAST, C., HORN, M. & GLÖCKNER, F. O. 2013. Evaluation of general 16S ribosomal RNA gene PCR primers for classical and next-generation sequencing-based diversity studies. *Nucleic Acids Research,* 41**,** e1-e1.

KOCSIS, A. K., LAKATOS, P. L., SOMOGYVARI, F., FUSZEK, P., PAPP, J., FISCHER, S., SZAMOSI, T., LAKATOS, L., KOVACS, A., HOFNER, P. & MANDI, Y. 2008. Association of beta-defensin 1 single nucleotide polymorphisms with Crohn's disease. *Scand J Gastroenterol,* 43**,** 299-307.

KOCZULLA, R., VON DEGENFELD, G., KUPATT, C., KROTZ, F., ZAHLER, S., GLOE, T., ISSBRUCKER, K., UNTERBERGER, P., ZAIOU, M., LEBHERZ, C., KARL, A., RAAKE, P., PFOSSER, A., BOEKSTEGERS, P., WELSCH, U., HIEMSTRA, P. S., VOGELMEIER, C., GALLO, R. L., CLAUSS, M. & BALS, R. 2003. An angiogenic role for the human peptide antibiotic LL-37/hCAP-18. *J Clin Invest,* 111**,** 1665-72.

KOON, H. W., SHIH, D. Q., CHEN, J., BAKIRTZI, K., HING, T. C., LAW, I., HO, S., ICHIKAWA, R., ZHAO, D., XU, H., GALLO, R., DEMPSEY, P., CHENG, G., TARGAN, S. R. & POTHOULAKIS, C. 2011. Cathelicidin signaling via the Toll-like receptor protects against colitis in mice. *Gastroenterology,* 141**,** 1852-63.e1-3.

KOREN, O., GOODRICH, J. K., CULLENDER, T. C., SPOR, A., LAITINEN, K., BÄCKHED, H. K., GONZALEZ, A., WERNER, J. J., ANGENENT, L. T., KNIGHT, R., BÄCKHED, F., ISOLAURI, E., SALMINEN, S. & LEY, R. E. 2012. Host remodeling of the gut microbiome and metabolic changes during pregnancy. *Cell,* 150**,** 470-80.

KOVACH, M. A., BALLINGER, M. N., NEWSTEAD, M. W., ZENG, X., BHAN, U., YU, F., MOORE, B. B., GALLO, R. L. & STANDIFORD, T. J. 2012. Cathelicidin Related Antimicrobial Peptide is Required for Effective Lung Mucosal Immunity in Gram-negative Bacterial Pneumonia. *J Immunol,* 189**,** 304-11.

KOVATCHEVA-DATCHARY, P., NILSSON, A., AKRAMI, R., LEE, Y. S., DE VADDER, F., ARORA, T., HALLEN, A., MARTENS, E., BJORCK, I. & BACKHED, F. 2015. Dietary Fiber-Induced Improvement in Glucose Metabolism Is Associated with Increased Abundance of Prevotella. *Cell Metab,* 22**,** 971-82.

KREUTER, A., JAOUHAR, M., SKRYGAN, M., TIGGES, C., STUCKER, M., ALTMEYER, P., GLASER, R. & GAMBICHLER, T. 2011. Expression of antimicrobial peptides in different subtypes of cutaneous lupus erythematosus. *J Am Acad Dermatol,* 65**,** 125-33.

KRUEGER, F., ANDREWS, S. R. & OSBORNE, C. S. 2011. Large scale loss of data in low-diversity illumina sequencing libraries can be recovered by deferred cluster calling. *PLoS One,* 6**,** e16607.

KUMAR, N., BEHERA, B., SAGIRI, S. S., PAL, K., RAY, S. S. & ROY, S. 2011. Bacterial vaginosis: Etiology and modalities of treatment—A brief note. *J Pharm Bioallied Sci.*

LAMBERT, J. A., JOHN, S., SOBEL, J. D. & AKINS, R. A. 2013. Longitudinal analysis of vaginal microbiome dynamics in women with recurrent bacterial vaginosis: recognition of the conversion process. *PLoS ONE,* 8**,** e82599-e82599.

LAMONT, R. F. 2015. Advances in the Prevention of Infection-Related Preterm Birth. *Front Immunol,* 6**,** 566.

LANDE, R., GANGULY, D., FACCHINETTI, V., FRASCA, L., CONRAD, C., GREGORIO, J., MELLER, S., CHAMILOS, G., SEBASIGARI, R., RICCIERI, V., BASSETT, R., AMURO, H., FUKUHARA, S., ITO, T., LIU, Y. J. & GILLIET, M. 2011. Neutrophils activate plasmacytoid dendritic cells by releasing self-DNA-peptide complexes in systemic lupus erythematosus. *Sci Transl Med,* 3**,** 73ra19.

LANGDON, A., CROOK, N. & DANTAS, G. 2016. The effects of antibiotics on the microbiome throughout development and alternative approaches for therapeutic modulation. *Genome Med,* 8**,** 39.

LANGILLE, M. G., MEEHAN, C. J., KOENIG, J. E., DHANANI, A. S., ROSE, R. A., HOWLETT, S. E. & BEIKO, R. G. 2014. Microbial shifts in the aging mouse gut. *Microbiome.*

LAPPAS, M., PERMEZEL, M. & RICE, G. E. 2003. N-Acetyl-cysteine inhibits phospholipid metabolism, proinflammatory cytokine release, protease activity, and nuclear factor-kappaB deoxyribonucleic acid-binding activity in human fetal membranes in vitro. *J Clin Endocrinol Metab,* 88**,** 1723-9.

LAPPAS, M. & RICE, G. E. 2009. Transcriptional regulation of the processes of human labour and delivery. *Placenta,* 30 Suppl A**,** S90-5.

LARKIN, M. A., BLACKSHIELDS, G., BROWN, N. P., CHENNA, R., MCGETTIGAN, P. A., MCWILLIAM, H., VALENTIN, F., WALLACE, I. M., WILM, A., LOPEZ, R., THOMPSON, J. D., GIBSON, T. J. & HIGGINS, D. G. 2007. Clustal W and Clustal X version 2.0. *Bioinformatics,* 23**,** 2947-8.

LAUKENS, D., BRINKMAN, B. M., RAES, J., DE VOS, M. & VANDENABEELE, P. 2016. Heterogeneity of the gut microbiome in mice: guidelines for optimizing experimental design. *FEMS Microbiol Rev,* 40**,** 117-32.

LAURENCE, M., HATZIS, C. & BRASH, D. E. 2014. Common contaminants in next-generation sequencing that hinder discovery of low-abundance microbes. *PLoS One,* 9**,** e97876.

LAVELLE, E. C., MURPHY, C., O'NEILL, L. A. & CREAGH, E. M. 2010. The role of TLRs, NLRs, and RLRs in mucosal innate immunity and homeostasis. *Mucosal Immunol,* 3**,** 17-28.

LAY, C., RIGOTTIER-GOIS, L., HOLMSTROM, K., RAJILIC, M., VAUGHAN, E. E., DE VOS, W. M., COLLINS, M. D., THIEL, R., NAMSOLLECK, P., BLAUT, M. & DORE, J. 2005. Colonic microbiota signatures across five northern European countries. *Appl Environ Microbiol,* 71**,** 4153-5.

LEE, C. C., SUN, Y., QIAN, S. & HUANG, H. 2011. Transmembrane Pores Formed by Human Antimicrobial Peptide LL-37. *Biophys J.*

LEE, J. K., CHANG, S. W., PERINPANAYAGAM, H., LIM, S. M., PARK, Y. J., HAN, S. H., BAEK, S. H., ZHU, Q., BAE, K. S. & KUM, K. Y. 2013. Antibacterial efficacy of a human beta-defensin-3 peptide on multispecies biofilms. *J Endod,* 39**,** 1625-9.

LEY, R. E., BACKHED, F., TURNBAUGH, P., LOZUPONE, C. A., KNIGHT, R. D. & GORDON, J. I. 2005. Obesity alters gut microbial ecology. *Proc Natl Acad Sci U S A,* 102**,** 11070-5.

LEY, R. E., TURNBAUGH, P. J., KLEIN, S. & GORDON, J. I. 2006. Microbial ecology: human gut microbes associated with obesity. *Nature,* 444**,** 1022-3.

LIGGINS, G. C. 1989. Initiation of labour. *Biol Neonate,* 55**,** 366-75.

LIM, J. H., KIM, M. H., HAN, Y. J., LEE, D. E., PARK, S. Y., HAN, J. Y., KIM, M. Y. & RYU, H. M. 2013. Cell-free fetal DNA and cell-free total DNA levels in spontaneous abortion with fetal chromosomal aneuploidy. *PLoS ONE,* 8**,** e56787-e56787.

LIM, R., BARKER, G. & LAPPAS, M. 2015. Human cathelicidin antimicrobial protein 18 (hCAP18/LL-37) is increased in foetal membranes and myometrium after spontaneous labour and delivery. *J Reprod Immunol,* 107**,** 31-42.

LINDSTRÖM, T. M. & BENNETT, P. R. 2005. The role of nuclear factor kappa B in human labour. *Reproduction (Cambridge, England),* 130**,** 569-81.

LINHARES, I. M., SUMMERS, P. R., LARSEN, B., GIRALDO, P. C. & WITKIN, S. S. 2011. Contemporary perspectives on vaginal pH and lactobacilli. *Am J Obstet Gynecol,* 204**,** 120.e1-5.

LIU, H., YU, H., GU, Y., XIN, A., ZHANG, Y., DIAO, H. & LIN, D. 2012. Human beta-defensin DEFB126 is capable of inhibiting LPS-mediated inflammation. *Applied microbiology and biotechnology*.

LIU, N., KAPLAN, A., LOW, J., NGUYEN, L., LIU, G., EQUILS, O. & HEWISON, M. 2009. Vitamin D Induces Innate Antibacterial Responses in Human Trophoblasts via an Intracrine Pathway1. *Biol Reprod,* 80**,** 398-406.

LOCKWOOD, C. J., ARCURI, F., TOTI, P., FELICE, C. D., KRIKUN, G., GULLER, S., BUCHWALDER, L. F. & SCHATZ, F. 2006. Tumor necrosis factor-alpha and interleukin-1beta regulate interleukin-8 expression in third trimester decidual cells: implications for the genesis of chorioamnionitis. *Am J Pathol,* 169**,** 1294-302.

LOZUPONE, C. & KNIGHT, R. 2005. UniFrac: a new phylogenetic method for comparing microbial communities. *Appl Environ Microbiol,* 71**,** 8228-35.

LOZUPONE, C. A., HAMADY, M., KELLEY, S. T. & KNIGHT, R. 2007. Quantitative and qualitative beta diversity measures lead to different insights into factors that structure microbial communities. *Appl Environ Microbiol,* 73**,** 1576-85.

MACINTYRE, D. A., CHANDIRAMANI, M., LEE, Y. S., KINDINGER, L., SMITH, A., ANGELOPOULOS, N., LEHNE, B., ARULKUMARAN, S., BROWN, R., TEOH, T. G., HOLMES, E., NICOHOLSON, J. K., MARCHESI, J. R. & BENNETT, P. R. 2015. The vaginal microbiome during pregnancy and the postpartum period in a European population. *Sci Rep,* 5**,** 8988.

MACINTYRE, D. A., LEE, Y. S., MIGALE, R., HERBERT, B. R., WADDINGTON, S. N., PEEBLES, D., HAGBERG, H., JOHNSON, M. R. & BENNETT, P. R. 2014. Activator protein 1 is a key terminal mediator of inflammation-induced preterm labor in mice. *Faseb j,* 28**,** 2358-68.

MACKLER, A. M., IEZZA, G., AKIN, M. R., MCMILLAN, P. & YELLON, S. M. 1999. Macrophage trafficking in the uterus and cervix precedes parturition in the mouse. *Biol Reprod,* 61**,** 879-83.

MACMANES, M. D. 2011. Promiscuity in mice is associated with increased vaginal bacterial diversity. *Naturwissenschaften,* 98**,** 951-60.

MACONES, G. A., PARRY, S., ELKOUSY, M., CLOTHIER, B., URAL, S. H. & STRAUSS, J. F., 3RD 2004. A polymorphism in the promoter region of TNF and bacterial vaginosis: preliminary evidence of gene-environment interaction in the etiology of spontaneous preterm birth. *Am J Obstet Gynecol,* 190**,** 1504-8; discussion 3A.

MAISETTA, G., BATONI, G., ESIN, S., RACO, G., BOTTAI, D., FAVILLI, F., FLORIO, W. & CAMPA, M. 2005. Susceptibility of Streptococcus mutans and Actinobacillus actinomycetemcomitans to bactericidal activity of human beta-defensin 3 in biological fluids. *Antimicrob Agents Chemother,* 49**,** 1245-8.

MARIAT, D., FIRMESSE, O., LEVENEZ, F., GUIMARAES, V., SOKOL, H., DORE, J., CORTHIER, G. & FURET, J. P. 2009. The Firmicutes/Bacteroidetes ratio of the human microbiota changes with age. *BMC Microbiol,* 9**,** 123.

MARTIN, D. H., ZOZAYA, M., LILLIS, R. A., MYERS, L., NSUAMI, M. J. & FERRIS, M. J. 2013. Unique vaginal microbiota that includes an unknown Mycoplasma-like organism is associated with Trichomonas vaginalis infection. *The Journal of infectious diseases,* 207**,** 1922-31.

MARTIN, J. A., OSTERMAN, M. J. & SUTTON, P. D. 2010. Are preterm births on the decline in the United States? Recent data from the National Vital Statistics System. *NCHS Data Brief***,** 1-8.

MARTIN, M. 2011. Cutadapt removes adapter sequences from high-throughput sequencing reads. *17*.

MARTINEAU, A. R., WILKINSON, K. A., NEWTON, S. M., FLOTO, R. A., NORMAN, A. W., SKOLIMOWSKA, K., DAVIDSON, R. N., SORENSEN, O. E., KAMPMANN, B., GRIFFITHS, C. J. & WILKINSON, R. J. 2007. IFN-gamma- and TNF-independent vitamin D-inducible human suppression of mycobacteria: the role of cathelicidin LL-37. *J Immunol,* 178**,** 7190-8.

MARTINEZ, R. C., FRANCESCHINI, S. A., PATTA, M. C., QUINTANA, S. M., GOMES, B. C., DE MARTINIS, E. C. & REID, G. 2009. Improved cure of bacterial vaginosis with single dose of tinidazole (2 g), Lactobacillus rhamnosus GR-1, and Lactobacillus reuteri RC-14: a randomized, double-blind, placebo-controlled trial. *Can J Microbiol,* 55**,** 133-8.

MCGRORY, T. & GARBER, G. E. 1992. Mouse intravaginal infection with Trichomonas vaginalis and role of Lactobacillus acidophilus in sustaining infection. *Infection and immunity,* 60**,** 2375-9.

MCLEAN, A. C., VALENZUELA, N., FAI, S. & BENNETT, S. A. 2012. Performing Vaginal Lavage, Crystal Violet Staining, and Vaginal Cytological Evaluation for Mouse Estrous Cycle Staging Identification. *J Vis Exp*.

MCMURDIE, P. J. & HOLMES, S. 2013. phyloseq: an R package for reproducible interactive analysis and graphics of microbiome census data. *PLoS One,* 8**,** e61217.

MCMURDIE, P. J. & HOLMES, S. 2014. Waste not, want not: why rarefying microbiome data is inadmissible. *PLoS Comput Biol,* 10**,** e1003531.

MEEHAN, C. J. & BEIKO, R. G. 2014. A phylogenomic view of ecological specialization in the Lachnospiraceae, a family of digestive tract-associated bacteria. *Genome Biol Evol,* 6**,** 703-13.

MEIS, P. J., KLEBANOFF, M., THOM, E., DOMBROWSKI, M. P., SIBAI, B., MOAWAD, A. H., SPONG, C. Y., HAUTH, J. C., MIODOVNIK, M., VARNER, M. W., LEVENO, K. J., CARITIS, S. N., IAMS, J. D., WAPNER, R. J., CONWAY, D., O'SULLIVAN, M. J., CARPENTER, M., MERCER, B., RAMIN, S. M., THORP, J. M., PEACEMAN, A. M. & GABBE, S. 2003. Prevention of recurrent preterm delivery by 17 alpha-hydroxyprogesterone caproate. *N Engl J Med,* 348**,** 2379-85.

MENARD, J. P. 2011. Antibacterial treatment of bacterial vaginosis: current and emerging therapies. *Int J Womens Health,* 3**,** 295-305.

MENDELSON, C. R. & CONDON, J. C. 2005. New insights into the molecular endocrinology of parturition. *J Steroid Biochem Mol Biol,* 93**,** 113-9.

MESIANO, S., CHAN, E. C., FITTER, J. T., KWEK, K., YEO, G. & SMITH, R. 2002. Progesterone withdrawal and estrogen activation in human parturition are coordinated by progesterone receptor A expression in the myometrium. *J Clin Endocrinol Metab,* 87**,** 2924-30.

MEYSICK, K. C. & GARBER, G. E. 1992. Interactions between Trichomonas vaginalis and vaginal flora in a mouse model. *The Journal of parasitology,* 78**,** 157-60.

MIDORIKAWA, K., OUHARA, K., KOMATSUZAWA, H., KAWAI, T., YAMADA, S., FUJIWARA, T., YAMAZAKI, K., SAYAMA, K., TAUBMAN, M. A., KURIHARA, H., HASHIMOTO, K. & SUGAI, M. 2003. Staphylococcus aureus Susceptibility to Innate Antimicrobial Peptides, β-Defensins and CAP18, Expressed by Human Keratinocytes. *Infect Immun.*

MIGALE, R., HERBERT, B. R., LEE, Y. S., SYKES, L., WADDINGTON, S. N., PEEBLES, D., HAGBERG, H., JOHNSON, M. R., BENNETT, P. R. & MACINTYRE, D. A. 2015. Specific Lipopolysaccharide Serotypes Induce Differential Maternal and Neonatal

Inflammatory Responses in a Murine Model of Preterm Labor. *Am J Pathol,* 185**,** 2390-401.

MIGALE, R., MACINTYRE, D. A., CACCIATORE, S., LEE, Y. S., HAGBERG, H., HERBERT, B. R., JOHNSON, M. R., PEEBLES, D., WADDINGTON, S. N. & BENNETT, P. R. 2016. Modeling hormonal and inflammatory contributions to preterm and term labor using uterine temporal transcriptomics. *BMC Med,* 14**,** 86.

MILANI, C., HEVIA, A., FORONI, E., DURANTI, S., TURRONI, F., LUGLI, G. A., SANCHEZ, B., MARTÍN, R., GUEIMONDE, M., VAN SINDEREN, D., MARGOLLES, A. & VENTURA, M. 2013. Assessing the Fecal Microbiota: An Optimized Ion Torrent 16S rRNA Gene-Based Analysis Protocol. *PLoS ONE,* 8**,** e68739-e68739.

MIRMONSEF, P., ZARIFFARD, M. R., GILBERT, D., MAKINDE, H., LANDAY, A. L. & SPEAR, G. T. 2012. Short-chain fatty acids induce pro-inflammatory cytokine production alone and in combination with toll-like receptor ligands. *Am J Reprod Immunol,* 67**,** 391-400.

MISHRA, B., GOLLA, R. M., LAU, K., LUSHNIKOVA, T. & WANG, G. 2016. Anti-Staphylococcal Biofilm Effects of Human Cathelicidin Peptides. *ACS Med Chem Lett,* 7**,** 117-21.

MITCHELL, C., GOTTSCH, M. L., LIU, C., FREDRICKS, D. N. & NELSON, D. B. 2013. Associations between vaginal bacteria and levels of vaginal defensins in pregnant women. *American journal of obstetrics and gynecology,* 208**,** 132.e1-7.

MITRA, A., SKRZYPCZAK, M., GINALSKI, K. & ROWICKA, M. 2015. Strategies for achieving high sequencing accuracy for low diversity samples and avoiding sample bleeding using illumina platform. *PLoS One,* 10**,** e0120520.

MOGENSEN, T. H. 2009. Pathogen Recognition and Inflammatory Signaling in Innate Immune Defenses. *Clin Microbiol Rev.*

MONTREEKACHON, P., CHOTJUMLONG, P., BOLSCHER, J. G., NAZMI, K., REUTRAKUL, V. & KRISANAPRAKORNKIT, S. 2011. Involvement of P2X(7) purinergic receptor and MEK1/2 in interleukin-8 up-regulation by LL-37 in human gingival fibroblasts. *J Periodontal Res,* 46**,** 327-37.

MOOKHERJEE, N., BROWN, K. L., BOWDISH, D. M. E., DORIA, S., FALSAFI, R., HOKAMP, K., ROCHE, F. M., MU, R., DOHO, G. H., PISTOLIC, J., POWERS, J.-P., BRYAN, J., BRINKMAN, F. S. L. & HANCOCK, R. E. W. 2006. Modulation of the TLR-mediated inflammatory response by the endogenous human host defense peptide LL-37. *Journal of immunology (Baltimore, Md. : 1950),* 176**,** 2455-64.

MOOKHERJEE, N., LIPPERT, D. N., HAMILL, P., FALSAFI, R., NIJNIK, A., KINDRACHUK, J., PISTOLIC, J., GARDY, J., MIRI, P., NASEER, M., FOSTER, L. J. & HANCOCK, R. E. 2009. Intracellular receptor for human host defense peptide LL-37 in monocytes. *J Immunol,* 183**,** 2688-96.

MORGAN, X. C., SEGATA, N. & HUTTENHOWER, C. 2013. Biodiversity and functional genomics in the human microbiome. *Trends Genet,* 29**,** 51-8.

MORRISON, G., KILANOWSKI, F., DAVIDSON, D. & DORIN, J. 2002. Characterization of the mouse beta defensin 1, Defb1, mutant mouse model. *Infection and immunity,* 70**,** 3053-60.

MOSER, C., WEINER, D. J., LYSENKO, E., BALS, R., WEISER, J. N. & WILSON, J. M. 2002. beta-Defensin 1 contributes to pulmonary innate immunity in mice. *Infect Immun,* 70**,** 3068-72.

MUHLEISEN, A. L. & HERBST-KRALOVETZ, M. M. 2016. Menopause and the vaginal microbiome. *Maturitas,* 91**,** 42-50.

MURAKAMI, M., LOPEZ-GARCIA, B., BRAFF, M., DORSCHNER, R. A. & GALLO, R. L. 2004. Postsecretory processing generates multiple cathelicidins for enhanced topical antimicrobial defense. *J Immunol,* 172**,** 3070-7.

NAGALINGAM, N. A., KAO, J. Y. & YOUNG, V. B. 2011. Microbial ecology of the murine gut associated with the development of DSS- colitis. *Inflamm Bowel Dis,* 17**,** 917-26.

NAGAOKA, I., TAMURA, H. & HIRATA, M. 2006. An antimicrobial cathelicidin peptide, human CAP18/LL-37, suppresses neutrophil apoptosis via the activation of formyl-peptide receptor-like 1 and P2X7. *J Immunol,* 176**,** 3044-52.

NAKADA, E., NAKADA, T. A., WALLEY, K. R., MCCONECHY, M., MCLAUGHLIN, L., VON DADELSZEN, P., SHOZU, M. & BOYD, J. H. 2011. mRNA induces RANTES production in trophoblast cells via TLR3 only when delivered intracellularly using lipid membrane encapsulation. *Placenta,* 32**,** 500-5.

NASU, K. & NARAHARA, H. 2010. Pattern recognition via the toll-like receptor system in the human female genital tract. *Mediators Inflamm,* 2010**,** 976024.

NELSON, D. B. & MACONES, G. 2002. Bacterial vaginosis in pregnancy: current findings and future directions. *Epidemiol Rev,* 24**,** 102-8.

NESS, R. B., HILLIER, S., RICHTER, H. E., SOPER, D. E., STAMM, C., BASS, D. C., SWEET, R. L. & RICE, P. 2003. Can known risk factors explain racial differences in the occurrence of bacterial vaginosis? *J Natl Med Assoc,* 95**,** 201-12.

NEUMANN, A., BERENDS, E. T., NERLICH, A., MOLHOEK, E. M., GALLO, R. L., MEERLOO, T., NIZET, V., NAIM, H. Y. & VON KOCKRITZ-BLICKWEDE, M. 2014. The antimicrobial peptide LL-37 facilitates the formation of neutrophil extracellular traps. *Biochem J,* 464**,** 3-11.

NHAN-CHANG, C. L., ROMERO, R., TARCA, A. L., MITTAL, P., KUSANOVIC, J. P., EREZ, O., MAZAKI-TOVI, S., CHAIWORAPONGSA, T., HOTRA, J., THAN, N. G., KIM, J. S., HASSAN, S. S. & KIM, C. J. 2010. Characterization of the transcriptome of chorioamniotic membranes at the site of rupture in spontaneous labor at term. *Am J Obstet Gynecol,* 202**,** 462 e1-41.

NIYONSABA, F., IWABUCHI, K., MATSUDA, H., OGAWA, H. & NAGAOKA, I. 2002. Epithelial cell-derived human beta-defensin-2 acts as a chemotaxin for mast cells through a pertussis toxin-sensitive and phospholipase C-dependent pathway. *Int Immunol,* 14**,** 421-6.

NIYONSABA, F., SOMEYA, A., HIRATA, M., OGAWA, H. & NAGAOKA, I. 2001. Evaluation of the effects of peptide antibiotics human beta-defensins-1/-2 and LL-37 on histamine release and prostaglandin D(2) production from mast cells. *Eur J Immunol,* 31**,** 1066-75.

NIYONSABA, F., USHIO, H., HARA, M., YOKOI, H., TOMINAGA, M., TAKAMORI, K., KAJIWARA, N., SAITO, H., NAGAOKA, I., OGAWA, H. & OKUMURA, K. 2010. Antimicrobial peptides human beta-defensins and cathelicidin LL-37 induce the secretion of a pruritogenic cytokine IL-31 by human mast cells. *J Immunol,* 184**,** 3526-34.

NIYONSABA, F., USHIO, H., NAKANO, N., NG, W., SAYAMA, K., HASHIMOTO, K., NAGAOKA, I., OKUMURA, K. & OGAWA, H. 2007. Antimicrobial peptides human beta-defensins stimulate epidermal keratinocyte migration, proliferation and production of proinflammatory cytokines and chemokines. *J Invest Dermatol,* 127**,** 594-604.

NIZET, V., OHTAKE, T., LAUTH, X., TROWBRIDGE, J., RUDISILL, J., DORSCHNER, R. A., PESTONJAMASP, V., PIRAINO, J., HUTTNER, K. & GALLO, R. L. 2001. Innate antimicrobial peptide protects the skin from invasive bacterial infection. *Nature,* 414**,** 454-7.

NOGUCHI, K., TSUKUMI, K. & URANO, T. 2003. Qualitative and quantitative differences in normal vaginal flora of conventionally reared mice, rats, hamsters, rabbits, and dogs. *Comparative medicine,* 53**,** 404-12.

NORMAN, J. E., MACKENZIE, F., OWEN, P., MACTIER, H., HANRETTY, K., COOPER, S., CALDER, A., MIRES, G., DANIELIAN, P., STURGISS, S., MACLENNAN, G., TYDEMAN, G., THORNTON, S., MARTIN, B., THORNTON, J. G., NEILSON, J. P. & NORRIE, J. 2009a. Progesterone for the prevention of preterm birth in twin pregnancy

(STOPPIT): a randomised, double-blind, placebo-controlled study and meta-analysis. *Lancet,* 373**,** 2034-40.

NORMAN, J. E., MARLOW, N., MESSOW, C. M., SHENNAN, A., BENNETT, P. R., THORNTON, S., ROBSON, S. C., MCCONNACHIE, A., PETROU, S., SEBIRE, N. J., LAVENDER, T., WHYTE, S. & NORRIE, J. 2016. Vaginal progesterone prophylaxis for preterm birth (the OPPTIMUM study): a multicentre, randomised, double-blind trial. *Lancet,* 387**,** 2106-16.

NORMAN, J. E., MORRIS, C. & CHALMERS, J. 2009b. The effect of changing patterns of obstetric care in Scotland (1980-2004) on rates of preterm birth and its neonatal consequences: perinatal database study. *PLoS Med,* 6**,** e1000153.

NORWITZ, E. R. & CAUGHEY, A. B. 2011. Progesterone Supplementation and the Prevention of Preterm Birth. *Rev Obstet Gynecol,* 4**,** 60-72.

NOSSA, C. W. 2010. Design of 16S rRNA gene primers for 454 pyrosequencing of the human foregut microbiome. *World Journal of Gastroenterology,* 16**,** 4135-4135.

O'NEIL, D. A., PORTER, E. M., ELEWAUT, D., ANDERSON, G. M., ECKMANN, L., GANZ, T. & KAGNOFF, M. F. 1999. Expression and regulation of the human beta-defensins hBD-1 and hBD-2 in intestinal epithelium. *J Immunol,* 163**,** 6718-24.

OPPENHEIM, J. J. & YANG, D. 2005. Alarmins: chemotactic activators of immune responses. *Curr Opin Immunol,* 17**,** 359-65.

OREN, Z., LERMAN, J. C., GUDMUNDSSON, G. H., AGERBERTH, B. & SHAI, Y. 1999. Structure and organization of the human antimicrobial peptide LL-37 in phospholipid membranes: relevance to the molecular basis for its non-cell-selective activity. *Biochem J,* 341**,** 501-13.

OSMAN, I., YOUNG, A., LEDINGHAM, M. A., THOMSON, A. J., JORDAN, F., GREER, I. A. & NORMAN, J. E. 2003. Leukocyte density and pro-inflammatory cytokine expression in human fetal membranes, decidua, cervix and myometrium before and during labour at term. *Mol Hum Reprod,* 9**,** 41-5.

OVERHAGE, J., CAMPISANO, A., BAINS, M., TORFS, E. C., REHM, B. H. & HANCOCK, R. E. 2008. Human host defense peptide LL-37 prevents bacterial biofilm formation. *Infect Immun,* 76**,** 4176-82.

PATIL, A., HUGHES, A. L. & ZHANG, G. 2004. Rapid evolution and diversification of mammalian alpha-defensins as revealed by comparative analysis of rodent and primate genes. *Physiological genomics,* 20**,** 1-11.

PATIL, A. A., CAI, Y., SANG, Y., BLECHA, F. & ZHANG, G. 2005. Cross-species analysis of the mammalian beta-defensin gene family: presence of syntenic gene clusters and preferential expression in the male reproductive tract. *Physiological genomics,* 23**,** 5-17.

PAULSEN, F., PUFE, T., CONRADI, L., VAROGA, D., TSOKOS, M., PAPENDIECK, J. & PETERSEN, W. 2002. Antimicrobial peptides are expressed and produced in healthy and inflamed human synovial membranes. *J Pathol,* 198**,** 369-77.

PAWELCZYK, E., NOWICKI, B. J., IZBAN, M. G., PRATAP, S., SASHTI, N. A., SANDERSON, M. & NOWICKI, S. 2010. Spontaneous preterm labor is associated with an increase in the proinflammatory signal transducer TLR4 receptor on maternal blood monocytes. *BMC pregnancy and childbirth,* 10**,** 66-66.

PETERSON, J., GARGES, S., GIOVANNI, M., MCINNES, P., WANG, L., SCHLOSS, J. A., BONAZZI, V., MCEWEN, J. E., WETTERSTRAND, K. A., DEAL, C., BAKER, C. C., DI FRANCESCO, V., HOWCROFT, T. K., KARP, R. W., LUNSFORD, R. D., WELLINGTON, C. R., BELACHEW, T., WRIGHT, M., GIBLIN, C., DAVID, H., MILLS, M., SALOMON, R., MULLINS, C., AKOLKAR, B., BEGG, L., DAVIS, C., GRANDISON, L., HUMBLE, M., KHALSA, J., LITTLE, A. R., PEAVY, H., PONTZER, C., PORTNOY, M., SAYRE, M. H., STARKE-REED, P., ZAKHARI, S., READ, J., WATSON, B. & GUYER, M. 2009. The NIH Human Microbiome Project. *Genome Res,* 19**,** 2317-23.

PIEBER, D., ALLPORT, V. C., HILLS, F., JOHNSON, M. & BENNETT, P. R. 2001. Interactions between progesterone receptor isoforms in myometrial cells in human labour. *Mol Hum Reprod,* 7**,** 875-9.

PINHEIRO DA SILVA, F., GALLO, R. L. & NIZET, V. 2009. Differing effects of exogenous or endogenous cathelicidin on macrophage toll-like receptor signaling. *Immunol Cell Biol,* 87**,** 496-500.

PIOLI, P. A., AMIEL, E., SCHAEFER, T. M., CONNOLLY, J. E., WIRA, C. R. & GUYRE, P. M. 2004. Differential expression of Toll-like receptors 2 and 4 in tissues of the human female reproductive tract. *Infect Immun,* 72**,** 5799-806.

PISTOLIC, J., COSSEAU, C., LI, Y., YU, J. J., FILEWOD, N. C., GELLATLY, S., REHAUME, L. M., BOWDISH, D. M. & HANCOCK, R. E. 2009. Host defence peptide LL-37 induces IL-6 expression in human bronchial epithelial cells by activation of the NF-kappaB signaling pathway. *J Innate Immun,* 1**,** 254-67.

POUND, L. D., PATRICK, C., EBERHARD, C. E., MOTTAWEA, W., WANG, G. S., ABUJAMEL, T., VANDENBEEK, R., STINTZI, A. & SCOTT, F. W. 2015. Cathelicidin Antimicrobial Peptide: A Novel Regulator of Islet Function, Islet Regeneration, and Selected Gut Bacteria. *Diabetes,* 64**,** 4135-47.

PRICE, M. N., DEHAL, P. S. & ARKIN, A. P. 2010. FastTree 2 – Approximately Maximum-Likelihood Trees for Large Alignments. *PLoS One.*

PRINCE, A. L., MA, J., KANNAN, P. S., ALVAREZ, M., GISSLEN, T., HARRIS, R. A., SWEENEY, E. L., KNOX, C. L., LAMBERS, D. S., JOBE, A. H., CHOUGNET, C. A., KALLAPUR, S. G. & AAGAARD, K. M. 2016. The placental membrane microbiome is altered among subjects with spontaneous preterm birth with and without chorioamnionitis. *Am J Obstet Gynecol,* 214**,** 627.e1-627.e16.

PUTSEP, K., CARLSSON, G., BOMAN, H. G. & ANDERSSON, M. 2002. Deficiency of antibacterial peptides in patients with morbus Kostmann: an observation study. *Lancet,* 360**,** 1144-9.

QUAST, C., PRUESSE, E., YILMAZ, P., GERKEN, J., SCHWEER, T., YARZA, P., PEPLIES, J. & GLÖCKNER, F. O. 2013. The SILVA ribosomal RNA gene database project: improved data processing and web-based tools. *Nucleic Acids Res.*

QUAYLE, A. J., PORTER, E. M., NUSSBAUM, A. A., WANG, Y. M., BRABEC, C., YIP, K. P. & MOK, S. C. 1998. Gene expression, immunolocalization, and secretion of human defensin-5 in human female reproductive tract. *The American journal of pathology,* 152**,** 1247-58.

RACICOT, K., CARDENAS, I., WÜNSCHE, V., ALDO, P., GULLER, S., MEANS, R. E., ROMERO, R. & MOR, G. 2013. Viral infection of the pregnant cervix predisposes to ascending bacterial infection. *Journal of immunology (Baltimore, Md. : 1950),* 191**,** 934-41.

RAJPAL, D. K., KLEIN, J. L., MAYHEW, D., BOUCHERON, J., SPIVAK, A. T., KUMAR, V., INGRAHAM, K., PAULIK, M., CHEN, L., VAN HORN, S., THOMAS, E., SATHE, G., LIVI, G. P., HOLMES, D. J. & BROWN, J. R. 2015. Selective Spectrum Antibiotic Modulation of the Gut Microbiome in Obesity and Diabetes Rodent Models. *PLoS One,* 10**,** e0145499.

RAPALA-KOZIK, M., BOCHENSKA, O., ZAWROTNIAK, M., WOLAK, N., TREBACZ, G., GOGOL, M., OSTROWSKA, D., AOKI, W., UEDA, M. & KOZIK, A. 2015. Inactivation of the Antifungal and Immunomodulatory Properties of Human Cathelicidin LL-37 by Aspartic Proteases Produced by the Pathogenic Yeast Candida albicans. *Infect Immun.*

RAVEL, J., GAJER, P., ABDO, Z., SCHNEIDER, G. M., KOENIG, S. S. K., MCCULLE, S. L., KARLEBACH, S., GORLE, R., RUSSELL, J., TACKET, C. O., BROTMAN, R. M., DAVIS, C. C., AULT, K., PERALTA, L. & FORNEY, L. J. 2011. Vaginal microbiome of reproductive-age women. *Proceedings of the National Academy of Sciences of the United States of America,* 108 Suppl**,** 4680-7.

RAVEL, J., GAJER, P., FU, L., MAUCK, C. K., KOENIG, S. S. K., SAKAMOTO, J., MOTSINGER-REIF, A. A., DONCEL, G. F. & ZEICHNER, S. L. 2012. Twice-daily application of HIV microbicides alter the vaginal microbiota. *mBio,* 3**,** 1-8.

RAVUSSIN, Y., KOREN, O., SPOR, A., LEDUC, C., GUTMAN, R., STOMBAUGH, J., KNIGHT, R., LEY, R. E. & LEIBEL, R. L. 2012. Responses of Gut Microbiota to Diet Composition and Weight Loss in Lean and Obese Mice. *Obesity (Silver Spring),* 20.

REID, G. & BURTON, J. 2002. Use of Lactobacillus to prevent infection by pathogenic bacteria. *Microbes and infection / Institut Pasteur,* 4**,** 319-24.

REINHOLZ, M., RUZICKA, T. & SCHAUBER, J. 2012. Cathelicidin LL-37: an antimicrobial peptide with a role in inflammatory skin disease. *Ann Dermatol,* 24**,** 126-35.

RESI, V., BASU, S., HAGHIAC, M., PRESLEY, L., MINIUM, J., KAUFMAN, B., BERNARD, S., CATALANO, P. & HAUGUEL-DE MOUZON, S. 2012. Molecular inflammation and adipose tissue matrix remodeling precede physiological adaptations to pregnancy. *Am J Physiol Endocrinol Metab.*

REZNIKOV, L. L., FANTUZZI, G., SELZMAN, C. H., SHAMES, B. D., BARTON, H. A., BELL, H., MCGREGOR, J. A. & DINARELLO, C. A. 1999. Utilization of endoscopic inoculation in a mouse model of intrauterine infection-induced preterm birth: role of interleukin 1beta. *Biology of reproduction,* 60**,** 1231-8.

RINALDI, S. F., CATALANO, R. D., WADE, J., ROSSI, A. G. & NORMAN, J. E. 2014. Decidual neutrophil infiltration is not required for preterm birth in a mouse model of infection-induced preterm labor. *J Immunol,* 192**,** 2315-25.

RINALDI, S. F., MAKIEVA, S., FREW, L., WADE, J., THOMSON, A. J., MORAN, C. M., NORMAN, J. E. & STOCK, S. J. 2015. Ultrasound-guided intrauterine injection of lipopolysaccharide as a novel model of preterm birth in the mouse. *Am J Pathol,* 185**,** 1201-6.

ROHRL, J., YANG, D., OPPENHEIM, J. J. & HEHLGANS, T. 2008. Identification and Biological Characterization of Mouse beta-defensin 14, the orthologue of human beta-defensin 3. *J Biol Chem,* 283**,** 5414-9.

ROHRL, J., YANG, D., OPPENHEIM, J. J. & HEHLGANS, T. 2010. Specific binding and chemotactic activity of mBD4 and its functional orthologue hBD2 to CCR6-expressing cells. *J Biol Chem,* 285**,** 7028-34.

ROMERO, R., ESPINOZA, J., GONCALVES, L. F., KUSANOVIC, J. P., FRIEL, L. & HASSAN, S. 2007. The role of inflammation and infection in preterm birth. *Semin Reprod Med,* 25**,** 21-39.

ROMERO, R., ESPINOZA, J., GONCALVES, L. F., KUSANOVIC, J. P., FRIEL, L. A. & NIEN, J. K. 2006. Inflammation in preterm and term labour and delivery. *Semin Fetal Neonatal Med,* 11**,** 317-26.

ROMERO, R., HASSAN, S. S., GAJER, P., TARCA, A. L., FADROSH, D. W., NIKITA, L., GALUPPI, M., LAMONT, R. F., CHAEMSAITHONG, P., MIRANDA, J., CHAIWORAPONGSA, T. & RAVEL, J. 2014. The composition and stability of the vaginal microbiota of normal pregnant women is different from that of non-pregnant women. *Microbiome,* 2**,** 4.

ROSENFELD, Y., PAPO, N. & SHAI, Y. 2006. Endotoxin (lipopolysaccharide) neutralization by innate immunity host-defense peptides. Peptide properties and plausible modes of action. *J Biol Chem,* 281**,** 1636-43.

ROUSE, D. J., CARITIS, S. N., PEACEMAN, A. M., SCISCIONE, A., THOM, E. A., SPONG, C. Y., VARNER, M., MALONE, F., IAMS, J. D., MERCER, B. M., THORP, J., SOROKIN, Y., CARPENTER, M., LO, J., RAMIN, S., HARPER, M. & ANDERSON, G. 2007. A trial of 17 alpha-hydroxyprogesterone caproate to prevent prematurity in twins. *N Engl J Med,* 357**,** 454-61.

ROYSE, K. E., KEMPF, M. C., MCGWIN, G., WILSON, C. M., TANG, J. & SHRESTHA, S. 2012. Toll-Like Receptor Gene Variants Associated with Bacterial Vaginosis among HIV-1 Infected Adolescents. *J Reprod Immunol,* 96**,** 84-9.

SAHL, H. G., PAG, U., BONNESS, S., WAGNER, S., ANTCHEVA, N. & TOSSI, A. 2005. Mammalian defensins: structures and mechanism of antibiotic activity. *J Leukoc Biol,* 77**,** 466-75.

SALMINEN, A., PAANANEN, R., VUOLTEENAHO, R., METSOLA, J., OJANIEMI, M., AUTIO-HARMAINEN, H. & HALLMAN, M. 2008. Maternal endotoxin-induced preterm birth in mice: fetal responses in toll-like receptors, collectins, and cytokines. *Pediatric research,* 63**,** 280-6.

SALTER, S. J., COX, M. J., TUREK, E. M., CALUS, S. T., COOKSON, W. O., MOFFATT, M. F., TURNER, P., PARKHILL, J., LOMAN, N. J. & WALKER, A. W. 2014. Reagent and laboratory contamination can critically impact sequence-based microbiome analyses. *BMC Biol,* 12**,** 87.

SALVADO, M. D., DI GENNARO, A., LINDBOM, L., AGERBERTH, B. & HAEGGSTROM, J. Z. 2013. Cathelicidin LL-37 induces angiogenesis via PGE2-EP3 signaling in endothelial cells, in vivo inhibition by aspirin. *Arterioscler Thromb Vasc Biol,* 33**,** 1965-72.

SALZMAN, N. H., DE JONG, H., PATERSON, Y., HARMSEN, H. J., WELLING, G. W. & BOS, N. A. 2002a. Analysis of 16S libraries of mouse gastrointestinal microflora reveals a large new group of mouse intestinal bacteria. *Microbiology,* 148**,** 3651-60.

SALZMAN, N. H., DE JONG, H., PATERSON, Y., HARMSEN, H. J. M., WELLING, G. W. & BOS, N. A. 2002b. Analysis of 16S libraries of mouse gastrointestinal microflora reveals a large new group of mouse intestinal bacteria. *Microbiology (Reading, England),* 148**,** 3651-60.

SALZMAN, N. H., GHOSH, D. & HUTTNER, K. M. 2003. Protection against enteric salmonellosis in transgenic mice expressing a human intestinal defensin. 422.

SALZMAN, N. H., HUNG, K., HARIBHAI, D., CHU, H., KARLSSON-SJÖBERG, J., AMIR, E., TEGGATZ, P., BARMAN, M., HAYWARD, M., EASTWOOD, D., STOEL, M., ZHOU, Y., SODERGREN, E., WEINSTOCK, G. M., BEVINS, C. L., WILLIAMS, C. B. & BOS, N. A. 2010. Enteric defensins are essential regulators of intestinal microbial ecology. *Nature immunology,* 11**,** 76-83.

SALZMAN, N. H., UNDERWOOD, M. A. & BEVINS, C. L. 2007. Paneth cells, defensins, and the commensal microbiota: a hypothesis on intimate interplay at the intestinal mucosa. *Seminars in immunology,* 19**,** 70-83.

SATO, T., MICHIZU, H., HASHIZUME, K. & ITO, A. 2001. Hormonal regulation of PGE2 and COX-2 production in rabbit uterine cervical fibroblasts. *Journal of applied physiology (Bethesda, Md. : 1985),* 90**,** 1227-31.

SCHAUBER, J., RIEGER, D., WEILER, F., WEHKAMP, J., ECK, M., FELLERMANN, K., SCHEPPACH, W., GALLO, R. L. & STANGE, E. F. 2006. Heterogeneous expression of human cathelicidin hCAP18/LL-37 in inflammatory bowel diseases. *Eur J Gastroenterol Hepatol,* 18**,** 615-21.

SCHER, J. U., SCZESNAK, A., LONGMAN, R. S., SEGATA, N., UBEDA, C., BIELSKI, C., ROSTRON, T., CERUNDOLO, V., PAMER, E. G., ABRAMSON, S. B., HUTTENHOWER, C. & LITTMAN, D. R. 2013. Expansion of intestinal Prevotella copri correlates with enhanced susceptibility to arthritis. *Elife,* 2**,** e01202.

SCHLOSS, P. D., GEVERS, D. & WESTCOTT, S. L. 2011. Reducing the effects of PCR amplification and sequencing artifacts on 16S rRNA-based studies. *PLoS One,* 6**,** e27310.

SCHLOSS, P. D., WESTCOTT, S. L., RYABIN, T., HALL, J. R., HARTMANN, M., HOLLISTER, E. B., LESNIEWSKI, R. A., OAKLEY, B. B., PARKS, D. H., ROBINSON, C. J., SAHL, J. W., STRES, B., THALLINGER, G. G., VAN HORN, D. J. & WEBER, C.

F. 2009. Introducing mothur: Open-Source, Platform-Independent, Community-Supported Software for Describing and Comparing Microbial Communities▽. *Appl Environ Microbiol.*

SCHROEDER, B. O., WU, Z., NUDING, S., GROSCURTH, S., MARCINOWSKI, M., BEISNER, J., BUCHNER, J., SCHALLER, M., STANGE, E. F. & WEHKAMP, J. 2011. Reduction of disulphide bonds unmasks potent antimicrobial activity of human β-defensin 1. *Nature,* 469**,** 419-23.

SCHUTTE, B. C., MITROS, J. P., BARTLETT, J. A., WALTERS, J. D., JIA, H. P., WELSH, M. J., CASAVANT, T. L. & MCCRAY, P. B. 2002. Discovery of five conserved β-defensin gene clusters using a computational search strategy. *Proc Natl Acad Sci U S A.*

SCHWARZER, M., MAKKI, K., STORELLI, G., MACHUCA-GAYET, I., SRUTKOVA, D., HERMANOVA, P., MARTINO, M. E., BALMAND, S., HUDCOVIC, T., HEDDI, A., RIEUSSET, J., KOZAKOVA, H., VIDAL, H. & LEULIER, F. 2016. Lactobacillus plantarum strain maintains growth of infant mice during chronic undernutrition. *Science,* 351**,** 854-7.

SCOTT, A., WELDON, S., BUCHANAN, P. J., SCHOCK, B., ERNST, R. K., MCAULEY, D. F., TUNNEY, M. M., IRWIN, C. R., ELBORN, J. S. & TAGGART, C. C. 2011. Evaluation of the ability of LL-37 to neutralise LPS in vitro and ex vivo. *PLoS One,* 6**,** e26525.

SCOTT, M. G., DAVIDSON, D. J., GOLD, M. R., BOWDISH, D. & HANCOCK, R. E. 2002. The human antimicrobial peptide LL-37 is a multifunctional modulator of innate immune responses. *J Immunol,* 169**,** 3883-91.

SCOTT, M. G., VREUGDENHIL, A. C., BUURMAN, W. A., HANCOCK, R. E. & GOLD, M. R. 2000. Cutting edge: cationic antimicrobial peptides block the binding of lipopolysaccharide (LPS) to LPS binding protein. *J Immunol,* 164**,** 549-53.

SEGAIN, J. P., RAINGEARD DE LA BLETIERE, D., BOURREILLE, A., LERAY, V., GERVOIS, N., ROSALES, C., FERRIER, L., BONNET, C., BLOTTIERE, H. M. & GALMICHE, J. P. 2000. Butyrate inhibits inflammatory responses through NFkappaB inhibition: implications for Crohn's disease. *Gut,* 47**,** 397-403.

SEGATA, N., IZARD, J., WALDRON, L., GEVERS, D., MIROPOLSKY, L., GARRETT, W. S. & HUTTENHOWER, C. 2011. Metagenomic biomarker discovery and explanation. *Genome Biol.*

SEMPLE, F., MACPHERSON, H., WEBB, S., COX, S. L., MALLIN, L. J., TYRRELL, C., GRIMES, G. R., SEMPLE, C. A., NIX, M. A., MILLHAUSER, G. L. & DORIN, J. R. 2011. Human β-defensin 3 affects the activity of pro-inflammatory pathways associated with MyD88 and TRIF. *European journal of immunology,* 41**,** 3291-300.

SEMPLE, F., MACPHERSON, H., WEBB, S., KILANOWSKI, F., LETTICE, L., MCGLASSON, S. L., WHEELER, A. P., CHEN, V., MILLHAUSER, G. L., MELROSE, L., DAVIDSON, D. J. & DORIN, J. R. 2015. Human beta-Defensin 3 [corrected] Exacerbates MDA5 but Suppresses TLR3 Responses to the Viral Molecular Pattern Mimic Polyinosinic:Polycytidylic Acid. *PLoS Genet,* 11**,** e1005673.

SEMPLE, F., WEBB, S., LI, H.-N., PATEL, H. B., PERRETTI, M., JACKSON, I. J., GRAY, M., DAVIDSON, D. J. & DORIN, J. R. 2010. Human beta-defensin 3 has immunosuppressive activity in vitro and in vivo. *European journal of immunology,* 40**,** 1073-8.

SENDER, R., SHAI & MILO, R. 2016. Revised estimates for the number of human and bacteria cells in the body.

SEVELSTED, A., STOKHOLM, J. & BISGAARD, H. 2016. Risk of Asthma from Cesarean Delivery Depends on Membrane Rupture. *J Pediatr,* 171**,** 38-42.e1-4.

SEVELSTED, A., STOKHOLM, J., BONNELYKKE, K. & BISGAARD, H. 2015. Cesarean section and chronic immune disorders. *Pediatrics,* 135**,** e92-8.

SHANNON, C. E. 1948. A Mathematical Theory of Communication. *Bell Labs Technical Journal,* 27**,** 379-423.

SHARP, G. C., HUTCHINSON, J. L., HIBBERT, N., FREEMAN, T. C., SAUNDERS, P. T. K. & NORMAN, J. E. 2016. Transcription Analysis of the Myometrium of Labouring and Non-Labouring Women. *PLoS One.*

SHI, J., AONO, S., LU, W., OUELLETTE, A. J., HU, X., JI, Y., WANG, L., LENZ, S., VAN GINKEL, F. W., LILES, M., DYKSTRA, C., MORRISON, E. E. & ELSON, C. O. 2007. A novel role for defensins in intestinal homeostasis: regulation of IL-1beta secretion. *Journal of immunology,* 179**,** 1245-53.

SHUYI, Y., FENG, W., JING, T., HONGZHANG, H., HAIYAN, W., PINGPING, M., LIWU, Z., ZWAHLEN, R. A. & HONGYU, Y. 2011. Human beta-defensin-3 (hBD-3) upregulated by LPS via epidermal growth factor receptor (EGFR) signaling pathways to enhance lymphatic invasion of oral squamous cell carcinoma. *Oral Surg Oral Med Oral Pathol Oral Radiol Endod,* 112**,** 616-25.

SHYNLOVA, O., NEDD-RODERIQUE, T., LI, Y., DOROGIN, A. & LYE, S. J. 2013a. Myometrial immune cells contribute to term parturition, preterm labour and post-partum involution in mice. *J Cell Mol Med,* 17**,** 90-102.

SHYNLOVA, O., NEDD-RODERIQUE, T., LI, Y., DOROGIN, A., NGUYEN, T. & LYE, S. J. 2013b. Infiltration of myeloid cells into decidua is a critical early event in the labour cascade and post-partum uterine remodelling. *J Cell Mol Med,* 17**,** 311-24.

SIMPSON, E. H. 1949. Measurement of diversity. *Nature*.

SIRIMA, S. B., SAWADOGO, R., MORAN, A. C., KONATE, A., DIARRA, A., YAMEOGO, M., PARISE, M. E. & NEWMAN, R. D. 2003. Failure of a chloroquine chemoprophylaxis program to adequately prevent malaria during pregnancy in Koupéla District, Burkina Faso. *Clinical infectious diseases : an official publication of the Infectious Diseases Society of America,* 36**,** 1374-82.

SNEGOVSKIKH, V., PARK, J. S. & NORWITZ, E. R. 2006. Endocrinology of parturition. *Endocrinol Metab Clin North Am,* 35**,** 173-91, viii.

SOBOLL, G., SCHAEFER, T. M. & WIRA, C. R. 2006. Effect of toll-like receptor (TLR) agonists on TLR and microbicide expression in uterine and vaginal tissues of the mouse. *American journal of reproductive immunology (New York, N.Y. : 1989),* 55**,** 434-46.

SOEHNLEIN, O., ZERNECKE, A., ERIKSSON, E. E., ROTHFUCHS, A. G., PHAM, C. T., HERWALD, H., BIDZHEKOV, K., ROTTENBERG, M. E., WEBER, C. & LINDBOM, L. 2008. Neutrophil secretion products pave the way for inflammatory monocytes. *Blood,* 112**,** 1461-71.

SORENSEN, O. E., FOLLIN, P., JOHNSEN, A. H., CALAFAT, J., TJABRINGA, G. S., HIEMSTRA, P. S. & BORREGAARD, N. 2001. Human cathelicidin, hCAP-18, is processed to the antimicrobial peptide LL-37 by extracellular cleavage with proteinase 3. *Blood,* 97**,** 3951-9.

SORENSEN, O. E., GRAM, L., JOHNSEN, A. H., ANDERSSON, E., BANGSBOLL, S., TJABRINGA, G. S., HIEMSTRA, P. S., MALM, J., EGESTEN, A. & BORREGAARD, N. 2003. Processing of seminal plasma hCAP-18 to ALL-38 by gastricsin: a novel mechanism of generating antimicrobial peptides in vagina. *J Biol Chem,* 278**,** 28540-6.

SPEAR, G. T., FRENCH, A. L., GILBERT, D., ZARIFFARD, M. R., MIRMONSEF, P., SULLIVAN, T. H., SPEAR, W. W., LANDAY, A., MICCI, S., LEE, B. H. & HAMAKER, B. R. 2014. Human alpha-amylase present in lower-genital-tract mucosal fluid processes glycogen to support vaginal colonization by Lactobacillus. *J Infect Dis,* 210**,** 1019-28.

SRINIVASAN, S. & FREDRICKS, D. N. 2008. The human vaginal bacterial biota and bacterial vaginosis. *Interdisciplinary perspectives on infectious diseases,* 2008**,** 750479-750479.

STEIN, B., BALDWIN, A. S., JR., BALLARD, D. W., GREENE, W. C., ANGEL, P. & HERRLICH, P. 1993. Cross-coupling of the NF-kappa B p65 and Fos/Jun transcription factors produces potentiated biological function. *EMBO J,* 12**,** 3879-91.

STEINSTRAESSER, L., LAM, M. C., JACOBSEN, F., PORPORATO, P. E., CHEREDDY, K. K., BECERIKLI, M., STRICKER, I., HANCOCK, R. E., LEHNHARDT, M., SONVEAUX, P., PREAT, V. & VANDERMEULEN, G. 2014. Skin electroporation of a plasmid encoding hCAP-18/LL-37 host defense peptide promotes wound healing. *Mol Ther,* 22**,** 734-42.

STRACHAN, D. P. 1989. Hay fever, hygiene, and household size. *Bmj,* 299**,** 1259-60.

SUDO, N. 2014. Microbiome, HPA axis and production of endocrine hormones in the gut. *Adv Exp Med Biol.* 2014/07/06 ed.

SUN, L., WANG, W., XIAO, W. & YANG, H. 2016. The Roles of Cathelicidin LL-37 in Inflammatory Bowel Disease. *Inflamm Bowel Dis,* 22**,** 1986-91.

SUZUKI, K., MURAKAMI, T., KUWAHARA-ARAI, K., TAMURA, H., HIRAMATSU, K. & NAGAOKA, I. 2011. Human anti-microbial cathelicidin peptide LL-37 suppresses the LPS-induced apoptosis of endothelial cells. *International immunology,* 23**,** 185-93.

SVARE, J. A., SCHMIDT, H., HANSEN, B. B. & LOSE, G. 2006. Bacterial vaginosis in a cohort of Danish pregnant women: prevalence and relationship with preterm delivery, low birthweight and perinatal infections. *BJOG : an international journal of obstetrics and gynaecology,* 113**,** 1419-25.

SYKES, L., HERBERT, B. R., MACINTYRE, D. A., HUNTE, E., PONNAMPALAM, S., JOHNSON, M. R., TEOH, T. G. & BENNETT, P. R. 2013. The CRTH2 agonist Pyl A prevents lipopolysaccharide-induced fetal death but induces preterm labour. *Immunology,* 139**,** 352-65.

TAHA, T. E., HOOVER, D. R., DALLABETTA, G. A., KUMWENDA, N. I., MTIMAVALYE, L. A., YANG, L. P., LIOMBA, G. N., BROADHEAD, R. L., CHIPHANGWI, J. D. & MIOTTI, P. G. 1998. Bacterial vaginosis and disturbances of vaginal flora: association with increased acquisition of HIV. *AIDS (London, England),* 12**,** 1699-706.

TAI, E. K., WONG, H. P., LAM, E. K., WU, W. K., YU, L., KOO, M. W. & CHO, C. H. 2008. Cathelicidin stimulates colonic mucus synthesis by up-regulating MUC1 and MUC2 expression through a mitogen-activated protein kinase pathway. *J Cell Biochem,* 104**,** 251-8.

TAI, E. K., WU, W. K., WANG, X. J., WONG, H. P., YU, L., LI, Z. J., LEE, C. W., WONG, C. C., YU, J., SUNG, J. J., GALLO, R. L. & CHO, C. H. 2013. Intrarectal administration of mCRAMP-encoding plasmid reverses exacerbated colitis in Cnlp(-/-) mice. *Gene Ther,* 20**,** 187-93.

TAKEDA, K. & AKIRA, S. 2001. Roles of Toll-like receptors in innate immune responses. *Genes Cells,* 6**,** 733-42.

TAN, W., CHEN, L., GUO, L., OU, X., XIE, D. & QUAN, S. 2014. Relationship between macrophages in mouse uteri and angiogenesis in endometrium during the peri-implantation period. *Theriogenology,* 82**,** 1021-7.

TEWARY, P., DE LA ROSA, G., SHARMA, N., RODRIGUEZ, L. G., TARASOV, S. G., HOWARD, O. M. Z., SHIROTA, H., STEINHAGEN, F., KLINMAN, D. M., YANG, D. & OPPENHEIM, J. J. 2013. β-Defensin 2 and 3 promote the uptake of self or CpG DNA, enhance IFN-α production by human plasmacytoid dendritic cells, and promote inflammation. *Journal of immunology (Baltimore, Md. : 1950),* 191**,** 865-74.

THINKHAMROP, J., HOFMEYR, G. J., ADETORO, O., LUMBIGANON, P. & OTA, E. 2015. Antibiotic prophylaxis during the second and third trimester to reduce adverse pregnancy outcomes and morbidity. *Cochrane Database Syst Rev***,** Cd002250.

THOMA, M. E., GRAY, R. H., KIWANUKA, N., ALUMA, S., WANG, M. C., SEWANKAMBO, N. & WAWER, M. J. 2011. Longitudinal changes in vaginal microbiota composition

assessed by gram stain among never sexually active pre- and postmenarcheal adolescents in Rakai, Uganda. *J Pediatr Adolesc Gynecol,* 24**,** 42-7.

TJABRINGA, G. S., AARBIOU, J., NINABER, D. K., DRIJFHOUT, J. W., SORENSEN, O. E., BORREGAARD, N., RABE, K. F. & HIEMSTRA, P. S. 2003. The antimicrobial peptide LL-37 activates innate immunity at the airway epithelial surface by transactivation of the epidermal growth factor receptor. *J Immunol,* 171**,** 6690-6.

TJABRINGA, G. S., NINABER, D. K., DRIJFHOUT, J. W., RABE, K. F. & HIEMSTRA, P. S. 2006. Human cathelicidin LL-37 is a chemoattractant for eosinophils and neutrophils that acts via formyl-peptide receptors. *Int Arch Allergy Immunol,* 140**,** 103-12.

TSAI, P. W., YANG, C. Y., CHANG, H. T. & LAN, C. Y. 2011. Human antimicrobial peptide LL-37 inhibits adhesion of Candida albicans by interacting with yeast cell-wall carbohydrates. *PLoS One,* 6**,** e17755.

TURNBAUGH, P. J., BACKHED, F., FULTON, L. & GORDON, J. I. 2008. Diet-induced obesity is linked to marked but reversible alterations in the mouse distal gut microbiome. *Cell Host Microbe,* 3**,** 213-23.

TURNBAUGH, P. J., HAMADY, M., YATSUNENKO, T., CANTAREL, B. L., DUNCAN, A., LEY, R. E., SOGIN, M. L., JONES, W. J., ROE, B. A., AFFOURTIT, J. P., EGHOLM, M., HENRISSAT, B., HEATH, A. C., KNIGHT, R. & GORDON, J. I. 2009. A core gut microbiome in obese and lean twins. *Nature,* 457**,** 480-4.

TURNBAUGH, P. J., LEY, R. E., MAHOWALD, M. A., MAGRINI, V., MARDIS, E. R. & GORDON, J. I. 2006. An obesity-associated gut microbiome with increased capacity for energy harvest. *Nature,* 444**,** 1027-31.

USSAR, S., GRIFFIN, N. W., BEZY, O., FUJISAKA, S., VIENBERG, S., SOFTIC, S., DENG, L., BRY, L., GORDON, J. I. & KAHN, C. R. 2015. Interactions between Gut Microbiota, Host Genetics and Diet Modulate the Predisposition to Obesity and Metabolic Syndrome. *Cell Metab,* 22**,** 516-30.

UZUN, A., DEWAN, A. T., ISTRAIL, S. & PADBURY, J. F. 2013. Pathway-Based Genetic Analysis of Preterm Birth. *Genomics,* 101**,** 163-70.

VALORE, E., PARK, C., IGRETI, S. & GANZ, T. 2002. Antimicrobial components of vaginal fluid. *American journal of obstetrics and gynecology,* 187**,** 561-568.

VALORE, E. V., PARK, C. H., QUAYLE, A. J., WILES, K. R., MCCRAY, P. B., JR. & GANZ, T. 1998. Human beta-defensin-1: an antimicrobial peptide of urogenital tissues. *J Clin Invest,* 101**,** 1633-42.

VAN MEIR, C. A., SANGHA, R. K., WALTON, J. C., MATTHEWS, S. G., KEIRSE, M. J. & CHALLIS, J. R. 1996. Immunoreactive 15-hydroxyprostaglandin dehydrogenase (PGDH) is reduced in fetal membranes from patients at preterm delivery in the presence of infection. *Placenta,* 17**,** 291-7.

VANDAMME, D., LANDUYT, B., LUYTEN, W. & SCHOOFS, L. 2012. A comprehensive summary of LL-37, the factotum human cathelicidin peptide. *Cell Immunol,* 280**,** 22-35.

VILO, C. & DONG, Q. 2012. Evaluation of the RDP Classifier Accuracy Using 16S rRNA Gene Variable Regions. *Metagenomics,* 1**,** 1-5.

VORA, S., ABBAS, A., KIM, C. J., SUMMERFIELD, T. L., KUSANOVIC, J. P., IAMS, J. D., ROMERO, R., KNISS, D. A. & ACKERMAN, W. E. T. 2010. Nuclear factor-kappa B localization and function within intrauterine tissues from term and preterm labor and cultured fetal membranes. *Reprod Biol Endocrinol,* 8**,** 8.

VRACHNIS, N., VITORATOS, N., ILIODROMITI, Z., SIFAKIS, S., DELIGEOROGLOU, E. & CREATSAS, G. 2010. Intrauterine inflammation and preterm delivery. *Annals of the New York Academy of Sciences,* 1205**,** 118-22.

WAKABAYASHI, A., SAWADA, K., NAKAYAMA, M., TODA, A., KIMOTO, A., MABUCHI, S., KINOSE, Y., NAKAMURA, K., TAKAHASHI, K., KURACHI, H. & KIMURA, T. 2013.

Targeting interleukin-6 receptor inhibits preterm delivery induced by inflammation. *Molecular human reproduction,* 0**,** 1-9.

WALIA, M. & SAINI, N. 2015. Relationship between periodontal diseases and preterm birth: Recent epidemiological and biological data. *Int J Appl Basic Med Res,* 5**,** 2-6.

WANG, A., CHEN, F., WANG, Y., SHEN, M., XU, Y., HU, J., WANG, S., GENG, F., WANG, C., RAN, X., SU, Y., CHENG, T. & WANG, J. 2013. Enhancement of antiviral activity of human alpha-defensin 5 against herpes simplex virus 2 by arginine mutagenesis at adaptive evolution sites. *J Virol,* 87**,** 2835-45.

WANG, G., LI, X. & WANG, Z. 2016. APD3: the antimicrobial peptide database as a tool for research and education. *Nucleic Acids Res,* 44**,** D1087-93.

WANG, J. M., XU, L., MURPHY, W. J., TAUB, D. D. & CHERTOV, O. 1996. IL-8-Induced T-Lymphocyte Migration: Direct as Well as Indirect Mechanisms. *Methods,* 10**,** 135-44.

WANG, Q., GARRITY, G. M., TIEDJE, J. M. & COLE, J. R. 2007. Naive Bayesian classifier for rapid assignment of rRNA sequences into the new bacterial taxonomy. *Appl Environ Microbiol,* 73**,** 5261-7.

WANG, R. F., BEGGS, M. L., ERICKSON, B. D. & CERNIGLIA, C. E. 2004a. DNA microarray analysis of predominant human intestinal bacteria in fecal samples. *Mol Cell Probes,* 18**,** 223-34.

WANG, T.-T., NESTEL, F. P., BOURDEAU, V., NAGAI, Y., WANG, Q., LIAO, J., TAVERA-MENDOZA, L., LIN, R., HANRAHAN, J. W., MADER, S., WHITE, J. H. & HANRAHAN, J. H. 2004b. Cutting edge: 1,25-dihydroxyvitamin D3 is a direct inducer of antimicrobial peptide gene expression. *Journal of immunology (Baltimore, Md. : 1950),* 173**,** 2909-12.

WANG, T. T., DABBAS, B., LAPERRIERE, D., BITTON, A. J., SOUALHINE, H., TAVERA-MENDOZA, L. E., DIONNE, S., SERVANT, M. J., BITTON, A., SEIDMAN, E. G., MADER, S., BEHR, M. A. & WHITE, J. H. 2010. Direct and indirect induction by 1,25-dihydroxyvitamin D3 of the NOD2/CARD15-defensin beta2 innate immune pathway defective in Crohn disease. *J Biol Chem,* 285**,** 2227-31.

WEHKAMP, J., HARDER, J., WEICHENTHAL, M., MUELLER, O., HERRLINGER, K. R., FELLERMANN, K., SCHROEDER, J. M. & STANGE, E. F. 2003. Inducible and constitutive beta-defensins are differentially expressed in Crohn's disease and ulcerative colitis. *Inflamm Bowel Dis,* 9**,** 215-23.

WEHKAMP, J. & STANGE, E. F. 2010. Paneth's disease. *J Crohns Colitis,* 4**,** 523-31.

WEN, L., LEY, R. E., VOLCHKOV, P. Y., STRANGES, P. B., AVANESYAN, L., STONEBRAKER, A. C., HU, C., WONG, F. S., SZOT, G. L., BLUESTONE, J. A., GORDON, J. I. & CHERVONSKY, A. V. 2008. Innate immunity and intestinal microbiota in the development of Type 1 diabetes. *Nature,* 455**,** 1109-13.

WESOLOWSKA-ANDERSEN, A., BAHL, M. I., CARVALHO, V., KRISTIANSEN, K., SICHERITZ-PONTEN, T., GUPTA, R. & LICHT, T. R. 2014. Choice of bacterial DNA extraction method from fecal material influences community structure as evaluated by metagenomic analysis. *Microbiome,* 2**,** 19.

WHITELEY, A. S., JENKINS, S., WAITE, I., KRESOJE, N., PAYNE, H., MULLAN, B., ALLCOCK, R. & O'DONNELL, A. 2012. Microbial 16S rRNA Ion Tag and community metagenome sequencing using the Ion Torrent (PGM) Platform. *Journal of microbiological methods,* 91**,** 80-8.

WIESENFELD, H. C., HILLIER, S. L., KROHN, M. A., LANDERS, D. V. & SWEET, R. L. 2003. Bacterial vaginosis is a strong predictor of Neisseria gonorrhoeae and Chlamydia trachomatis infection. *Clinical infectious diseases : an official publication of the Infectious Diseases Society of America,* 36**,** 663-8.

WIRA, C. R., FAHEY, J. V., GHOSH, M., PATEL, M. V., HICKEY, D. K. & OCHIEL, D. O. 2010. Sex hormone regulation of innate immunity in the female reproductive tract: the

role of epithelial cells in balancing reproductive potential with protection against sexually transmitted pathogens. *Am J Reprod Immunol,* 63**,** 544-65.

WOO, P. C., LAU, S. K., TENG, J. L., TSE, H. & YUEN, K. Y. 2008. Then and now: use of 16S rDNA gene sequencing for bacterial identification and discovery of novel bacteria in clinical microbiology laboratories. *Clin Microbiol Infect,* 14**,** 908-34.

WORLD HEALTH, O. 2013. SEXUALLY TRANSMITTED INFECTIONS (STIs).

WU, Z., HOOVER, D. M., YANG, D., BOULÈGUE, C., SANTAMARIA, F., OPPENHEIM, J. J., LUBKOWSKI, J. & LU, W. 2003. Engineering disulfide bridges to dissect antimicrobial and chemotactic activities of human beta-defensin 3. *Proceedings of the National Academy of Sciences of the United States of America,* 100**,** 8880-5.

YALLAMPALLI, C., GARFIELD, R. E. & BYAM-SMITH, M. 1993. Nitric oxide inhibits uterine contractility during pregnancy but not during delivery. *Endocrinology,* 133**,** 1899-902.

YAMAGUCHI, Y., FUKUHARA, S., NAGASE, T., TOMITA, T., HITOMI, S., KIMURA, S., KURIHARA, H. & OUCHI, Y. 2001. A novel mouse beta-defensin, mBD-6, predominantly expressed in skeletal muscle. *J Biol Chem,* 276**,** 31510-4.

YAMAGUCHI, Y., NAGASE, T., TOMITA, T., NAKAMURA, K., FUKUHARA, S., AMANO, T., YAMAMOTO, H., IDE, Y., SUZUKI, M., TERAMOTO, S., ASANO, T., KANGAWA, K., NAKAGATA, N., OUCHI, Y. & KURIHARA, H. 2007. Beta-defensin overexpression induces progressive muscle degeneration in mice. *American journal of physiology. Cell physiology,* 292**,** C2141-9.

YAMASAKI, K., SCHAUBER, J., CODA, A., LIN, H., DORSCHNER, R. A., SCHECHTER, N. M., BONNART, C., DESCARGUES, P., HOVNANIAN, A. & GALLO, R. L. 2006. Kallikrein-mediated proteolysis regulates the antimicrobial effects of cathelicidins in skin. *Faseb j,* 20**,** 2068-80.

YAN, X., SUN, M. & GIBB, W. 2002. Localization of nuclear factor-kappa B (NF kappa B) and inhibitory factor-kappa B (I kappa B) in human fetal membranes and decidua at term and preterm delivery. *Placenta,* 23**,** 288-93.

YANG, D., CHERTOV, O., BYKOVSKAIA, S. N., CHEN, Q., BUFFO, M. J., SHOGAN, J., ANDERSON, M., SCHRODER, J. M., WANG, J. M., HOWARD, O. M. & OPPENHEIM, J. J. 1999. Beta-defensins: linking innate and adaptive immunity through dendritic and T cell CCR6. *Science,* 286**,** 525-8.

YAO, J., CARTER, R. A., VUAGNIAUX, G., BARBIER, M., ROSCH, J. W. & ROCK, C. O. 2016. A Pathogen-Selective Antibiotic Minimizes Disturbance to the Microbiome. *Antimicrob Agents Chemother,* 60**,** 4264-73.

YARBROUGH, V. L., WINKLE, S. & HERBST-KRALOVETZ, M. M. 2015. Antimicrobial peptides in the female reproductive tract: a critical component of the mucosal immune barrier with physiological and clinical implications. *Hum Reprod Update,* 21**,** 353-77.

YARZA, P., YILMAZ, P., PRUESSE, E., GLOCKNER, F. O., LUDWIG, W., SCHLEIFER, K. H., WHITMAN, W. B., EUZEBY, J., AMANN, R. & ROSSELLO-MORA, R. 2014. Uniting the classification of cultured and uncultured bacteria and archaea using 16S rRNA gene sequences. *Nat Rev Microbiol,* 12**,** 635-45.

YIN, L., CHINO, T., HORST, O. V., HACKER, B. M., CLARK, E. A., DALE, B. A. & CHUNG, W. O. 2010. Differential and coordinated expression of defensins and cytokines by gingival epithelial cells and dendritic cells in response to oral bacteria. *BMC Immunol,* 11**,** 37.

YIN, Y., WANG, Y., ZHU, L., LIU, W., LIAO, N., JIANG, M., ZHU, B., YU, H. D., XIANG, C. & WANG, X. 2013. Comparative analysis of the distribution of segmented filamentous bacteria in humans, mice and chickens. *Isme j,* 7**,** 615-21.

YOUSSEF, R. E., LEDINGHAM, M. A., BOLLAPRAGADA, S. S., O'GORMAN, N., JORDAN, F., YOUNG, A. & NORMAN, J. E. 2009. The role of toll-like receptors (TLR-2 and -4)

and triggering receptor expressed on myeloid cells 1 (TREM-1) in human term and preterm labor. *Reprod Sci,* 16**,** 843-56.

YU, G., FADROSH, D., GOEDERT, J. J., RAVEL, J. & GOLDSTEIN, A. M. 2015. Nested PCR Biases in Interpreting Microbial Community Structure in 16S rRNA Gene Sequence Datasets. *PLoS One,* 10**,** e0132253.

YUAN, M., JORDAN, F., MCINNES, I. B., HARNETT, M. M. & NORMAN, J. E. 2009. Leukocytes are primed in peripheral blood for activation during term and preterm labour. *Mol Hum Reprod,* 15**,** 713-24.

ZANVIT, P., KONKEL, J. E., JIAO, X., KASAGI, S., ZHANG, D., WU, R., CHIA, C., AJAMI, N. J., SMITH, D. P., PETROSINO, J. F., ABBATIELLO, B., NAKATSUKASA, H., CHEN, Q., BELKAID, Y., CHEN, Z. J. & CHEN, W. 2015. Antibiotics in neonatal life increase murine susceptibility to experimental psoriasis. *Nat Commun,* 6**,** 8424.

ZEUTHEN, L. H., FINK, L. N. & FROKIAER, H. 2008. Epithelial cells prime the immune response to an array of gut-derived commensals towards a tolerogenic phenotype through distinct actions of thymic stromal lymphopoietin and transforming growth factor-beta. *Immunology,* 123**,** 197-208.

ZHOU, Y. S., WEBB, S., LETTICE, L., TARDIF, S., KILANOWSKI, F., TYRRELL, C., MACPHERSON, H., SEMPLE, F., TENNANT, P., BAKER, T., HART, A., DEVENNEY, P., PERRY, P., DAVEY, T., BARRAN, P., BARRATT, C. L. & DORIN, J. R. 2013. Partial deletion of chromosome 8 beta-defensin cluster confers sperm dysfunction and infertility in male mice. *PLoS Genet,* 9**,** e1003826.

ZHU, C., TAN, H., CHENG, T., SHEN, H., SHAO, J., GUO, Y., SHI, S. & ZHANG, X. 2013. Human beta-defensin 3 inhibits antibiotic-resistant Staphylococcus biofilm formation. *J Surg Res,* 183**,** 204-13.

ZUCHT, H. D., GRABOWSKY, J., SCHRADER, M., LIEPKE, C., JURGENS, M., SCHULZ-KNAPPE, P. & FORSSMANN, W. G. 1998. Human beta-defensin-1: A urinary peptide present in variant molecular forms and its putative functional implication. *Eur J Med Res,* 3**,** 315-23.

Appendices

Appendices

Materials and Methods

***In-vivo* Mouse Experiments**	**Source**
Hamilton 33-gauge needle	Sigma Aldrich, Poole, Dorset, UK
Hamilton syringe	Sigma Aldrich, Poole, Dorset, UK
Sodium Chloride 0.9% (physiological saline)	Sigma Aldrich, Poole, Dorset, UK
LPS Ultrapure (*E. coli* 0111:B4)	Sigma Aldrich, Poole, Dorset, UK
Vetergesic	Alstoe Ltd, York, UK
Isoflurane	Merial Animal Health Ltd, Harlow, Essex, UK
RNAlater®	Sigma Aldrich, Poole, Dorset, UK
Paraformaldehyde	Sigma Aldrich, Poole, Dorset, UK
Povidone Iodine (10% w/v)	Sigma Aldrich, Poole, Dorset, UK
Coated Vicryl (W9443) Violet 4/0 16mm 3/8 circle conventional cutting needle	MidMeds Ltd, Waltham Abbey, UK
Mersilk (W580) Black 5/0 12mm 3/8 circle reverse cutting needle	MidMeds Ltd, Waltham Abbey, UK
BD Microtainer® Blood Collection Tubes Clot Activator/ SST Gel	Becton, Dickinson and Company, New Jersey, USA
Ultrasound; Visualsonics high resolution Vevo 770 ultrasound scanner	FUJIFILM VisualSonics, Inc, Ontario, Canada
Ultrasound; Vevo 770 Imaging Station (Integrated Rail System)	FUJIFILM VisualSonics, Inc, Ontario, Canada
D1 Digital Video Recorder	Swann, UK

Estrus Cycling and Staging	**Source**
PMSG	Sigma Aldrich, Poole, Dorset, UK
hCG	Sigma Aldrich, Poole, Dorset, UK
Crystal Violet	Sigma Aldrich, Poole, Dorset, UK

***Ex-vivo* Experiments**	**Source**
hBD3 (chemically synthesized and folded)	Peptide Institute (#4382-s)
LPS Ultrapure (*E. coli* 0111:B4)	Sigma Aldrich, Poole, Dorset, UK
Scrambled LL-37	Almac, Gladsmuir, UK
Recombinant LL-37	Almac, Gladsmuir, UK
RPMI 1640 medium	Sigma Aldrich, Poole, Dorset, UK
Fetal Calf Serum	Mycoplex, Teddington, UK
Penicillin	Sigma Aldrich, Poole, Dorset, UK
Streptomycin	Sigma Aldrich, Poole, Dorset, UK
Culture plates (6 well and 12 well)	Corning Costar, High Wycombe, UK

ELISA	**Source**
MaxiSorp®, Nunc, Flat-bottomed 96-well plates	Affymetrix, California, USA
3,3′,5,5′-Tetramethylbenzidine (TMB) Liquid Substrate	Sigma Aldrich, Poole, Dorset, UK
Tween 20	Sigma Aldrich, Poole, Dorset, UK
Reagent Diluent Concentrate 2 (10x)	R&D Systems, Abingdon, UK
Dulbeccos Phosphate buffered saline 1x (PBS)	Gibco, Life Technologies Ltd, Paisley, UK
DuoSet ELISA	R&D Systems, Abingdon, UK

RNA Exaction	Source
TRI reagent®	Sigma Aldrich, Poole, Dorset, UK
Phase Lock Gel Heavy 2 ml tubes	5 PRIME, Inc, Gaithersburg, USA
1-Bromo-3-chloropropane	Sigma Aldrich, Poole, Dorset, UK
RNeasy Mini Kit	Qiagen, Crawley, West Sussex, UK
Nanodrop ND-1000	Thermo Fisher Scientific, Waltham, USA
TissueLyser I	Qiagen, Crawley, West Sussex, UK
Precellys®24	Bertin Corp, Rockville, USA
Chloroform	Sigma Aldrich, Poole, Dorset, UK
Isopropanol	Sigma Aldrich, Poole, Dorset, UK
RNA Bee - RNA Isolation Reagent	AMS Biotechnology Ltd, Abingdon, UK
Lysing Matrix D, 2 mL	MP Biomedicals, California, USA
RNase and DNase-free water	Sigma Aldrich, Poole, Dorset, UK

RT-qPCR	Source
High-Capacity cDNA Reverse Transcription Kit	Applied Biosystems, Life Technologies Ltd, Paisley, UK
DNase 1	Qiagen, Crawley, West Sussex, UK
TaqMan® Gene Expression Master Mix (x2)	Applied Biosystems, Life Technologies Ltd, Paisley, UK
TaqMan® Assays Probes	Applied Biosystems, Life Technologies Ltd, Paisley, UK
Human ACTB (Beta Actin) Endogenous Control (FAM™/MGB probe)	Applied Biosystems, Life Technologies Ltd, Paisley, UK
Eukaryotic 18S rRNA Endogenous Control (FAM™/MGB probe)	Applied Biosystems, Life Technologies Ltd, Paisley, UK
Mouse ACTB (Actin, Beta) Endogenous Control (FAM™ Dye/MGB probe)	Applied Biosystems, Life Technologies Ltd, Paisley, UK
ABI PRISM® 7000 Sequence Detection System	Applied Biosystems, Life Technologies Ltd, Paisley, UK
The LightCycler® 480 Real-Time PCR System	Roche Diagnostics Limited, Life Technologies Ltd, Paisley, UK

16S rRNA qPCR	Source
LightCycler® 480 SYBR Green II Master’	Life Technologies Ltd, Paisley, UK

Microbiome	**Source**
PowerSoil® DNA Isolation Kit	MO BIO, Carlsbad, USA
FastDNA® SPIN Kit	MP Biomedicals, Santa Ana, USA
FastPrep® Instrument	MP Biomedicals, Santa Ana, USA
Q5® High-Fidelity DNA Polymerase kit	New England Biolabs, Massachusetts, USA
Agilent 2100 Bioanalyzer	Agilent Technologies, California, USA
Bioanalyzer Chips DNA 1000	Agilent Technologies, California, USA
Bioanalyzer Chips DNA High Sensitivity	Agilent Technologies, California, USA
Qubit™ 2 Fluorometer	Thermo Fisher Scientific, Waltham, USA
Qubit dsDNA HS Assay Kit	Thermo Fisher Scientific, Waltham, USA
Qubit dsDNA BS Assay Kit	Thermo Fisher Scientific, Waltham, USA
100bp ladder	New England Biolabs, Massachusetts, USA
Loading Dye	New England Biolabs, Massachusetts, USA
Agarose	Sigma Aldrich, Poole, Dorset, UK
Ethidium Bromide	Sigma Aldrich, Poole, Dorset, UK
ExoSAP-IT®	Affymetrix, California, USA
dNTPs	Life Technologies Ltd, Paisley, UK
Ion Torrent PGM	Life Technologies Ltd, Paisley, UK
KAPA Library Quantification kit	KAPA Biosystems
Ion OneTouchTM 400 Template Kit v2	Life Technologies Ltd, Paisley, UK
MiSeq Reagent v3 kit	Illumina, California, USA,

Galaxy Workflow

Step	Annotation
Step 1: Input dataset	Input FASTQ File
Input Dataset *select at runtime*	
Step 2: FastQC:Read QC	
Short read data from your current history Output dataset 'output' from step 1 Title for the output file - to remind you what the job was for FastQC Contaminant list *select at runtime*	
Step 3: Cutadapt	Discard Reads With Homopolymers >7bp
Fastq file to trim Output dataset 'output' from step 1 **3' Adapters** **3' Adapters 1** Source Enter custom sequence Enter custom 3' adapter sequence AAAAAAA **3' Adapters 2** Source Enter custom sequence Enter custom 3' adapter sequence TTTTTTT **3' Adapters 3** Source Enter custom sequence Enter custom 3' adapter sequence GGGGGGG **3' Adapters 4** Source Enter custom sequence Enter custom 3' adapter sequence CCCCCCC **5' or 3' (Anywhere) Adapters** Maximum error rate 0.0 Match times 1 Minimum overlap length 1 Discard Trimmed Reads False Minimum length 150 Maximum length 0 Quality cutoff 0 Additional output options Default	
Step 4: Cutadapt	Trim The 5' Primer Off Reads
Fastq file to trim Output dataset 'output' from step 3 **3' Adapters** **5' or 3' (Anywhere) Adapters**	

5' or 3' (Anywhere) Adapters 1 Source Enter custom sequence Enter custom 5' or 3' adapter sequence AGTTTGATYMTGGCTCAG Maximum error rate 0.22 Match times 1 Minimum overlap length 3 Discard Trimmed Reads False Minimum length 175 Maximum length 0 Quality cutoff 0 Additional output options Additional output files Rest of Read False Too Short Reads False Untrimmed Reads True	
Step 5: Cutadapt Fastq file to trim Output dataset 'output' from step 4 **3' Adapters** **3' Adapters 1** Source Enter custom sequence Enter custom 3' adapter sequence ACTCCTACGGRAGGCAGCA **5' or 3' (Anywhere) Adapters** Maximum error rate 0.22 Match times 1 Minimum overlap length 3 Discard Trimmed Reads False Minimum length 150 Maximum length 0 Quality cutoff 0 Additional output options Additional output files Rest of Read True Too Short Reads True Untrimmed Reads True	Trim The 3'' Primer Off Reads
Step 6: FASTQ Quality Trimmer	Full Length Reads (i.e

FASTQ File Output dataset 'output' from step 5 Keep reads with zero length False Trim ends 3' only Window size 6 Step Size 1 Maximum number of bases to exclude from the window during aggregation 0 Aggregate action for window mean of scores Trim until aggregate score is >= Quality Score 25.0	3' primer was trimmed) sent for Quality Filtering
Step 7: FASTQ Quality Trimmer FASTQ File Output dataset 'untrimmed_output' from step 5 Keep reads with zero length False Trim ends 3' only Window size 6 Step Size 1 Maximum number of bases to exclude from the window during aggregation 0 Aggregate action for window mean of scores Trim until aggregate score is >= Quality Score 25.0	Not Full Length Reads (i.e 3' primer was Not trimmed) sent for Quality Filtering
Step 8: Filter FASTQ FASTQ File Output dataset 'output_file' from step 6 Minimum Size 200 Maximum Size 450 Minimum Quality 0.0 Maximum Quality 0.0 Maximum number of bases allowed outside of quality range 0 This is paired end data False **Quality Filter on a Range of Bases**	Filter Trimmed Reads by Size
Step 9: Filter FASTQ FASTQ File Output dataset 'output_file' from step 7 Minimum Size 200 Maximum Size 450	Filter Not Trimmed Reads by Size

Minimum Quality 0.0 Maximum Quality 0.0 Maximum number of bases allowed outside of quality range 0 This is paired end data False **Quality Filter on a Range of Bases**	
Step 10: FastQC:Read QC Short read data from your current history Output dataset 'output_file' from step 8 Title for the output file - to remind you what the job was for FastQC Contaminant list *select at runtime*	FastQC output
Step 11: Concatenate datasets Concatenate Dataset Output dataset 'output_file' from step 8 **Datasets** **Dataset 1** Select Output dataset 'output_file' from step 9	Combine Datasets
Step 12: FastQC:Read QC Short read data from your current history Output dataset 'output_file' from step 9 Title for the output file - to remind you what the job was for FastQC Contaminant list *select at runtime*	FastQC output
Step 13: FastQC:Read QC Short read data from your current history Output dataset 'out_file1' from step 11 Title for the output file - to remind you what the job was for FastQC Contaminant list *select at runtime*	FastQC output
Step 14: FASTQ to FASTA FASTQ file to convert Output dataset 'out_file1' from step 11	Convert FASTQ to FASTA. Output Enter QIIME Workflow.

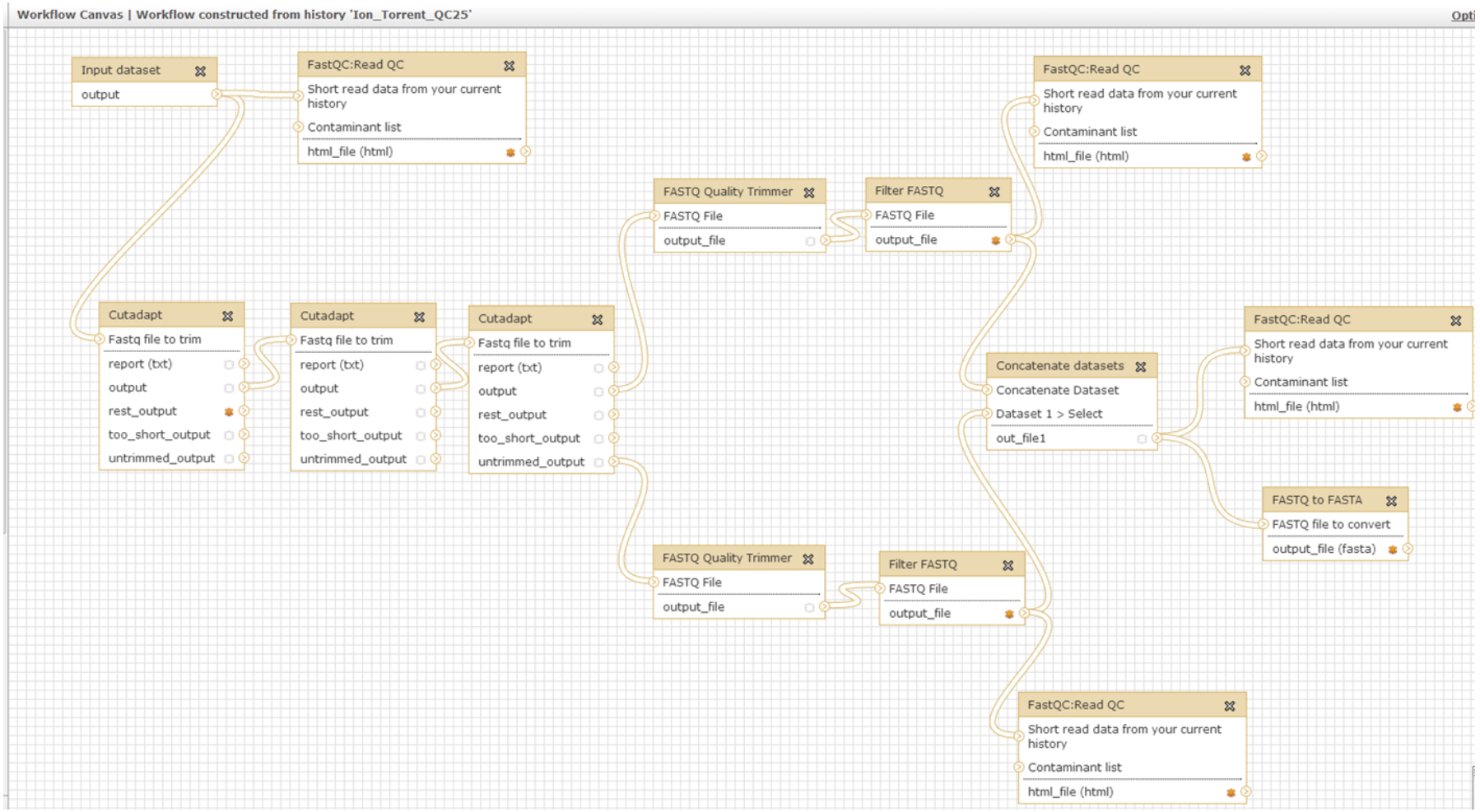
Workflow Canvas | Workflow constructed from history 'Ion_Torrent_QC25'
Opti
Input dataset
output
FastQC:Read QC
Short read data from your current history
Contaminant list
html_file (html)
FastQC:Read QC
Short read data from your current history
Contaminant list
html_file (html)
FASTQ Quality Trimmer
FASTQ File
output_file
Filter FASTQ
FASTQ File
output_file
Cutadapt
Fastq file to trim
report (txt)
output
rest_output
too_short_output
untrimmed_output
Cutadapt
Fastq file to trim
report (txt)
output
rest_output
too_short_output
untrimmed_output
Cutadapt
Fastq file to trim
report (txt)
output
rest_output
too_short_output
untrimmed_output
Concatenate datasets
Concatenate Dataset
Dataset 1 > Select
out_file1
FastQC:Read QC
Short read data from your current history
Contaminant list
html_file (html)
FASTQ to FASTA
FASTQ file to convert
output_file (fasta)
FASTQ Quality Trimmer
FASTQ File
output_file
Filter FASTQ
FASTQ File
output_file
FastQC:Read QC
Short read data from your current history
Contaminant list
html_file (html)

Full Taxonomic Classifications (LEfSe)

Full Taxonomic Classification	Annotated Classification
Bacteria.Bacteroidetes.Bacteroidia.Bacteroidales.Prevotellaceae	p.Bacteroidetes.f.Prevotellaceae
Bacteria.Bacteroidetes.Bacteroidia.Bacteroidales.Prevotellaceae.Prevotella	p.Bacteroidetes.g.Prevotella
Bacteria.Bacteroidetes.Bacteroidia.Bacteroidales.Prevotellaceae.Prevotella.Otu00045	p.Bacteroidetes.g.Prevotella.Otu00045
Bacteria.Bacteroidetes.Bacteroidia.Bacteroidales.Prevotellaceae.Prevotella.Otu00089	p.Bacteroidetes.g.Prevotella.Otu00089
Bacteria.Firmicutes.Clostridia.Clostridiales.Lachnospiraceae.Blautia.Otu00017	p.Firmicutes.g.Blautia.Otu00017
Bacteria.Firmicutes.Clostridia.Clostridiales.Lachnospiraceae.Blautia.Otu00037	p.Firmicutes.g.Blautia.Otu00037
Bacteria.Firmicutes.Clostridia.Clostridiales.Lachnospiraceae.Blautia.Otu00042	p.Firmicutes.g.Blautia.Otu00042
Bacteria.Firmicutes.Clostridia.Clostridiales.Lachnospiraceae.Blautia.Otu00060	p.Firmicutes.g.Blautia.Otu00060
Bacteria.Firmicutes.Clostridia.Clostridiales.Lachnospiraceae.Blautia.Otu00105	p.Firmicutes.g.Blautia.Otu00105
Bacteria.Firmicutes.Erysipelotrichia	p.Firmicutes.c.Erysipelotrichia
Bacteria.Firmicutes.Erysipelotrichia.Erysipelotrichales	p.Firmicutes.o.Erysipelotrichales
Bacteria.Firmicutes.Erysipelotrichia.Erysipelotrichales.Erysipelotrichaceae	p.Firmicutes.f.Erysipelotrichaceae
Bacteria.Firmicutes.Erysipelotrichia.Erysipelotrichales.Erysipelotrichaceae.Allobaculum	p.Firmicutes.g.Allobaculum
Bacteria.Firmicutes.Erysipelotrichia.Erysipelotrichales.Erysipelotrichaceae.Allobaculum.Otu00019	p.Firmicutes.g.Allobaculum.Otu00019
Bacteria.Bacteroidetes.Bacteroidia.Bacteroidales.S24_7.unclassified.Otu00003	p.Bacteroidetes.f.S24_7.Otu00003
Bacteria.Bacteroidetes.Bacteroidia.Bacteroidales.S24_7.unclassified.Otu00022	p.Bacteroidetes.f.S24_7.Otu00022
Bacteria.Bacteroidetes.Bacteroidia.Bacteroidales.unclassified.unclassified.Otu00039	p.Bacteroidetes.g.unclassified.Otu00039
Bacteria.Firmicutes.Clostridia.Clostridiales.Lachnospiraceae.Blautia.Otu00069	p.Firmicutes.g.Blautia.Otu00069
Bacteria.Firmicutes.Clostridia.Clostridiales.Lachnospiraceae.unclassified.Otu00043	p.Firmicutes.f.Lachnospiraceae.unclassified.Otu00043
Bacteria.Firmicutes.Clostridia.Clostridiales.Lachnospiraceae.unclassified.Otu00047	p.Firmicutes.f.Lachnospiraceae.unclassified.Otu00047
Bacteria.Firmicutes.Clostridia.Clostridiales.Lachnospiraceae.unclassified.Otu00170	p.Firmicutes.f.Lachnospiraceae.unclassified.Otu00170
Bacteria.Firmicutes.unclassified.unclassified.unclassified.unclassified	p.Firmicutes.g.unclassified
Bacteria.Tenericutes.Mollicutes.Anaeroplasmatales	p.Tenericutes.o.Anaeroplasmatales
Bacteria.Tenericutes.Mollicutes.Anaeroplasmatales.Anaeroplasmataceae	p.Tenericutes.f.Anaeroplasmataceae
Bacteria.Tenericutes.Mollicutes.Anaeroplasmatales.Anaeroplasmataceae.Anaeroplasma	p.Tenericutes.g.Anaeroplasma
Bacteria.Tenericutes.Mollicutes.Anaeroplasmatales.Anaeroplasmataceae.Anaeroplasma.Otu00072	p.Tenericutes.g.Anaeroplasma.Otu00072
Bacteria.Bacteroidetes.Bacteroidia.Bacteroidales.Prevotellaceae	p.Bacteroidetes.f.Prevotellaceae
Bacteria.Bacteroidetes.Bacteroidia.Bacteroidales.Prevotellaceae.Prevotella	p.Bacteroidetes.g.Prevotella
Bacteria.Bacteroidetes.Bacteroidia.Bacteroidales.Prevotellaceae.Prevotella.Otu00045	p.Bacteroidetes.g.Prevotella.Otu00045
Bacteria.Bacteroidetes.Bacteroidia.Bacteroidales.Prevotellaceae.Prevotella.Otu00089	p.Bacteroidetes.g.Prevotella.Otu00089